ISSN 1881-7815 Online ISSN 1881-7823

BST
BioScience Trends

Volume 14, Number 4
August, 2020

IRCA
BSSA

IACMHR

www.biosciencetrends.com

BST
BioScience Trends

ISSN: 1881-7815
Online ISSN: 1881-7823
CODEN: BTIRCZ
Issues/Year: 6
Language: English
Publisher: IACMHR Co., Ltd.

BioScience Trends is one of a series of peer-reviewed journals of the International Research and Cooperation Association for Bio & Socio-Sciences Advancement (IRCA-BSSA) Group and is published bimonthly by the International Advancement Center for Medicine & Health Research Co., Ltd. (IACMHR Co., Ltd.) and supported by the IRCA-BSSA and Shandong University China-Japan Cooperation Center for Drug Discovery & Screening (SDU-DDSC).

BioScience Trends devotes to publishing the latest and most exciting advances in scientific research. Articles cover fields of life science such as biochemistry, molecular biology, clinical research, public health, medical care system, and social science in order to encourage cooperation and exchange among scientists and clinical researchers.

BioScience Trends publishes Original Articles, Brief Reports, Reviews, Policy Forum articles, Case Reports, News, and Letters on all aspects of the field of life science. All contributions should seek to promote international collaboration.

Editorial Board

Editorial Office

Pearl City Koishikawa 603,
2-4-5 Kasuga, Bunkyo-ku, Tokyo 112-0003, Japan
E-mail: office@biosciencetrends.com

BioScience Trends

Editorial and Head Office

Pearl City Koishikawa 603, 2-4-5 Kasuga, Bunkyo-ku,
Tokyo 112-0003, Japan

E-mail: office@biosciencetrends.com
URL: www.biosciencetrends.com

CONTENTS

Volume 14, Number 4, 2020

Policy Forum

Original Article

Policy Forum

DOI: 10.5582/bst.2020.03093

An international comparison analysis of reserve and supply system for emergency medical supplies between China, the United States, Australia, and Canada

Xu Wang[1,§], Wenhui Wu[2,§], Peipei Song[3], Jiangjiang He[1,*]

[1] Department of Health Policy Research, Shanghai Health Development Research Center (Shanghai Medical Information Center), Shanghai, China;
[2] Division of Drug Administration, Shanghai Municipal Health Commission, Shanghai, China;
[3] Institute for Global Health Policy Research, Bureau of International Health Cooperation, National Center for Global Health and Medicine, Tokyo, Japan.

SUMMARY Coronavirus disease 19 (COVID-19) has become a pandemic around the world. With the explosive growth of confirmed cases, emergency medical supplies are facing global shortage, which restricts the treatment of seriously ill patients and protection of medical staff. Taking China, the United States, Australia, and Canada as examples, this study compares and analyzes the reserve and supply systems of emergency medical supplies and problems exposed in response to the COVID-19 epidemic. Some common problems were found, such as insufficient types and quantities of emergency medical supplies in reserve, insufficient emergency production capacity, and imperfect command mechanism for emergency supplies deployment and transportation. A sound reserve system of emergency medical supplies is the basis and guarantee for dealing with public health emergencies such as major outbreaks. Based on the comparison of systems and practical experience, countries around the world should further improve the reserve and supply system of emergency medical supplies, and improve the coordination and cooperation mechanism for emergency supplies for international public health emergencies, so as to cope with increasingly severe public health emergencies in the context of globalization.

Keywords emergency medical supplies, reserve and supply, COVID-19

1. Introduction

Recently, COVID-19 has become a pandemic and affects almost all countries worldwide. As of April 12, 2020, 1,696,588 confirmed COVID-19 cases and 105,952 deaths have been reported around the world (*1*). Particularly, the United States, Italy and Spain are seriously affected. At the same time, shortage of medical supplies has become a global problem. The world health organization (WHO) has declared that global medical supplies - such as surgical masks, detection reagents, ventilators, *et al.*- are extremely scarce due to the outbreak of COVID-19 (*2*), resulting in many patients failing to get timely treatment. In addition, shortage of personal protective equipment endangers medical staff and the epidemic prevention and control situation worldwide, leading to frequent infections of front-line medical staff in some seriously affected countries (*3*). According to statistical data released by the Italian higher health institute on March 23, the number of confirmed COVID-19 cases among Italian medical staff has risen to 4,824, accounting for 9% of the total confirmed cases in Italy (*4*).

On March 23, 2020, WHO declared that the global outbreak of COVID-19 may affect production and supply of emergency medical supplies and their raw materials, aggravate the shortage of emergency medical supplies and cause unexpected consequences. WHO called for global-level political commitment and coordination, making joint efforts to increase output of emergency medical supplies (*5*).

This study intends to summarize and analyze the national emergency supplies reserve and supply system of China, the United States, Australia, and Canada, aiming to provide a reference for further improving emergency medical supplies reserve and the supply mechanism for public health emergencies.

2. Reserve and supply system of emergency medical supplies in China

In the early stage of the epidemic, the number of

confirmed COVID-19 cases in China increased rapidly from 571 on January 23 to 74,185 on February 19 (Figure 1A) (*6*), leading to an explosive increase in demand for medical supplies and a serious shortage of medical supplies. In 1997, China proposed to strengthen the management of the medical reserve (*7*), required establishment of a central and local two-level medical reserve system and implementation of a system of dynamic reserve and paid redeployment program. It was clarified that the central medical reserve was mainly responsible for storing special medicines and medical devices needed for major disasters, epidemics, major emergencies, and strategic reserves. The local medical reserve was mainly responsible for storing medicines and medical devices needed for prevention and treatment of regional or general disasters, epidemics, emergencies, and local common diseases and frequently-occurring diseases. When it is necessary to make urgent use of the national reserved medicines and medical devices, the local reserve shall be responsible for the supply and the central reserve shall supplement the supply in principle. According to the level and involved region of disasters, epidemics, and emergencies, the order of the medicine reserve use is stipulated. In 1998, the Ministry of Finance of the People's Republic of China issued *financial management measures for the national medical reserve fund* to ensure its effective use (*8*). When there are no emergencies such as catastrophic disasters or epidemics, more than 70% of the medical reserve funds allocated by the state should be stored in physical form in the reserve enterprises. The storage sites are located in the northeast, north, northwest, and middle regions of China, and the modern logistics system ensures timely allocation of medicines.

In 1999, China further promulgated the *National Pharmaceutical Reserve Management Measures* (*9*) and clarified that the Ministry of Industry and Information Technology was the main management department of the national medical reserve. The Ministry of Industry and Information Technology is responsible for the coordination of national medical reserve work, organizing and making the annual plan of the central medical reserve, and collaborating with relevant departments to timely adjust the kinds of medicines and medical devices

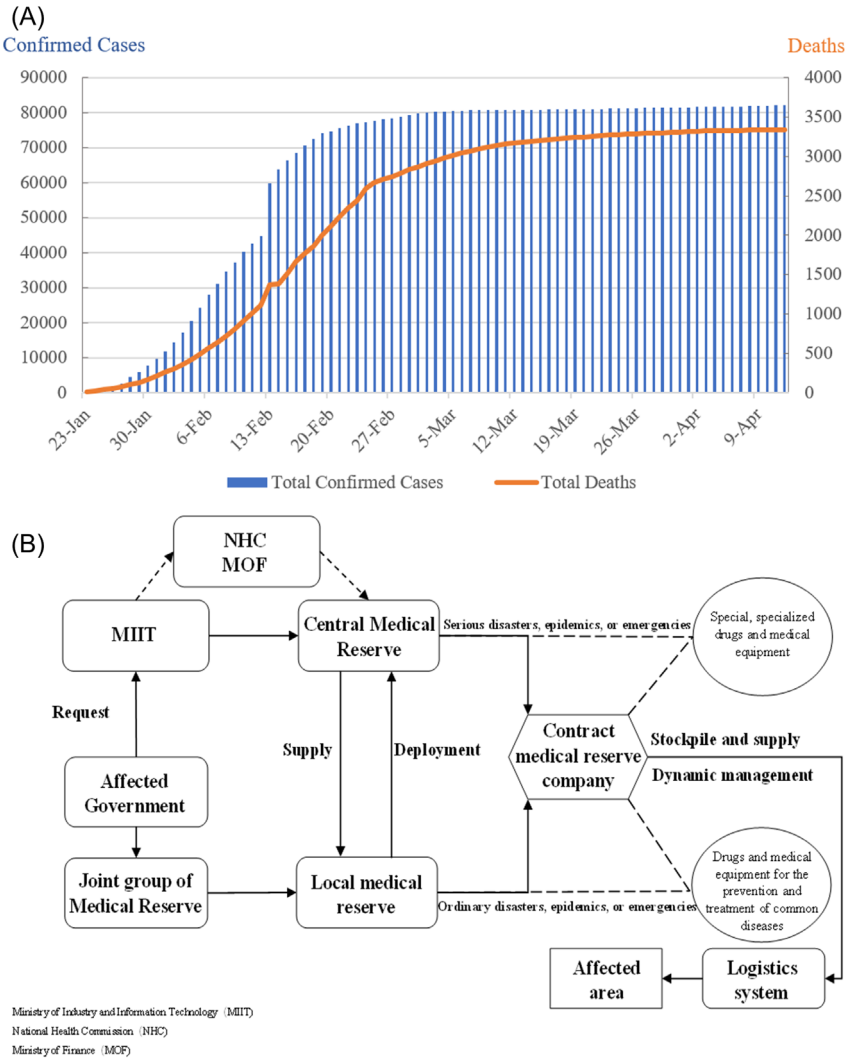

Figure 1. (A) Trends in the number of confirmed COVID-19 cases and deaths in China; (B) Reserve and supply system of emergency medical supplies in China.

in the central reserve. Enterprises that undertake medical reserves are responsible for implementing the medical reserve plan issued by the medical reserve management department and rotating reserve medicines and medical devices in a timely fashion to ensure the quality of the reserve medicines and medical devices (Figure 1B). Since the Severe Acute Respiratory Syndrome (SARS) broke out in 2003, China officially issued documents such as *Regulations on Preparedness and Responses to Emergent Public Health Hazards* (*10*) and further improved the emergency medical reserve and supply system. In 2004, under the unified deployment of the State Council, the National Development and Reform Commission organized the National Medical Reserve Emergency Plan, established the basic system and operation mechanism of emergency management of medical reserves, and strengthened the basic work of emergency management. In 2008, China formulated the *(Draft) Catalogue of health emergency personnel and equipment* (*11*), where the types and standards of emergency supplies were clearly stipulated. The reserves mainly include special and conventional reserves types. The special reserves are aimed at emergencies and epidemics such as anti-terrorism, SARS, AIDS, avian influenza, H1N1 influenza, *et al.* The special reserves include biological vaccine products, killing drugs, treatment medicines for chemical poisoning, antiviral drugs, *etc.* The conventional reserves, including medical devices and medicines such as antibiotics, analgesics, and narcotics, are required for general disasters, epidemics, and emergencies (*12,13*).

3. Reserve and supply system of emergency medical supplies in the United States

Since March, the number of confirmed COVID-19 cases in the United States has shown explosive growth. From 62 cases reported on March 1 to 492,881 cases on April 12, the United States has become the country with the most confirmed cases in the world (Figure 2A) (*14*). Under these circumstances, the shortage of emergency medical supplies such as masks, detection kits, protective equipment, and ventilators emerge continuously. In 1999, the United States Congress authorized the Department

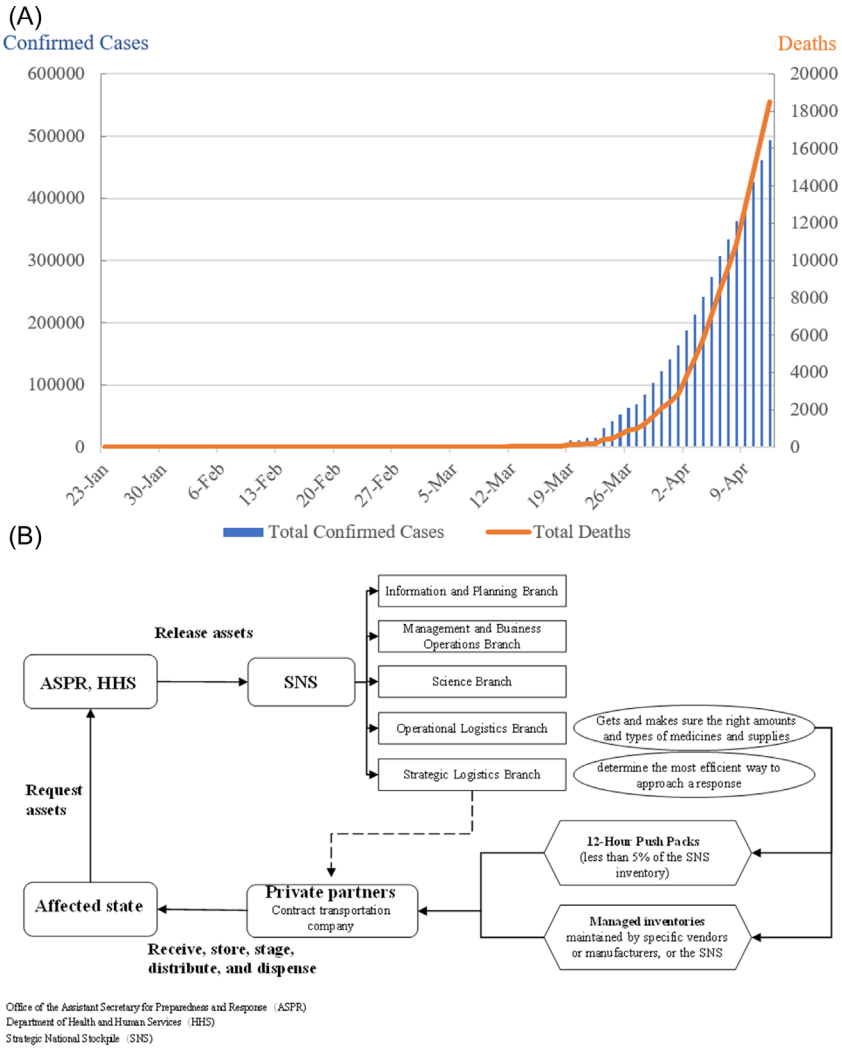

Figure 2. (A) Trends in the number of confirmed COVID-19 cases and deaths in the United States; (B) Reserve and supply system of emergency medical supplies in the United States.

of Health and Human Services (HHS) and subordinate Centers for Disease Control and Prevention (CDC) to implement the National Pharmaceutical Stockpile (NPS) plan (*15,16*), aiming to procure medicines and vaccines for storage and deal with the threat of potential biological, chemical and major infectious diseases. In 2003, NPS became the Strategic National Stockpile (SNS). Since 2018, SNS was mainly managed by the Office of the Assistant Secretary for Preparedness and Response (ASPR) under HHS. ASPR is responsible for management, maintenance, and delivery of SNS assets. All states and local governments must formulate plans for receiving, storing, deploying and distributing SNS assets. SNS plans to establish and maintain a national medical supplies repository that can be quickly deployed to emergency sites *via* the federal government purchasing and storing large amounts of medical supplies in installments and batches. SNS includes information and planning branch, management and business operation branch, operation logistics branch, science branch, and strategic logistics branch. The operation logistics branch is responsible for the procurement and storage of medicines, devices, and vaccines, and makes sure the right amounts and types of medicines and supplies are available to respond to an emergency. The strategic logistics branch is responsible for coordination of relations between public health and other federal agencies and private partners, and coordinates information sharing with states and locals, determining the most efficient way to approach a response (*17*).

The storage form of emergency medical supplies mainly includes 12-hour push packages, which are usually stored in 12 locations in the United States; the management inventory maintained by a specific vendor or SNS, which is stored and maintained by the vendor or directly managed by SNS (*18*). The use of national strategic reserve supplies requires a series of procedures. The requests to call SNS assets before emergencies require solid evidence that there may be biological, chemical, radiological, national public health emergencies, or that emergency events have occurred such as major earthquake, pandemic influenza, smallpox, biology and chemistry, and a serious shortage of medical supplies has appeared. In the above case, the state health department and the governor or designated agent of the affected place can apply directly to HHS for national strategic reserve supplies support, and HHS and other federal agencies quickly evaluate the application and make a decision on whether to allocate. After obtaining approval, the assets provided by SNS will be delivered to any affected states within the United States by the fastest land or air transportation (Figure 2B). At the same time, HHS will regularly inspect the threats and risks of international public health emergencies. On the basis of this, medicines and medical supplies, such as antivirals, ventilators, masks, and gloves, will be added to the SNS reserve (*19*).

4. Reserve and supply system of emergency medical supplies in Australia

In late March, COVID-19 spread rapidly in Australia, with more than 100 cases diagnosed daily (Figure 3A) (*14*). Since 2002, the Australian Government has officially established the National Medical Stockpile (NMS), aiming to prevent public health emergencies such as epidemic outbreaks and biochemical weapon attacks (*20*). In June 2006, the Australian Health Ministers' Advisory Council (AHMAC) established the Australian Health Protection Principal Committee (AHPPC) (*19*). AHPPC is composed of state and regional chief health officers, disaster health experts and other experts in related fields. The purpose is to provide AHMAC with advice on preparedness for public health emergencies and coordinate national emergency response for major incidents. The Health Emergency Management Branch (HEMB) of the Australian Department of Health and Ageing (DHA) Health Protection Office is responsible for the planning and management of NMS, including inventory management, and planning and developing Memoranda of Understanding with states and territories for deployment of the stockpile. The responsibility of HEMB is to provide effective risk assessments, coordinate relevant national health departments to respond to public health emergencies, which may be caused by natural causes or terrorist activities, and to the government's overall emergency management activities. Secondly, HEMB is also responsible for providing strategic advice to AHPC.

NMS is mainly composed of emergency reserves of vaccines, antidotes, highly specialized medicines and protective equipment. The NMS protects Australians from, chemical, biological and radio-nuclear (CBRN) health disasters or pandemic influenza (*21*). The purpose is to supplement medicines and protective equipment held by state and territory health authorities, ensuring that medical supplies are not in short supply due to public health emergencies. NMS is kept in various strategic locations around Australia, and according to the contract managed by DHA, the inventory is stored in facilities operated by logistics companies. They will be quickly delivered to the places where they are needed if necessary. For security reasons, the exact location and content of these inventories are kept confidentially. All jurisdictions possess a pharmaceutical stockpile separate from the NMS, and all jurisdictions have pre-placed strategic reserves of medicines and personal protective equipment to quickly respond to CBRN health disasters or pandemic influenza. The NMS inventory includes 42 products and more than 110 million items. The products are mainly related to pandemic influenza prevention (*20*).

The Australian states and territories have constitutional responsibilities within their responsibility. They are responsible for coordinating and planning for disaster and emergency response, as well as for the

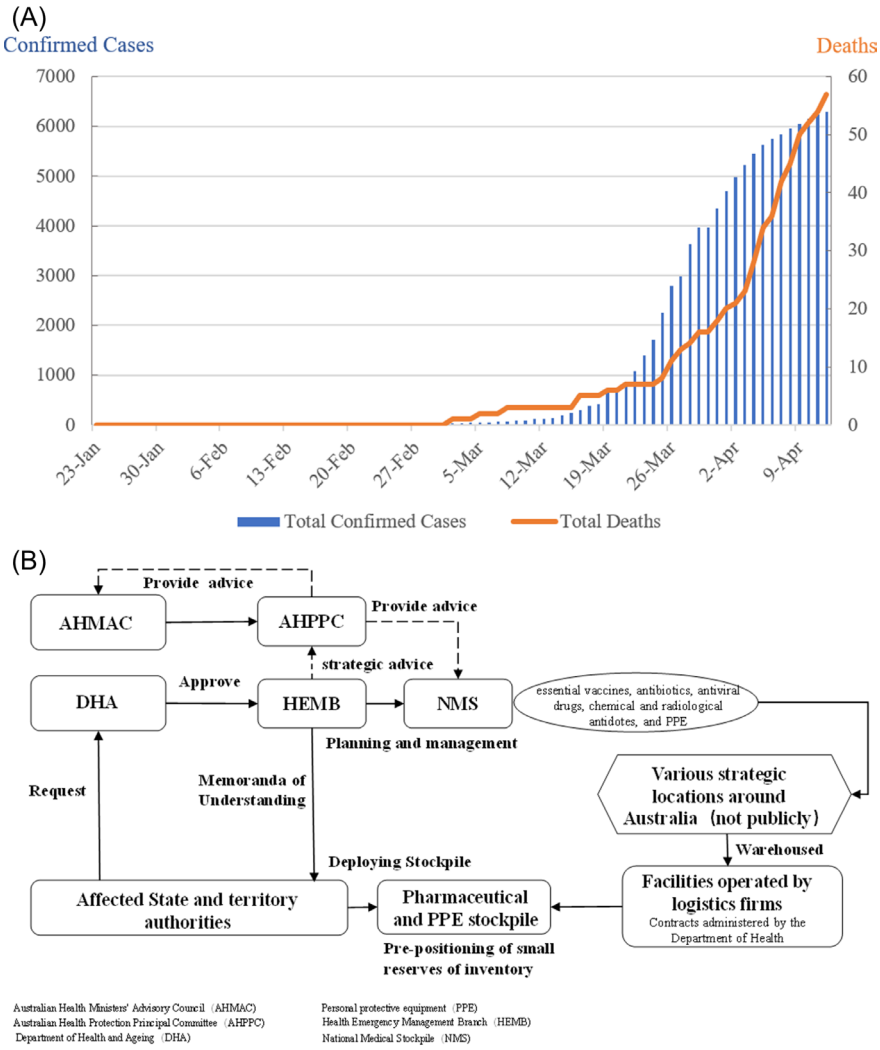

Figure 3. (A) Trends in the number of confirmed COVID-19 cases and deaths in Australia; (B) Reserve and supply system of emergency medical supplies in Australia.

deployment of inventory items in their jurisdictions during national health emergencies. When the total supplies of the affected state or territory cannot reasonably meet the needs of the situation, the state or territory government can seek the assistance of the Government of Australia. The Minister of Health and the Australian Chief Medical Officer have authority for approval to deploy inventory according to the request of state or territory authority. The AHPPC conducts key decision-making consultations on inventory management in consideration of broader health emergency response arrangements (Figure 3B) (*19*).

After the SARS epidemic, the DHA signed a long-term contract with vaccine manufacturers in 2004. The purpose is to rapidly develop and supply pandemic vaccines, antiviral agents and Personal Protective Equipment, in response to the next possible pandemic. In 2009, NMS further purchased 21 million doses of H1N1 vaccine in response to the threat of H1N1 influenza, expecting to cover 50% of the population (*19*).

5. Reserve and supply system of emergency medical supplies in Canada

The number of confirmed COVID-19 cases in Canada increased rapidly from 1,739 reported on March 25 to 22,544 on April 12 (Figure 4A) (*14*). Critical medical supplies are in short supply. In 1952, the Canadian Cabinet authorized the National Health and Welfare Department to reserve basic hygiene products (*22,23*). Subsequently, the national medical supplies reserve continued to develop, gradually forming National Emergency Strategic Stockpile (NESS), enabling the federal government to respond to changing public health risks in society such as new diseases, natural disasters, and CBRN disasters. In 2004, after the outbreak of SARS, Canada established the Public Health Agency of Canada (PHAC) to manage public health emergencies and improve cooperation within and between jurisdictions (*24*). The assets of NESS have also been transferred to the newly established Public Health Agency for management and maintenance. The NESS plan is one of the plans of the Office of Emergency Response Services (OERS), Centre for Emergency

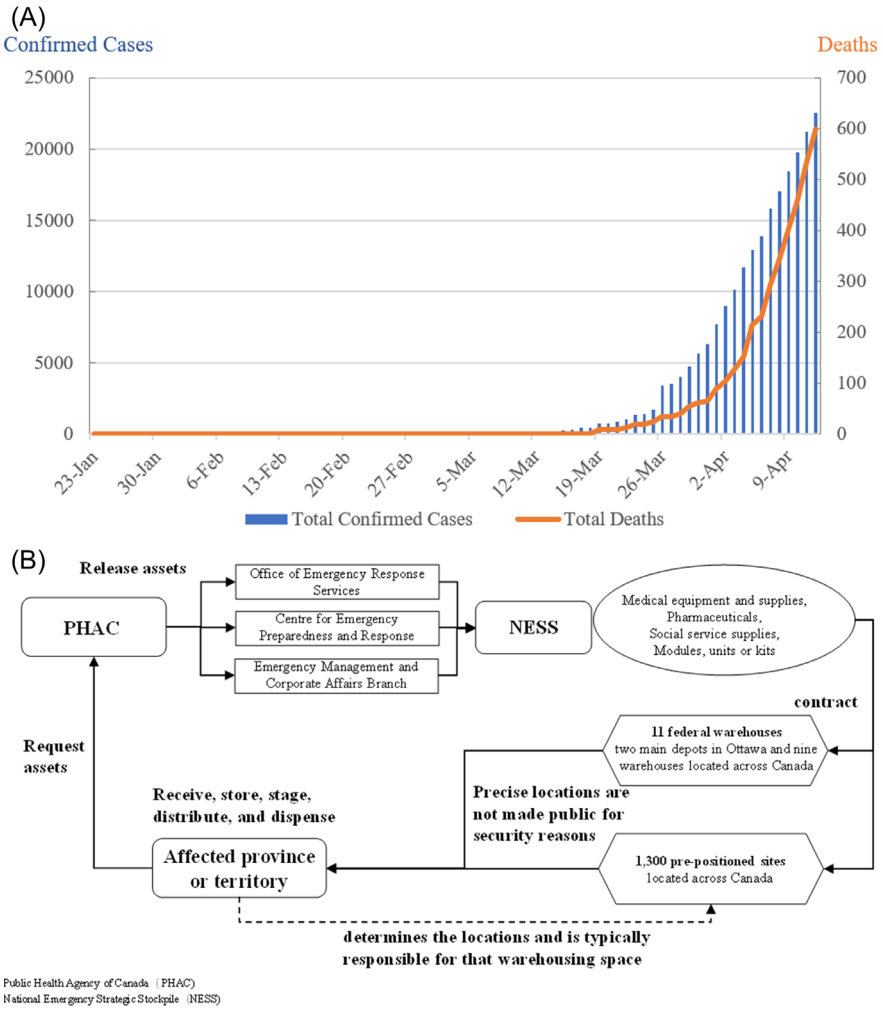

Figure 4. (A) Trends in the number of confirmed COVID-19 cases and deaths in Canada; (B) Reserve and supply system of emergency medical supplies in Canada.

Preparedness and Response, Emergency Management and Corporate Affairs Branch of the PHAC.

The NESS is mainly stored in 11 strategic warehouses leased by PHAC and 1,300 pre-location sites (*25,26*), including two main warehouses in the National Capital Region (Ottawa) and nine warehouses located across Canada. The specific location of pre-location sites is in the charge of each province or territory. The program indicated that 66% of supplies deployed are released from the Ottawa depots, 12% from the other federal warehouses located in the provinces, and 22% from pre-positioned sites. For safety reasons, the precise location of any warehouse or pre-positioning point will not be disclosed. NESS mainly contains medical equipment and supplies such as ventilators, personal protective equipment, medicines such as antibiotics and antivirals, social service supplies such as beds and generators, and various modules or kits, such as mini-clinics and reception center kits. If the local emergency situation overwhelms the available municipal resources, the municipality will contact the provincial or regional emergency management department to obtain more resources. When provinces and territories are unable to provide required resources, they can request for assistance to the PHAC. Emergency supplies can be quickly deployed to any place in the country within 24 hours after a province or region sends a request. The deployment of emergency supplies is coordinated by the provincial or regional health or social services department (Figure 4B). Meanwhile, the assets of NESS have been increasing in response to the pandemic of infectious diseases since the outbreak of SARS. After the H1N1 outbreak in 2009, the scope of supply reserves has been further expanded, including antiviral drugs, ventilators, and related oxygen supply equipment, personal protection equipment, *etc.* (*27*).

6. International comparison of issues and challenges in the reserve and supply system of emergency medical supplies

Although China, the United States, Australia and Canada have established corresponding reserve and supply systems of emergency medical supplies, the problem of emergency medical reserve and supply is more acute in China and the United States, where the cumulative

number of confirmed cases is significantly higher than in Australia and Canada.

6.1. Catalogue

In 2008, China formulated a reference catalogue of equipment for health emergency teams. However, the national medical reserve catalogue and standards have not been adjusted and updated for many years, which can no longer meet the needs of today's society (*12*). Some of the medicines and devices, which are necessary for COVID-19 treatment are not in the national medical reserve catalog (*28,29*). Some commodities cannot be rotated by the enterprises due to outdated varieties. Although the United States, Australia, Canada, and other countries have updated the reserve scope of emergency medical supplies according to major international public health emergencies such as SARS and H1N1, the shortage of medical protection supplies is still a prominent issue in various countries during the fight against the COVID-19 epidemic (*30,31*). For instance, there are close to 12,700 ventilators in the reserve of the United States, but with the growing severity of the COVID-19 epidemic, the reserves are far from enough to respond to such a serious public health emergency. The state medical institutions are facing a shortage of ventilators (*32-34*).

6.2. Procurement

China issued the reserve catalogue through the medical reserve management department, and the reserve task of the medicines and medical devices was undertaken by the enterprises in accordance with the catalogue. However, the outbreak of COVID-19 quickly spread across the country, and the first-level response was launched at the same time all over the country. Due to the direct requisition of production enterprises by the provinces and municipalities, the lack of information sharing about supplies procurement and provision, coupled with the lack of raw materials, the shortage of employees, and corporate vacations during the Spring Festival, the shortage of emergency medical supplies was exacerbated in some provinces, cities, and regions. In response to this situation, China promptly established a medical supplies support group under the State Council's joint prevention and control of the COVID-19 epidemic. With the Ministry of Industry and Information Technology as the unified coordinating department, the major medical supply production enterprises were mobilized to accelerate the resumption of production, and international procurements were expanded actively through various methods. The shortage of medical emergency supplies has been alleviated to a certain extent (*35*). The United States mainly purchases medicines and devices that are in urgent need through SNS. However, the national strategic reserve is difficult to deal with during such a serious national epidemic in response to this COVID-19 outbreak. State governments such as Washington DC have stated that the medical supplies received from the federal government are not enough to deal with the epidemic. At the same time, because the federal government has not issued a national emergency supply procurement measure for the COVID-19 epidemic, each state can only procure supplies from various channels on their own (*36,37*).

6.3. Reserve

China requires governments above the county level to "*reserve medicines, medical devices and other supplies for the prevention and treatment of infectious diseases*" (*38*). However, at the beginning of the COVID-19 outbreak, it was revealed that the emergency medical supplies reserves in China were insufficient. The reason may be that the emergency medical supplies reserves in China are mainly in the form of physical and capital reserves. The reserve form is relatively simple and the production capacity reserve, information reserve, technical reserve, and other forms are lacking. It is difficult to meet the needs of complex, diverse and unpredictable public health emergencies (*29*). The main supplies in Australia and Canada are stored in strategic warehouses across the country. Meanwhile, emergency medical supplies are pre-stored in states and regions in the form of pre-positioning sites to quickly respond to CBRN disasters or pandemic infectious diseases. However, during the COVID-19 epidemic prevention and control process, the problem that the emergency medical supply rotation and update system has not been effectively implemented was exposed. For example, Ontario, Canada, as a key area for epidemic prevention and control, the strategic reserve of N95 masks is nearly 55 million. However, more than 80% of the inventory has expired (*39*).

6.4. Delivery and distribution

China, as the country with the earliest outbreak of COVID-19, in the early stage of response to the epidemic, some key logistics express delivery companies received multi-channel emergency logistics transportation needs from relevant government departments, the military, and local governments. Decentralized demand makes the enterprises feel overwhelmed, coupled with high requirements and insufficient transport capacity during Spring Festival, the enterprises have difficulty in effectively deploying resources and optimizing security. After a large amount of medical supplies from the national emergency allocation, procurement and social donations arrived in Wuhan, they could not be hierarchically classified, managed, and scientifically used. The medical supplies stayed in warehouses for too long and could not be distributed to the urgently

needed hospitals. Other areas with lighter epidemics have improper use of emergency medical supplies to a certain extent, such as high allocation and waste. The United States has also exposed the problem of uneven distribution of emergency supplies. Currently, some states only receive 10% of the applied supplies; some states have received more supplies than the number on their applications; and some cities have failed to get any assistance from the state government (*40*). In addition, inter-regional road conditions and unreasonable seizure issues have also hindered the timely transportation and distribution of emergency medical supplies to a certain extent.

7. Suggestions for improving the reserve and supply system of emergency medical supplies

7.1. Formulate a scientific dynamic list of emergency supply reserve requirements

Each emergency has specific needs for emergency medical supplies. By continuous reference, accumulation, and learning, the regularity and characteristics of the actual occurrence of public health emergencies can be grasped. The emergency medical reserve supply lists and standards can be studied and formulated. The scope, type and quantity of emergency medical supplies reserves suitable for each country or region can be determined. The reserve catalogue and standards can be updated according to the practical situation.

7.2. Improve the storage form of emergency medical supplies

Owing to the uncertainty of the scope and extent of public health emergencies, supplies can be reserved through physical, capital, production capacity, technology, information, socialized reserves, and other forms according to the storage and use characteristics of emergency supplies. Meanwhile, an emergency medical supplies dynamic rotation updates, supervision and assessment system is suggested to be established, aiming to ensure the quality of emergency medical supplies. It is recommended to build a national (regional) emergency supplies reserve warehouse in areas with convenient transportation and wide radiation range. By the introduction of modern logistics management, the rapid transportation of emergency medical supplies can be achieved.

7.3. Establish a unified dispatch system for emergency medical supplies

It is recommended to establish a coordinated management organization for emergency medical supplies logistics support, aiming to coordinate and solve urgent problems encountered in prevention and control promptly. At the same time, clear operation guidelines and plans should be formulated to ensure the unified operation of emergency supply production, storage, transfer, reception, distribution, transportation, *et al.* When necessary, logistics enterprises, military technical equipment, personnel and vehicles can be utilized to achieve classified and targeted distribution.

7.4. Strengthen international cooperation in the supply guarantee of emergency medical supplies

The epidemic situation of major infectious diseases often spreads around the world, and the duration is long and the harm is great. It is suggested that the international community establish a higher-level global coordination and cooperation mechanism for public health, led by international organizations to establish a global system for the procurement and supply of emergency medical supplies. At the same time, specialized departments can be established to coordinate the production, procurement, delivery, and distribution of medical supplies in response to major public health emergencies worldwide.

Acknowledgements

This paper was supported by grants from the China Medical Board Collaborating Project "Establishing Health Policy Transformation Network of China (Project number: CMB-CP 14-190)" (to He Jiangjiang and Wang Xu).

References

1. World Health Organization. Coronavirus disease 2019 (COVID-19) Situation report - 80. *https://www.who.int/docs/default-source/coronaviruse/situation-reports/20200409-sitrep-80-covid-19.pdf?sfvrsn=1b685d64_2* (accessed April 10, 2020).
2. World Health Organization. Coronavirus disease (COVID-19) technical guidance: COVID-19 Critical Items. *https://www.who.int/emergencies/diseases/novel-coronavirus-2019/technical-guidance/covid-19-critical-items* (accessed March 30, 2020).
3. World Health Organization. Shortage of personal protective equipment endangering health workers worldwide. *https://www.who.int/news-room/detail/03-03-2020-shortage-of-personal-protective-equipment-endangering-health-workers-worldwide* (accessed March 24, 2020).
4. Xinhuanews. Coronavirus: death toll among doctors in Italy up to 24. *http://www.xinhuanet.com/english/europe/2020-03/24/c_138911288.htm* (accessed March 24, 2020). (in Chinese)
5. World Health Organization. WHO Director-General's opening remarks at the media briefing on COVID-19 - 23 March 2020. *https://www.who.int/dg/speeches/detail/who-director-general-s-opening-remarks-at-the-media-briefing-on-covid-19---23-march-2020* (accessed March 24, 2020).

6. National Health Commission of the People's Republic of China. Outbreak Notification. *http://www.nhc.gov.cn/xcs/yqtb/list_gzbd.shtml* (accessed April 10, 2020). (in Chinese)
7. Law Yearbook of China. Notice of the State Council on Reforming and Strengthening the Management of Pharmaceutical Stockpile. *http://www.pkulaw.cn/fulltext_form.aspx?Db=qikan&gid=1510046077* (accessed March 24, 2020). (in Chinese)
8. The State Economic and Trade Commission. Financial Management Measures for National Medicine Reserve Fund. *http://www.ccdi.gov.cn/fgk/law_display/4016* (accessed March 24, 2020). (in Chinese)
9. The State Economic and Trade Commission. Provisions for National Pharmaceutical Stockpile. *http://www.ccdi.gov.cn/fgk/law_display/3502* (accessed March 24, 2020). (in Chinese)
10. The Central People's Government of the People's Republic of China. National Contingency Plan for Public Health Emergencies. *http://www.gov.cn/yjgl/2006-02/26/content_211654.htm* (accessed February 4, 2020). (in Chinese)
11. National Health Commission of the People's Republic of China. (Draft) Catalogue of health emergency personnel and equipment. *https://wenku.baidu.com/view/b8261d33f111f18583d05aa6.html* (accessed March 24, 2020). (in Chinese)
12. Cui Y. Perfection of the Research on the State Pharmaceutical Reserve System. Review of Economic Research, 2014; 61: 36-41. (in Chinese)
13. Yu WX, Shi LW, Wang YT. On the Problems of Current Medical Reserve System and Some Policy Proposal for System Reformation in China. China Pharmacy. 2011; 22:780-782. (in Chinese)
14. World Health Organization. Coronavirus disease (COVID-2019) situation reports. *https://www.who.int/emergencies/diseases/novel-coronavirus-2019/situation-reports/* (accessed April 10, 2020).
15. U.S. Department of Health & Human Services. Strategic National Stockpile (SNS). *https://chemm.nlm.nih.gov/sns.htm* (accessed March 24, 2020).
16. Esbitt D. The Strategic National Stockpile: roles and responsibilities of health care professionals for receiving the stockpile assets. Disaster Manag Response. 2003; 1:68-70.
17. U.S. Department of Health & Human Services. About the Strategic National Stockpile. *https://www.phe.gov/about/sns/Pages/about.aspx* (accessed March 24, 2020).
18. U.S. Department of Health & Human Services. Stockpile Products. *https://www.phe.gov/about/sns/Pages/products.aspx* (accessed March 24, 2020).
19. Government of Canada. Appendix G: Evaluation of the National Emergency Stockpile System (NESS) – International studies. *https://www.canada.ca/en/public-health/corporate/mandate/about-agency/office-evaluation/evaluation-reports/evaluation-national-emergency-stockpile-system/appendix-g.html* (accessed March 24, 2020).
20. Australian National Audit Office (ANAO). Management of the National Medical Stockpile. *https://www.anao.gov.au/sites/default/files/AuditReport_2013-2014_53.pdf* (accessed March 24, 2020).
21. Australian National Audit Office (ANAO). Australia's Preparedness for a Human Influenza Pandemic. *https://www.anao.gov.au/sites/default/files/ANAO_Report_2007-2008_06.pdf* (accessed March 24, 2020).
22. Government of Canada. National Emergency Strategic Stockpile. *https://www.canada.ca/en/public-health/services/emergency-preparedness-response/national-emergency-strategic-stockpile.html* (accessed March 24, 2020).
23. Hacon WS. The employment of emergency medical units of the National Medical Stockpile. Can Med Assoc J.1967; 96:185-191.
24. Government of Canada. Canadian Pandemic Influenza Preparedness: Planning Guidance for the Health Sector. *https://www.canada.ca/en/public-health/services/flu-influenza/canadian-pandemic-influenza-preparedness-planning-guidance-health-sector.html* (accessed March 24, 2020).
25. Government of Canada. Section 2: Evaluation of the National Emergency Stockpile System (NESS) – Background. *https://www.canada.ca/en/public-health/corporate/mandate/about-agency/office-evaluation/evaluation-reports/evaluation-national-emergency-stockpile-system/background-context.html#background-1* (accessed March 24, 2020).
26. Government of Canada. Appendix A: Evaluation of the National Emergency Stockpile System (NESS) – Life-cycle management. *https://www.canada.ca/en/public-health/corporate/mandate/about-agency/office-evaluation/evaluation-reports/evaluation-national-emergency-stockpile-system/appendix-a.html* (accessed March 24, 2020).
27. Government of Canada. Appendix B: Evaluation of the National Emergency Stockpile System (NESS) – Technical annex. *https://www.canada.ca/en/public-health/corporate/mandate/about-agency/office-evaluation/evaluation-reports/evaluation-national-emergency-stockpile-system/appendix-b.html* (accessed March 24, 2020).
28. China Net. The National Medicine Reserve should be replaced. *http://finance.china.com.cn/roll/20140411/2327951.shtml* (accessed March 24, 2020). (in Chinese)
29. Yuan HSB, Huang YM, Fan MS, Shao R. The improvement of the medical reserve form in China. Chinese Journal of Pharmaceuticals. 2018; 49: 869-874. (in Chinese)
30. Kokudo N, Sugiyama H. Call for international cooperation and collaboration to effectively tackle the COVID-19 pandemic. Global Health & Medicine. 2020; 2:60-62.
31. Villa S, Lombardi A, Mangioni D, Bozzi G, Bandera A, Gori A, Raviglione MC. The COVID-19 pandemic preparedness... or lack thereof: from China to Italy. Global Health & Medicine. 2020; 2:73-77.
32. ABC NEWS. Hospitals fear shortage of ventilators for virus patients. *https://abcnews.go.com/Health/wireStory/hospitals-fear-shortage-ventilators-virus-patients-69651300* (accessed March 30, 2020).
33. China Daily Global. US hospitals press for ventilators. *http://www.chinadaily.com.cn/a/202003/25/WS5e7ae160a310128217281e32.html* (accessed March 30, 2020).
34. CNN. The COVID-19 ranking system that could decide who gets a ventilator. *https://us.cnn.com/videos/us/2020/04/03/hospital-point-system-griffin-lead-pkg-vpx.cnn/video/playlists/top-news-videos/* (accessed April 4, 2020).
35. Wang X, Zhang X, He JJ. Challenges to the system of

reserve medical supplies for public health emergencies: reflections on the outbreak of the severe acute respiratory syndrome coronavirus 2 (SARS-CoV-2) epidemic in China. BioSci Trends. 2020; 14:3-8.
36. CNN. Trump administration edits national stockpile website a day after it contradicted Jared Kushner. *https://edition.cnn.com/2020/04/03/politics/stockpile-website-edited-kushner-claim/index.html* (accessed April 4, 2020).
37. CNBC. Cuomo says coronavirus is 'more dangerous' than expected as New York cases jump 14% overnight to 75,795. *https://www.cnbc.com/2020/03/31/gov-cuomo-says-coronavirus-is-more-dangerous-than-expected-as-new-york-cases-jump-14percent-overnight-to-75795.html?&qsearchterm=Cumo%20says%20coronavirus%20is%20more* (accessed April 4, 2020).
38. The Central People's Government of the People's Republic of China. The 2004 Revised Law of the People's Republic of China on the Prevention and Treatment of Infectious Diseases. *http://www.gov.cn/gongbao/content/2004/content_62975.htm* (accessed March 25, 2020). (in Chinese)
39. Exclusive: Millions of masks stockpiled in Canada's Ontario expired before coronavirus hit. *http://www.yidianzixun.com/article/0OpB8wvI?s=yunos&appid=s3rd_yunos* (accessed March 24, 2020). (in Chinese)
40. Guanchacn. How many federal supplies can the US states take? It depends on the relationship between the governor and Trump? *https://www.guancha.cn/internation/2020_04_01_544987.shtml* (accessed April 4, 2020). (in Chinese)

Received April 15, 2020; Revised May 6, 2020; Accepted May 8, 2020

[§]These authors contributed equally to this work.
**Address correspondence to:*
Jiangjiang He, Shanghai Health Development Research Center (Shanghai Medical Information Center), No.1477 Beijing (W) Road, Jing'an District, Shanghai 200040, China.
E-mail: hejiangjiang@shdrc.org

Released online in J-STAGE as advance publication May 9, 2020.

Original Article

DOI: 10.5582/bst.2020.03146

Descriptive epidemiology of high frequency component based on heart rate variability from 10-second ECG data and daily physical activity among community adult residents: the Nagahama Study

Naomi Takahashi[1,*], Yoshimitsu Takahashi[1], Yasuharu Tabara[2], Takahisa Kawaguchi[2], Akira Kuriyama[1], Kenji Ueshima[3], Shinji Kosugi[4], Akihiro Sekine[5], Ryo Yamada[2], Fumihiko Matsuda[2], Takeo Nakayama[1], On behalf of the Nagahama Study Group

[1] Department of Health Informatics, Kyoto University School of Public Health, Kyoto, Japan;
[2] Center for Genomic Medicine, Graduate School of Medicine, Kyoto University, Kyoto, Japan;
[3] Department of EBM Research, Institute for Advancement of Clinical and Translational Science, Kyoto University Hospital, Kyoto, Japan;
[4] Department of Medical Ethics and Medical Genetics, Kyoto University School of Public Health, Kyoto, Japan;
[5] Department of Omics-based Medicine, Clinical Preventive Medical Sciences, Center for Preventive Medical Sciences, Chiba University, Chiba, Japan.

SUMMARY Characteristics of high frequency (HF) component based on heart rate variability (HRV) in a large general population remain unclear, particularly on the relationship with daily physical activity. We aimed to characterize the distribution of HF component and examine the association with daily physical activity among community residents. We performed spectral analysis of HRV from 10-second ECG recordings among 9135 residents aged 30 to 74 years in Nagahama City, Japan. HF components were log-transformed to consider the distribution. Simple correlations between HF and age were determined. Age-adjusted mean values of HF component were calculated for each questionnaire item related to daily physical activity. Multiple regression analysis was performed to examine the effect of daily physical activity on HF component value. Mean values of logarithmically-transformed HF component (lnHF) were higher in women than in men ($p < 0.001$). lnHF was inversely associated with age ($r = -0.40$, -0.49 for men, women, respectively). Adjusted mean lnHF for physically active people was significantly higher than that in inactive people ($p < 0.001$). HF components from 10-second ECG recordings were moderately and negatively correlated with age in both sexes, and positively correlated with daily physical activity in the general adult population. Maintaining the level of daily physical activity, especially to exercise regularly could keep the parasympathetic function high.

Keywords parasympathetic function, spectral analysis, short ECG recordings

1. Introduction

One way to evaluate autonomic nervous system function is to analyze heart rate variability (HRV), a parameter that can offer a pathophysiologic perspective on cardiovascular disease (CVD) including coronary artery disease, heart failure, and arrhythmias (*1,2*). In particular, spectral analysis of HRV using the Fast Fourier Transform (FFT) (*3,4*), the autoregressive model (AR model) (*4,5*), or the Maximum Entropy Method (MEM) (*4*) allows for the separate evaluation of sympathetic and parasympathetic nervous activity. These methods are all based on the fact that sympathetic and parasympathetic nerves reflect HRV of specific frequency bands (*1,2*). High-frequency (HF) component (0.15-0.4 Hz) is an index of the parasympathetic nerve function, which is subject to the respiration. Low-frequency (LF) component (0.04-0.15 Hz) is influenced by both of parasympathetic and sympathetic nerve activity, and thus the ratio of LF to HF (LF/HF) is considered as an index of the sympathetic nerve function. Some studies have examined the relationships between HRV and various diseases, and have found that decreased parasympathetic function is associated with coronary heart disease (CHD) risk and mental stress (*6,7*). However, the distribution and characteristics of the HF and LF components have not been fully elucidated in a general population. When electrocardiogram (ECG) is used for general evaluations of parameters such as autonomic nervous function, a basic ECG is run for 5 minutes (*2,8*). Some large cohort

studies had their findings based on analyzed HRV from ECG recordings shorter than 5 minutes (*7,9*). The results of HRV analysis from shorter ECG recordings comparing with longer recordings was previously validated (*10,11*).

It is well known that exercise can positively affect health, and the presence or absence of exercise habits has greatly impacted the health maintenance of the human mind and body (*12,13*). Physical activity such as exercise can have soothing effects on the autonomic nervous system (*14,15*). Some studies have found an association between certain lifestyle habits and HRV in large-scale studies of community residents, but the association between daily physical activity habits and HRV has not been fully elucidated (*16-18*).

In Japan, mass health checkups for adults are typically conducted in community settings, and where an ECG is to be recorded for only 10 seconds. We previously validated 10-second recording of ECG to estimate HF component comparing with 5-minute recording (*19*). It became possible to estimate HF component from routine short ECG recording in mass surveys, and large number of ECG data would be available for this purpose.

We hypothesized that the HF component values obtained from 10-second ECG data were reflective of exercise habits. However, the little evidence is available to suggest a relationship between HF component analyzed from short ECG recordings and physical activity. The present study aimed to estimate the HF component on the 10-second ECG and examine the association between daily physical activity and HF component in a large community population.

2. Methods

2.1. Study design and study population

A cross-sectional study was conducted using baseline data from the Nagahama Prospective Genome Cohort for Comprehensive Human Bioscience (The Nagahama Study (*20*)). This cohort comprising healthy community residents (aged 30 to 74 years) of Nagahama City (population, 125,000), Shiga Prefecture, located in the center of Japan, was recruited from 2008 to 2010. Out of the eligible resident, 10,082 people who agreed to participate after receiving the explanation of a community-based genome-epidemiologic study, the "Nagahama Zero (0)-ji Prevention Cohort Project" were selected as participants in the Nagahama Study. We had recruited participants of health checkups from about 70,000 eligible people by through public relations activities with the Nagahama city and nonprofit organization Zeroji Club, and participating in voluntary. Of the 10,082 participants, we excluded 278 people for the following reasons: participants in the pilot study (n = 273; due to the improvement of the health checkup contents for this survey based on the pilot's implementation, missing questionnaire (n = 2), missing almost blood and physiological tests (n = 3). Finally, 9,804 participants were confirmed as the Nagahama Study 1st phase cohort data. We applied our study inclusion criteria to this 1st phase cohort data. Of the 9,804 participants, we excluded certain individuals due to missing ECG data, ECG recordings shorter than 10 seconds, presence of an arrhythmia and missing necessary questionnaire item (Figure 1). Inappropriate arrhythmia types for spectral analysis were determined according to the Minnesota code (*21,22*) through discussion among co-authors (NT: registered nurse, AK & TN: general physician, KU: cardiologist). The study protocol was approved by Kyoto University Graduate School and Faculty of Medicine, Ethics Committee (E1495 and G278).

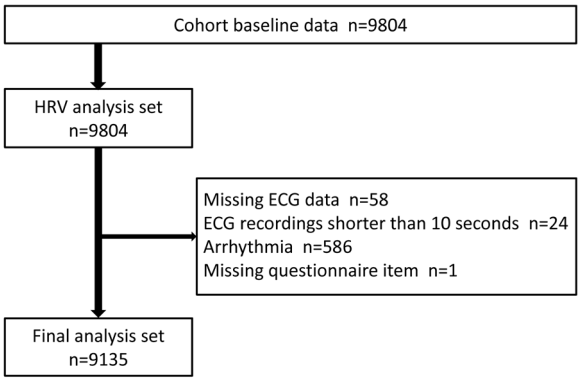

Figure 1. Flowchart of study subject selection.

2.2. Electrocardiogram and spectral analysis of HRV

Standard 12-lead electrocardiograms (FCP-7431, Fukuda Denshi, Tokyo, Japan) were recorded for 10 seconds in the supine position in the baseline survey of The Nagahama Study. ECG recordings in our study were performed between 9:00 a.m. and 4:00 p.m.

We used the MemCalc method in this study, so we used software MemCalc/Win (Suwa Trust, Tokyo, Japan) for HRV analysis. This method is a type of time-series data analysis using the Maximum Entropy Method (MEM) for spectral analysis of the frequency domain, and the nonlinear least squares model for analysis of the time domain (reproduction of the time series) to determine underlying variation in the time series (*5,23,24*). As the ECG data length required in the frequency band was calculated as 1/frequency (seconds), the minimum data lengths required for analysis of HF and LF components were 6.7 and 25 seconds, respectively. As our ECG data from the baseline study of the Nagahama Study were from 10-second ECGs, we were only able to evaluate the HF component.

2.3. Daily physical activity habits

From the baseline questionnaire, the following three

items were used for the present purpose: "Are you in the habit of exercising to the point of light sweating for over 30 minutes per session, twice weekly, for over a year?" ("Yes" or "No"); "In your daily life do you walk or do an equivalent amount of physical activity for more than one hour a day?" ("Yes" or "No"); and "How would you describe your physical activity level in your daily life?" ("Insufficiently active", "Sufficiently active", or "Highly active")

2.4. Statistical analysis

Descriptive statistics of participants' characteristics (age, height, weight, body mass index (BMI), blood pressure, and brain natriuretic peptide (BNP)), HF component, R-R interval, and heart rate from R-R interval were described. The *t*-test and Wilcoxon rank sum test to compare continuous values, and chi-square test to compare categorical values were used. Pearson's correlation analysis was conducted to examine the association between age and HF components. The normality of crude values of the HF component was examined by histograms, box plots, normal probability plots, and the Shapiro-Wilk test. Pearson's correlation coefficients were calculated between age and HF component values, systolic blood pressure (SBP), and diastolic blood pressure (DBP). For the HF component, analysis of covariance for each questionnaire item related to physical activity was carried out, and means were calculated for the HF component value after adjusting for age. In addition, in order to examine the effect of physical activity on the HF component value, three multiple regression models were created with logarithmically-transformed values of HF component as the response variable and physical activity habits, age, sex, and BMI as explanatory variables (Model A: age, sex, BMI, and exercise to the point of sweating; Model B: age, sex, BMI, and physical activity > 1 h; Model C: age, sex, BMI, and physical activity level). All statistical analyses were performed with Stata SE Ver.13.1 (College Station, TX). Statistical significance tests were two-sided and $P < 0.05$ was considered significant.

3. Results

3.1. Selection of participants for analysis

Of the 9,804 participants, we excluded 669 people for the following reasons: missing ECG data ($n = 58$), ECG recordings shorter than 10 seconds ($n = 24$), presence of an arrhythmia ($n = 586$), and missing necessary questionnaire item ($n = 1$) (Figure 1).

3.2. Participant characteristics

Table 1 shows characteristics of the 9,135 participants selected for analysis and the results of the HRV analysis. Mean participant ages were 55.4 and 52.4 years for men and women, respectively, with relatively few participants in their 40s (14%) and 70s (11%). As normality of the HF component was not evident, logarithmic transformation was applied for analysis. The mean logarithmically-transformed HF component (lnHF) value for women (5.34) was higher than that for men (5.11) ($p < 0.001$).

Table 2 shows means of lnHF values for each age group among those in their 30s to 50s, women had a higher mean HF component value than men, while among those in their 60s to 70s, the men exhibited a higher mean HF component value than women. Mean lnHF values decreased with increases in age group. The

Table 1. Participant characteristics and heart rate variability from 10-second ECG data

	Total (n = 9,135)	Men (n = 2,932)	Women (n = 6,203)	P value
Age group				< 0.001
30-39 years	2167 (24%)	611 (21%)	1556 (25%)	
40-49 years	1313 (14%)	360 (12%)	953 (15%)	
50-59 years	1811 (20%)	456 (16%)	1355 (22%)	
60-69 years	2885 (32%)	1091 (37%)	1794 (29%)	
70-79 years	959 (11%)	414 (14%)	545 (9%)	
Age (years)	53.3 ± 13.3	55.4 ± 13.5	52.4 ± 13.1	< 0.001
Height (cm)	159.9 ± 8.4	168.3 ± 6.5	155.9 ± 5.9	< 0.001
Weight (kg)	57.2 ± 10.9	66.5 ± 10.2	52.9 ± 8.1	< 0.001
BMI (kg/m^2)	22.3 ± 3.3	23.4 ± 3.1	21.7 ± 3.2	< 0.001
Blood pressure (mm Hg)				
SBP	121.8 ± 17.0	128.5 ± 15.7	118.7 ± 16.7	< 0.001
DBP	75.3 ± 11.1	79.9 ± 10.8	73.2 ± 10.6	< 0.001
BNP (pg/mL)	12.3 [7.3, 20.2]	10.1 [5.9, 18]	13.1 [8.1, 21.4]	< 0.001
Heart rate(bpm)	64 [58, 70]	62 [57, 68]	64 [59, 70]	< 0.001
R-R (ms)	946.5 ± 127.7	968.5 ± 136.7	936.1 ± 121.8	< 0.001
lnHF	5.26 ± 1.48	5.11 ± 1.47	5.34 ± 1.48	< 0.001

SBP: systolic blood pressure; DBP: diastolic blood pressure; BNP: brain natriuretic peptide; R-R: mean variation in R-R interval; lnHF: log-transformed HF component values; Mean ± SD: Age, Height, Weight, BMI, Blood pressure, R-R, lnHF. Median [first quartile, third quartile]: BNP, Heart rate. Comparisons between men and women: *P*-value for age group, chi-square test; *P*-value for mean, *t*-test; *P*-value for median, Wilcoxon rank sum test.

Table 2. Mean ± SD of lnHF from 10-second ECG data

Age (years)	Total (n = 9,135)	Men (n = 2,932)	Women (n = 6,203)	P value
30-39	6.30 ± 1.19	6.11 ± 1.23	6.38 ± 1.16	< 0.001
40-49	5.75 ± 1.26	5.53 ± 1.35	5.83 ± 1.21	< 0.001
50-59	5.02 ± 1.26	4.94 ± 1.31	5.05 ± 1.25	0.097
60-69	4.68 ± 1.38	4.71 ± 1.39	4.66 ± 1.38	0.377
70-79	4.46 ± 1.46	4.49 ± 1.44	4.45 ± 1.47	0.688
Total	5.26 ± 1.48	5.11 ± 1.47	5.34 ± 1.48	< 0.001

SD: Standard deviation; lnHF: log-transformed HF component values; Comparisons between men and women: P value for mean, t-test.

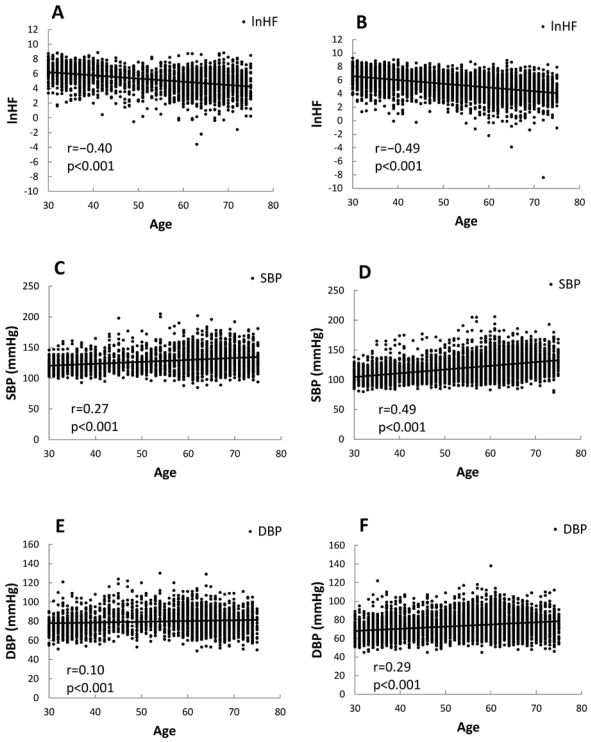

Figure 2. Scatter plots for log-transformed values of HF and age, systolic blood pressure, and diastolic blood pressure. (A): lnHF *vs.* age (Men), **(B)**: lnHF *vs.* age (Women), **(C)**: SBP *vs.* age (Men), **(D)**: SBP *vs.* age (Women), **(E)**: DBP *vs.* age (Men), **(F)**: DBP *vs.* age (Women). lnHF: log-transformed HF component values; SBP: systolic blood pressure; DBP: diastolic blood pressure.

results of trend test for the lnHF value of age groups showed a tendency for the lnHF value to decrease monotonically with increases in age group. This trend was observed in men, women, and in both sexes combined (each P value for trend < 0.001).

3.3. Correlation between lnHF and age

Figure 2 shows scatter plots and the Pearson correlation coefficient between age and lnHF(r = −0.46). For comparison, we also show scatter plots and the Pearson correlation coefficients of age with SBP (0.42) and with DBP (0.22). In addition, the partial correlation coefficient excluding the effect of age for lnHF and SBP was r = −0.29 (P < 0.001), indicating a weak negative correlation.

3.4. Adjusted mean lnHF for each physical activity habit

Figure 3 shows adjusted means of lnHF for each questionnaire item related to physical activity habits (adjusted for age) and the 95% confidence intervals. The adjusted mean lnHF for the group with a greater degree of physical activity was higher than that for the lesser degree of physical activity.

3.5. Impact of physical activity habits on HF component

Table 3 shows multiple regression analysis results. We checked the variance inflation factor (VIF) for each of our models and found no multicollinearity problem (VIF < 3 in all cases). Regression coefficients of physical activity habits were 0.133 [95% confidence interval (95%CI): 0.065-0.201] in Model A and 0.063 [0.008-0.118] in Model B. Coefficients for physical activity level in Model C were 0.079 [−0.017-0.176] (Sufficiently active) and 0.170 [0.062-0.278] (Highly active).

4. Discussion

Using 10-second ECG recordings for 9,135 general residents in a Japanese community, we found a moderate negative correlation between HF component values and age, in both sexes. The mean HF component value was higher in women than in men. HF component values increased with daily physical activity. This is one of the largest population studies that described the distributions of HF component values by age and sex, and found the positive relationship with daily physical activities.

We estimated and characterized the HF component values from 10-second ECG recordings for 9,135 adult residents in a Japanese community. Consistent with previous studies (*8,25,26*), we confirmed lower HF component values with increased age. In addition, we clarified that women had relatively higher HF component values than men. Among those in their 30s to 50s, women had a higher HF component value than men, while those over 60 years of age showed only a small sex-dependent difference in HF component value. Thus, it is possible that age-related deterioration in parasympathetic function is more marked in women than in men. It is generally known that SBP is correlated with age (*27*). As shown in Figure 2, the strength of the

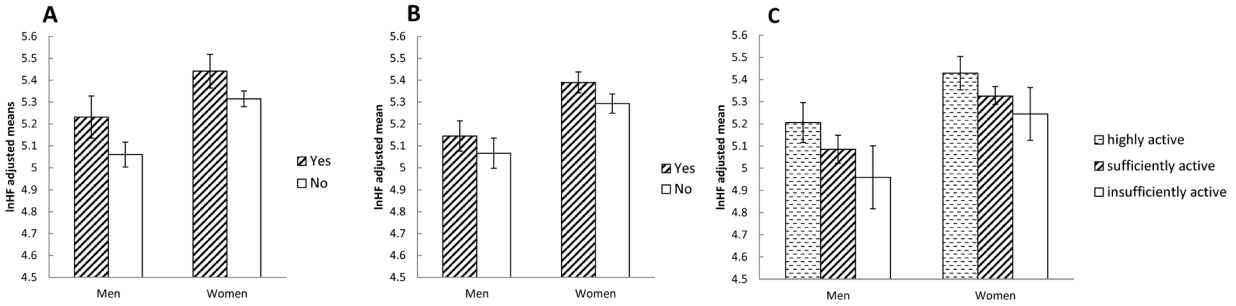

Figure 3. Adjusted mean lnHF corresponding to each question related to physical activity (adjusted for age). (A): Are you in the habit of exercising to the point of light sweating for over 30 minutes per session, twice weekly, for over a year? 0: No, 1: Yes. **(B)**: In your daily life do you walk or do an equivalent amount of physical activity for more than one hour a day? 0: No, 1: Yes. **(C)**: How would you describe your physical activity level in your daily life? 1: Insufficiently active, 2: Sufficiently active, 3: Highly active. Error bar: 95% confidence interval. $P < 0.001$ for all adjusted means.

Table 3. Regression model for lnHF for each question related to physical activity

Model	Explanatory variable	Coef.	95%CI		*P* value	Adj R^2
Model A	Age	−0.051	−0.055	−0.049	< 0.001	0.225
	Men		Reference			
	Women	0.031	−0.028	0.090	0.299	
	BMI	−0.035	−0.044	−0.027	< 0.001	
	Exercise to the point of sweating: Yes	0.133	0.065	0.201	< 0.001	
Model B	Age	−0.051	−0.053	−0.049	< 0.001	0.224
	Men		Reference			
	Women	0.025	−0.034	0.084	0.410	
	BMI	−0.035	−0.043	−0.026	< 0.001	
	Physical activity > 1 h: Yes	0.063	0.008	0.118	0.024	
Model C	Age	−0.050	−0.052	−0.048	< 0.001	0.225
	Men		Reference			
	Women	0.030	−0.029	0.090	0.321	
	BMI	−0.034	−0.043	−0.026	< 0.001	
	Physical activity level					
	Insufficiently active		Reference			
	Sufficiently active	0.079	−0.017	0.176	0.108	
	Highly active	0.170	0.062	0.278	0.002	

Coef.: regression coefficient, 95%CI: 95% confidence interval, Adj R^2: adjusted R squired. Exercise to the point of sweating: Are you in the habit of exercising to the point of light sweating for over 30 minutes per session, twice weekly, for over a year? 0: No, 1: Yes. Physical activity > 1 h: In your daily life do you walk or do an equivalent amount of physical activity for more than one hour a day? 0: No, 1: Yes. Physical activity level: How would you describe your physical activity level in your daily life? 1: Insufficiently active, 2: Sufficiently active, 3: Highly active.

negative correlation between age and HF component is quite comparable to the strength of the positive correlation between SBP and age. While autonomic nerve function has not been examined sufficiently in population settings, it may be one of the more important and easily assessed markers of aging. Kuo TB *et al.* pointed out that gender differences in parasympathetic function begin to decrease around age 50 (*28*).

The mean HF component values were greater in those who exercised regularly, relative to those who only performed regular light physical activity, even after adjusting for age. Similar findings pertaining to HF component were reported in a meta-analysis by Sandercock *et al.* (*29*). The HF component is an index of parasympathetic function. As the present study conducted spectral analyses of ECG data from 10-second measurements (which did not include the LF component), we were unable to determine whether parasympathetic dominance or sympathetic dominance was evident. However, as Aeschbacher *et al.* demonstrated, adopting a healthy lifestyle has an important effect on autonomic function (*16*), and we would surmise that maintaining good parasympathetic activity may be possible by performing regular physical activity. There are few studies that analyzed directly the relationship between daily physical activity habits and HRV in a large sample size. Several studies treated physical activity habits as theme in HRV analyses studies (*30-34*). Concerning the study on HRV and physical activity, community-based studies using subjective physical activity data were at most about 5,000 subjects (*30,31*). Studies using objective physical activity data were at most about 200 subjects (*32-34*). The present findings were based on one of the largest population studies that examined the relationships between HF component values and age, sex, and daily physical activities.

Further empirical evidence is required in order to establish the utility of estimating autonomic nerve function from short ECG recordings to predict health outcomes. When HRV is measured in order to evaluate autonomic nervous function (*2,8*), ECGs are conducted under strict experimental settings, and participants are prohibited from taking alcohol or caffeine for 24 hours prior to ECG measurement. Participants are also required to rest in the supine position for at least 15 minutes. Unfortunately, these processes make the measurement somewhat troublesome for screening examinees. At health checkups and clinical practice in Japan, the routine ECG recording time is approximately 10 seconds. In Japan, ECG is routinely used in daily clinical settings and for health checkups, and has been used in the National Survey on Circulatory Disorders to assess the health status among Japanese people (*35*). If remarkable parasympathetic dysfunction is found at this point, it may be possible to address early on any dysfunction in the autonomic nervous system. If the evaluation using 10-second ECG data proves to have the same or nearly similar accuracy as that for the conventional evaluation, this could be highly beneficial in outpatient therapy for cases such as patients with diabetic autonomic neuropathy or menopausal disorders in women. de Bruyne *et al.* found that an HRV analysis from 10-second ECG data was able to explain cardiac mortality among 5,272 elderly individuals (*9*). While there are many advantages of ECG in clinical practice, few studies have assessed the possibilities of using shorter duration ECG data to evaluate autonomic function. Further studies are needed to improve and disseminate knowledge on the potential clinical uses of HRV evaluation, particularly in terms of recording time and preconditioning.

The present study has some limitations. First, we were unable to consider the balance between the HF component and LF component when making conclusions on the relationship between physical activity habits and HF component. Second, it is known that HF component amplitude is reduced by increases in respiratory rate or decreased tidal volume, but we were only able to determine visually the presence or absence of breathing from the R-R interval fluctuation plot. Researchers' subjectivity must also be taken into account, so the presence/absence of breathing was not considered. However, respiratory influence might have occurred randomly among each age group, sex, and category of physical activity, thus there are little possibility of serious bias to the present findings. Moreover, we carefully investigated whether sleep or anxiety might be a confounding factor in examining the relationship between HF components and physical activity, but no remarkable relationship was found. Therefore, we focused simply on the relationship between HF components and physical activity. However, the present data concerning sleep and anxiety were collected only by self-administered questionnaire, thus, further studies are desirable with objective data on this issue.

In conclusion, we, using 10-second ECG data of community adult residents, found a moderate negative correlation between HF component values and age, in both sexes, although the mean HF component value was higher in women than in men. Increases in mean HF component values were also noted with increases in the level of daily physical activity. Maintaining the level of daily physical activity, especially to exercise regularly could keep the parasympathetic function high.

Acknowledgements

The authors would like to thank all participants, the Nagahama City Office, and the nonprofit organization Zeroji Club for their help in performing the Nagahama Study.

***Funding*:** This study was supported by a research grant from the Takeda Science Foundation and university grants.

References

1. Akselrod S, Gordon D, Ubel FA, Shannon DC, Berger AC, Cohen RJ. Power spectrum analysis of heart rate fluctuation: a quantitative probe of beat-to-beat cardiovascular control. Science. 1981; 213:220-222.
2. Task Force of the European Society of Cardiology and the North American Society of Pacing and Electrophysiology. Heart rate variability: standards of measurement, physiological interpretation and clinical use. Circulation. 1996; 93:1043-1065.
3. Cooley JW, Tukey JW. An algorithm for the machine calculation of complex fourier series. Math Comput. 1965; 19:297-301.
4. Ohtomo, N, Tanaka Y. New method of time series analysis and "MemCalc". In: A Recent Advance in Time-Series Analysis by Maximum Entropy Method (Saito K, eds.). Hokkaido University Press, Sapporo, Japan, 1994; pp. 11-29.
5. Akaike H. Power spectrum estimation through autoregressive model fitting. Ann Inst Stat Math. 1969; 21:407-419.
6. Friederich HC, Schild S, Schellberg D, Quenter A, Bode C, Herzog W, Zipfel S. Cardiac parasympathetic regulation in obese women with binge eating disorder. Int J Obes (Lond). 2006; 30:534-542.
7. Liao D, Cai J, Rosamond WD, Barnes RW, Hutchinson RG, Whitsel EA, Rautaharju P, Heiss G. Cardiac autonomic function and incident coronary heart disease: a population-based case-cohort study. The ARIC Study. Atherosclerosis Risk in Communities Study. Am J Epidemiol. 1997; 145:696-706.
8. Hayano J. Shinpakuhendou ni yoru Jiritushinkeikinou Kaiseki (The autonomic function analysis by heart rate variability.). In: Junkankishikkan to Jiritushinkeikinou (Cardiovascular disease and Autonomic function.) (Inoue H, eds.), 2nd Edition. IGAKU-SHOIN Inc., Tokyo, Japan, 2001; pp. 75-77. (in Japanese)
9. de Bruyne MC, Kors JA, Hoes AW, Klootwijk P, Dekker

JM, Hofman A, van Bemmel JH, Grobbee DE. Both decreased and increased heart rate variability on the standard 10-second electrocardiogram predict cardiac mortality in the elderly: the Rotterdam Study. Am J Epidemiol. 1999; 150:1282-1288.
10. Schroeder EB, Whitsel EA, Evans GW, Prineas RJ, Chambless LE, Heiss G. Repeatability of heart rate variability measures. J Electrocardiol. 2004; 37:163-172.
11. Nussinovitch U, Elishkevitz KP, Katz K, Nussinovitch M, Segev S, Volovitz B, Nussinovitch N. Reliability of Ultra-Short ECG Indices for Heart Rate Variability. Ann Noninvasive Electrocardiol. 2011; 16:117-122.
12. Blair SN, Kohl HW, Gordon NF, Paffenbarger RS, Jr. How much physical activity is good for health? Annu Rev Public Health. 1992; 13:99-126.
13. Paffenbarger RS, Jr., Hyde RT, Wing AL, Steinmetz CH. A natural history of athleticism and cardiovascular health. JAMA. 1984; 252:491-495.
14. Albinet CT, Boucard G, Bouquet CA, Audiffren M. Increased heart rate variability and executive performance after aerobic training in the elderly. Eur J Appl Physiol. 2010; 109:617-624.
15. Rezende Barbosa MP, Netto Junior J, Cassemiro BM, de Souza NM, Bernardo AF, da Silva AK, Pastre CM, Vanderlei LC. Impact of functional training on cardiac autonomic modulation, cardiopulmonary parameters and quality of life in healthy women. Clin Physiol Funct Imaging. 2016; 36:318-325.
16. Aeschbacher S, Bossard M, Ruperti Repilado FJ, Good N, Schoen T, Zimny M, Probst-Hensch NM, Schmidt-Trucksass A, Risch M, Risch L, Conen D. Healthy lifestyle and heart rate variability in young adults. Eur J Prev Cardiol. 2016; 23:1037-1044.
17. Kluttig A, Schumann B, Swenne CA, Kors JA, Kuss O, Schmidt H, Werdan K, Haerting J, Greiser KH. Association of health behaviour with heart rate variability: a population-based study. BMC Cardiovasc Disord. 2010; 10:58.
18. Britton A, Shipley M, Malik M, Hnatkova K, Hemingway H, Marmot M. Changes in heart rate and heart rate variability over time in middle-aged men and women in the general population (from the Whitehall II Cohort Study). Am J Cardiol. 2007; 100:524-527.
19. Takahashi N, Kuriyama A, Kanazawa H, Takahashi Y, Nakayama T. Validity of spectral analysis based on heart rate variability from 1-minute or less ECG recordings. Pacing Clin Electrophysiol. 2017; 40:1004-1009.
20. Tabara Y, Takahashi Y, Kohara K, Setoh K, Kawaguchi T, Terao C, Igase M, Yamada R, Kosugi S, Sekine A, Miki T, Nakayama T, Matsuda F. Association of longer QT interval with arterial waveform and lower pulse pressure amplification: the Nagahama Study. Am J Hypertens. 2013; 26:973-980.
21. Toyoshima H, Usami T, Chishaki A, Horibe H, Nichijunkyo shindenzu code 2005 no kaihatsu to sono keii (The development and background of the Nichijunkyo [The Japanese Society of Cardiovascular Disease Prevention] ECC code 2005 [compliant with 1982 version Minnesota code]). Nichijunyoboushi, 2005; 40:138-154. (in Japanese).
22. Prineas RJ, Crow RS, Zhang ZM. The Minnesota Code Manual of Electrocardiographic Findings, 2nd Edition. Springer-Verlag London Ltd, London, UK, 2010.
23. Sawada Y, Ohtomo N, Tanaka Y, Tanaka G, Yamakoshi K, Terachi S, Shimamoto K, Nakagawa M, Satoh S, Kuroda S, Iimura O. New technique for time series analysis combining the maximum entropy method and non-linear least squares method: its value in heart rate variability analysis. Med Biol Eng Comput. 1997; 35:318-322.
24. Takusagawa M, Komori S, Umetani K, Ishihara T, Sawanobori T, Kohno I, Sano S, Yin D, Ijiri H, Tamura K. Alterations of autonomic nervous activity in recurrence of variant angina. Heart. 1999; 82:75-81.
25. Shannon DC, Carley DW, Benson H. Aging of modulation of heart rate. Am J Physiol. 1987; 253:H874-877.
26. Hrushesky WJ, Fader D, Schmitt O, Gilbertsen V. The respiratory sinus arrhythmia: a measure of cardiac age. Science. 1984; 224:1001-1004.
27. Franklin SS, Gustin Wt, Wong ND, Larson MG, Weber MA, Kannel WB, Levy D. Hemodynamic patterns of age-related changes in blood pressure. The Framingham Heart Study. Circulation. 1997; 96:308-315.
28. Kuo TB, Lin T, Yang CC, Li CL, Chen CF, Chou P. Effect of aging on gender differences in neural control of heart rate. Am J Physiol. 1999; 277:H2233-2239.
29. Sandercock GR, Bromley PD, Brodie DA. Effects of exercise on heart rate variability: inferences from meta-analysis. Med Sci Sports Exerc. 2005; 37:433-439.
30. Jandackova VK, Scholes S, Britton A, Steptoe A. Are Changes in Heart Rate Variability in Middle-Aged and Older People Normative or Caused by Pathological Conditions? Findings From a Large Population-Based Longitudinal Cohort Study. J Am Heart Assoc. 2016; 5.
31. Soares-Miranda L, Sattelmair J, Chaves P, Duncan GE, Siscovick DS, Stein PK, Mozaffarian D. Physical activity and heart rate variability in older adults: the Cardiovascular Health Study. Circulation. 2014; 129:2100-2110.
32. Buchheit M, Simon C, Viola AU, Doutreleau S, Piquard F, Brandenberger G. Heart rate variability in sportive elderly: relationship with daily physical activity. Med Sci Sports Exerc. 2004; 36:601-605.
33. Hautala AJ, Karjalainen J, Kiviniemi AM, Kinnunen H, Makikallio TH, Huikuri HV, Tulppo MP. Physical activity and heart rate variability measured simultaneously during waking hours. Am J Physiol Heart Circ Physiol. 2010; 298:H874-880.
34. Soares-Miranda L, Sandercock G, Vale S, Santos R, Abreu S, Moreira C, Mota J. Metabolic syndrome, physical activity and cardiac autonomic function. Diabetes Metab Res Rev. 2012; 28:363-369.
35. Horibe H, Kasagi F, Kagaya M, Matsutani Y, Okayama A, Ueshima H. A nineteen-year cohort study on the relationship of electrocardiographic findings to all cause mortality among subjects in the national survey on circulatory disorders, NIPPON DATA80. J Epidemiol. 2005; 15:125-134.

Received May 8, 2020; Revised June 21, 2020; Accepted June 24, 2020.

*Address correspondence to:
Naomi Takahashi, Department of Health Informatics, Kyoto University School of Public Health, Yoshida Konoe-cho, Sakyo-ku, Kyoto 606-8501, Japan.
E-mail: ntakahashi@kuhp.kyoto-u.ac.jp

Released online in J-STAGE as advance publication July 4 2020.

Original Article

DOI: 10.5582/bst.2020.03194

Insecticide Resistance of *Aedes albopictus* in Zhejiang Province, China

Juan Hou[§], Qinmei Liu[§], Jinna Wang, Yuyan Wu, Tianqi Li, Zhenyu Gong[*]

Zhejiang Provincial Center for Disease Control and Prevention, Hangzhou, Zhejiang, China.

SUMMARY From 2003 until 2018, a total of 12 outbreaks with 1,654 confirmed dengue cases have been reported in Zhejiang Province. The emergence of insecticide resistance in mosquitoes will affect the control of dengue. Our study aims to investigate the current situation of insecticide resistance of *Ae. albopictus* in Zhejiang Province and compares it with the situation in 2016. *Ae. albopictus* were collected from 12 Zhejiang Province cities in 2019. Resistance to three major categories of insecticides, including 8 commonly used insecticides, was evaluated according to the tube test protocol recommended by China CDC. *Ae. albopictus* in all cities, except Hangzhou, Wenzhou, Lishui and Shaoxing, showed decreased susceptibility to beta-cypermethrin, deltamethrin and permethrin. For malathion, 3 cities *Ae. albopictus* have developed resistance, 3 cities *Ae. albopictus* have decreased susceptibility. For propoxur, in 3 cities *Ae. albopictus* showed decreased susceptibility with mortality ranging from 94.24% to 96.67%. The resistance to alpha-cypermethrin, lambda-cyhalothrin and fenitrothion is rare in *Ae. albopictus* in that only Zhoushan's mosquitoes showed decreased susceptibility to alpha-cypermethrin. The resistance to beta-cypermethrin, deltamethrin and permethrin was significantly correlated with each other. Compared to the situation in 2016, the insecticide resistance of *Ae. albopictus* in Zhejiang Province has become more common in 2019. In the emergency preparedness for future mosquito-borne diseases, two things should be done: 1) the selection of insecticides should be made based on information from insecticide resistance surveillance 2) the use of insecticide should follow scientific guidance.

Keywords *Aedes albopictus*, insecticide resistance, mosquito-borne disease, dengue fever, Zhejiang Province

1. Introduction

Aedes albopictus, also known as Asian tiger mosquito, originates from South-East Asia and spreads to all continents except Antarctica, making it the most invasive mosquito in the world (*1*). It is widely distributed across different regions in China in that cases have been reported from warm south areas, such as Hainan Island and Guangdong Province, as well as cold north regions, like Tibet plateau and Shenyang Province(*2*). Zhejiang Province, located on the southeast coast of China, has a subtropical monsoon climate. The local natural resources, annual average temperature of 15~18°C, and abundant rainfall make it an ideal environment for mosquito's growth and reproduction. Although *Aedes aegypti* has not been discovered yet, *Ae. albopictus* has been discovered in many places in Zhejiang Province.

Ae. albopictus, as the secondary vector, plays an important role in transmission of dengue virus and Chikungunya virus (*3-5*). It may also be a potential vector of Zika virus (*6-8*). Of note, *Ae. albopictus* is the main vector of Aedes-borne disease in China and the sole vector in Zhejiang Province (*9,10*). With the expansion of *Ae. albopictus* distribution, the global health burden caused by Aedes-borne diseases is increasing. Taking dengue fever as an example, it is estimated that 50 million population in over 100 countries contract this disease every year, and about half of the world's population are at risk for contracting dengue virus (*11-13*). In China, dengue fever first emerged in the southeast coast of China (Fujian Province and Guangdong Province), and then spread to the southwest and central area (including Yunnan Province, Henan Province and Shandong Province) (*14-16*). It is estimated that dengue fever has influence on one billion Chinese residents' health (*16*).

Dengue fever also severely threatens the population's health in Zhejiang Province and impedes social and economic development. From 2014 to now, autochthonous dengue outbreak happens in Zhejiang Province every year (*17,18*). In 2017, there was a large-scale dengue outbreak in Hangzhou City with 1,136

cases confirmed (*18*). Also, in that same year there was a autochthonous Chikungunya outbreak in Zhejiang Province (*19*).

At present, for most mosquito-borne diseases, there is no effective vaccine or specific therapeutic drug available. Therefore, controlling mosquito vectors has become a paramount measure of the global mosquito-borne disease control strategy (*20*). Because of high efficacy and low cost for manufacture, chemical insecticides are used as the major tool in mosquito control (especially for mosquito-borne disease control). For example, during the outbreak of dengue in Guangzhou in 2014, a large amount of pyrethroids and temephos were used to control *Ae. albopictus* (*21*). Although the use of chemical insecticides can quickly reduce mosquito density, the improper use of insecticides (*i.e.*, used at high frequency, excessive amount of insecticide used per time, and other incorrect use behaviors) will lead to selection pressure on mosquitoes, which induces insecticide resistance in the survivors (*22*). The emergence of insecticide resistance will make this mosquito control strategy ineffective and eventually lead to the resurgence of mosquito-borne diseases (*23*).

Therefore, to maximize the control effect on mosquitoes and delay their insecticide resistance development, it is crucial to guide people to use insecticides properly. And the guidance should be made on the basis of monitoring and evaluating the situation of insecticide resistance in mosquito species in Zhejiang Province. In this study, *Ae. Albopictus* were collected from 11 prefecture-level cities and Yiwu City of Zhejiang Province in 2019 and eight commonly used insecticides were included in insecticide resistance testing.

2. Materials and Methods

2.1. Mosquito collection and feeding

Ae. albopictus were collected from 11 prefecture-level cities (including Hangzhou, Ningbo, Quzhou, Wenzhou, Lishui, Jinhua, Taizhou, Huzhou, Zhoushan, Jiaxing and Shaoxing) and Yiwu City in Zhejiang Province. In order to obtain the resistance level of the whole city using a multi-point sampling method, the larvae of *Ae. albopictus* were collected from at least three localities in each city (Figure 1). Then larvae were raised with dechlorinated tap water and fed with mouse feed. The adults were identified as species by morphology. Adult mosquitoes were fed with 10% glucose water. *Ae. albopictus* were maintained in a controlled laboratory, where temperature was 27 ± 2˚C, relative humidity was 75 ± 10%, and light: dark cycle was 14 h:10 h.

2.2. Insecticide-impregnated paper

According to frequency of use, three major categories of insecticides were selected for resistance bioassays (pyrethroids: beta-cypermethrin, deltamethrin, permethrin, alpha-cypermethrin, lambda-cyhalothrin; organophosphates: malathion, fenitrothion; carbamate: propoxur.). The discriminating doses used in this study were offered by the staff of China CDC, based on the laboratory susceptible strain of *Ae. Albopictus*. They also provided the insecticide-impregnated papers (0.4% beta-cypermethrin, 0.1% deltamethrin, 3% permethrin, 0.5% malathion, 0.05% propoxur, 1.4% alpha-cypermethrin, 0.2% fenitrothion, 0.5% lambda-cyhalothrin) and control papers for this study.

2.3. Adult resistance bioassays

The bioassays were carried out in 2019, according to the tube test protocol recommended by China CDC. The temperature, humidity and light in the testing room were the same as those in the feeding room. Both test group and control group consisted of the F1 generation of non-blood fed female mosquitoes (3~5days old). For each insecticide test, the test group was exposed to insecticide-impregnated paper for one hour with three replicates. There were 12 control groups, each of which was repeated three times. After exposure, the mosquitoes were fed with 10% glucose water.

Mortality counts were conducted 24 hours after the end of the bioassay. Mosquitoes, which were unable to fly when they were given mechanical stimulation were considered dead. If the control mortality is ≥ 5% and < 20%, the mortality should be corrected by Abbott's formula, as follows:

$$\text{Corrected mortality} = \frac{(\%\text{observed mortality} - \%\text{control mortality})}{\text{Corrected mortality}} \times 100$$

If the mortality of control group was ≥ 20%, the bioassay should be redone. Resistant status was classified into three categories by mortality rate: resistance if mortality < 90%, probable resistance if mortality was between 90 and 98%, and susceptibility if mortality > 98%.

2.4. Statistical Analysis

The correlation of the mortality between different insecticides was analyzed by Pearson correlation. Statistical analyses were performed using SPSS (version 20.0) software and a value of < 0.05 was considered to be statistically significant.

3. Results

The mosquitoes in all cities, except Hangzhou and Wenzhou, showed a decreased susceptibility to the

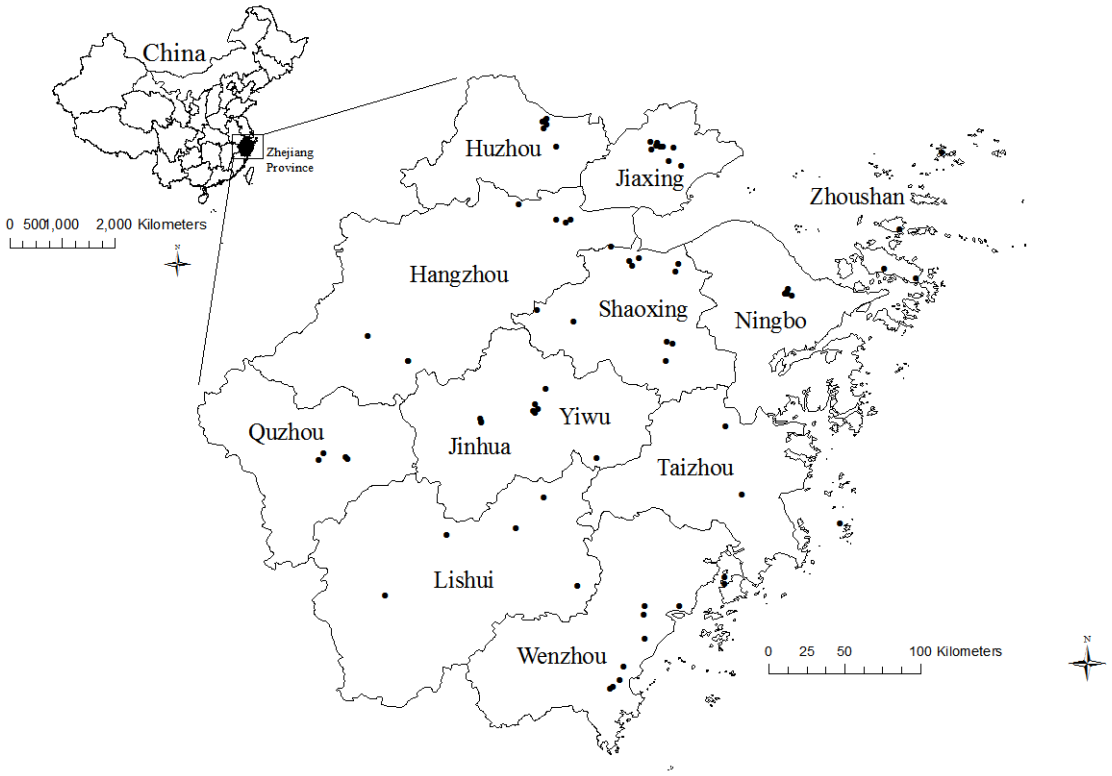

Figure 1. The sampling sites of *Ae. albopictus* in Zhejiang Province, China. The sampling sites of *Ae. albopictus* in 11 prefecture-level cities of Zhejiang Province.

three major categories of insecticides tested (Table 1, Figure 2). Mosquitoes in Ningbo and Huzhou showed a probable resistance to one of the pyrethroids; mosquitoes in Lishui showed a probable resistance to malathion; mosquitoes in Jinhua showed a probable resistance to one of the pyrethroids and propoxur; mosquitoes in Jiaxing showed a probable resistance to two of the pyrethroids and malathion; mosquitoes in Taizhou showed a probable resistance and resistance to three pyrethroids and malathion; mosquitoes in Quzhou showed a resistance to deltamethrin, permethrin and malathion, with a mortality of 82.73-88.68%, and showed to be probably resistant to beta-cypermethrin and propoxur. The city with most serious insecticide resistance problem is Yiwu, in which the mosquitoes showed a resistance to the pyrethroids tested, with a mortality of 61.15-80.00%, and showed a probable resistance to propoxur.

For beta-cypermetrin, mosquitoes in Yiwu and Taizhou had developed resistance, while mosquitoes in Quzhou, Jinhua and Jiaxing had developed probable resistance. For deltamethrin, mosquitoes in Yiwu, Quzhou and Zhoushan had developed resistance, while mosquitoes in Ningbo, Taizhou and Jiaxing had developed probable resistance. For permethrin, mosquitoes in Yiwu and Quzhou had developed resistance, while mosquitoes in Zhoushan, Taizhou and Huzhou had probable resistance. For malathion, mosquitoes in Shaoxing, Quzhou and Taizhou had developed resistance, while mosquitoes in Zhoushan, Jiaxing and Lishui have probable resistance. For propoxur, mosquitoes in Quzhou, Yiwu and Jinhua had probable resistance. For alpha-cypermethrin, lambda-cyhalothrin and fenitrothion, only mosquitoes in Zhoushan had developed probable resistance, while mosquitoes in other cities are all susceptible.

Table 2 shows the correlation of the mortality between different insecticides. The mortality of beta-cypermethrin was related with that of deltamethrin and permethrin, and the r was 0.834 ($P < 0.001$) and 0.864 ($P < 0.001$), respectively. The mortality of deltamethrin was significantly associated with that of permethrin and the r of 0.960 ($P < 0.0001$).

4. Discussion

As the increasing health burden caused by arboviral diseases, mosquito-borne disease has become a major international public health concern. Mosquito control is the key part of the global strategy for mosquito-borne disease prevention, and insecticides are the most critical component of this work. In the past, the use of insecticides (such as long-lasting insecticidal nets; indoor residual spraying; space spraying) has effectively reduced the incidence of mosquito-borne diseases and has saved millions of people (*24*). However, with the overuse of chemical insecticides, mosquitoes have developed resistance to protect their lives. The first case

Table 1. The mortalities of *Ae.albopictus* in twelve cities exposed to discriminating does of eight insecticides

Cities	Beta-cypermethrin		Deltamethrin		Permethrin		Malathion		Propoxur		Alpha-cypermethrin		Lambda-cyhalothrin		Fenitrothion	
	No.	M (%)	No.	M (%)	No.	M (%)	No.	M (%)	No.	M (%)	No.	M (%)	No.	M (%)	No.	M (%)
Hangzhou	80	100.00	82	98.78	80	100.00	82	100.00	76	100.00	83	100.00	80	98.75	72	100.00
Ningbo*	90	98.75	90	91.25	90	98.75	90	98.75	90	100.00	90	98.75	-	-	-	-
Quzhou*	60	90.57	59	82.73	60	88.68	60	86.79	59	94.24	-	-	-	-	-	-
Yiwu	66	65.15	60	61.67	60	80.00	70	98.57	60	96.67	-	-	-	-	-	-
Wenzhou	78	100.00	81	100.00	-	-	79	100.00	84	100.00	-	-	80	100.00	-	-
Lishui	90	100.00	84	100.00	87	100.00	83	95.18	86	100.00	-	-	-	-	-	-
Jinhua	90	92.22	90	100.00	90	100.00	90	100.00	90	96.67	-	-	-	-	-	-
Taizhou*	66	82.37	66	94.71	79	94.11	67	89.58	63	100.00	-	-	-	-	-	-
Huzhou*	69	100.00	67	98.41	68	96.87	73	100.00	65	100.00	-	-	-	-	-	-
Zhoushan	91	98.90	92	89.13	90	94.44	91	91.21	95	100.00	92	94.57	-	-	-	-
Jiaxing	75	96.00	75	97.33	75	98.67	75	92.00	75	98.67	-	-	-	-	-	-
Shaoxing	60	100.00	60	100.00	60	100.00	60	85.00	60	100.00	-	-	-	-	-	-

No.: number of *Ae.albopictus*; M: mortality; *The mortality corrected by Abbott's formula.

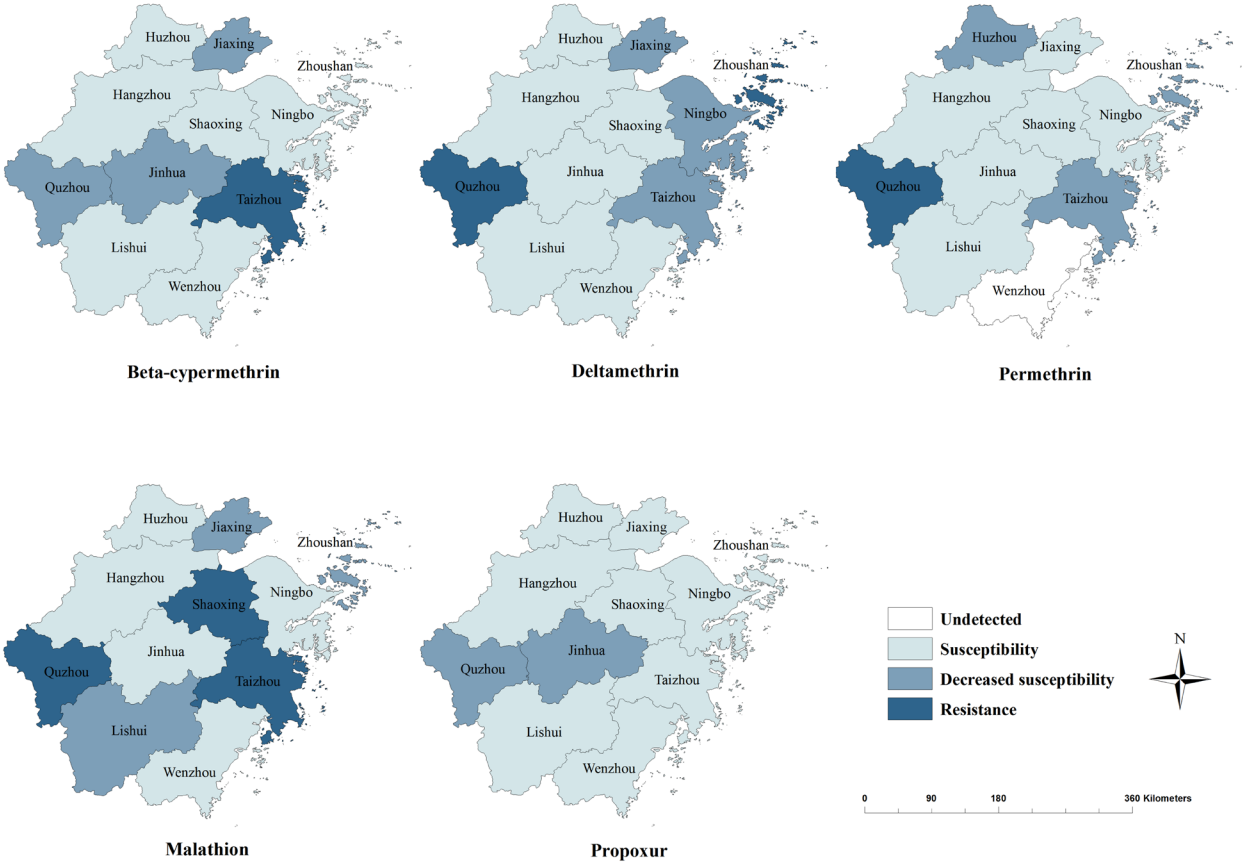

Figure 2. The resistance to five insecticides in Zhejiang Province. Beta--cypermethrin: The resistance level of *Ae. albopictus* to beta--cypermethrin in 11 prefecture-level cities. **Deltamethrin**: The resistance level of *Ae. albopictus* to deltamethrin in 11 prefecture-level cities. **Permethrin**: The resistance level of *Ae. albopictus* to permethrin in 11 prefecture-level cities. **Malathion**: The resistance level of *Ae. albopictus* to malathion in 11 prefecture-level cities. **Propoxur**: The resistance level of *Ae. albopictus* to propoxur in 11 prefecture-level cities.

of insecticide resistance in mosquitoes was reported in 1952, and later on similar cases were reported across the world (*25-29*). The emergence of resistance negatively influenced the control of mosquito-borne diseases (*30-32*) and promoted scientists to develop new insecticide-based methods (*33*). For example, insect-attractive targeted sugar baits are being developed to control mosquitoes (*34-36*). However, such methods will undergo the same pattern as previous tools did in that the method works out at the beginning, but the

Table 2. Correlation of mortality between different insecticides

	Beta-cypermethrin		Deltamethrin		Permethrin		Malathion		Propoxur	
	r	*P*	*r*	*P*	*r*	*P*	*r*	*P*	*r*	*P*
Beta-cypermethrin	1	-								
Deltamethrin	0.834	0.001*	1	-						
Permethrin	0.864	0.001*	0.960	0.000*	1	-				
Malathion	0.004	0.990	0.022	0.947	0.066	0.847	1	-		
Propoxur	0.511	0.089	0.552	0.063	0.582	0.060	0.162	0.615	1	-

*$p < 0.05$

effectiveness would decrease in a short time because mosquitoes develop resistance (*33*).

We investigated the *Ae. albopictus* adults' resistance to five commonly used insecticides in Zhejiang Province in 2016 (*37*). Generally, after insecticide exposure, a population with a mortality < 90% is considered to be resistant, a population with a mortality > 90% and < 98% is considered to be probably resistant, and a population with mortality > 98% is considered to be susceptible. According to this, for the three pyrethroids, only Shaoxing showed resistance for beta-cypermethrin in 2016. However, the number of cities in Zhejiang Province where mosquitoes are resistant to the three pyrethroids increased in 2019. For beta-cypermathrin tested for mosquitoes in Ningbo, Quzhou, Yiwu, Jinhua, Taizhou, and Jiaxiang, the mortality in 2019 is lower than the rate in 2016, suggesting a decrease in mosquitoes' susceptibility to beta-cypermathrin. For deltamethrin tested for mosquitoes in Hangzhou, Ningbo, Quzhou, Yiwu, Taizhou, Huzhou, Zhoushan and Jiaxing, the morality in 2019 is lower than the rate in 2016. In addition, for permethrin tested for mosquitoes in Quzhou, Yiwu, Taizhou, Huzhou, Zhoushan, the morality in 2019 is lower than the rate in 2016.

In 2019, mosquitoes in Yiwu and Taizhou newly developed resistance to beta-cypermetrin; mosquitoes in Yiwu, Quzhou and Zhoushan newly developed resistance to deltamethrin; and mosquitoes in Yiwu and Quzhou have developed resistance to permethrin. These results informed us that there are more cities in Zhejiang province in which mosquitoes develop insecticide resistance.

Different from pyrethroids resistance, malathion resistance in Zhejiang Province in 2019 has been mitigated, by comparison with the situation in 2016, only for Shaoxing, Taizhou and Quzhou, mosquitoes in these cities still show resistance to malathion. The resistance status of propoxur was similar to the status in 2016 that mosquitoes in most cities are still susceptible.

Notably, a relatively intense resistance to beta-cypermetrin, deltamethrin and permethrin was observed in mosquitoes in Yiwu and the mortality was 65.15%, 61.67% and 80%, respectively in 2019. Yiwu is the largest wholesale market for small commodities in the world in that about 15,000 foreign businessmen from more than 100 countries and regions reside here. Our surveillance data shows that the number of imported cases of dengue fever in Yiwu is the largest in Zhejiang Province. The annual number of imported cases from 2016 to 2019 was 9, 12, 12 and 35 respectively. The local government attaches great importance to mosquito-borne diseases. The government exterminates mosquitoes in each place where any mosquito-related cases were identified, and regularly organizes large-scale mosquito control campaigns. Beta cypermetrin, deltamethrin and permethrin are often used to kill mosquitoes and flies. Large scale and high frequency use of insecticides can lead to development of resistance, which may be the explanation for resistance of adult mosquitoes in Yiwu city.

In recent years, not only has *Ae. albopictus* in Zhejiang Province developed resistance to pyrethroids, but also has the indigenous house fly. We studied the resistance of house flies in 2011, 2014 and 2017, and found that the resistance to pyrethroids was very common (*38*). The increase of vector resistance may be attributed to large-scale use of chemical insecticides. With the increasing challenge of mosquito-borne diseases prevention and control, the frequency of using pyrethroids increased. Wei *et al.* investigated the resistance of *Ae. albopictus* in the early and late stages of emergency dengue fever control in Hangzhou in 2017, and found that after 3 months of wide-ranging use of insecticides, the resistance of *Ae. albopictus* to pyrethroids increased (*39*). Correlations among beta-cypermethrin, deltamethrin and permethrin suggested that cross resistance may exist between them.

Through this study, we found that the resistance of *Ae. Albopictus* in Zhejiang Province has increased significantly in the past three years, and there are several implications from the study results: 1) the local government and healthcare facilities should highlight the use of insecticides resistance surveillance; 2) the insecticides should be used in a more strategic and sustainable way to reduce insecticide resistance 3) scientific management of infectious disease vectors should be developed. Guo *et al.* constructed "mosquito-free village" in rural areas mainly by cultivating the health literacy of villagers to reduce mosquito breeding areas (*40*). The success of the "mosquito-free village"

construction suggests that we can control mosquito density at a lower level with less or no insecticides. Therefore, we are calling on the government and health institutions to use the environment management and environment modification method to create an environment not conducive to mosquitoes' survival. This activity should be affiliated with other measures, such as an anti-mosquito education program to prevent future mosquito-borne disease in Zhejiang Province.

In summary, our study found that mosquitoes in most cities had resistance or probable resistance to the three major categories of tested insecticides. For beta-cypermetrin and permethrin, 2 cities' mosquitoes have developed resistance, and 3 cities' mosquitoes have decreased susceptibility. For deltamethrin and malathion, 3 cities' mosquitoes have developed resistance, and 3 cities' mosquitoes have decreased susceptibility. Few cities' mosquitoes had resistance to alpha-cypermethrin, lambda-cyhalothrin and fenitrothion. In the future daily mosquito control, the government and health institutions should adopt a comprehensive management of mosquito control, which involves environment management, biocontrol, physical control, and chemical control. To more efficiently reduce the density of mosquitoes and lower the risk of mosquito-borne disease in Zhejiang Province, the next objective is to strengthen activities in eliminating mosquito breeding sites within this province. To achieve this, the government and health institutions should launch anti-mosquito campaigns to raise citizen awareness of mosquito control strategies and guide healthcare workers to use insecticides properly. In the emergency preparedness for future mosquito-borne diseases, two things should be done: 1) the selection of insecticides should be made based on information obtained from insecticide resistance surveillance 2) the use of insecticide should strictly follow scientific guidance.

Acknowledgements

This work was financially supported by grants from the State Project for Scientific & Technological Development of the 13th Five Year Plan (grant number: 2017ZX10303404). We thank Fengxia Meng and Chunchun Zhao from the China CDC for providing insecticide-impregnated papers with diagnostic doses and control papers. We also appreciate those who support this work: our colleagues from Center for Disease Control and Prevention of 11 prefecture-level cities and Yiwu city.

References

1. Benedict MQ, Levine RS, Hawley WA, Lounibos LP. Spread of the tiger: global risk of invasion by the mosquito *Aedes albopictus*. Vector Borne Zoonotic Dis. 2007; 7:76-85.
2. Liu Q. The sustainable control strategy and key technology of Aedes vector. Electronic Journal of Emerging Infectious Diseases. 2018; 3:75-79. (in Chinese)
3. Gratz NG. Critical review of the vector status of *Aedes albopictus*. Med Vet Entomol. 2004; 18:215-227.
4. Paupy C, Delatte H, Bagny L, Corbel V, Fontenille D. *Aedes albopictus*, an arbovirus vector: from the darkness to the light. Microbes Infect. 2009; 11:1177-1185.
5. Rezza G. Dengue and chikungunya: long-distance spread and outbreaks in naïve areas. Pathog Glob Health. 2014; 108:349-355.
6. Gardner LM, Chen N, Sarkar S. Global risk of Zika virus depends critically on vector status of *Aedes albopictus*. Lancet Infect Dis. 2016; 16:522-523.
7. McKenzie BA, Wilson AE, Zohdy S. *Aedes albopictus* is a competent vector of Zika virus: a meta-analysis. PLoS One. 2019; 14:e0216794-e0216794.
8. Wong P-SJ, Li M-zI, Chong C-S, Ng L-C, Tan C-H. Aedes (Stegomyia) albopictus (Skuse): a potential vector of Zika virus in Singapore. PLoS Negl Trop Dis. 2013; 7:e2348-e2348.
9. Guo Y-h, Wu H-x, Liu X-b, Yue Y-j, Ren D-s, Zhao N, Li G-c, Song X-p, Lu L, Liu Q-y. National vectors surveillance report on mosquitoes in China, 2018. Chin J Vector Biol & Control. 2019; 30:134-138. (in Chinese)
10. Wu Y, Gong Zy, Hou J, Guo S, Wang Jn, Ling F. Analysis of vector surveillance from 2011 to 2013 in Zhejiang province, China. Chin J Vector Biol & Control. 2015; 26:394-397. (in Chinese)
11. Bhatt S, Gething PW, Brady OJ, *et al*. The global distribution and burden of dengue. Nature. 2013; 496:504-507.
12. Brady OJ, Gething PW, Bhatt S, Messina JP, Brownstein JS, Hoen AG, Moyes CL, Farlow AW, Scott TW, Hay SI. Refining the global spatial limits of dengue virus transmission by evidence-based consensus. PLoS Negl Trop Dis. 2012; 6:e1760-e1760.
13. Messina JP, Brady OJ, Pigott DM, Brownstein JS, Hoen AG, Hay SI. A global compendium of human dengue virus occurrence. Sci Data. 2014; 1:140004.
14. Chen Q, Song W, Mu D, Li Y, Yin W, Li Z. Analysis on epidemiological characteristics of dengue fever in China, as of 31th August, 2017. Disease Surveillance. 2017; 32:801-804. (in Chinese)
15. Ning W, Lu L, Ren H, Liu Q. Spatial and Temporal Variations of Dengue Fever Epidemics in China from 2004 to 2013. Journal of Geo-Information Science. 2015; 17:614-621. (in Chinese)
16. Zhang F. The current situation of dengue fever in China. Electronic Journal of Emerging Infectious Diseases. 2018; 3:65-66. (in Chinese)
17. Ai L, Chen E, Jimin S, Jiangping R. Analysis on spatial and temporal clustering of dengue fever epidemic in Zhejiang,2004-2016. Disease Surveillance. 2019; 34:27-31. (in Chinese)
18. Yu H, Kong Q, Wang J, Qiu X, Wen Y, Yu X, Liu M, Wang H, Pan J, Sun Z. Multiple Lineages of Dengue Virus Serotype 2 Cosmopolitan Genotype Caused a Local Dengue Outbreak in Hangzhou, Zhejiang Province, China, in 2017. Sci Rep. 2019; 9:7345-7345.
19. Pan J, Fang C, Yan J, Yan H, Zhan B, Sun Y, Liu Y, Mao H, Cao G, Lv L, Zhang Y, Chen E. Chikungunya Fever Outbreak, Zhejiang Province, China, 2017. Emerg Infect Dis. 2019; 25:1589-1591.
20. Abramides GC, Roiz D, Guitart R, Quintana S, Giménez N. Control of the Asian tiger mosquito (*Aedes albopictus*) in

a firmly established area in Spain: risk factors and people's involvement. Trans R Soc Trop Med Hyg. 2013; 107:706-714.
21. Su X, Guo Y, Deng J, Xu J, Zhou G, Zhou T, Li Y, Zhong D, Kong L, Wang X, Liu M, Wu K, Yan G, Chen X-G. Fast emerging insecticide resistance in *Aedes albopictus* in Guangzhou, China: Alarm to the dengue epidemic. PLoS Negl Trop Dis. 2019; 13:e0007665-e0007665.
22. Yavaşoglu Sİ, Yaylagül EÖ, Akıner MM, Ülger C, Çağlar SS, Şimşek FM. Current insecticide resistance status in Anopheles sacharovi and Anopheles superpictus populations in former malaria endemic areas of Turkey. Acta Trop. 2019; 193:148-157.
23. Liu N. Insecticide resistance in mosquitoes: impact, mechanisms, and research directions. Annu Rev Entomol. 2015; 60:537-559.
24. Bhatt S, Weiss DJ, Cameron E, *et al.* The effect of malaria control on Plasmodium falciparum in Africa between 2000 and 2015. Nature. 2015; 526:207-211.
25. Bharati M, Rai P, Saha D. Insecticide resistance in *Aedes albopictus* Skuse from sub-Himalayan districts of West Bengal, India. Acta Trop. 2019; 192:104-111.
26. Kamgang B, Marcombe S, Chandre F, Nchoutpouen E, Nwane P, Etang J, Corbel V, Paupy C. Insecticide susceptibility of *Aedes aegypti* and *Aedes albopictus* in Central Africa. Parasit Vectors. 2011; 4:79-79.
27. Fotakis EA, Chaskopoulou A, Grigoraki L, Tsiamantas A, Kounadi S, Georgiou L, Vontas J. Analysis of population structure and insecticide resistance in mosquitoes of the genus Culex, Anopheles and Aedes from different environments of Greece with a history of mosquito borne disease transmission. Acta Trop. 2017; 174:29-37.
28. Cui F, Raymond M, Qiao C-L. Insecticide resistance in vector mosquitoes in China. Pest Manag Sci. 2006; 62:1013-1022.
29. Chuaycharoensuk T, Juntarajumnong W, Boonyuan W, Bangs MJ, Akratanakul P, Thammapalo S, Jirakanjanakit N, Tanasinchayakul S, Chareonviriyaphap T. Frequency of pyrethroid resistance in *Aedes aegypti* and *Aedes albopictus* (Diptera: Culicidae) in Thailand. J Vector Ecol. 2011; 36:204-212.
30. Benelli G, Beier JC. Current vector control challenges in the fight against malaria. Acta Trop. 2017; 174:91-96.
31. Marcombe S, Carron A, Darriet F, Etienne M, Agnew P, Tolosa M, Yp-Tcha MM, Lagneau C, Yébakima A, Corbel V. Reduced efficacy of pyrethroid space sprays for dengue control in an area of Martinique with pyrethroid resistance. Am J Trop Med Hyg. 2009; 80:745-751.
32. Gnankiné O, Bassolé IHN, Chandre F, Glitho I, Akogbeto M, Dabiré RK, Martin T. Insecticide resistance in Bemisia tabaci Gennadius (Homoptera: Aleyrodidae) and Anopheles gambiae Giles (Diptera: Culicidae) could compromise the sustainability of malaria vector control strategies in West Africa. Acta Trop. 2013; 128:7-17.
33. Catteruccia F. Malaria-carrying mosquitoes get a leg up on insecticides. Nature. 2020; 577:319-320.
34. Gu ZY, He J, Teng XD, Lan CJ, Shen RX, Wang YT, Zhang N, Dong YD, Zhao TY, Li CX. Efficacy of orally toxic sugar baits against contact-insecticide resistant culex quinquefasciatus. Acta Trop. 2020; 202:105256-105256.
35. Qualls WA, Müller GC, Revay EE, Allan SA, Arheart KL, Beier JC, Smith ML, Scott JM, Kravchenko VD, Hausmann A, Yefremova ZA, Xue R-D. Evaluation of attractive toxic sugar bait (ATSB)-Barrier for control of vector and nuisance mosquitoes and its effect on non-target organisms in sub-tropical environments in Florida. Acta Trop. 2014; 131:104-110.
36. Revay EE, Schlein Y, Tsabari O, Kravchenko V, Qualls W, De-Xue R, Beier JC, Traore SF, Doumbia S, Hausmann A, Müller GC. Formulation of attractive toxic sugar bait (ATSB) with safe EPA-exempt substance significantly diminishes the Anopheles sergentii population in a desert oasis. Acta Trop. 2015; 150:29-34.
37. Hou J, Meng F, Wu Y, Wang J, Guo S, Gong Z. Resistance of adult *Aedes albopictus* to commonly used insecticides in Zhejiang province. Chin J Vector Biol & Control. 2017; 28:230-232. (in Chinese)
38. Wang JN, Hou J, Wu Y-Y, Guo S, Liu Q-M, Li T-Q, Gong Z-Y. Resistance of House Fly, Musca domestica L. (Diptera: Muscidae), to Five Insecticides in Zhejiang Province, China: The Situation in 2017. Can J Infect Dis Med Microbiol. 2019; 2019:4851914-4851914.
39. Wei L, Kong Q, Wang H, Wang Y, Shen L, Cao Y. Comparison of insecticide resistance of *Aedes albopictus* before and after emergency control of dengue fever in Hangzhou, China, 2017. Chin J Vector Biol & Control. 2019; 30:678-681. (in Chinese)
40. Guo S, Huang W, Sun J, Gong Z, Ling F, Wu H, Chen E. "Mosquito-Free Villages": Practice, Exploration, and Prospects of Sustainable Mosquito Control-Zhejiang, China. China CDC Weekly. 2019; 1:70-74.

Received May 26, 2020; Revised June 22, 2020; Accepted June 24, 2020.

[§]These authors contributed equally to this work.
**Address correspondence to:*
Zhenyu Gong, Zhejiang Provincial Center for Disease Control and Prevention, 3399 Binsheng Road, Binjiang District, Hangzhou 310051, Zhejiang Province, China.
E-mail: gongzhenyu2020@163.com

Released online in J-STAGE as advance publication June 27, 2020.

Original Article

DOI: 10.5582/bst.2020.03085

Exploration of *Salmonella* effector mutant strains on MTR4 and RRP6 degradation

Xiaoning Sun[1,2], Kentaro Kawata[1], Atsuko Miki[1], Youichiro Wada[1,2], Masami Nagahama[3], Akiko Takaya[4,5], Nobuyoshi Akimitsu[1,*]

[1] Isotope Science Center, The University of Tokyo, Tokyo, Japan;
[2] Advanced Interdisciplinary Studies, Engineering Department, The University of Tokyo, Tokyo, Japan;
[3] Laboratory of Molecular and Cellular Biochemistry, Meiji Pharmaceutical University, Tokyo, Japan;
[4] Department of Natural Products Chemistry, Graduate School of Pharmaceutical Sciences, Chiba University, Chiba, Japan;
[5] Medical Mycology Research Center, Chiba University, Chiba, Japan.

SUMMARY *Salmonella enterica* serovar Typhimurium (*Salmonella*), a pathogenic bacterium, is a major cause of foodborne diseases worldwide. *Salmonella* injects multiple virulence factors, called effectors, into cells and causes multiple rearrangements of cellular biological reactions that are important for *Salmonella* proliferation and virulence. Previously, we reported that *Salmonella* infection causes loss of MTR4 and RRP6, which are nuclear RNA degradation factors, resulting in the stabilization and accumulation of unstable nuclear RNAs. This accumulation is important for the cellular defense for *Salmonella* infection. In this study, we examined a series of *Salmonella* mutant strains, most of which are strains with genes related to effectors translocated by T3SSs encoded on *Salmonella* pathogenic islands, SPI-1 and SPI-2, that have been depleted. Among 42 *Salmonella* mutants, 6 mutants' infections canceled loss of MTR4 and RRP6. Proliferation assay of *Salmonella* in the cell revealed that six mutants showed poor proliferation in the host cell, demonstrating that poor proliferation contributed to cancellation of MTR4 and RRP6 loss. This result indicates that certain events associated with *Salmonella* proliferation in host cells cause loss of MTR4 and RRP6.

Keywords T3SSs, SPI-1, SPI-2, Flagella, MTR4, RRP6

1. Introduction

Salmonella enterica serovar Typhimurium (*Salmonella*), a pathogenic bacterium, is a major cause of foodborne diseases worldwide. The *Salmonella* genome carries two particular regions involved in virulence, *Salmonella* pathogenicity islands named SPI-1 and SPI-2. T3SSs are nanosyringe-like organelles expressed by *Salmonella*, including T3SS-1 and T3SS-2, which are encoded on SPI-1 and SPI-2, respectively. T3SSs consist of a basal body and a needle-like complex through which *Salmonella* derived effector proteins are secreted into the cytoplasm of the host cell (*1,2*). T3SS-1 mainly facilitates the invasion of *Salmonella* into host cells, and T3SS-2 facilitates the pathogenesis of *Salmonella* and is necessary for the formation of the *Salmonella*-containing vacuole (SCV), the intracellular niche of replication (*3*).

Virulence genes located on SPI-1 and SPI-2 are required at different stages, specifically, the intestinal and the systemic phases of infection, respectively (*4*). Both pathogenicity islands contain many operons, the expression of which is primarily governed by highly integrated transcriptional regulators. HilA, HilC and HilD, for instance, are regulators in SPI-1 (*5,6*). A series of operons, including *prg/org*, *inv/spa* and *sic/sip* in SPI-1 encode the components of T3SS machine and primary effector proteins (*7*). SsrA/B, the two-component regulatory system encoded in SPI-2, controls the expression of genes in SPI-2. By developing an *in vitro* system, Bustamante *et al.* revealed a cross-talk mechanism between SPI-1 and SPI-2 in which HilD encoded in SPI-1 differently regulates the regulons of SPI-1 and SPI-2 in the growth phase (*8*). In addition, Moest *et al.* pointed out that growing evidence suggests that the two T3SSs' regulation can be interdependent and the periods of secreting bacterium proteins overlap (*2*).

Salmonella has another T3SS, the flagellar system (*9*). The flagellar T3SS exports substrate subunits that assemble into a functional flagellum and regulatory factors that control the assembly process. Flagellar gene expression is under spatiotemporal control by a transcriptional hierarchy of three promoter classes.

flhDC, controlled by a class 1 promoter, encodes a flagellar master regulator. A $FlhD_4C_2$ complex activates class 2 promoter transcription. FliZ, controlled by the class 2 promoter, activates SPI1 gene regulation through HilD-posttranscriptional regulation (*10*). The SPI1 master regulator HilD activates *flhDC* gene expression (*11*). Furthermore, the SsaB protein encoded on SPI-2 is involved in flagella assembly by affecting the post-transcription expression of *flhDC* (*12*). Therefore, the cross-regulation network between SPI-1, SPI-2 and the flagellar system likely contributes to *Salmonella* virulence.

A large number of RNAs are continuously being produced in eukaryotic nuclei, and RNA degradation systems are recruited to keep the balance of these genomic outputs, such as by discarding the transcriptional byproducts and malformed transcripts (*13*). The RNA exosome, a 3′–5′ ribonuclease complex, facilitates the degradation of some labile nuclear RNAs (*14*). The RNA exosome consists of nine core subunits and an essential catalytic subunit, RRP44 (*15*). Among them, six subunits surround a central channel and contain domains, which are homologous to the bacterial phosphorolytic ribonuclease RNase PH (*16,17*); three subunits, which are positioned on top of the RNase PH-like ring, harbor S1 or KH RNA-binding domains (*18*). RRP44 is believed to interact with the "bottom" of the PH-ring (*16*), and RRP6 is believed to be located next to the exosome entrance, on the opposite side of RRP44 (*19*). The active ribonucleases RRP6 and RRP44 (DIS3) in human nuclei facilitate the nine subunits' large and inert core of the RNA exosome to obtain its catalytic activity (*20,21*). In addition, RRP6 is involved in interactions with other cofactors such as RRP47 and MTR4 (*22*).

The NEXT complex, composed of MTR4, Zn-finger protein ZCCHC8, and RNA-binding factor RBM7, mainly targets early and unprocessed RNA by recruiting the nuclear RNA exosome complex (*23*). In addition, the PAXT complex, which also contains MTR4, mainly targets long and polyadenylated RNA by recruiting the nuclear RNA exosome complex (*13*). MTR4 is an RNA helicase that interacts with several protein adaptors and facilitates the RNA exosome recognizing its target (*24*). Thus, MTR4 and RRP6 are important components of the RNA exosome in the nuclear RNA degradation pathway. Recently, we revealed that the unstable nuclear ncRNAs are mainly degraded by the MTR4-mediated nuclear RNA decay pathway. In addition, RRP6 and MTR4 are dramatically decreased upon *Salmonella* infection, resulting in stabilizing the labile nuclear ncRNAs (*25*).

Because effectors of *Salmonella* are the main influence for cell physiology in *Salmonella* infection, we considered whether any effectors are involved in the degradation of MTR4 and RRP6. To test this idea, we constructed a series of *Salmonella* mutant strains and examined the effect of these mutants for loss of MTR4 and RRP6. Among the 42 *Salmonella* mutants examined in this study, 6 canceled loss of MTR4 and RRP6. A proliferation assay of *Salmonella* in the cell revealed that 6 mutants showed poor proliferation in the host cell, demonstrating that poor proliferation attributed in cancellation of loss of MTR4 and RRP6. This result indicates that certain events associated with *Salmonella* proliferation in the host cell causes loss of MTR4 and RRP6. Thus, this is the first report of exploring *Salmonella* effectors that may be involved in degrading the components of the RNA exosome among many *Salmonella* mutant strains. Our study has the potential to lay a good foundation for future research on *Salmonella* effector and RNA exosome upon *Salmonella* infection.

2. Materials and Methods

2.1. Cell lines and culture

Hela TO cells, purchased from Clontech (Palo Alto, CA), were maintained in Dulbecco's modified Eagle's medium (DMEM) purchased from Wako (Tokyo, Japan), supplying with 10% fetal bovine serum (FBS) purchased from Life Technologies (Grand Island, NY). FBS was heat-inactivated at 56°C for 30 min. Hela TO cells were cultured in a humidified incubator (Thermo Fisher Scientific) with 5% CO_2 at 37°C.

2.2. Construction of *Salmonella* mutant strains

Salmonella enterica serovar Typhimurium (*Salmonella*) mutant strains were constructed based on wild type *Salmonella*. The detailed information about these mutants is shown in Tables 1 and 2.

2.3. *Salmonella* culture

Salmonella was cultured with 5 mL LB5 at 37°C overnight (around 16.5 h) in a shaking bath. A total of 50 μL of the full growth was inoculated with a fresh 5 mL LB5 at 37°C for 2 h. *Salmonella* was collected by centrifuge and resuspended with a corresponding volume of 1 × PBS before infection.

2.4. Heat-killed *Salmonella*

After resuspending the subcultured *Salmonella* with a corresponding volume of 1 × PBS, the *Salmonella* was incubated at 80°C for 1 h to heat-kill it.

2.5. *Salmonella* infection

A 12-well plate was used in this study, and 2×10^5 Hela cells were plated in each well. Hela cells were infected with WT-*Salmonella*, *Salmonella* mutant strains or heat-killed *Salmonella* at 100 multiplicity of infection (moi). After infection with 100 moi *Salmonella* or 1 μg/mL LPS (WAKO, Japan), Hela cells were incubated at 37°C for 1

Table 1. 42 *Salmonella* mutant strains

Strains	Relevant characteristics	References
S. enterica serovar Typhimurium		
χ3306	Virulent strain, *gyrA1816* pStSR1001^{+}	Gulig and Curtiss, 1987
χ3337	Virulence plasmid-cured derivative of x3306, gyrA1816 *pStSR1001*, *spv*$^{-}$	Gulig and Curtiss, 1987
χ3306*phoP*	*phoP*::*aph*-ΔTer in χ3306, ΔPhoP	Matsui *et al.*, 2000 Microbiol. ImmunoL, 44(6), 447-454, 2000
CS2007	*clpP*::Cm in χ3306, ΔClpXP	Yamamoto *et al.* IAI 60: 3164-74. 2001
CS2022	Δ*lon*::Cm in χ3306, ΔLon	Takaya et la., IAI 71: 690-6. 2003
CS2609	*flhD*::Tn*10* in χ3306, ΔFlhDΔFlhC	Tomoyasu *et al.* MM 48: 443-52. 2003
CS2725	Δ*hilD* in χ3306, ΔHilD	Takaya *et al.* MM 55: 839-52. 2005
CS2802	Δ*hilC* Δ*hilD* in χ3306, ΔHilCΔHilD	Takaya *et al.* MM 55: 839-52. 2005
CS3752	Δ*sptP*::Km in χ3306, ΔSptP	This study
CS3754	Δ*sopD2*::Km in χ3306, ΔSopD2	This study
CS3794	Δ*avrA*::Km in χ3306, ΔAvrA	This study
CS3802	Δ*pipA*::FRT in χ3306, ΔPipA	This study
CS3803	Δ*pipB*::FRT in χ3306, ΔPipB	This study
CS3804	Δ*gtgA*::FRT in χ3306, ΔGtgA	This study
CS3809	Δ*pipC*::Km in χ3306, ΔPipC	This study
CS3822	Δ*gogA*::FRT in χ3306, ΔGogA	This study
CS4022	Δ*prgI*::FRT in χ3306, ΔPrgI	This study
CS4037	Δ*sspH2*::Km in χ3306, ΔSspH2	This study
CS4844	Δ*gogB*::Cm in χ3306, ΔGogB	This study
CS4845	Δ*sseK1*::Km in χ3306, ΔSseK1	This study
CS4846	Δ*sseI*::Km in χ3306, ΔSseI	This study
CS4848	Δ*sseL*::Km in χ3306, ΔSseL	This study
CS4850	Δ*sseK2*::Cm in χ3306, ΔSseK2	This study
CS4852	Δ*sifA*::Cm in χ3306, ΔSifA	This study
CS4853	Δ*sseJ*::Km in χ3306, ΔSseJ	This study
CS4854	Δ*steC*::Km in χ3306, ΔSteC	This study
CS4856	Δ*pipB2*::Cm in χ3306, ΔPipB2	This study
CS4857	Δ*sifB*::Cm in χ3306, ΔSifB	This study
CS4862	Δ*ssaB*::FRT in χ3306, ΔSsaB	This study
CS4863	Δ*gtgE*::FRT in χ3306, ΔGtgE	This study
CS4864	Δ*sseFG*::FRT in χ3306, ΔSseFG	This study
CS10004	Δ*aroA*::FRT in χ3306, ΔAroA	This study
CS10135	Δ*ssaG*::FRT in χ3306, ΔSsaG	Takaya *et al.*, JBC (2019)
CS10216	Δ*srfJ*::FRT in χ3306, ΔSrfJ	This study
CS10218	Δ*steD*::Cm in χ3306, ΔSteD	This study
CS10221	Δ*steA*::FRT in χ3306, ΔSteA	This study
CS10222	Δ*steB*::FRT in χ3306, ΔSteB	This study
CS10223	Δ*steD*::FRT in χ3306, ΔSteD	This study
CS10224	Δ*sseK3*::FRT in χ3306, ΔSseK3	This study
CS10225	Δ*steE*::Cm in χ3306, ΔSteE	This study
CS10226	Δ*steE*::FRT in χ3306, ΔSteE	This study
CS10227	Δ*slrP*::FRT in χ3306, ΔSlrP	This study
CS10228	Δ*sarA*::Cm in χ3306, ΔSarA	This study

Km: Kanamycin-resistant gene, 25 μg/mL; Cm: Chloramphenicol-resistant gene, 20 μg/mL; FRT: Flp recognition target.

h, followed by two washings with 1 × PBS. Then, 1-mL/well DMEM supplied with 10% heat-inactivated FBS and 100 μg/mL gentamicin was added into the well. The infected Hela cells were continually incubated at 37°C in the humidified incubator with 5% CO_2 for another 16 h.

2.6. Quantitative real-time polymerase chain reaction (qPCR)

SYBR Premix Ex Taq II (Takara) was employed to amplify the genomic DNA. A Thermal Cycler Dice Real Time System (Takara) was used to conduct qPCR analysis.

2.7. Western blot (WB)

Cells were collected with 80 μL 2 × SDS loading buffer, followed by ultrasonication, centrifugation at 4°C, and boiling at 98°C for 3 min. Lysates were resolved by 10% SDS-PAGE and a semi-dry blotter (Bio-Rad Laboratories, Hercules, CA) was used to transfer to polyvinylidene difluoride (PVDF) membranes (Millipore). After being blocked with 3% BSA for 1 h at room temperature, the PVDF membranes were incubated with the indicated primary antibodies (anti-MTR4 antibody was generated during a previous study (*25*), anti-RRP6 was purchased from abcam in the UK) for 1 h at room temperature, followed by incubating with the corresponding secondary antibodies conjugated to horseradish peroxidase (HRP) (Millipore, USA) for 1 h at room temperature. The chemiluminescence signals were detected with a Luminescent Image Analyzer (LAS-4000, Fujifilm) after addition of HRP substrate (Millipore).

Table 2. Oligonucleotides used for construction of mutant strains and plasmids in this study: Construction of *Salmonella* mutants

Primer	Sequence
AroA-P1-F	tccctgacgttacaacccatcgcgcgggtcgatggcgccagtgtaggctggagctgcttc
AroA-P2-R	ggtccaggatcgtaactggcgtatcggacagtgcgaccagcatatgaatatcctccttag
AroA-check-F	gtgttgttggcggtatgcgc
AroA-check-R	gtcgactggcgcaacagaag
GogB-P1-F	agccatattgcaatatgcatatacaagtaacgaggcgacagtgtaggctggagctgcttc
GogB-P2-R	gatcatcatgtcgattccgatatacccatcttagctcatgcatatgaatatcctccttag
GogB-check-F	ttgctgaatcggctaacagc
GogB-check-R	catgtagtctagagttaggg
GtgE-P1-F	taggcagcgtttacagaagtaatacagcaactcctcaggggtgtaggctggagctgcttc
GtgE-P2-R	aactatcataaaatggtacaccagtctttccaggaggaggcatatgaatatcctccttag
GtgE-check-F	tagccacctccccaaaatcc
GtgE-check-R	ttcaccccatagcttccccg
PipB2-P1-F	tgataaattttatcatgcactgtgttgctgtctctgggaggtgtaggctggagctgcttc
PipB2-P2-R	tgtttgtgtgcttgtagacattgtggcgtcttcagtacgccatatgaatatcctccttag
PipB2-check-F	gcagcacatgcaacttgaag
PipB2-check-R	ctcagctactattcagtagc
SifA-P1-F	gtgaaatccttaccaactccccaaggaatacgaaagaagcgtgtaggctggagctgcttc
SifA-P2-R	aacagccgctttgttgttctgagcgaacgtgtagcgtggtcatatgaatatcctccttag
SifA-check-F	cgcagttgagataaaaaggg
SifA-check-R	ggaagtacgtgagtaaaccc
SifB-P1-F	aaagagtgagatgttttctcaaagtgctatctctcaacgcgtgtaggctggagctgcttc
SifB-P2-R	atactatttatggtgtgatcaactctggtgatgagcctcacatatgaatatcctccttag
SifB-check-F	tcaggtgtttcaccgatagg
SifB-check-R	cgagccaattcgttccatag
SrfJ-P1-F	ccggaacttccctatgaaaggcagactcatctcttccgatccggtgtaggctggagctgcttc
SrfJ-P2-R	catagcaacgtactggcgcctgacggcggcagcgttaacgcatatgaatatcctccttag
SrfJ-check-F	atcgtctgaacgcaggattg
SrfJ-check-R	tccgcccagctttcgctatc
SsaB-P1-F	ctcccatttatgtctgaggagggattcatgctggcagtttgtgtaggctggagctgcttc
SsaB-P2-R	tgtggtataataaccgtttaaccatcccccatccgctgtgcatatgaatatcctccttag
SseF-P1-F	gcggcaagtaatatagtcgatggtaatagtcctccttccggtgtaggctggagctgcttc
SseF-check-F	gttatgcggatgcctcatgg
SseG-P2-R	tccggcgcacgttgttctggcgttacctgagccagcaaaccatatgaatatcctccttag
SseI-P1-F	catattggaagcggatgtcttcccgccatcatcagtaaccgtgtaggctggagctgcttc
SseI-P2-R	gttctgacagacgtcctccacggtgcgcttacattttacccatatgaatatcctccttag
SseI-check-F	gaaattaaggccaggaagag
SseI-check-R	ctgtcatctgtgatagtgtc
SseJ-P1-F	gcgtgtttaataaagtaaggaggacactatgccattgagtggtgtaggctggagctgcttc
SseJ-P2-R	tgctcaaggcgtaccgcagccgatggaactttattcagtgcatatgaatatcctccttag
SseJ-check-F	atgtaccaggcattaacctc
SseJ-check-R	cggtggcgatttatcgactc
SseK1-P1-F	ttatgatcccaccattaaatagatatgttcccgcgctttcgtgtaggctggagctgcttc
SseK1-P2-R	ccatttccgctactgcacatgcctcgcccatgaactttgccatatgaatatcctccttag
SseK1-check-F	tagctgacagcgattgcaac
SseK1-check-R	atatctccgttctgaacagc
SseK2-P1-F	aagtaatactcaaaccatcgcacctacgctcagtccacctgtgtaggctggagctgcttc
SseK2-P2-R	ggctatcatgattacctccaagaactggcagttaaactgccatatgaatatcctccttag
SseK2-check-F	cgcttaggtttagagacctc
SseK2-check-R	tggctctcaacttctcactc
SseK3-P1-F	gcaactccagctattactctgccttcatcaggtagtgcaaacgtgtaggctggagctgcttc
SseK3-P2-R	gccttagcccaccgcagacaccatcaatgtatggatcgcccatatgaatatcctccttag
SseL-P1-F	aagaggtgagcgatgaggcgcttacattgttgtttagcgcgtgtaggctggagctgcttc
SseL-P2-R	tactggagactgtattcatatatttgccgccgggtttgggcatatgaatatcctccttag
SseL-check-F	tgtatcgacgcgttaccagc
SseL-check-R	gtggttgaatcattgacggc
SteA-P1-F	gttgattgacatatcgtcataatgagagaggagtaggacgtgtaggctggagctgcttc
SteA-P2-R	agttatggtagcgagcttttatgtcggccgcccattgcgccatatgaatatcctccttag
SteA-check-F	cggcagtgattgcgttgc
SteA-check-R	ctgaggcggatatcgctg
SteB-P1-F	atctcaaccctgtgtctttccaggcttagtcaatgtggacgtgtaggctggagctgcttc
SteB-P2-R2	ctgtggaatagcaatgccgggaaggacatggcatgacactcatatgaatatcctccttag
SteB-check-F	gcagatgtcagtcttgtaag
SteB-check-R	gaccagaagatgggcactct
SteC-P1-F	gcgagatgaagactgtacacgatggcgccccctttcttggagtgtaggctggagctgcttc
SteC-P2-R	atacctagccacaagagtcccttcctccggcgcggctagcatatgaatatcctccttag
SteC-check-F	cagaggatgagacatatgccg

3. Results

3.1. Live *Salmonella*, but neither heat-killed *Salmonella* nor LPS, induces loss of MTR4 and RRP6

Our previous study showed that *Salmonella* infection induces loss of MTR4 and RRP6, which are important components of the RNA exosome for RNA degradation in the nucleus, thus stabilizing the labile lncRNAs (*25*).

Table 2. Oligonucleotides used for construction of mutant strains and plasmids in this study: Construction of *Salmonella* mutants (continued)

Primer	Sequence
SteC-check-R	atctgtagcgaatgtgcccc
SteD-P1-F	atgaatgtcacttcaggcgtgaatgcgcaaacgccattgcgtgtaggctggagctgcttc
SteD-P2-R	ctatgacttgctgtgtttgctcatttatggccaggctggccatatgaatatcctccttag
SteD-check-F	gtgcagtcgacgtgcatgaagaggtttatatg
SteD-check-R	ggctcttgaatacataacacc
SteE-P1-F	gcgcgtttaacgcaggcgccacgttggtggtggattaccagtgtaggctggagctgcttc
SteE-P2-R	atgcaggccgcgccgtgtaataacgcctgtcttttagccacatatgaatatcctccttag
SteE-check-F	gcaaaccgatgtcgatgg
SteE-check-R	agcgccgaatcgcaatcc
sarA-P1-F	taatagtactaacagggtggcgagcacaatcgctccatatgcatgtggtgtaggctggagctgcttc
sarA-P2-R	gatataaccggacggtgggttatgactggctggggtagtgcaactggcatatgaatatcctccttag
pipA-P1	gctccggtcacctacagattaatacctcaaagcggagtagtgtaggctggagctgcttc
pipA-P2	agatgtagaccattctgggaggtgaaggatgccccatctccatagaatatcctccttag
pipA-check-F	cgctaacatgtccggtgtaa
pipA-check-R	ggtcaatgtgccgctatttc
gtgA-P1	gtgtcttgctgaataccttatctctggaccaggaggaatggtgtaggctggagctgcttc
gtgA-P2	cgtaggcgattcttggtggtgatgtgtgacccatctctttcatatgaatatcctccttag
gtgA-check-F	aaatggttgggttgcagggt
gtgA-check-R	gaacttacccagagcggtgt
gogA-P1	ggattatccaatcctcatgacagcaaggtatttccagaccgtgtaggctggagctgcttc
gogA-P2	ctagattcgtaggcgattcttggtggtgatgtgtgacccacatatgaatatcctccttag
gogA-check-F	atctggggccacgcatttttt
gogA-check-R	ttactacacccacggcgtaa
avrA -P1	tggtagcctggctcaatcattgaggcatatttttgcaggcgtgtaggctggagctgcttc
avrA-P2	agtcttatggcgctggaaggatttcctctggcaggcaacccatatgaatatcctccttag
avrA-check-F	gccacaggccacaaaagaaa
avrA-check-R	atcctgtttggggatatgct
sptP-P1	attgctaaggaaaatactgataaggcatatgttgcgcctggtgtaggctggagctgcttc
sptP-P2	cagcttgccgtcgtcataagcaactgggcttgcattgcttcatatgaatatcctccttag
sptP-check-F	taatggtgaactggctgcga
sptP-check-R	tgtgggcgcctccattttat
pipB-P1	gagttctatcattgtaatccgggagtggagtaggggtatggtgtaggctggagctgcttc
pipB-P2	tgcatgcggccggtaccggtacgaaagaagcaatgaaaagcatatgaatatcctccttag
pipB-check-F	ggtttttacgccatctacgc
pipB-check-R	aatatcggggaaaacaggtg
pipC-P1	tacgtatcgcgttttatctcattaagaaagtatgttgacggtgtaggctggagctgcttc
pipC-P2	cgtttatatgacgcgttaggcctggatgcgccagaagatgcatatgaatatcctccttag
pipC-check-F	agatcgtacagggatgatgg
pipC-check-R	tgagtaggtgtctggcatct
sopD2-P1	ggggccttttaatgacttttttatataagcatattgcgacgtgtaggctggagctgcttc
sopD2-P2	cggctagcccgtttgatgagtcctgataaagaagaagcgccatatgaatatcctccttag
sopD2-check-F	ctgtttatgatccgcctctt
sopD2-check-R	gcaggtctgatggatggtta
prgI-P1	ccaggccattggtatttcccaagcccactttaatttaacggtgtaggctggagctgcttc
prgI-P2	ggacaatagttgcaatcgacataatccaccttataactgacatatgaatatcctccttag
prgI check-F	caagaaagagctcgaggtgt
prgI check-R	gcaagggtcattaccagcag
sspH2-P1-	tggaagcggatgtcttcccgccaccatcagtaatcgccgcgtgtaggctggagctgcttc
sspH2-P2	ctaaggaggatattcatatgcaggtgaatgaggtgcggtgcgacaaagatattcccggac
sspH2-check-F	cagcagagtatgatgctgtc
sspH2-check-R	gattgtatctggtaaccggc
slrP-P1	gcatcaaagtattagcaatgaggcctcaacagaggtgcctgtgtaggctggagctgcttc
slrP-P2	ctaaggaggatattcatatgcggtgtaaacaggcttctgataagcgcagcgtcgtcggta
slrP-check-F	ccctgtatgccaacagtaatc
slrP-check-R	gaaggacctcaacctacaag

First, we considered whether only live *Salmonella* induces loss of MTR4 and RRP6. MTR4 and RRP6 were not decreased upon heat-killed *Salmonella* infection (Figure 1). In addition, LPS did not decrease MTR4 and RRP6. These show that live *Salmonella*, but not dead *Salmonella*, induces MTR4 and RRP6 degradation.

3.2. MTR4 and RRP6 decrement upon *Salmonella* infection

Both MTR4 and RRP6 are important components of the RNA exosome in the mammalian nucleus. Upon wild type *Salmonella* infection, both MTR4 and RRP6 decreased dramatically (25). We hypothesized that MTR4 and RRP6 are not degraded by infection if important effector(s) involved in the degradation of these proteins are mutated. As shown in Table 1, 42 *Salmonella* mutant strains were constructed. WB analysis was performed to examine the degradation of MTR4 and RRP6 upon infection of these mutant strains. As shown in Figure 2, all 36 strains induced loss of MTR4 and RRP6, except ΔHilCΔHilD, ΔHilD, ΔPrgI, ΔFlhDΔFlhC, ΔClpXP and ΔAroA.

3.3. Examination of proliferation of *Salmonella* mutant strains

Considering the growth condition of these mutant strains, next, we examined the proliferation of mutant strains in HeLa cells by monitoring the amount of the 16S ribosomal RNA gene (16S rRNA gene). Among these mutants, six mutant strains, ΔHilD, ΔHilCΔHilD, ΔPrgI, ΔFlhDΔFlhC, ΔClpXP, and ΔAroA, did not grow well in the cells. HilC and HilD, transcriptional regulators encoded in SPI-1, are co-regulated and directly activate the expression of HilA (*26*), the central player of T3SS-1 regulation. In addition, HilD is necessary for activating regulons of both SPI-1 and SPI-2 (*8*). PrgI constitutes the needle of the T3SSs and is of great importance to effector translocation (*27*). T3SSs derive from flagella and still share regulatory mechanisms with them (*28-30*), after mutating the gene of the flagellum, the mutant strain ΔFlhDΔFlhC also showed a poor proliferation (shown in Figure 3). The ClpXP protease, a member of the ATP-dependent protease family, is reported to regulate flagellum synthesis and SPI-1 expression negatively through $FlhD_4C_2$ degradation (*10,31,32*). As an auxotrophic mutation, deletion of *aroA* is commonly studied for attenuation without losing the ability of immunostimulation. Felgner *et al.* found that deletion of *aroA* affects flagellin phase variation and the expression of virulence-associated the *arnT* and *ansB* genes (*33*). These genes, which show a poor proliferation, may greatly contribute to *Salmonella* invasion and/or proliferation in host cells.

4. Discussion

Salmonella infection induces an immune response in the host cells by invading and replicating inside the host cells. Lundberg *et al.* found that the expression of several invasion genes are growth phase regulated and correlate

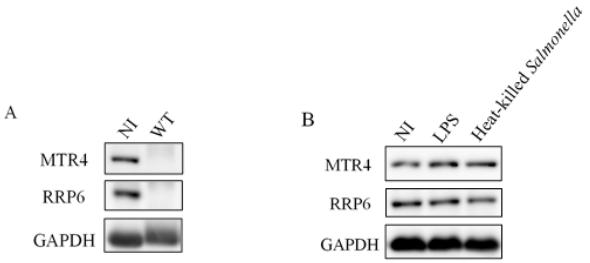

Figure 1. Alive *Salmonella*, but not heat-killed *Salmonella* or LPS, induced loss of MTR4 and RRP6. (A) MTR4 and RRP6 degradation upon *Salmonella* infection. NI: no infection; WT: wild type *Salmonella*. **(B)** LPS and heat-killed *Salmonella* did not induce loss of MTR4 and RRP6.

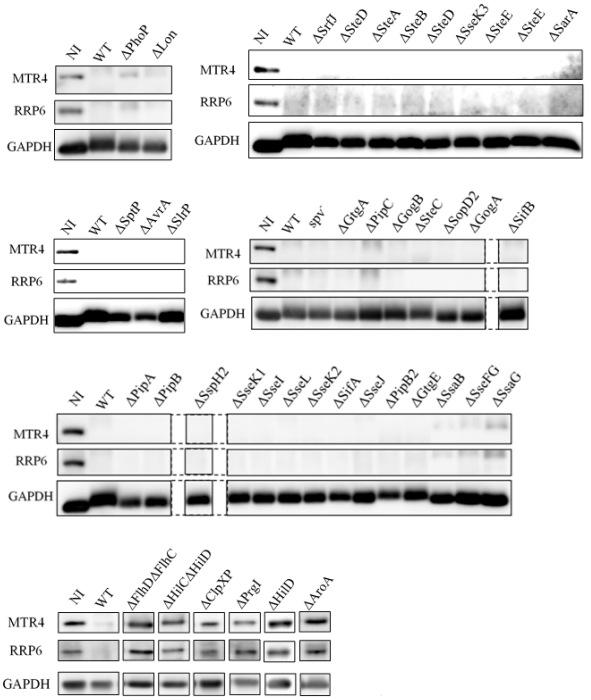

Figure 2. Investigation of loss of MTR4 and RRP6 in response to infection of *Salmonella* mutant strains. MTR4 and RRP6 were determined by WB.

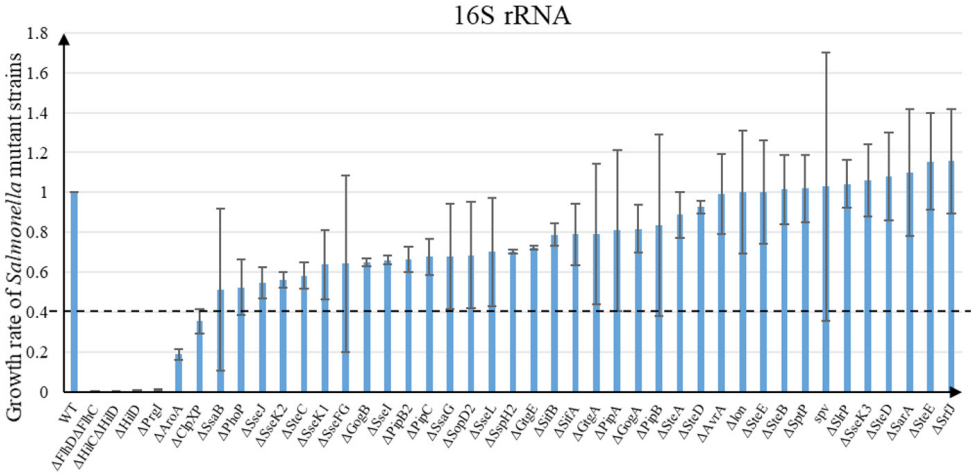

Figure 3. Proliferation of the 42 *Salmonella* mutant strains. To examine proliferation of *Salmonella* mutant strains, increment of 16S rRNA gene was measured by genomic PCR. 6 bars below the dashed line indicate the 6 mutant strains which did not grow well (< 40%). Data are shown as mean ± SD (n = 3).

with apoptosis induction (*34*). Together with a series of effectors translocated by T3SSs, several regulators were also examined in our study. Our results showed that *Salmonella* mutant strains ΔClpXP, ΔHilD, ΔHilCΔHilD, ΔPrgI, and ΔAroA show poor proliferation, suggesting that *clpP*, *hilD*, *hilC*, *prgI*, and *aroA* are important factors for invasion and/or proliferation in host cells. Flagella are essential structures of bacteria. They provide the motility of *Salmonella* and increase adhesion to the host cells, thus facilitating the invasion process during host cell infection and triggering of the host immune system (*35*). Thus, the *Salmonella* mutant strain ΔFlhDΔFlhC showed a poor proliferation in host cells after the flagellum gene (*flhD*) mutated. The poor proliferation may have been caused by attenuate adhesion or invasion abilities after the *flhD* mutated. In addition, ClpXP and AroA were reported to be involved in flagellum synthesis or flagellin phase variation (*31,33*).

In this study, although we mainly explored the effectors contributing to the degradation of MTR4 and RRP6, none of the well grown mutant strains canceled the degradation of MTR4 and RRP6. Several possibilities may contribute to this result. First, there may be no such effector for inducing loss of MTR4 and RRP6; instead, the loss might be the result of a complex immune response rather than a specific gene. In addition, a previous study showed that killed *Salmonella* or its LPS cannot induce lncRNA or eRNA, which may indicate that only those *Salmonella*e that are alive and able to invade the host cells can induce loss of MTR4 and RRP6 (*25*). Our study indicates that certain events associated with *Salmonella* proliferation in the host cell causes loss of MTR4 and RRP6, resulting in nuclear RNA stabilization. Because limited mutants were examined here, we cannot exclude the possibility that there might be such genes, but they are not included in the mutants that we constructed.

Acknowledgements

This work was supported by a MEXT grant KAKENHI (18H02570 and 17KK0163) and Takeda Science Foundation.

References

1. Moest T, Méresse S. *Salmonella* T3SSs: Successful mission of the secret (ion) agents. Curr Opin Microbiol. 2013; 16:38-44.
2. Hansen-Wester I, Hensel M. *Salmonella* pathogenicity islands encoding type III secretion systems. Microbes Infect. 2001; 3:549-559.
3. Figueira R, Holden D. Functions of the *Salmonella* pathogenicity island 2 (SPI-2) type III secretion system effectors. Microbiology. 2012; 158:1147-1161.
4. Bäumler AJ, Tsolis R, Ficht T, Adams L. Evolution of host adaptation in *Salmonella enterica*. Infect Immu. 1998; 66: 4579-4587.
5. Ellermeier C, Ellermeier J, Slauch J. HilD, HilC and RtsA constitute a feed forward loop that controls expression of the SPI1 type three secretion system regulator hilA in *Salmonella enterica* serovar Typhimurium. Mol Microbiol. 2005; 57:691-705.
6. Ellermeier J, Slauch J. Adaptation to the host environment: regulation of the SPI1 type III secretion system in *Salmonella enterica* serovar Typhimurium. Curr Opin Microbiol. 2007; 10:24-29.
7. Lim S, Lee B, Kim M, Kim D, Yoon H, Yong K, Kang D, Ryu S. Analysis of HilC/D-dependent invF promoter expression under different culture conditions. Microb Pathog. 2012; 52:359-366.
8. Bustamante V, Martínez L, Santana F, Knodler L, Steele-mortimer O, Puente J. HilD-mediated transcriptional cross-talk between SPI-1 and SPI-2. Proc Natl Acad Sci U S A. 2008; 105:14591-14596.
9. Gophna U, Ron EZ, Graur D. Bacterial type III secretion systems are ancient and evolved by multiple horizontal-transfer events. Gene. 2003; 312:151-163.
10. Kage H, Takaya A, Ohya M, Yamamoto T. Coordinated regulation of expression of *Salmonella* pathogenicity island 1 and flagellar type III secretion systems by ATP-dependent ClpXP protease. J Bacteriol. 2008; 190:2470-2478.
11. Singer H, Kühne C, Deditius JA, Hughes KT, Erhardt M. The *Salmonella* Spi1 virulence regulatory protein HilD directly activates transcription of the flagellar master operon *flhDC*. J Bacteriol. 2014; 196:1448-1457.
12. Uchiya K, Sugita A, Nikai T. Involvement of SPI-2-encoded SpiC in flagellum synthesis in *Salmonella enterica* serovar Typhimurium. BMC Microbiol. 2009; 9:1-10.
13. Meola N, Domanski M, Karadoulama E, Chen Y, Gentil C, Pultz D, Vitting-Seerup K, Lykke-Andersen S, Andersen J, Sandelin A, Jensen T. Identification of a Nuclear Exosome Decay Pathway for Processed Transcripts. Mol Cell. 2016; 64:520-533.
14. Schneider C, Tollervey D. Threading the barrel of the RNA exosome. Trends Biochem Sci. 2013; 38:485-493.
15. Han J, van Hoof A. The RNA Exosome Channeling and Direct Access Conformations Have Distinct In Vivo Functions. Cell Rep. 2016; 16:3348-3358.
16. Hernández H, Dziembowski A, Taverner T, Séraphin B, Robinson C. Subunit architecture of multimeric complexes isolated directly from cells. EMBO Rep. 2006; 7:605-610.
17. Liu Q, Greimann J, Lima C. Reconstitution, Activities, and Structure of the Eukaryotic RNA Exosome. Cell. 2006; 127:1223-1237.
18. Shen V, Kiledjian M. A View to a Kill: Structure of the RNA Exosome. Cell. 2006; 127:1093-1095.
19. Cristodero M, Böttcher B, Diepholz M, Scheffzek K, Clayton C. The Leishmania tarentolae exosome: Purification and structural analysis by electron microscopy. Mol Biochem Parasitol. 2008; 159:24-29.
20. Allmang C, Petfalski E, Podtelejnikov A, Mann M, Tollervey D, Mitchell P. The yeast exosome and human PM-Scl are related complexes of 3→5 exonucleases. Genes Dev. 1999; 13:2148-2158.
21. Tomecki R, Kristiansen M, Lykke-Andersen S, Chlebowski A, Larsen K, Szczesny R, Drazkowska K, Pastula A, Andersen J, Stepien P, Dziembowski A, Jensen T. The human core exosome interacts with differentially localized processive RNases: HDIS3 and hDIS3L. EMBO J. 2010; 29:2342-2357.
22. Schuch B, Feigenbutz M, Makino D, Falk S, Basquin C,

Mitchell P, Conti E. The exosome-binding factors Rrp6 and Rrp47 form a composite surface for recruiting the Mtr4 helicase. EMBO J. 2014; 33:2829-2846.
23. Lubas M, Christensen M, Kristiansen M, Domanski M, Falkenby L, Lykke-Andersen S, Andersen J, Dziembowski A, Jensen T. Interaction Profiling Identifies the Human Nuclear Exosome Targeting Complex. Mol Cell. 2011; 43:624-637.
24. Kilchert C, Wittmann S, Vasiljeva L. The regulation and functions of the nuclear RNA exosome complex. Nat Rev Mol Cell Biol. 2016; 17:227-239.
25. Imamura K, Takaya A, Ishida Y, , *et al.* Diminished nuclear RNA decay upon *Salmonella* infection upregulates antibacterial noncoding RNAs. EMBO J. 2018; 37:e97723.
26. Boddicker JD, Knosp BM, Jones BD. Transcription of the *Salmonella* invasion gene activator, hilA, requires HilD activation in the absence of negative regulators. J Bacteriol. 2003; 185:525-33.
27. Loquet A, Sgourakis N, Gupta R, Giller K, Riedel D, Goosmann C, Griesinger C, Kolbe M, Baker D, Becker S, Lange A. Atomic model of the type III secretion system needle. Nature. 2012; 486:276-279.
28. Lin D, Rao CV, Slauch JM. The *Salmonella* SPI1 type three secretion system responds to periplasmic disulfide bond status *via* the flagellar apparatus and the RcsCDB system. J Bacteriol. 2008; 190:87-97.
29. Pallen MJ, Beatson SA, Bailey CM. Bioinformatics, genomics and evolution of non-flagellar type-III secretion systems: a Darwinian perspective. FEMS Microbiol Rev. 2005; 29:201-229.
30. Wang Q, Zhao Y, McClelland M, Harshey RM. The RcsCDB signaling system and swarming motility in *Salmonella enterica* serovar typhimurium: dual regulation of flagellar and SPI-2 virulence genes. J Bacteriol. 2007; 189:8447-8457.
31. Tomoyasu T, Ohkishi T, Ukyo Y, Tokumitsu A, Takaya A, Suzuki M, Sekiya K, Matsui H, Kutsukake K, Yamamoto T. The ClpXP ATP-dependent protease regulates flagellum synthesis in *Salmonella enterica* serovar typhimurium. J Bacteriol. 2002; 184:645-653.
32. Tomoyasu T, Takaya A, Isogai E, Yamamoto T. Turnover of FlhD and FlhC, master regulator proteins for *Salmonella* flagellum biogenesis, by the ATP-dependent ClpXP protease. Mol Microbiol. 2003; 48:443-452.
33. Felgner S, Frahm M, Kocijancic D, Rohde M, Eckweiler D, Bielecka A, Bueno E, Cava F, Abraham W, Curtiss R, Häussler S, Erhardt M, Weiss S. *aroA*-Deficient *Salmonella enterica* Serovar Typhimurium Is More Than a Metabolically Attenuated Mutant. mBio. 2016; 7:e01220-16.
34. Lundberg U, Vinatzer U, Berdnik D, Von Gabain A, Baccarini M. Growth phase-regulated induction of *Salmonella*-induced macrophage apoptosis correlates with transient expression of SPI-1 genes. J Bacteriol. 1999; 181:3433-3437.
35. Ramos H, Rumbo M, Sirard J. Bacterial flagellins: Mediators of pathogenicity and host immune responses in mucosa. Trends Microbiol. 2004; 12:509-517.

Received April 13, 2020; Revised April 25, 2020; Accepted April 27, 2020

**Address correspondence to:*
Nobuyoshi Akimitsu, Isotope Science Center, The University of Tokyo, 2-11-16 Yayoi, Bunkyo-ku, Tokyo 113-0032, Japan.
E-mail: akimitsu@ric.u-tokyo.ac.jp

Released online in J-STAGE as advance publication April 30, 2020.

Original Article

DOI: 10.5582/bst.2020.03125

The cytotoxicity of advanced glycation end products was attenuated by UCMSCs in human vaginal wall fibroblasts by inhibition of an inflammatory response and activation of PI3K/AKT/PTEN

Lisha Li[1,2,3], Yizhen Sima[1], Yan Wang[1], Jing Zhou[1,2,3], Ling Wang[1,2,3,*], Yisong Chen[1,*]

[1] Obstetrics and Gynecology Hospital of Fudan University, Shanghai, China;
[2] The Academy of Integrative Medicine of Fudan University, Shanghai, China;
[3] Shanghai Key Laboratory of Female Reproductive Endocrine-related Diseases, Shanghai, China.

SUMMARY Pelvic organ prolapse (POP) occurs when the pelvic organs (bladder, bowel or uterus) herniate into the vagina, causing incontinence, voiding, and bowel and sexual dysfunction, negatively impacting upon a woman's quality of life. Intermediate intermolecular cross-links and advanced glycation cross-links increase in prolapsed tissue. Stem cells are able to participate in tissue repair due to their ability to differentiate into multiple lineages, and thus into various types of connective tissue cells, so they therefore hold great promise for treating pelvic floor dysfunction. The current study found that advanced glycation end products (AGEs) inhibited the viability and proliferation of human vaginal wall fibroblasts (VWFs), were cytotoxic to VWFs, and also induced the apoptosis of VWFs. In contrast, umbilical cord-derived mesenchymal stem cells (UCMSCs) secreted anti-inflammation cytokines to protect against the cytotoxic effects of fibroblasts induced by AGEs and attenuated the cytotoxic effect of AGE on fibroblasts by activation of the PI3K/Akt-PTEN pathway. This study demonstrated that UCMSCs inhibited the cytotoxic effect of AGE in cells from patients with POP by inducing an anti-inflammatory reaction and activating the PI3K/AKT/PTEN signaling pathway. The current results provide important insights into use of stem cells to treat POP.

Keywords pelvic organ prolapse; advanced glycation end products; umbilical cord-derived mesenchymal stem cells; cytokines; PI3K-AKT

1. Introduction

Pelvic floor dysfunction (PFD) is the term for a group of clinical conditions, including stress urinary incontinence (SUI), pelvic organ prolapse (POP), overactive bladder syndrome, and fecal incontinence (*1,2*). In the general population, POP is an exceedingly common condition for mature women, with an estimated 41% presenting to their primary gynecologist with prolapse (*3*). PFD is primarily caused by aging and parity, and there are bimodal peaks of POP in these women at the ages of 46 and 71 (*4*). Treatments for this condition are still conservative and symptom-based. Women with symptoms who failed to respond to or who chose not to receive conservative treatment are candidates for surgery. Traditionally, surgeries include anterior, posterior, or total repair of the vagina, with concomitant hysterectomy, but the rate of recurrence can be as high as 20-30 % (*5,6*). Synthetic and biomaterial meshes have recently been used during surgery to provide improved long-term outcomes; however, about one-third of meshes cause scarring, erosion, and pain (*7*). Alternative methods are therefore needed to promote the repair and regeneration of damaged tissues.

In the supportive system of the pelvic floor, fibrous connective tissues surrounding the pelvic organs form fascia and ligaments to provide mechanical strength to support the vagina and its adjacent organs. Due to their specific anatomical location, these tissues are subjected to constant mechanical tensile loading from abdominal pressure and gravity (*8*). The fascia and ligaments of the pelvic floor mainly consist of dense connective tissues containing fibroblasts and extracellular matrix (ECM) secreted by fibroblasts.

Advanced glycation end products (AGEs), the products of nonenzymatic glycation and oxidation of proteins and lipids, accumulate in diverse biological settings including: diabetes, inflammation, renal failure, and aging (*9*). In a study examining the actual role of AGEs in the pathological physiology of POP, Jackson *et al.* found that both intermediate intermolecular cross-links and advanced glycation cross-links increased in

prolapsed tissue (*10,11*). AGEs can affect the metabolism of collagen through the receptor for AGEs (RAGE) but not directly through changes in expression or structure. AGEs activate the p-p38 MAPK and NF-κB-p-p65 pathways, thereby regulating collagen metabolism, although other pathways may also be involved (*12*). Taken together, these findings provide an enhanced understanding of the mechanism through which AGEs contribute to collagen metabolism in pelvic tissue of POP and the pathophysiology of POP.

Stem cells are able to participate in tissue repair due to their ability to differentiate into multiple lineages, and thus into various types of connective tissue cells, so they therefore hold great promise for treating PFD (*13*). Bone marrow-derived mesenchymal stem cells (BMSCs) are one of the most well-characterized stem cell sources, have great differentiation capability, and secrete bioactive factors that facilitate tissue repair (*14,15*). In animal models of SUI, periurethral injection of BMSCs restored the damaged external urethral sphincter and significantly alleviated SUI symptoms (*16*). Tissue engineering (TE) approaches have been used in different areas of medicine to improve long-term outcomes of surgical interventions (*17*). BMSCs are believed to regulate the repair process at sites of injured tissue by interacting with essential endogenous cells involved in the healing process: fibroblasts, endothelial cells, and epithelial cells (*18,19*). Umbilical cord-derived mesenchymal stem cells (UCMSCs) are isolated from the human umbilical cord and have better cell content and greater ability to proliferate than BMSCs. UCMSCs have lower immunogenicity than BMSCs, are easy to obtain, and cause no ethical controversy, so they have attracted increasing attention from researchers (*20*).

The current study investigated the anti-inflammatory role of UCMSCs and signaling pathways to inhibit the cytotoxic effect of AGEs in POP. Those findings were analyzed to determine if UCMSCs could serve as a potential treatment that reduces cell damage.

2. Materials and Methods

2.1. Culture of human UCMSCs and human vaginal wall fibroblasts (VWFs)

Human UCMSCs were purchased from the Shanghai Branch of Chinese Academy of Science and cultured in Gibco Dulbecco's Modified Eagle Medium: Nutrient Mixture F-12 (DMEM/F-12) containing 10% fetal bovine serum (FBS), 100 U/mL penicillin, and 100 mg/mL streptomycin at 37°C in a 5% CO_2 atmosphere.

Human fibroblasts derived from the vaginal wall were obtained from patients suffering from POP or other diseases who underwent a hysterectomy at the Obstetrics and Gynecology Hospital of Fudan University. Ethical approval was obtained from the Ethics Committee of the Obstetrics and Gynecology Hospital of Fudan University. Briefly, fresh vaginal wall tissue specimens from the surgical margin of the free womb were rinsed 3 times with phosphate-buffered saline (PBS) (containing 1% penicillin, streptomycin, amphotericin B) at 4˚C for 5 min and digested at 37˚C for 30 min in PBS containing 2% collagenase. After separation, the cells were cultured in Dulbecco's modified Eagle's medium (DMEM) (containing 10% fetal bovine serum, 1% penicillin, streptomycin, and amphotericin B) at 37.5˚C in a 5% CO_2 atmosphere, with replacement of the culture medium every 2-3 days. VWFs were identified using anti-vimentin antibody staining and subsequently stored in liquid nitrogen for further study.

2.2. Co-culture of human UCMSCs with VWFs

Human UCMSCs were co-cultured with VWFs by seeding UCMSCs (5×10^4 cells/dish) and fibroblasts (1×10^5 cells/dish) onto DMEM/F-12 culture medium.

2.3. Cell treatment and chemicals

VWFs or co-cultured cells were treated with AGEs at various concentrations (0, 25, 50, 100, and 200 μg/mL) in DMEM/F-12 containing 10% FBS for 2 days and then used for subsequent experiments. Untreated cells served as the control group (con). The PI3K inhibitor LY294002 and the Akt inhibitor GSL 690693 were purchased from Selleckchem (Houston, TX, USA).

2.4. Annexin V/PI double-staining

The fibroblasts from each treatment group were harvested and washed with PBS twice before being labeled with Annexin V/PI double-staining (KeyGen Biotech, China) in the dark, as described previously. All samples were analyzed with flow cytometry (Becton Dickinson, Franklin Lakes, NJ, USA) using the analytical software Cell Quest (BD, USA).

2.5. Real-time cell analyzer (RTCA) system

The xCELLigence RTCA DP System (ACEA Biosciences, San Diego, California, USA) allows label-free and real-time monitoring of cellular processes, such as cell proliferation, cytotoxicity, adhesion, viability, invasion, and migration, using electronic cell sensor array technology.

In brief, 50 μL of cell culture medium at room temperature was added to each well of E-plate 16 plates for analysis with the xCELLigence RTCA DP System. The E-plate 16 was then connected to the cell culture incubator and electrical contacts were checked. Background impedance was measured for 24 hours. UCMSCs were resuspended in cell culture medium and

adjusted to 5,000 cells/well. The cell suspension (100 μL) was added to wells containing 50 μL of medium on the E-plate 16 in order to determine the optimum cell concentration. After incubation at room temperature for 30 minutes, the E-plate 16 was placed in the cell culture incubator. Cell adhesion, growth, and proliferation were monitored every hour for a period of up to 24 hours *via* the incorporated sensor electrode arrays of the E-plate 16. After 24 hours, different concentrations of AGEs were added to 200 μL of cell culture medium, and live cells were monitored every 15 minutes for a period of up to 96 hours. Electrical impedance was measured with the RTCA-integrated software of the xCELLigence system as a dimensionless parameter termed CI.

2.6. RNA extraction and real-time RT-PCR

For PCR analysis, total RNA was extracted with an RNA extraction Kit (Axygen, CA, USA) according to the manufacturer's protocol, and the purity and concentration of RNA were measured with a NanoDrop 2000c (Thermo, Fisher, MA, USA). RNA (1 μg) was converted into cDNA using reverse transcriptase (Promega, Madison, USA). The normalization controls for mRNA and miRNA were GAPDH and U6 RNA, respectively. Threshold cycle (Ct) values were calculated using the software supplied with the Applied Biosystems 7900 Real-time PCR system.

2.7. Cytokine analysis

A Bio-Rad Bio-plex 200 suspension array system was used to measure the cytokine levels in cell culture medium. This bead-based Luminex technology allows for analysis of multiple proteins in a single sample. The experimental protocol allows for simultaneous reporting of standards, controls, blanks, and cytokines of interest in duplicate. The human cytokine 15-plex kit included the following cytokines: IL-1β, IL-4, IL-6, IL-10, IL-17A, IL-17F, IL-21, IL-22, IL-23, IL-25, IL-31, IL-33, IFN-γ, sCD40L, and TNF-α. Bio-Rad Bio-plex Data Pro software was used for data analysis to identify the extreme values, data distribution, and to select the range.

2.8. Cell Counting Kit-8 (CCK-8) Assay

Following the protocol for the CCK8 assay (Do-jindo Laboratories, Kumamoto, Japan), cell growth by transfected cells in 96-well plates was assessed at 48 hours. A spectrophotometer (Thermo Fisher Scientific, Waltham, MA, USA) was used to measure the absorbance at 450 nm.

2.9. Statistical analyses

Data were analyzed using the software GraphPad Prism (Version 7). Experimental results were expressed as the mean ± standard error of the mean (SEM). Each value is the mean of the data from an assay performed in triplicate. Data were subjected to analysis of variance (ANOVA), and the Tukey test was used to separate the means. Differences were considered statistically significant at $p < 0.05$.

3. Results

3.1. AGEs inhibited the viability and proliferation of VWFs from patients with PFD

To analyze the effect of AGEs on PFD, human fibroblasts were obtained from the vaginal wall of patients with POP. These fibroblasts were isolated, cultured, and treated with different concentrations of AGEs. Changes in biological function including cell viability, cell apoptosis, and cell proliferation were detected. A CCK-8 assay was used to detect cellular dehydrogenase activity to evaluate the viability of fibroblasts. AGEs were found to significantly decrease the viability of fibroblasts in a dose-dependent manner in all treated groups compared to the control group (Figure 1A). Annexin V/PI double-staining was performed to examine cell apoptosis. AGEs significantly induced the apoptosis of fibroblasts in a dose-dependent manner compared to control cells (Figure 1B). The xCELLigence RTCA DP System was used to monitor cell proliferation in real time. AGEs markedly inhibited the growth of treated cells in a time- and concentration-dependent manner (Figure 1C).

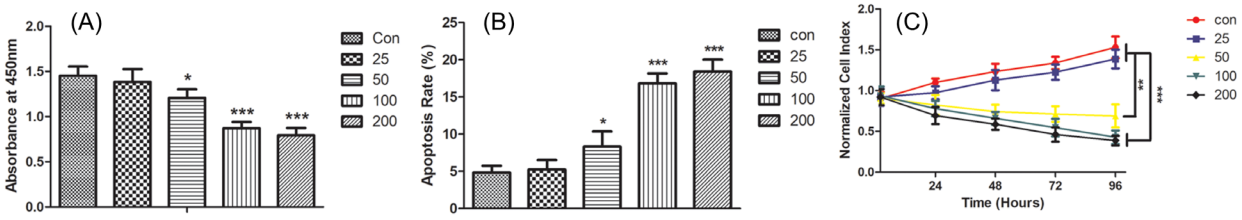

Figure 1. Effect of different concentrations of AGEs on cell viability, apoptosis, and proliferation of vaginal wall fibroblasts from patients with pelvic floor dysfunction. (A) AGEs decreased the viability of fibroblasts in a dose-dependent manner in all treated groups compared to the control group. **(B)** AGEs induced the apoptosis of fibroblasts in a dose-dependent manner compared to control cells. **(C)** AGEs inhibited the growth of treated cells in a time- and concentration-dependent manner. $^{*}p < 0.05$. All results are expressed as the mean ± SEM, and data are representative of at least three experiments.

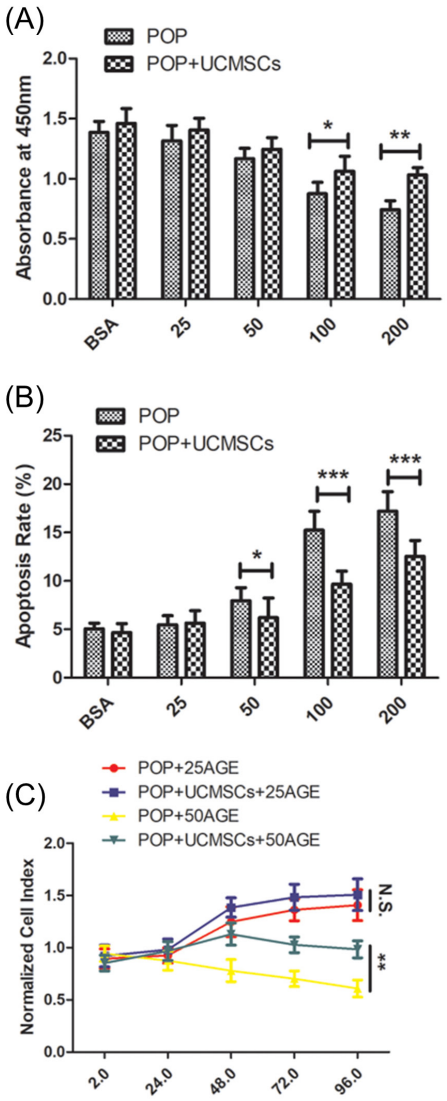

Figure 2. UCMSCs inhibited the cytotoxic effects of fibroblasts induced by AGEs. (A) The viability of fibroblasts co-cultured with UCMSCs and treated with AGEs increased at the concentrations of 100 μg/mL and 200 μg/mL compared to the control. **(B)** UCMSCs decreased the rate of apoptosis in POP treated with AGEs. **(C)** UCMSCs attenuated the inhibitory effect of AGEs on cell proliferation. $^{*}p < 0.05$. All results are expressed as the mean ± SEM, and data are representative of at least three experiments.

3.2. UCMSCs protect fibroblasts against cytotoxic effects induced by AGEs

To determine whether UCMSCs protected against the cytotoxic effects of AGEs, fibroblasts were co-cultured with human UCMSCs and then treated with different concentration of AGEs. Directly cultured fibroblasts treated with different concentration of AGEs served as the corresponding control group. UCMSCs significantly increased the viability of fibroblasts until treatment with AGEs at a concentration of 100 μg/mL compared to the control (Figure 2A). Compared to the control group, cells co-cultured with UCMSCs exhibited a significant reduction in the rate of apoptosis starting at the concentration of 50 μg/mL when treated with AGEs

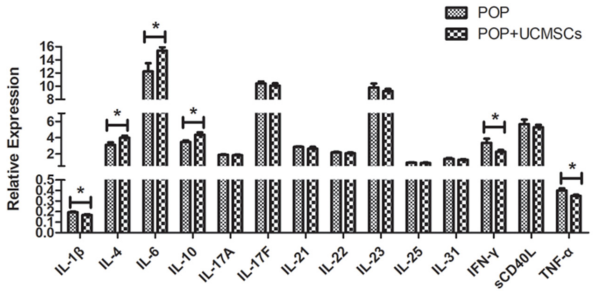

Figure 3. UCMSCs secrete anti-inflammation cytokines to attenuate the cytotoxic effect of AGE in POP. Cytokines from the supernatant of UCMSCs co-cultured with fibroblasts were treated with AGEs at a concentration of 100 μg/mL. $^{*}p < 0.05$. All results are expressed as the mean ± SEM, and data are representative of at least three experiments.

(Figure 2B), and co-culturing attenuated the inhibitory effect of AGEs on cell proliferation (Figure 2C).

3.3. UCMSCs secrete anti-inflammation cytokines to attenuate the cytotoxic effect of AGEs

To explore whether UCMSCs secreted cell factors that affect the cytotoxic effect of AGEs, cytokines from the supernatant of UCMSCs co-cultured with fibroblasts that were treated with AGEs at a concentration of 100 μg/mL were analyzed. The anti-inflammatory cytokines IL-4, IL-6, and IL-10 increased in UCMSCs while the pro-inflammatory cytokines IL-1β, IFN-γ, and TNF-α decreased in UCMSCs compared to fibroblasts cultured alone (Figure 3).

3.4. UCMSCs attenuate the cytotoxic effect of AGE on fibroblasts by activating the PI3K/Akt/PTEN pathway

Compared to the control, co-culturing with UCMSCs significantly enhanced the expression of PI3K and Akt mRNA in fibroblasts that were treated with 100 μg/mL of AGEs. The signaling pathway for that effect was analyzed. PEN modulates apoptosis, and the expression of PTEN mRNA decreased in co-cultured cells (Figure 4A).

Fibroblasts were pre-treated with the PI3K inhibitor LY294002 and the Akt inhibitor GSK 690693. An enhanced cytotoxic effect of AGEs at a concentration of 100 μg/mL was noted in UCMSCs co-cultured with fibroblasts; the rate of apoptosis increased compared to that in untreated cells (Figure 4B). Treatment with these inhibitors had an additive inhibitory effect on proliferation (Figure 4C) and cell viability (Figure 4D).

4. Discussion

The current study investigated whether UCMSCs could attenuate the cytotoxic effect of AGE-induced cell apoptosis in POP and the possible molecular mechanisms allowing UCMSCs to resist AGE-induced cytotoxicity

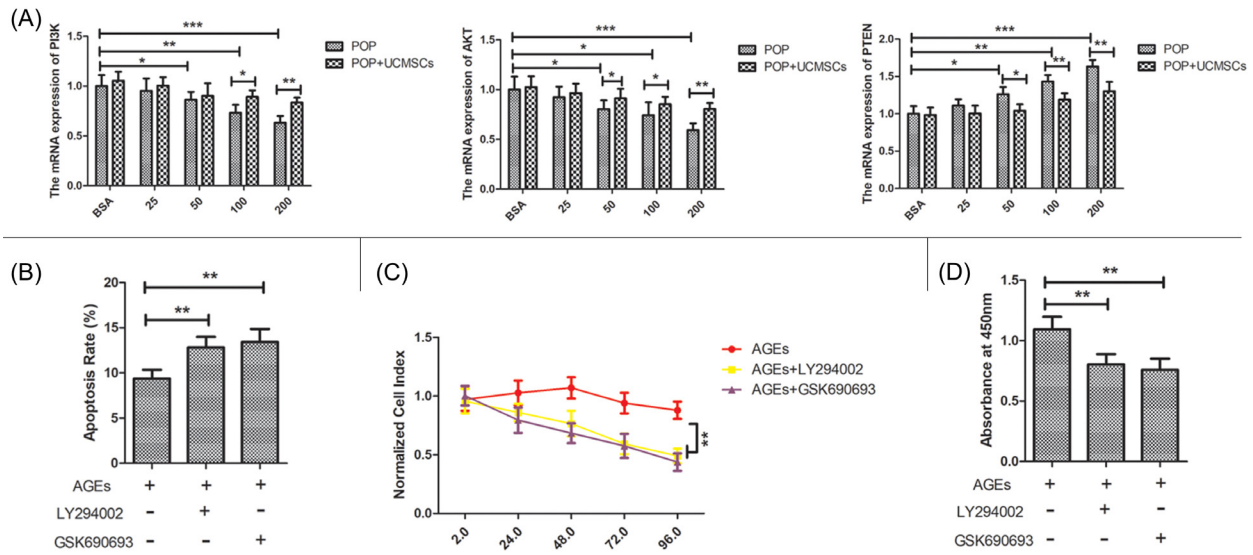

Figure 4. UCMSCs attenuate the cytotoxic effect of AGE on fibroblasts by activating the PI3K/Akt/PTEN pathway. (A) The levels of expression of PI3K, AKT, and PTEN mRNA in POP and co-cultured UCMSCs treated with different concentrations of AGEs. **(B)** The PI3K inhibitor LY294002 and the Akt inhibitor GSK 690693 increased the rate of apoptosis in co-cultured UCMSCs treated with 100 μg/mL of AGEs. **(C)** The PI3K inhibitor LY294002 and the Akt inhibitor GSK 690693 inhibited proliferation in co-cultured UCMSCs treated with 100 μg/mL of AGEs. **(D)** The PI3K inhibitor LY294002 and the3 Akt inhibitor GSK 690693 inhibited cell viability in co-cultured UCMSCs treated with 100 μg/mL of AGEs. $^{*}p < 0.05$. All results are expressed as the mean ± SEM, and data are representative of at least three experiments.

in POP. The current study found that AGEs inhibit the proliferation of VWFs and have dose-dependent cytotoxic effects on those cells. AGEs also induce the apoptosis of VWFs. In contrast, UCMSCs protect fibroblasts against the cytotoxic effects of AGEs by secreting anti-inflammatory cytokines to improve cell proliferation and cell viability and decrease the rate of apoptosis. Moreover, the PI3K/AKT/PTEN pathway is involved in UCMSCs inhibiting the cytotoxic effect of AGE-mediated cell apoptosis.

Human fibroblasts have the advantages of being easily harvested, cultured, and expanded *in vitro*, which make them an ideal cell source for regenerative medicine. VWFs play an important role in the pathophysiology of POP, which controls the integrity of collagen, and thereby impacts the mechanical properties of the pelvic floor (*21,22*). Primary culture of VWFs is commonly used to evaluate connective tissue in POP (*23*). Previous studies have described the impacts of AGEs on fibroblast proliferation. One study reported that AGEs promote the proliferation of fibroblasts, but another reported that AGEs induced the apoptosis of or inhibited the proliferation of fibroblasts (*24,25*). In the current study, the proliferation of fibroblasts from patients with POP was significantly inhibited by increasing concentrations of AGEs, suggesting that fibroblasts are more likely to be inhibited in POP. These results explain the smaller number of fibroblasts in the pelvic floor of patients with POP.

MSCs have been extensively used as cell-based therapies predominantly for their anti-inflammatory and immunomodulatory non-stem cell properties (*26*). They have also potential for tissue engineering purposes for regenerating new tissues or promoting the activity of endogenous stem cells (*27*). MSC populations have the capacity for self-renewal, a high proliferative potential, and differentiate into a variety of mesodermal and other lineages. Recent advances in cellular identification using more specific markers has shown that MSCs can be extracted from most tissues including bone marrow, the umbilical cord, the placenta, adipose tissue, and the endometrium, although not all of these sources have demonstrated clonogenicity for their MSC populations (*28,29*).

Typically, MSCs actively respond to stress or injury in a similar manner to the way cells of the innate immune system respond to pathogen exposure. When supplied systemically, exogenous MSCs home in on sites of injury in response to inflammation (*30,31*). There, MSCs operate in a paracrine manner secreting large amounts of diverse proteins, growth factors, cytokines, and chemokines that promote a variety of actions including neo-angiogenesis, tissue regeneration and remodeling, immune cell activation, suppression of inflammation, and cellular recruitment (*32*).

The potential of MSCs to serve as a cell-based therapy has recently been explored in numerous clinical applications. The ability to direct BMSCs to differentiate into other cell types and lineages has shown that these cells maintain a phenotype lacking tissue-specific characteristics until they are exposed to signals in damaged tissues (*33,34*). MSCs obtained from dental pulp have been used to repair related tissues such as the periodontal ligament, dental papilla, and dental follicle (*35*). The ability of adipose tissue and bone marrow MSCs to act as precursor cells has also

been exploited by directing their differentiation toward the chondrogenic lineage in order to produce cartilage-synthesizing chondrocytes (*36*). Although MSCs show promise as cell-based therapies, greater understanding of their mechanism of action and their potential is needed. Early use of MSCs has not always met expectations, often leading to inconsistent results. This may be due to lesser refined methods of isolating and cultivating MSCs resulting in the administration of fibroblasts and myofibroblasts rather than undifferentiated MSCs. Production of significant numbers of MSCs posed a challenge until recently since the regenerative potential of MSC declined during culture expansion, which is required due to the small numbers of perivascular MSC present within tissues (*37*).

POP is a common hidden disease burden for large numbers of women. Compounding this burden is the inadequacies of current surgeries with or without mesh. Recent advances in cellular phenotyping and gene profiling suggest endometrial MSCs as a possible complement to mesh-based POP treatment (*38*). The capacity of eMSCs to regenerate tissue is exemplified during a woman's reproductive life, where they regenerate at least one centimeter of endometrial lining each menstrual cycle for over 400 menstrual cycles. Seeding eMSCs onto polyamide/gelatin composite mesh and implanting them into the vaginal wall allow favorable modulation of the innate immune response and accelerate organized tissue repair. The first attempt at combining eMSCs and mesh to treat a fascial defect was successful in rodent models. This is encouraging, suggesting that further development of this approach using an ovine model is warranted (*39-41*).

In a recent *in vivo* study on PFD, transplantation of BMSCs resulted in new tissue growth and collagen deposition in a wound healing model. In the context of PFD, an appropriate amount of elastic fibers in the connective tissue is extremely crucial to functionally restoring pelvic floor support. Simple deposition of collagen would cause formation of dense connective tissues and eventually scar tissues (*42,43*).

UCMSCs have shown great potential in regenerative medicine for their extensive sources, potential to differentiate into multiple lineages, low immunogenicity, and self-renewal ability (*44*). The safety and therapeutic potential of human UCMSCs have been increasingly studied in the context of regenerative medicine and immune modulation. The immunosuppressive and anti-inflammatory properties of cultured/expanded UCMSCs have led these cells to be tested for their therapeutic potential in preclinical animal models since the mid-2000s, and their differentiation characteristics and responses to external environment have been extensively documented in *in vitro* single and co-culture setups (*45-47*). They have multiple advantages such as easy isolation and harvesting, no posing of ethical concerns, no tumor susceptibility, and low immunogenicity (*48*). As a result, UCMSCs hold significant promise for tissue engineering and regenerative medicine applications (*49*). To date, UCMSCs have been widely used in multiple studies to treat conditions such as acute lung injury, insulin-resistant diabetes, Alzheimer's disease (AD), acute myocardial infarction, graft-versus-host diseases (GVHD), aplastic anemia, arthritis, liver disease, spinal cord injury, systemic lupus erythematosus, and stroke (*50-52*).

Previous studies demonstrated that phosphatase and tensin homolog (PTEN) can negatively regulate the PI3K/AKT pathway, which in turn influences the nuclear factor kappa-light- chain-enhancer of activated B cells (NF-κB) signalling to modulate cell survival, migration, and proliferation. AGEs adjust the metabolism of target proteins through RAGE and activate an array of signal transduction cascades, such as MAPK, ROS, p38, NO, and NF-κB (*53,54*). The current authors hypothesized that the PI3K/Akt/PTEN pathway may be involved in governing the observed effects of UCMSCs to resist the cytotoxic effect of AGEs in POP. PI3K is a lipid kinase that induces cell cycle progression, cell survival, and cell migration, and many pieces of evidence have indicated that PI3K/AKT signaling is constitutively activated in many tumors with PTEN dysfunction.

The current findings further substantiate the contention that UCMSCs play a beneficial anti-inflammatory role by inhibiting the cytotoxic effect of AGEs. PI3K-AKT signaling, which is closely related to cell proliferation, is firmly considered to be involved in inflammatory action as well (*55*). In the current study, the anti-inflammatory conditions created by cells co-cultured with UCMSCs inhibited the expression of PTEN to reverse the apoptosis and improve cell proliferation in POP.

In conclusion, the anti-inflammatory role of UCMSCs may help to reverse the cytotoxic effect of AGEs in patients with POP and activate the PI3K/AKT/PTEN signaling pathway to increase proliferation and decrease apoptosis. These roles might provide important insights into the use of UCMSCs to treat POP.

Acknowledgements

This work was supported by grants from the National Natural Science Foundation of China (No. 81671439 to Yisong Chen), the National Natural Science Foundation of China (Nos. 31571196 and 30801502 to Ling Wang), and the Fund for Young Scientists of the Shanghai Municipal Health and Family Planning Commission (No. 20184Y0218 to Lisha Li).

References

1. Arnouk A, De E, Rehfuss A, Cappadocia C, Dickson S, Lian F. Physical, Complementary, and alternative medicine in the treatment of pelvic floor disorders. Curr

Urol Rep. 2017; 18:47.
2. Easley DC, Abramowitch SD, Moalli PA. Female pelvic floor biomechanics: Bridging the gap. Curr Opin Urol. 2017; 27:262-267.
3. Tinetti A, Weir N, Tangyotkajohn U, Jacques A, Thompson J, Briffa K. Help-seeking behaviour for pelvic floor dysfunction in women over 55: Drivers and barriers. Int Urogynecol J. 2018; 29:1645-1653.
4. Cardenas-Trowers O, Meyer I, Markland AD, Richter HE, Addis I. A Review of phytoestrogens and their association with pelvic floor conditions. Female Pelvic Med Reconstr Surg. 2018; 24:193-202.
5. Weintraub AY, Glinter H, Marcus-Braun N. Narrative review of the epidemiology, diagnosis and pathophysiology of pelvic organ prolapse. Int Braz J Urol. 2020; 46:5-14.
6. Wallace SL, Miller LD, Mishra K. Pelvic floor physical therapy in the treatment of pelvic floor dysfunction in women. Curr Opin Obstet Gynecol. 2019; 31:485-493.
7. Taithongchai A, Sultan AH, Wieczorek PA, Thakar R. Clinical application of 2D and 3D pelvic floor ultrasound of mid-urethral slings and vaginal wall mesh. Int Urogynecol J. 2019; 30:1401-1411.
8. Hong S, Hong L, Li B, Wu D, Liu C, Min J, Guo W, Hu M, Tang J, Li Y. The role of GPX1 in the pathogenesis of female pelvic organ prolapse. PLoS One. 2017; 12: e0181896.
9. Deluyker D, Evens L, Bito V. Advanced glycation end products (AGEs) and cardiovascular dysfunction: Focus on high molecular weight AGEs. Amino Acids. 2017; 49:1535-1541.
10. Jackson S, James M, Abrams P. The effect of oestradiol on vaginal collagen metabolism in postmenopausal women with genuine stress incontinence. BJOG. 2002; 109:339-344.
11. Sferra R, Pompili S, D'Alfonso A, Sabetta G, Gaudio E, Carta G, Festuccia C, Colapietro A, Vetuschi A. Neurovascular alterations of muscularis propria in the human anterior vaginal wall in pelvic organ prolapse. J Anat. 2019; 235:281-288.
12. Chen YS, Wang XJ, Feng W, Hua KQ. Advanced glycation end products decrease collagen I levels in fibroblasts from the vaginal wall of patients with POP *via* the RAGE, MAPK and NF-κB pathways. Int J Mol Med. 2017; 40:987-998.
13. Clevers H, Loh KM, Nusse R. Stem cell signaling. An integral program for tissue renewal and regeneration: Wnt signaling and stem cell control. Science. 2014; 346:1248012.
14. Fu X, Liu G, Halim A, Ju Y, Luo Q, Song AG. Mesenchymal stem cell migration and tissue repair. Cells. 2019; 8:784.
15. Jin M, Chen Y, Zhou Y, Mei Y, Liu W, Pan C, Hua X. Transplantation of bone marrow-derived mesenchymal stem cells expressing elastin alleviates pelvic floor dysfunction. Stem Cell Res Ther. 2016; 7:51.
16. Du XW, Wu HL, Zhu YF, Hu JB, Jin F, Lv RP, Sun S, Wang HY, Xu JW. Experimental study of therapy of bone marrow mesenchymal stem cells or muscle-like cells/ calcium alginate composite gel for the treatment of stress urinary incontinence. Neurourol Urodyn. 2013; 32:281-286.
17. Mangir N, Aldemir Dikici B, Chapple CR, MacNeil S. Landmarks in vaginal mesh development: Polypropylene mesh for treatment of SUI and POP. Nat Rev Urol. 2019; 16:675-689.
18. Wang YJ, Yan J, Zou XL, Guo KJ, Zhao Y, Meng CY, Yin F, Guo L. Bone marrow mesenchymal stem cells repair cadmium-induced rat testis injury by inhibiting mitochondrial apoptosis. Chem Biol Interact. 2017; 271:39-47.
19. Han S1, Wang B2, Li X1,3, Xiao Z1, Han J1, Zhao Y1, Fang Y4, Yin Y1, Chen B1, Dai J1. Bone marrow-derived mesenchymal stem cells in three-dimensional culture promote neuronal regeneration by neurotrophic protection and immunomodulation. J Biomed Mater Res A. 2016; 104:1759-1769.
20. Płusa T, Baranowska A, Baranowski P. [Stem cells in contemporary medicine]. Pol Merkur Lekarski. 2019; 46:5-8.
21. Lu Y, Chen HY, Wang XQ, Wang JX. Correlations between mitofusin 2 expression in fibroblasts and pelvic organ prolapse: An *in vitro* study. Chin Med J (Engl). 2017; 130:2951-2959.
22. Ruiz-Zapata AM, Kerkhof MH, Ghazanfari S, Zandieh-Doulabi B, Stoop R, Smit TH, Helder MN. Vaginal fibroblastic cells from women with pelvic organ prolapse produce matrices with increased stiffness and collagen content. Sci Rep. 2016; 6:22971.
23. Medel S, Alarab M, Kufaishi H, Drutz H, Shynlova O. Attachment of primary vaginal fibroblasts to absorbable and nonabsorbable implant materials coated with platelet-rich plasma: Potential application in pelvic organ prolapse surgery. Female Pelvic Med Reconstr Surg. 2015; 21:190-197.
24. Dai J, Chen H, Chai Y. Advanced glycation end products (AGEs) induce apoptosis of fibroblasts by activation of NLRP3 inflammasome *via* reactive oxygen species (ROS) signaling pathway. Med Sci Monit. 2019; 25:7499-7508.
25. Nonaka K, Kajiura Y, Bando M, Sakamoto E, Inagaki Y, Lew JH, Naruishi K, Ikuta T, Yoshida K, Kobayashi T, Yoshie H, Nagata T, Kido J. Advanced glycation end-products increase IL-6 and ICAM-1 expression *via* RAGE, MAPK and NF-κB pathways in human gingival fibroblasts. J Periodontal Res. 2018; 53:334-344.
26. Hejretová L, Čedíková M, Dolejšová M, Vlas T, Jindra P, Lysák D, Holubová M. Comparison of the immunomodulatory effect of single MSC batches versus pooled MSC products. Cell Tissue Bank. 2019; 21:119-129.
27. Marolt Presen D, Traweger A, Gimona M, Redl H. Mesenchymal stromal cell-based bone regeneration therapies: From cell transplantation and tissue engineering to therapeutic secretomes and extracellular vesicles. Front Bioeng Biotechnol. 2019; 7:352.
28. Hass R, Kasper C, Böhm S, Jacobs R. Different populations and sources of human mesenchymal stem cells (MSC): A comparison of adult and neonatal tissue-derived MSC. Cell Commun Signal. 2011; 9:12.
29. Toh WS, Lai RC, Zhang B, Lim SK. MSC exosome works through a protein-based mechanism of action. Biochem Soc Trans. 2018; 46:843-853.
30. Vinci P, Bastone A, Schiarea S, Cappuzzello C, Del Prete A, Dander E, Biondi A, D'Amico G. Mesenchymal stromal cell-secreted chemerin is a novel immunomodulatory molecule driving the migration of ChemR23-expressing cells. Cytotherapy. 2017; 19:200-210.
31. Saparov A, Ogay V, Nurgozhin T, Jumabay M, Chen WC. Preconditioning of human mesenchymal stem cells to enhance their regulation of the immune response. Stem

Cells Int. 2016; 2016:3924858.
32. Rackham CL, Amisten S, Persaud SJ, King AJF, Jones PM. Mesenchymal stromal cell secretory factors induce sustained improvements in islet function pre- and post-transplantation. Cytotherapy. 2018; 20:1427-1436.
33. Brown C, McKee C, Bakshi S, Walker K, Hakman E, Halassy S, Svinarich D, Dodds R, Govind CK, Chaudhry GR. Mesenchymal stem cells: Cell therapy and regeneration potential. J Tissue Eng Regen Med. 2019; 13:1738-1755.
34. Atashi F, Modarressi A, Pepper MS. The role of reactive oxygen species in mesenchymal stem cell adipogenic and osteogenic differentiation: A review. Stem Cells Dev. 2015; 24:1150-1163.
35. Sharpe PT. Dental mesenchymal stem cells. Development. 2016; 143:2273-2280.
36. Liu Y, Lin L, Zou R, Wen C, Wang Z, Lin F. MSC-derived exosomes promote proliferation and inhibit apoptosis of chondrocytes *via* lncRNA-KLF3-AS1/miR-206/GIT1 axis in osteoarthritis. Cell Cycle. 2018; 17:2411-2422.
37. Oryan A, Kamali A, Moshiri A, Baghaban Eslaminejad M. Role of mesenchymal stem cells in bone regenerative medicine: What is the evidence? Cells Tissues Organs. 2017; 204:59-83.
38. Edwards SL, Ulrich D, White JF, Su K, Rosamilia A, Ramshaw JA, Gargett CE, Werkmeister JA. Temporal changes in the biomechanical properties of endometrial mesenchymal stem cell seeded scaffolds in a rat model. Acta Biomater. 2015; 13:286-294.
39. Emmerson SJ, Gargett CE. Endometrial mesenchymal stem cells as a cell based therapy for pelvic organ prolapse. World J Stem Cells. 2016; 8:202-215.
40. Darzi S, Deane JA, Nold CA, Edwards SE, Gough DJ, Mukherjee S, Gurung S, Tan KS, Vashi AV, Werkmeister JA, Gargett CE. Endometrial mesenchymal stem/stromal cells modulate the macrophage response to implanted polyamide/gelatin composite mesh in immunocompromised and immunocompetent Mice. Sci Rep. 2018; 8:6554.
41. Su K, Edwards SL, Tan KS, White JF, Kandel S, Ramshaw JAM, Gargett CE, Werkmeister JA. Induction of endometrial mesenchymal stem cells into tissue-forming cells suitable for fascial repair. Acta Biomater. 2014; 10:5012-5020.
42. Zhao B, Hu M, Wu H, Ren C, Chen J, Zhang X, Cui S. Peroxisome proliferator-activated receptor-γ and its related pathway in bone marrow mesenchymal stem cell differentiation co-cultured with mechanically stretched ligament fibroblasts. Int J Mol Med. 2018; 42:219-227.
43. Dandia H, Makkad K, Tayalia P. Glycated collagen – A 3D matrix system to study pathological cell behavior. Biomater Sci. 2019; 7:3480-3488.
44. Chandravanshi B, Bhonde RR. Human umbilical cord-derived stem cells: Isolation, characterization, differentiation, and application in treating diabetes. Crit Rev Biomed Eng. 2018; 46:399-412.
45. Zheng Q, Fu X, Jiang J, Zhang N, Zou L, Wang W, Ding M, Chen H. Umbilical cord mesenchymal stem cell transplantation prevents chemotherapy-induced ovarian failure *via* the NGF/TrkA pathway in rats. Biomed Res Int. 2019; 2019:6539294.
46. De Witte SFH, Peters FS, Merino A, Korevaar SS, Van Meurs JBJ, O'Flynn L, Elliman SJ, Newsome PN, Boer K, Baan CC, Hoogduijn MJ. Epigenetic changes in umbilical cord mesenchymal stromal cells upon stimulation and culture expansion. Cytotherapy. 2018; 20:919-929.
47. Wang P, Zeng F, He L, Wang J, Zhang T, Zhang D. Alteration of the immune status of umbilical cord mesenchymal stem cells stimulated by TLR1/2 agonist, Pam3Csk. Mol Med Rep. 2016; 14:2206-2212.
48. Meng M, Liu Y, Wang W, Wei C, Liu F, Du Z, Xie Y, Tang W, Hou Z, Li Q. Umbilical cord mesenchymal stem cell transplantation in the treatment of multiple sclerosis. Am J Transl Res. 2018; 10:212-223.
49. Zhang Y, Xing Y, Jia L, Ji Y, Zhao B, Wen Y, Xu X. An *in vitro* comparative study of multisource derived human mesenchymal stem cells for bone tissue engineering. Stem Cells Dev. 2018; 27:1634-1645.
50. Guan LX, Guan H, Li HB, Ren CA, Liu L, Chu JJ, Dai LJ. Therapeutic efficacy of umbilical cord-derived mesenchymal stem cells in patients with type 2 diabetes. Exp Ther Med. 2015; 9:1623-1630.
51. Xu Z, Nan W, Zhang X *et al.* Umbilical cord mesenchymal stem cells conditioned medium promotes Aβ25-35 phagocytosis by modulating autophagy and aβ-degrading enzymes in BV2 cells. J Mol Neurosci. 2018; 65:222-233.
52. Alshareeda AT, Alsowayan B, Almubarak A, Alghuwainem A, Alshawakir Y, Alahmed M. Exploring the potential of mesenchymal stem cell sheet on the development of hepatocellular carcinoma *in vivo*. J Vis Exp. 2018;139.57805
53. Kim J, Park JC, Lee MH, Yang CE, Lee JH, Lee WJ. High-mobility group box 1 mediates fibroblast activity *via* RAGE-MAPK and NF-κB signaling in keloid scar formation. Int J Mol Sci. 2017; 19:76.
54. Chen XJ, Wu WJ, Zhou Q, Jie JP, Chen X, Wang F, Gong XH. Advanced glycation end-products induce oxidative stress through the Sirt1/Nrf2 axis by interacting with the receptor of AGEs under diabetic conditions. J Cell Biochem. 2018; doi: 10.1002/jcb.27524.
55. Jin QS, Huang LJ, Zhao TT, Yao XY, Lin LY, Teng YQ, Kim SH, Nam MS, Zhang LY, Jin YJ. HOXA11-AS regulates diabetic arteriosclerosis-related inflammation *via* PI3K/AKT pathway. Eur Rev Med Pharmacol Sci. 2018; 22:6912-6921.

Received April 28, 2020; Revised May 22, 2020; Accepted May 28, 2020.

Address correspondence to:
Yisong Chen and Ling Wang, Obstetrics & Gynecology Hospital of Fudan University, 419 Fangxie Road, Shanghai 200011, China.
E-mail: cys373900207@163.com (Chen YS), Dr.wangling@fudan.edu.cn (Wang L)

Released online in J-STAGE as advance publication June 3, 2020.

Original Article

DOI: 10.5582/bst.2020.03262

Regulatory effects of Ningdong granule on microglia-mediated neuroinflammation in a rat model of Tourette's syndrome

Lin Zhao[1], Nan Cheng[2], Bo Sun[3], Shuzhen Wang[4], Anyuan Li[1], Zhixue Wang[1], Yuan Wang[1], Fanghua Qi[1,*]

[1] Department of Traditional Chinese Medicine, Shandong Provincial Hospital affiliated to Shandong University, Ji'nan, China;
[2] Department of Intensive Care Unit, Shandong Provincial Hospital affiliated to Shandong University, Ji'nan, China;
[3] Shandong Medical Imaging Research Institute affiliated to Shandong University, Ji'nan, China;
[4] Department of Pediatry, The First Affiliated Hospital of Shandong First Medical University, Ji'nan, China.

SUMMARY Tourette's syndrome (TS) is an inherited neurologic disorder characterized by involuntary stereotyped motor and vocal tics. Its pathogenesis is still unclear and its treatment remains limited. Recent research has suggested the involvement of immune mechanisms in the pathophysiology of TS. Microglia are the brain's resident innate immune cells. They can mediate neuroinflammation and regulate brain development and homeostasis. A traditional Chinese medicine (TCM), Ningdong granule (NDG), has been found to be efficacious in the treatment of TS while causing few adverse reactions. In the current study, a rat model of 3,3'-iminodipropionitrile (IDPN)-induced TS was used to explore the regulating effects and mechanisms of NDG on microglia-mediated neuroinflammation. IDNP led to robust pathological changes and neurobehavioral complications, with activation of microglia in the striatum of rats with TS. After activation by IDNP, microglia strongly responded to this specific injury, and TNF-α, IL-6, and MCP-1 were released in the striatum and/or serum of rats with TS. Interestingly, NDG inhibited the activation of microglia and decreased the abnormal expression of TNF-α, IL-6, and MCP-1 in the striatum and/or serum of rats with TS, thus controlling tics. However, there were no significant changes in the striatum and/or serum of rats with TS after treatment with haloperidol. The anti-TS action of haloperidol might occur not through microglial activation and neuroinflammation but through the DAT system, thus controlling tics. In conclusion, microglia might play key roles in mediating neuroinflammatory responses in TS, triggering the release of TNF-α, IL-6, and MCP-1. NDG inhibited tics in rats with TS, and this mechanism may be associated with a reduction in the increased number of activated microglia and a decrease in the expression of pro-inflammatory cytokines and chemokines in the striatum and/or serum.

Keywords Tourette's syndrome (TS), Ningdong granule (NDG), microglia, immunoregulation, neuroinflammation

1. Introduction

Gilles de la Tourette syndrome, or Tourette's syndrome (TS), is an inherited neurologic disorder characterized by involuntary stereotyped motor and vocal tics, with a variety of behavioral comorbidities in most cases, such as attention deficit hyperactivity disorder, obsessive compulsive disorder, and other impulse control disorders (*1*). TS usually starts in childhood, with a peak age between 7 to 15 years. Its prevalence is estimated to be four to six per 1,000 children and adolescents, with an incidence in males 3-4 times higher than that in females (*2*). In terms of its clinical course, TS can cause lifelong impairment in 5 to 10% of patients and even life-threatening symptoms in some, including mild self-injurious behaviors and borderline personality disorders (*3*).

Currently, the detailed etiological and pathophysiological mechanism of TS is still unclear. The etiology is complex, with polygenic, immunological, and hormonal contributions and potential involvement of environmental factors (*4*). The pathophysiology involves the dysfunction of both motor and non-motor basal ganglia-thalamo-cortical circuitries, with a variety of neurotransmitters implicated including dopamine (DA), serotonin (5-TH), and gamma-amino butyric acid (GABA) (*5*). Mounting evidence has shown that immune dysregulation contributes to the pathophysiology of TS. Neuroimmune interactions are increasingly appreciated as an important

regulator of normal brain development and function and a potential contributor to the pathophysiology of a range of neuropsychiatric illnesses, including TS (*6*).

Microglia are the principal resident immune cells of the brain involved in homeostasis and host defense against pathogens and central nervous system (CNS) disorders (*7*). Microglia survival and maintenance depend on cytokines and transcription factors. Activated microglia will produce pro-inflammatory tumor necrosis factor (TNF)-α, the cytokines interleukin (IL)-1 and IL-6, and other substances (*8*). Recent studies have suggested that there is abnormal activation of microglia in patients with TS. Lennington *et al.* performed the first unbiased and comprehensive characterization of changes in gene expression based on RNA sequencing of specimens from the basal ganglia of patients with TS (*9*). They found that the top-scoring up-regulated module was enriched in immune-related genes including TNF-α, IL-6, and IL-12, consistent with activation of microglia in patients' striatum. The activation of microglia was mainly evident as an increased number of $CD45^+$ cells in the caudate of patients with TS. Another study also observed bilateral inflammatory microglial activation in the caudate nuclei of children with TS (*10*). Therefore, the potential involvement of microglia dysregulation in TS maybe an intriguing area for future study.

At present, there is still no ideal pharmacological treatment for TS. Haloperidol (Hal) is approved by the US Food and Drug Administration for treatment of TS. It can effectively inhibit the excitability of the cortical motor area by suppressing the activity of DA receptors (*11*). However, an extremely high proportion of patients eventually refuse further therapy with Hal because of adverse reactions, including sedation, dizziness, dyskinesia tarda, and extrapyramidal symptoms (*e.g.*, acute dystonia and akathisia) (*12*). Therefore, novel drugs for treatment of TS need to be developed soon.

Traditional Chinese medicine (TCM) has been widely used in the treatment of various diseases, including nervous system diseases, in China, Japan, South Korea, and other Asian countries for thousands of years (*13*). Ningdong granule (NDG), a TCM used to treat TS in accordance with the therapeutic principles of TCM, has been used as an anti-tic agent in Chinese clinics for several years. A previous study by the current authors indicated that NDG had a total efficacy of 79.3% in patients with TS while causing few apparent adverse reactions or toxicities (*14*). Moreover, the NDG group displayed a 41.39% reduction in tic severity and frequency compared to the placebo group (10.79%) (*15*). Previous studies by the current authors also indicated that NDG regulates the disturbance of DA, DA transporter (DAT), 5-TH, and GABA in animals and patients with TS (*11,12,16*). In addition, NDG modulates abnormal serum levels of IL-12 and TNF-α in patients with TS, and NDG might be an immune mechanism for treating TS (*14*). However, the possible immune mechanisms by which NDG treats TS are still unclear. The aim of the current study was to explore the possible mechanism by which NDG immunoregulates microglia in rats with TS.

2. Materials and Methods

2.1. Preparation of NDG

NDG was provided by 999 Modern Chinese Medicine Co. Ltd. (999 Co. Ltd., Shenzhen, China). As shown in Table 1, NDG contains 8 ingredients. After the ingredients were mixed in proportion, they were macerated with distilled water for 1 h at room temperature, and the whole mixture was decocted twice for 30 min each time. The filtrates were mixed and condensed and then dried with a vacuum-drier at 60°C. The resulting granules were stored at 4°C.

2.2. Laboratory animals and behavior recordings

Forty male Wistar rats (4 weeks old, weight: 100 ± 20 g) were purchased from Shandong Laboratory Animal Center (Jinan, China) and housed in an air-conditioned animal room with a 12-h light/dark cycle, a temperature of 22 ± 2°C, and a humidity of 50 ± 10%. Rats were constantly provided with a laboratory diet and water *ad libitum*.

After one week, the rats were randomly divided into a control group (n = 10) and TS model group (n = 30). Rats in the TS model group were intraperitoneally injected (*i.p.*) with 3,3'-iminodipropionitrile (IDPN) (150mg/kg, *i.p.*), while the control group received normal saline (NS) (5 mL/kg, *i.p.*). After IDPN was administered once a day for 7 consecutive days, rats in the model group with IDPN-induced TS were further divided into 3

Table 1. Components of Ningdong granule (NDG)

Components	Part used	Amount used (g)
Gastrodia elata Blume	rhizome	6
Codonopsis pilosula (Franch) Nannf.	root	9
Ophiopogon japonicus (L.f.) Ker-Gawl	root tuber	6
Paeonia lactiflora Pall.	root	12
Ostrea gigas Thunb.	shell	15
Fossil fragments	skeletal fossils	15
Pheretima aspergillum	whole polypide	6
Glycyrrhiza uralensis Fisch.	root	6

Table 2. Standards for evaluation of stereotypical behaviors

Score	Stereotypical behaviors
0	Asleep, resting in place, or normal activity in place.
1	Occasional sniffing and head raising.
2	Frequent sniffing and body raising
3	Frequent sniffing, self-grooming with head and body raising primarily in one place, and an occasional rapid burst of loco motor activity (2-5 steps).
4	Continuous sniffing, biting, head bobbing, and repetitive body raising/wall climbing in place.
5	Continuous sniffing, biting, licking, head bobbing, and continuous body rising/wall climbing whereby the forepaws do not touch the cage floor.

groups: a model group (n = 10), an NDG group (n = 10), and a haloperidol (Hal) group (n = 10). The rats were administered normal saline by gastric perfusion (0.9%) at 10 mL/kg (control group and model group), NDG at 370 mg/kg (NDG group), or haloperidol at 1.0 mg/kg (Hal group) once a day for 8 weeks.

Stereotyped behaviors were counted according to evaluation standards described previously (Table 2) (*17*). Counts were conducted once every 2 weeks by trained observers who were blinded to the group's treatment. Each animal was observed for one min of every 10 min for a total of 6 observation periods.

At the end of the experiment, all rats were sacrificed under anesthesia and the striatal tissues were extracted from the brain by the method described by Hida *et al.* (*18*). Right striatal tissues were removed and fixed overnight at 4°C by immersion in a 4% formalin solution for immunohistochemistry, and the left striatal tissues were stored at -80°C until analysis.

2.3. Immunohistochemistry

Ionized calcium-binding adaptor molecule-1 (Iba-1) is a marker of microglial activation. To analyze the microglial activation in the striatal tissues of rats with TS, the expression of Iba-1 was detected immunohistochemically as follows. Three samples were randomly selected from each group. Sections of striatal tissues were routinely processed, embedded in paraffin, and sectioned in 5-μm serial sections. Two sections were randomly selected from each sample. For Iba-1immunohistochemistry, sections were washed three times in a 0.1 M phosphate buffer solution (PBS) for 10 minutes each. Afterwards, sections were treated with 3% H_2O_2 in PBS for 20 minutes at room temperature. Sections were incubated in a blocking solution containing PBS/10% filtered goat serum (v/v) for 1 hour at room temperature followed by incubation with goat polyclonal anti-Iba1 (dilution 1:1,000, ab5076, Abcam, Cambridge, UK) overnight at 4°C. Next, the paraffin sections were washed thrice in PBS for 8 minutes each and were then incubated with secondary antibody (dilution 1:200; KIT-9901, Maixin Biotechnologies, Fuzhou, China) for 30min at room temperature followed by washes and colorimetric development (DAB: DAB-2031, Maixin Biotechnologies, Fuzhou, China). Immuno-stained sections were mounted on slides and covered. The number of Iba1-positive cells, activated cells with large cell bodies and thick processes, was counted in five 400× non-overlapping microscopic fields in each section.

2.4. Levels of TNF-α, IL-1, IL-6, and monocyte chemoattractant protein 1in the striatum and serum

The levels of TNF-α, IL-1, IL-6, and monocyte chemoattractant protein 1 (MCP-1) in the striatum and serum were measured using anenzyme-linked immunosorbent assay (ELISA) according to the manufacturer's instructions (TNF-α: JYM0635Ra, IL-1: JYM0418Ra, IL-6: JYM0646Ra, MCP-1: JYM0495Ra, Wuhan ColorfulGene Biological Technology Co., Ltd, Wuhan, China). Briefly, dispensed antigen standards and samples were added to each well of 96-wellplates pre-coated with primary antibody. After a biotin conjugate reagent and an enzyme conjugate reagent were added to each well, the plates were incubated at 37°C for 60 min. The plates were then rinsed 5 times with distilled water. After a chromogenic reaction, absorbance was measured within 30 min at 450 nm with a microtiter plate reader.

2.5. Statistical analysis

Data are expressed as the mean ± standard deviation (SD). Statistical analysis was performed using one-way analysis of variance ANOVA. A repeated measures ANOVA was used to analyze the stereotypic behaviors of the rats. All analyses were performed using the statistical software package SPSS (Version 21.0, SPSS Inc., Chicago, IL, USA), and $p < 0.05$ was considered statistically significant.

3. Results

3.1. Behavioral study

Repeated measures ANOVA indicated that the IDPN-induced TS model had significant group effects. Administration of IDPN produced multiple stereotypical behaviors in rats compared to control rats throughout the study ($p < 0.01$). After treatment with NDG or Hal, scores for stereotypical behaviors in both

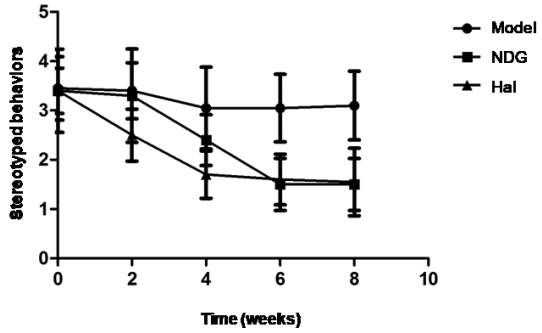

Figure 1. Stereotypical behavior of rats in the three experimental groups over an 8-week period. The data represent the mean ± S.D. (n = 10). Administration of IDPN produced multiple stereotypical behaviors in rats ($p < 0.01$). The stereotypical behavior scores at the baseline did not differ among groups ($p > 0.05$). After treatment with NDG or Hal, dyskinetic-hyperkinetic syndrome scores in IDPN-induced rats decreased significantly ($p < 0.01$).

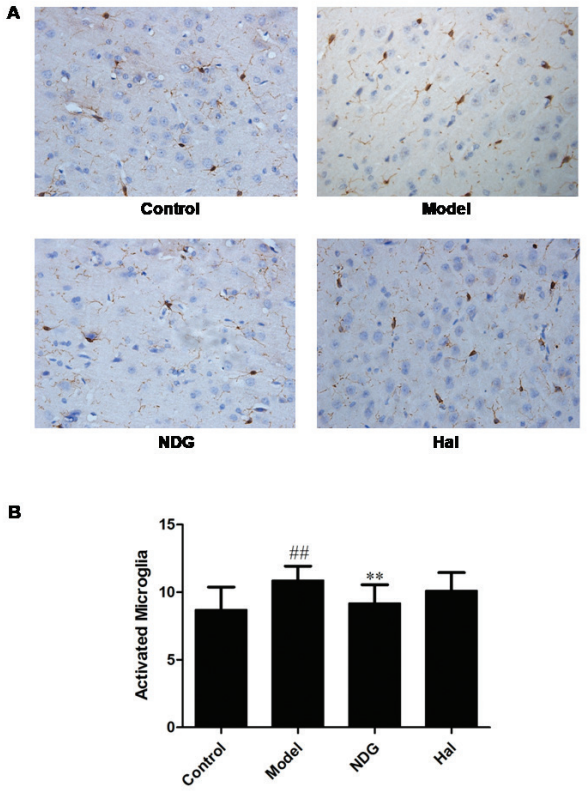

Figure 2. The number of activated microglia in the striatum of rats with TS. The data represent the mean ± S.D. (n = 10). **(A)** The activated microglia in the striatum were detected using immunohistochemistry. **(B)** The number of activated microglia in the striatum was calculated based on images from immunohistochemistry. The number of Iba1-positive cells, activated cells with large cell bodies and thick processes, was counted in five 400× non-overlapping microscopic fields in each section. Note: $^{\#\#}p < 0.01$ *vs.* control group, and $^{**}p < 0.01$ *vs.* model group.

the NDG group and Hal group decreased significantly compared to scores in the model group ($p < 0.01$), and there were no marked differences in scores between the two treatments ($p > 0.05$) (Figure 1).

3.2. Microglial activation in the striatum

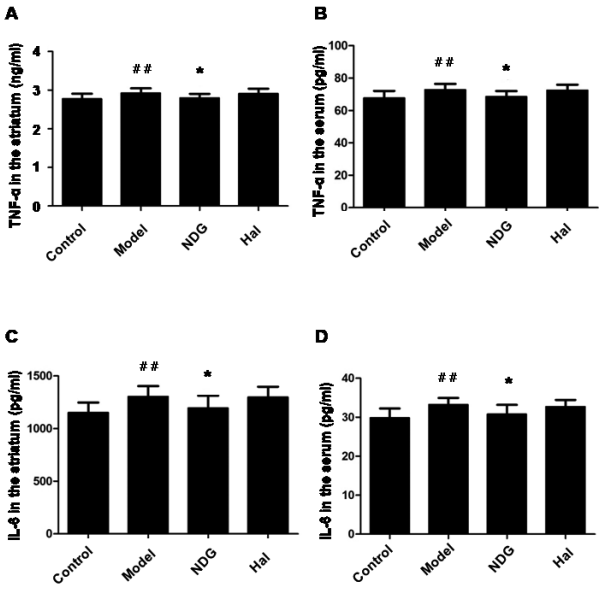

Figure 3. The levels of TNF-α and IL-6 in the striatum and serum of rats with TS. The data represent the mean ± S.D. (n = 10). **(A)** The levels of TNF-α in the striatum, **(B)** The levels of TNF-α in serum, **(C)** The levels of IL-6 in the striatum, and **(D)** The levels of IL-6 in serum. Note: $^{\#\#}p < 0.01$ *vs.* control group, and $^{*}p < 0.05$ *vs.* model group.

The number of activated microglia (Iba-1+) in the striatal tissues of rats with TS was detected immunohistochemically. As shown in Figure 2, the number of activated microglia in the striatum increased significantly in the model group compared to that in the control group ($p < 0.01$). After treatment with NDG or Hal, NDG down-regulated the increased number of activated microglia in the striatum of rats with TS ($p < 0.05$); while there were no significant changes in the number of activated microglia in the Hal group compared to the number in the model group ($p > 0.05$) (Figure 2).

3.3. Levels of TNF-α, IL-6, and IL-1 in the striatum and serum

Activated microglia produce pro-inflammatory TNF-α, IL-1, IL-6, and other substances. Here, the levels of TNF-α, IL-6, and IL-1 were detected in the striatum and serum of rats with TS using ELISA. As shown in Figure 3, IDPN regulated the levels of TNF-α and IL-6 in the striatum and serum of rats. There was a significant increase in the TNF-α (Figures 3A and 3B) and IL-6 (Figures 3C and 3D) levels in the striatum and serum of the model group (TNF-α: $p < 0.01$, IL-6: $p < 0.01$) compared to levels in the control group. After treatment with NDG or Hal, the levels of TNF-α and IL-6in the striatum and serum of the NDG group decreased significantly compared to levels in the model group (TNF-α: $p < 0.05$, IL-6: $p < 0.05$); there were no significant changes in the levels of TNF-α and IL-6 in the striatum and serum of the Hal group compared to levels in the model group ($p > 0.05$). Interestingly, there were no significant differences in the levels of IL-1 in

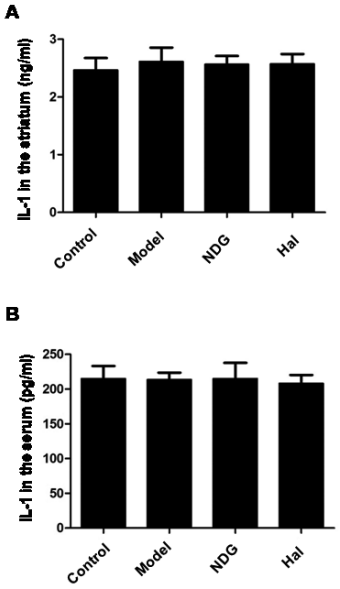

Figure 4. The levels of IL-1 in the striatum and serum of rats with TS. The data represent the mean ± S.D. (n = 10). **(A)** The levels of IL-1 in the striatum and **(B)** in serum. Note: $^{\#\#}p < 0.01$ *vs.* control group, and $^{*}p < 0.05$ *vs.* model group.

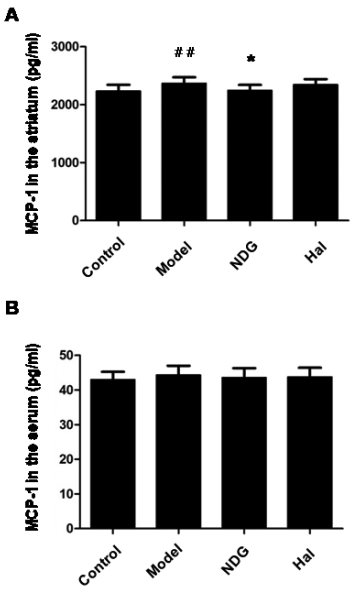

Figure 5. The levels of MCP-1 in the striatum and serum of rats with TS. The data represent the mean ± S.D. (n = 10). **(A)** The levels of MCP-1 in the striatum and **(B)** in serum. Note: $^{\#\#}p < 0.01$ *vs.* control group, and $^{*}p < 0.05$ *vs.* model group.

the striatum and serum of the four groups ($p > 0.05$) (Figures 4A and 4B).

3.4. Levels of MCP-1 in the striatum and serum

MCP-1 is a chemokine regulating monocyte chemotaxis and T-lymphocyte differentiation, and it plays a crucial role in the pathogenesis of inflammatory diseases, atherosclerosis, and cancer (19). The current study detected the levels of MCP-1 in the striatum and serum of rats with TS using ELISA. As shown in Figure 5A, the levels of MCP-1 in the striatum and serum of the model group increased significantly compared to levels in the control group ($p < 0.01$). After treatment with NDG or Hal, the levels of MCP-1in the striatum of the NDG group decreased significantly compared to levels in the model group ($p < 0.05$); there were no significant changes in the levels of MCP-1in the striatum of the Hal group compared to levels in the model group ($p > 0.05$). Interestingly, there were no significant differences in the levels of MCP-1 in the serum of the four groups ($p > 0.05$) (Figure 5B).

4. Discussion

Recent research has suggested that immune mechanisms might be involved in the pathophysiology of TS. According to previous animal and post-mortem studies, microglia play a crucial role in neural-immune crosstalk in TS and other related disorders (*20,21*). Microglia, as the primary resident immune cells of the CNS, are the first line of defense of the brain's innate immune response against infection, injury, and diseases (*22*). They play an important role in maintaining normal brain function. When the body is healthy, they are known as surveying microglia because they examine the tissue to maintain homeostasis; when disease develops, they are activated and, along with other functions, become phagocytic to clear cellular debris. The current study found that NDG inhibits tics in rats with TS by regulating the activation of microglia.

In the CNS, microglia serve as resident phagocytes that dynamically survey the environment, playing crucial roles in CNS tissue maintenance, injury response, and pathogen defense (*23*). Microglia can respond quickly to various CNS injuries including trauma, ischemia, and infection, and the maintain the homeostasis of the CNS. However, this response is not always beneficial, and sometimes it worsens damage. Studies have indicated that microglia might act as a double-edged sword in various neurological diseases. In general, microglial activation and the increased expression of cytokines are intended to protect the CNS and benefit the host organism. Nonetheless, amplified, exaggerated, or chronic microglial activation can lead to robust pathological changes and neurobehavioral complications such as depression and cognitive deficits (*24*).

Microglial abnormalities are implicated in a range of neuropsychiatric pathologies, including TS and autism. A recent postmortem analysis of brains from patients with TS indicated an increased number of $CD45^{+}$ microglial cells in the striatum and revealed that these cells had morphological changes consistent with neuro-toxic activation (*9*). A recent positron emission tomography study similarly suggested increased microglial activation in patients with TS

(*10*). These findings are consistent with the results of a study by the current authors which found that the neurotoxic drug IDNP can lead to robust pathological changes and neurobehavioral complications with microglial activation in the striatum of rats with TS. After intervention with NDG, the increase in activated microglia decreased and tics were alleviated (Figures 1 and 2).

Neuroinflammation is defined as an inflammatory response within the brain or spinal cord. Microglia play key roles in mediating these neuroinflammatory responses. For example, in infection or disease, microglia become 'activated' and function as inflammatory cellular mediators. Upon activation, resident microglial cells transform from a ramified form to an amoeboid form and acquire the ability to phagocytose and release pro-inflammatory cytokines, chemokines, and growth factors, including ILs (*e.g.*, IL-1 and IL-6), TNF-α, and MCP-1 (*25*).

TS is largely genetic. Recent research has identified a hypomorphic mutation in L-histidine decarboxylase (Hdc) as a rare but high-penetrance genetic cause of TS. TheHdc-KO (knockout of the Hdc gene) model thus serves as a unique platform to probe the pathophysiology of TS and related conditions (*26*). After administration of lipopolysaccharide (LPS) as an inflammatory challenge, microglial activation in the striatum of Hdc-KO mice was enhanced, with greater expression of Iba1 than that in wild-type controls (*27*). This was accompanied by increased production of IL-1β and TNF-α, confirming an increased inflammatory response. Morer *et al.* evaluated the expression of genes encoding selected inflammatory factors including interferon-γ, IL-2, IL-1β, MCP-1, and CD45 in post-mortem specimens from adults with TS (*20*). They noted significantly increased expression of MCP-1 and IL-2 in patients with TS (a 6.5-fold and a 2.3-fold increase, respectively), supporting the notion of inflammatory processes in the basal ganglia of patients with TS.

In the current study, microglia in rats were activated by the neurotoxic drug IDNP and then strongly responded to this specific injury, releasing TNF-α and IL-6 in the striatum and serum (Figure 3). After intervention with NDG, tics were alleviated, and the levels of TNF-α and IL-6in the striatum and serum of rats with TS decreased. TNF-α plays an integral role in immunological responses to infection as a potent regulator of the immune system and inflammatory processes, recruiting macrophages, activating T-cells, and inducing the expression of downstream cytokines and other immune mediators during infection (*28*). IL-6 is an important mediator of neuroinflammation and is involved in microglial priming under neuroinflammatory conditions. IL-6-mediated cell-cell interactions may be an attractive therapeutic target for brain inflammation (*29*). The increase in TNF-α and IL-6 may increase the permeability of the blood-brain barrier. These changes might lead to an enhanced autoimmune response and even abnormal release of neurotransmitters in the basal ganglia, which in turn contributes to the clinical symptoms of TS and related disorders.

MCP-1, also called chemokine (CC motif) ligand 2 (CCL2), is a key chemokine involved in neuroinflammation, and a MCP-1 deficiency protects against inflammation in the brain. Mounting evidence suggests that MCP-1 is significantly involved in the activation of microglia (*30*). The current study found that microglia were activated by the neurotoxic drug IDNP, and they strongly responded to this specific injury by releasing MCP-1 in the striatum of rats with TS (Figure 5A). After intervention with NDG, tics were alleviated, and the levels of MCP-1in the striatum of rats with TS decreased. However, there were no significant differences in the levels of MCP-1 in the serum of the four groups (the control group, the IDNP-induced TS group, the NDG group, and the Hal group) (Figure 5B). The speculation is that MCP-1 might be mainly expressed in brain tissue, a finding that is similar to the results of a previous study which found that MCP-1 and its receptor CCR2 are primarily expressed by microglia in the mouse and human brain (*31*).

IL-1 is one of the most well-known pro-inflammatory cytokines that acts within the brain during insults and neurodegenerative diseases. The IL-1 system involves two essential agonists, IL-1αand IL-1β, as well as IL-1's endogenous antagonist, IL-1 receptor antagonist (IL-1RN) (*32*). In the brain, IL-1 is mainly synthesized and released by activated microglia and involved in neuroinflammation during various neurological diseases. He *et al.* investigated the relationship between single-nucleotide polymorphisms (SNPs) of IL-1α and IL-1RN and the susceptibility to TS in the Chinese Han population (*33*), and they found that IL-1α rs17561 and IL-1RN rs315952 polymorphisms might not be associated with susceptibility to TS in that population. In addition, Morer *et al.* found that the levels of IL-1β expression were below detection limits in both patients with TS and controls (*20*). Interestingly, the current study found no significant differences in the levels of IL-1 both in the striatum and serum of the four groups (the control group, the IDNP-induced TS group, the NDG group, and the Hal group) (Figures 4A and 4B). The speculation is that IL-1 might be not involved in neuroinflammation and microglial activation in TS.

NDG, a TCM to treat TS in accordance with the therapeutic principles of TCM, has been used as an anti-tic agent in Chinese clinics for several years. Pharmacological studies have found that NDG contains a number of active substances such as saponins (*e.g.*, gastrodin and paeoniflorin), steroid saponins, carbohydrates and their glycosides, alkaloids, organic acids, and flavonoids, which have proven to have antioxidant action, to protect brain neurons, to reduce

and allay excitement (*34*).The current study found that NDG inhibited the activation of microglia and decreased the abnormal expression of TNF-α, IL-6, and MCP-1 in the striatum and/or serum of rats with TS, thus controlling tics. However, there were no significant changes in the striatum and/or serum of rats with TS after treatment with Hal. The anti-TS action of Hal might occur not through microglial activation and neuroinflammation but through the DAT system, thus controlling tics (*16*).

In conclusion, microglia might play key roles in mediating neuroinflammatory responses in TS, triggering the release of TNF-α, IL-6, and MCP-1. NDG inhibited tics in rats with TS, and this mechanism may be associated with a reduction in the increased number of activated microglia and a decrease in the expression of pro-inflammatory cytokines and chemokines in the striatum and/or serum.

Acknowledgements

The study was supported by the National Natural Science Foundation of China (grant Nos. 81503613 and 81273798), the Natural Science Foundation of Shandong Province (grant Nos. BS2015YY030 and ZR2012HM030), a Project funded by the China Postdoctoral Science Foundation (grant No. 2014M551924), a Shandong Province Project for Development of Science and Technology in Traditional Chinese Medicine (grant No. 2013ZDZK-085), and Shandong Province Project for Scientific and Technological Development (grant No. 2011GSF11903).

References

1. Stern JS. Tourette's syndrome and its borderland. Pract Neurol. 2018; 18:262-270.
2. Leckman JF. Tourette's syndrome. Lancet. 2002; 360:1577-1586.
3. Hallett M. Tourette syndrome: Update. Brain Dev. 2015; 37:651-655.
4. Swain JE, Scahill L, Lombroso PJ, King RA, Leckman JF. Tourette syndrome and tic disorders: A decade of progress. J Am Acad Child Adolesc Psychiatry. 2007; 46:947-968.
5. Efron D, Dale RC. Tics and Tourette syndrome. J Paediatr Child Health. 2018; 54:1148-1153.
6. Frick L, Pittenger C. Microglial dysregulation in OCD, Tourette syndrome, and PANDAS. J Immunol Res. 2016; 2016:8606057.
7. Hickman S, Izzy S, Sen P, Morsett L, El Khoury J. Microglia in neurodegeneration. Nat Neurosci. 2018; 21:1359-1369.
8. Bilbo SD, Schwarz JM. Early-life programming of later-life brain and behavior: Acritical role for the immune system. Front Behav Neurosci. 2009; 3:14.
9. Lennington JB, Coppola G, Kataoka-Sasaki Y, Fernandez TV, Palejev D, Li Y, Huttner A, Pletikos M, Sestan N, Leckman J, Vaccarino F. Transcriptome analysis of the human striatum in Tourette syndrome. Biol Psychiatry. 2016; 79:372-382.
10. Kumar A, Williams MT, Chugani HT. Evaluation of basal ganglia and thalamic inflammation in children with pediatric autoimmune neuropsychiatric disorders associated with streptococcal infection and tourette syndrome: A positron emission tomographic (PET) study using 11C-[R]-PK11195. J Child Neurol. 2015; 30:749-756.
11. Lv H, Li A, Ma H, Liu F, Xu H. Effects of Ningdong granule on the dopamine system of Tourette's syndrome rat models. J Ethnopharmacol. 2009; 124:488-492.
12. Wang S, Qi F, Li J, Zhao L, Li A. Effects of Chinese herbal medicine Ningdong granule on regulating dopamine (DA)/serotonin (5-TH) and gamma-amino butyric acid (GABA) in patients with Tourette syndrome. Biosci Trends. 2012; 6:212-218.
13. Wang JJ, Qi FH, Wang ZX, Zhang ZK, Pan N, Huai L, Qu SY, Zhao L. A review of traditional Chinese medicine for treatment of glioblastoma. Biosci Trends. 2019; 13:476-487.
14. Tang HX, Li AY, Li JJ, Hou GS, Zhang F. Effect of Ningdong Granule on the levels of IL-12 and TNF-alpha in children patients with Tourette's syndrome. Zhongguo Zhong Xi Yi Jie He Za Zhi. 2014; 34:435-438. (in Chinese).
15. Zhao L, Li AY, Lv H, Liu FY, Qi FH. Traditional Chinese medicine Ningdong granule: The beneficial effects in Tourette's disorder. J Int Med Res. 2010; 38:169-175.
16. Zhao L, Qi F, Zhang F, Wang Z, Mu L, Wang Y, En Q, Li J, Du Y, Li A. Dual regulating effect of Ningdong granule on extracellular dopamine content of two kinds of Tourette's syndrome rat models. Biosci Trends. 2015; 9:245-251.
17. Zhang F, Li A. Dual restoring effects of gastrodin on dopamine in rat models of Tourette's syndrome. Neurosci Lett. 2015; 588:62-66.
18. Hida H, Fukuda A, Fujimoto I, Shimano Y, Nakajima K, Hashitani T, Nishino H. Dopamine-denervation enhances the trophic activity in striatum: Evaluation by morphological and electrophysiological development in PC12D cells. Neurosci Res. 1997; 28:209-221.
19. Bianconi V, Sahebkar A, Atkin SL, Pirro M. The regulation and importance of monocyte chemoattractant protein-1. Curr Opin Hematol. 2018; 25:44-51.
20. Morer A, Chae W, Henegariu O, Bothwell AL, Leckman JF, Kawikova I. Elevated expression of MCP-1, IL-2 and PTPR-N in basal ganglia of Tourette syndrome cases. Brain Behav Immun. 2010; 24:1069-1073.
21. Hong JJ, Loiselle CR, Yoon DY, Lee O, Becker KG, Singer HS. Microarray analysis in Tourette syndrome postmortem putamen. J Neurol Sci. 2004; 225:57-64.
22. Nadal-Nicolás FM, Jiménez-López M, Salinas-Navarro M, Sobrado-Calvo P, Vidal-Sanz M, Agudo-Barriuso M. Microglial dynamics after axotomy-induced retinal ganglion cell death. J Neuroinflammation. 2017; 14:218.
23. Prinz M, Jung S, Priller J. Microglia biology: One century of evolving concepts. Cell. 2019; 179:292-311.
24. Wolf SA, Boddeke HW, Kettenmann H. Microglia in physiology and disease. Annu Rev Physiol. 2017; 79:619-643.
25. DiSabato DJ, Quan N, Godbout JP. Neuroinflammation: The devil is in the details. J Neurochem. 2016; 139 Suppl 2:136-153.
26. Pittenger C. Histidine Decarboxylase Knockout Mice as a model of the pathophysiology of Tourette syndrome and

related conditions. Handb Exp Pharmacol. 2017; 241:189-215.
27. Frick L, Rapanelli M, Abbasi E, Ohtsu H, Pittenger C. Histamine regulation of microglia: Gene-environment interaction in the regulation of central nervous system inflammation. Brain Behav Immun. 2016; 57:326-337.
28. Parker-Athill EC, Ehrhart J, Tan J, Murphy TK. Cytokine correlations in youth with tic disorders. J Child Adolesc Psychopharmacol. 2015; 25:86-92.
29. Matsumoto J, Dohgu S, Takata F, Machida T, Hatip F, Hatip-Al-Khatib I, Yamauchi A, Kataoka Y. TNF-α-sensitive brain pericytes activate microglia by releasing IL-6 through cooperation between IκB-NFκB and JAK-STAT3 pathways. Brain Res. 2018; 1692:34-44.
30. Zhang K, Wang H, Xu M, Frank JA, Luo J. Role of MCP-1 and CCR2 in ethanol-induced neuroinflammation and neurodegeneration in the developing brain. J Neuroinflammation. 2018; 15:197.
31. Conductier G, Blondeau N, Guyon A, Nahon JL, Rovère C. The role of monocyte chemoattractant protein MCP1/CCL2 in neuroinflammatory diseases. J Neuroimmunol. 2010; 224:93-100.
32. Dinarello CA. A clinical perspective of IL-1β as the gatekeeper of inflammation. Eur J Immunol. 2011; 41:1203-1217.
33. Chou IC, Lin HC, Wang CH, Lin WD, Lee CC, Tsai CH, Tsai FJ. Polymorphisms of interleukin 1 gene IL1RN are associated with Tourette syndrome. Pediatr Neurol. 2010; 42:320-324.
34. Zhao L. The clinical and molecular biological mechanismstudy of Ningdong granule on Tourette's syndrome [D]. Jinan: Medical College of Shandong University. 2010; PP. 22-24. (in Chinese)

Received July 6, 2020; Revised July 26, 2020; Accepted July 29, 2020.

*Address correspondence to:
Fanghua Qi, Department of Traditional Chinese Medicine, Shandong Provincial Hospital affiliated to Shandong University, No.324, Jingwuweiqi Road, Ji'nan, Shandong 250021, China.
E-mail: qifanghua2006@126.com

Released online in J-STAGE as advance publication July 31, 2020.

Original Article

DOI: 10.5582/bst.2020.03136

Correlation between reticulum ribosome-binding protein 1 (RRBP1) overexpression and prognosis in cervical squamous cell carcinoma

Jiaqi Zhu[§], Ruixue Zhao[§], Wei Xu, Jing Ma, Xin Ning, Rong Ma[*], Fanling Meng[*]

Department of Gynecology, Harbin Medical University Cancer Hospital, Harbin, Heilongjiang, China.

SUMMARY Our purpose was to evaluate the correlation between endoplasmic reticulum ribosomal binding protein 1 (RRBP1) expression in cervical squamous cell carcinoma (CSCC) and poor patient prognosis. RRBP1 is a nascent transporter that is situated on the rough endoplasmic reticulum (ER). It adjusts to the secretion of proteins in cells and alleviates ER stress, thus stimulating cell proliferation. An immunohistochemical (IHC) study was conducted to detect the expression level of RRBP1 on 96 CSCC tissue samples. Western blot and Quantitative real-time polymerase chain reaction (qRT-PCR) were performed to compare the expression levels of RRBP1 in cervical squamous cell carcinoma with healthy cervical tissues. An overexpression of RRBP1 was observed in CSCC tissues, and the expression level was associated with FIGO stage (Stage I *vs.* II: 52.6% *vs.* 74.1%, $p = 0.030$), and lymph node metastasis (No *vs.* Yes: 61.5% *vs.* 92.3%, $p = 0.031$) but not patient age and tissue differentiation. Univariate survival analysis indicated that prognosis was associated with the expression level of RRBP1 and tissue differentiation and lymph node metastasis. Analysis of the multi-factor survival Cox model proved that RRBP1 was an independent prognostic factor. In conclusion, compared with healthy cervical tissues, RRBP1 was overexpressed in CSCC tissues, illustrating that RRBP1 may be a new biomarker for the diagnosis of CSCC. The study on RRBP1 may contribute to exploring the pathogenesis of CSCC and may also guide targeted therapy for CSCC in the future.

Keywords cervical squamous cell carcinoma (CSCC), endoplasmic reticulum ribosome binding protein 1 (RRBP1), diagnosis, prognosis

1. Introduction

Cervical cancer (CC) is the fourth most common cancer in women and the fourth leading cause of cancer-related death (*1*). With the popularity of cervical cancer screening and the application of the human papilloma virus (HPV) vaccine in recent years, its incidence and mortality are declining, but the 5-year overall survival (OS) rate for advanced CC patients remains at only 52% and still plagues women (*2*). In recent years, individualized treatment based on gene targets has become a trend, and it has been proven that MALAT1 is involved in the development of CC (*3*). Although the discovery of these genes has certain significance for the early diagnosis and personalized treatment of CC, some of these diagnostic techniques or treatments cannot be widely applied to the clinic due to low accuracy or high expense. Cervical squamous cell carcinoma (CSCC) is the most common pathologic type of CC (*4*). Therefore, the identification of high-precision CSCC molecular markers is imperative, which will guide the early diagnosis and treatment of CSCC.

Endoplasmic reticulum ribosomal-binding protein 1 (RRBP 1) is a transport protein with a molecular weight of 180 KD that is located on the rough endoplasmic reticulum (ER) membrane (*5,6*). Its most notable feature of primary structure is a highly conserved sequence containing 10 amino acids that is repeated 54 times for a series near the NH2 end of the protein (*7*). According to previous studies, we found that low RRBP1 expression is related to deposition of the extracellular matrix in myogenic progenitor cells (*8*). RRBP1 plays an important role in intestinal maturation and can be expressed during osteoblast differentiation and at neuromuscular junctions (*9,10*). In recent years, RRBP1 has been determined to be overexpressed in lung cancer and involved in the mRNA stability control of unfolded protein response (UPR) components, thus diminishing ER stress and assisting tumor cell survival (*11,12*). In addition, we determined that RRBP1 was

related to multiple cancers, such as, liver cancer, prostate cancer, colorectal cancer, lung cancer, breast cancer, esophageal cancer, endometrial cancer and ovarian cancer according to previous studies (*11,13-19*). All of the above findings suggest that RRBP1 may be related to the proliferation of tumor cells, indicating that it may also act as a new biomarker and become a new target for therapy of malignant tumors.

However, few studies have explored expression levels of RRBP1 in CSCC, and the relationship with clinicopathological features. Our study aimed to investigate whether RRBP1 was expressed in CSCC using Immunohistochemical (IHC), Western blot and Quantitative real-time polymerase chain reaction (qRT-PCR) methods.

2. Materials and Methods

2.1. Patients and clinical samples

A total of 96 CSCC tissue samples were collected from 96 patients who had undergone cervical cancer stage surgery at Department of Gynecology Harbin Medical University Cancer Hospital between January 10, 2010 and November 20, 2012. None of these patients had any therapy before surgery, including immunotherapy, chemotherapy, or radiotherapy. The paraffin-embedded sections of the 96 clinical samples were made for IHC analysis after fixation, dehydration, transparency, wax transparency, embedding, sectioning, patching, staining, transparency, and paraffin embedding. The clinical pathological features of the patients enrolled were obtained from the medical record system of the hospital. The patients were followed from the day of surgery until November 30, 2018 (the follow-up period was 11-105 months, average 81 months). We also collected 36 fresh surgical specimens for Western blot and qRT-PCR analysis at Harbin Medical University Cancer Hospital from November 2018 to May 2019, including 10 normal cervical tissues and 26 CSCC tissues. The study was approved by the Harbin Municipal Ethics Committee and all enrolled participants have signed informed consent after being fully informed.

2.2. IHC

First, the reagents were prepared according to the manufacturer's instructions. Then the 96 paraffin-embedded sections were treated with antigen retrieval and serum blocking. The primary anti-RRBP1 antibody (1:1,000, Abcam, Ab95983, UK) was added to all samples and then incubated at 4°C overnight. After rinsing with phosphate buffered saline (PBS), the biotin-labelled secondary antibody (goat anti-rabbit lgG-HRP, Wanleibio, WLA023, China) was added to samples and incubated at 37°C for 30 minutes. After staining all samples with Diaminobenzidine (DAB) chromogen, the samples were incubated at room temperature for 1 hour. Finally, the samples were counterstained with hematoxylin after rinsing with PBS. The negative control is a diluent.

2.3. IHC result judgment

IHC results were evaluated by two pathologists and RRBP1 staining was analyzed by semi-quantitative methods. The intensity was scored as follows: colourlessness (0), light yellow (1), brownish yellow (2), and brown (3). The percentage of positive cells was scored as follows: 0 indicates < 5%, 1 indicates 5-25%, 2 indicates 26-50%, 3 indicates 51-75%, and 4 indicates > 75%. The final score was evaluated by multiplying the above two scores together, and a score ≥ 4 was considered overexpression and a score < 4 was considered low expression.

2.4. Western blot analysis

First, the reagents and polyacrylamide gels were prepared according to manufacturer's instructions. For protein extraction, the lysate (containing 1% PMSF) was aliquoted on the basis of the demands of the experiment and added to each sample. The lysate was centrifuged at 12,000 rpm for 5 minutes at 4°C. Then, total protein was quantified using a BCA protein concentration determination kit (Wanleibio, WLA004, China). The complex protein mixture was separated using Sodium dodecyl sulfate-polyacrylamide gel (SDS-PAGE) (Wanleibio, WLA013, China) and transferred to a Polyvinylidene difluoride (PVDF) membrane (Millipore, IPVH00010, USA) using normal methods. The primary RRBP1 antibody (1:1,000) was added to 36 samples which were then incubated at 4°C overnight. Then, the secondary antibody, goat anti-rabbit lgG-HRP (1:5,000), was added and incubated for 45 minutes at 37°C. Finally, the chemiluminescent reagent was added to the membrane and slowly shaken. The membrane was placed on X-ray film in a dark room before final development, and the exposure time was adjusted according to the strength of the signal. Gel-Pro-Analyzer software was used to analyze the optical density value of the target band. A β-actin antibody (Wanleibio, WL01845, China) was used as an internal reference antibody.

2.5. Real-time PCR analysis

First, mRNA was extracted from 36 samples according to instructions, and the concentration of RNA was measured using a NanoDrop 2000 UV spectrophotometer (NanoDrop 2000, Thermo, USA). cDNA was then synthesized in a PCR instrument (Real-Time PCR, Exicycler 96, BIONEER, Korea) using Super M-MLV reverse transcriptase (BioTeke, PR6502, Beijing), and the products underwent quantitative fluorescence analysis

with the $2^{-\Delta\Delta Ct}$ method. The RRBP1-F primer sequence is 5'-TCCATCCAGAGTCTCACTTC-3', and the RRBP1-R primer sequence is 5'-GCCCTCGTTGAACACCAT-3'. The GAPDH-F primer sequence of is 5'-GGCACCCAG CACAATGAA-3', and the GAPDH-R primer sequence of is 5'-TAGAAGCATTTGCGGTGG-3'.

2.6. Statistical analysis

The IHC results were analyzed using the chi-square test. The Western blot result was assessed by the gray value of the electrophoretic band, which was analyzed by GraphPad Prism 8.0.2 (GraphPad Software Inc., San Diego, California, United States) and plotted as a peak curve where the peak area represented protein concentration. Finally, the results were plotted as a histogram. The PCR results were analyzed by the $2^{-\Delta\Delta Ct}$ method, and the products of PCR were subjected to quantitative fluorescence analysis. Finally, the results were drawn into a histogram by GraphPad Prism. OS and DFS of all samples were estimated by Kaplan-Meier method, and were tested by the log-rank test. Finally, multivariate analysis was conducted with Cox regression models (proportional risk models). A P value < 0.05 was deemed statistically significant. All the above data analyses were performed using Windows SPSS software V25.0 (IBM SPSS, Inc., Chicago, IL, USA).

3. Results

3.1. Patient pathological characteristics

To analyze the immunity of RRBP1 in all tissue samples, we examined 96 untreated CSCC tissue samples by IHC. As shown in Table 1, 45 were obtained from patients > 49 years old, and 51 were ≤ 49 years old. Of the 96 patients, 38 patients were in stage I (according to FIGO cervical cancer staging in 2009), and 58 patients were in stage II.

Table 1. Association analyses between the expression levels of RRBP1 and the clinicopathological characteristics of Cervical squamous cell carcinoma (CSCC)

Variables	Patients (*n*)	RRBP1 expression		P^a
		Low	High	
Age (years)				0.667
> 49	45	14	31	
≤ 49	51	19	32	
FIGO stage				0.030
I	38	18	20	
II	58	15	43	
Histological grade				0.071
G1	23	12	11	
G2	65	20	45	
G3	8	1	7	
lymph node metastasis				0.031
No	83	32	51	
Yes	13	1	12	

G1, well differentiated; G2, moderately differentiated; G3, poorly differentiated; [a]Chi-square test.

3.2. Expression of RRBP1 was extremely obvious in CSCC

We analyzed 26 fresh CSCC specimens by Western blot and qRT-PCR and compared them with 10 normal cervical specimens, and the results showed that the expression of RRBP1 increased obviously at both the protein (Figure 1B, $p < 0.001$) and mRNA level (Figure 2, $p < 0.001$) in CSCC tissue.

To analyze the association between the expression of RRBP 1 and the pathological features of CSCC patients, we performed an IHC analysis on 96 samples. The IHC outcomes showed that RRBP1 was situated in the cytoplasm of CSCC (Figure 3). As shown in Table 1, there were 33 patients with low RRBP1 expression and 63 patients with high RRBP1 expression. Moreover, in CSCC tissue, the high expression of RRBP1 was related to FIGO stage (Stage I *vs.* II: 52.6% *vs.* 74.1%, $p = 0.030$), and lymph node metastasis (No *vs.* Yes: 61.5% *vs.* 92.3%, $p = 0.031$), but not patient age ($p = 0.667$) and tissue differentiation ($p = 0.071$) (Table 1).

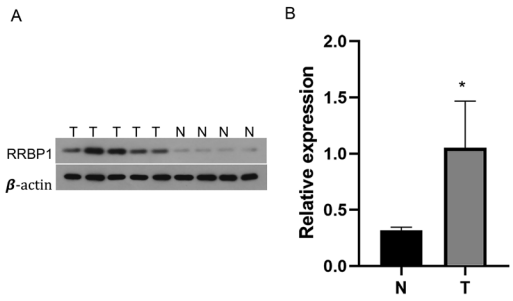

Figure 1. (A), Representative protein samples obtained from frozen normal cervical tissues (N) and cervical squamous cell carcinoma tissues (T) were analyzed by Western blot. The levels of β-actin were used as an internal control; **(B)**, Histogram of pooled data from N (n = 10) and cervical squamous cell carcinoma cells (CSCCs) ($n = 26$**).** RRBP1 expression was elevated in CSCCs compared with that in N. The data are presented as the mean ± SD ($^*p < 0.001$).

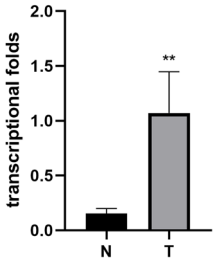

Figure 2. Histogram of RRBP1 mRNA expression in normal cervical tissues and cervical squamous cell carcinoma tissues (N, normal cervical tissues; T, cervical squamous cell carcinoma tissues). The levels of β-actin were used as an internal control, and the RRBP1 mRNA expression was calculated by $2^{-\Delta\Delta Ct}$ method. RRBP1 mRNA expression was elevated in CSCCs compared with normal cervical tissues. The data are presented as the mean ± SD ($^{**}p < 0.001$).

3.3. Association between overexpression of RRBP1 in CSCC and patient unfavorable prognosis.

We analyzed the OS and DFS of 96 patients using the Kaplan-Meier method. The results showed that high RRBP1 expression significantly shortened OS (Figure 4A, $p = 0.018$) and DFS (Figure 4B, $p = 0.008$). Univariate survival analysis indicated that RRBP1 high expression and tissue differentiation and lymph node metastasis were related to unfavorable prognosis of CSCC (Table 2); Table 2 manifests OS ($p = 0.001$) and DFS ($p < 0.001$) of patients with RRBP1 overexpression, and OS ($p = 0.045$) and DFS ($p = 0.016$) of patients with lymph node metastasis, and OS ($p = 0.010$) and DFS ($p = 0.003$) of patients with tissue differentiation.

Furthermore, multivariate survival evaluation was conducted with Cox regression models. RRBP1 is an independent prognostic factor. The estimation of OS (95% Cl = 1.305 -73.315, $p = 0.026$) and DFS (95% Cl = 1.712- 95.598, $p = 0.013$) is shown in Table 3.

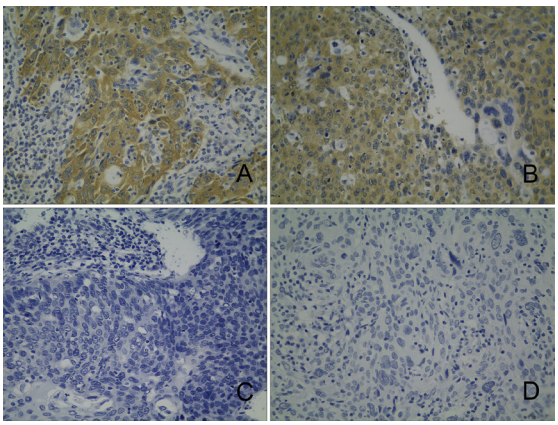

Figure 3. Immunohistochemical staining of RRBP1 in CSCC specimens. A and B, High expression of RRBP1 in CSCCs; C and D, Low expression of RRBP1 in CSCCs.

4. Discussion

In this study, we analyzed the association between the expression level of RRBP1 in CSCC and patient prognosis. It seems to be the first published assessment

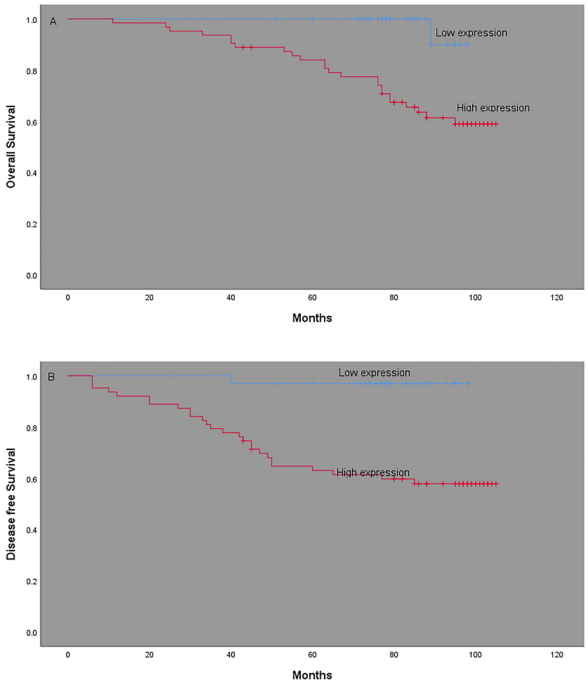

Figure 4. Kaplan-Meier analysis of overall survival and disease-free survival related to expression of RRBP1. Patients with high expression of RRBP1 had a poorer prognosis than those with low expression of RRBP1. **(A),** overall survival curves of CSCC according to their RRBP1 expression status, ($p = 0.018$); **(B)**, disease-free survival curves of CSCC patients according to their RRBP1 expression status, ($p = 0.008$).

Table 2. Univariate survival analysis of OS and DFS in 96 patients with Cervical squamous cell carcinoma (CSCC)

Variables	*n*	OS		P^a	DFS		P^a
		Mean ± SE (month)	95% CI		Mean ± SE (month)	95% CI	
Age(years)							
> 49	45	96 ± 3	91 - 102	0.200	91 ± 4	82 - 99	0.164
≤ 49	51	88 ± 4	81 - 95		80 ± 5	70 - 89	
FIGO stage							
I	38	93 ± 3	86 - 100	0.767	85 ± 5	76 - 95	0.667
II	58	91 ± 3	85 - 97		84 ± 4	76 - 93	
Histological grade							
G1	23	95 ± 3	90 - 100	0.010	89 ± 6	77 - 100	0.003
G2	65	94 ± 3	88 - 99		87 ± 4	79 - 95	
G3	8	65 ± 10	44 - 85		54 ± 11	32 - 76	
lymph node metastasis							
No	83	94 ± 2	89 - 99	0.045	88 ± 3	82 - 95	0.016
Yes	13	82 ± 5	71 - 92		65 ± 9	47 - 83	
RRBP1							
Low expression	38	97 ± 1	95 - 99	0.001	96 ± 2	93 - 100	< 0.001
High expression	58	87 ± 3	81 - 94		77 ± 5	68 - 86	

G1, well differentiated; G2, moderately differentiated; G3, poorly differentiated; OS, overall survival; DFS, disease-free survival; [a]Log-rank test.

Table 3. Multivariate survival analysis of OS and DFS in 96 patients with Cervical squamous cell carcinoma (CSCC)

Variables	OS			OS		
	Exp(B)	95% CI	P^a	Exp(B)	95% CI	P^a
lymph node metastasis	0.617	0.729 - 4.714	0.195	0.672	0.822 - 4.664	0.129
Histological grade	0.693	0.913 - 4.380	0.083	0.709	0.983 - 4.203	0.056
RRBP1	2.281	1.305 - 73.315	0.026	2.549	1.712 - 95.598	0.013

OS overall survival; DFS disease-free survival; CI confidence interval; [a]Cox regression test.

of RRBP1 expression levels in CSCC tissue.

RRBP1 was originally found in Saccharomyces cerevisiae, which is also located on the ER membrane, with a primary structure containing an immensely repetitive tandem sequence (*7*). Previous studies have shown that the function of the internal ribosome entry site (IRES) is to maintain or enhance the expression of regulatory proteins (*20,21*). Gao *et al.* demonstrated that in liver cancer cells, the 5'-untranslated region (UTR) of the RRBP1 protein contains an IRES and the overexpression of RRBP1 was mainly to enhance protein synthesis (*13*). Fulda *et al.* have shown that enhanced ER activity is necessary for the rapid proliferation of tumor cells, and ER stress will promote the UPR, initiating the mitogen-activated protein kinase (MAPK) family signaling pathway (*12*). Tsai *et al.* demonstrated in lung cancer tissue that RRBP1 may participate in the adjustment of the normality of GRP78 (a UPR component) mRNA, thereby reducing ER stress and helping tumor cells survive (*11,22,23*). Diefenbach *et al.* demonstrated that RRBP1 interacted with cell microtubules by binding to kinase family member 5B (KIF5B) (*24*). Lee *et al.* discovered that the RRBP1-ALK fusion genes were a novel and recurrent carcinogenic mechanism in invasive epithelioid inflammatory myofibroblastic sarcoma (*25*). In recent years, overexpression of RRBP1 has been found in many kinds of cancers and is closely related to poor prognosis (*11, 13-19*). Through our study, it is indicated that RRBP1 may be involved in the occurrence of CSCC and has important clinical significance for exploring the carcinogenic mechanism of CSCC in the future. We confirmed that RRBP1 is an independent prognostic factor, indicating that RRBP1 may be a potential biological marker for CSCC.

We used the same methods as previous studies. The pathogenesis of RRBP1 in CSCC is not clearly understood yet and still needs further investigation. All of our samples were squamous cell carcinomas; therefore, many other kinds of pathological types are needed to fully evaluate the association between the expression level of RRBP1 in CC and patient prognosis.

In conclusion, RRBP1 may become a new biomarker for CSCC and has important clinical significance for exploring the carcinogenic mechanism of CSCC in the future. RRBP1 may play an important role in early diagnosis, individualized therapy of CSCC patients.

Acknowledgements

This work was supported by grants from the Liande Wu Science Foundation for Young Scholars of Harbin Medical University Cancer Hospital (WLD-QN1705) and the Postdoctoral Research Startup Fund of Heilongjiang Province (LBH-Q16162) and Outstanding Young Scholars fund of Harbin Medical University Cancer Hospital (JCQN2019-05). The funders had no role in study design, data collection and analysis, decision to publish, or preparation of the manuscript. We express our thanks to Dr. Qi Huang for evaluation procedures.

References

1. Bray F, Ferlay J, Soerjomataram I, Siegel RL, Torre LA, Jemal A. Global cancer statistics 2018: GLOBOCAN estimates of incidence and mortality worldwide for 36 cancers in 185 countries. CA Cancer J Clin. 2018; 68:394-424.
2. Green JA, Kirwan JM, Tierney JF, Symonds P, Fresco L, Collingwood M, Williams CJ. Survival and recurrence after concomitant chemotherapy and radiotherapy for cancer of the uterine cervix: a systematic review and meta-analysis. Lancet. 2001; 358:781-786.
3. Guo F, Li Y, Liu Y, Wang J, Li Y, Li G. Inhibition of metastasis-associated lung adenocarcinoma transcript 1 in CaSki human cervical cancer cells suppresses cell proliferation and invasion. Acta Biochim Biophys Sin (Shanghai). 2010; 42:224-229.
4. Bhatla N, Aoki D, Sharma DN, Sankaranarayanan R. Cancer of the cervix uteri. Int J Gynaecol Obstet. 2018; 143 Suppl 2:22-36.
5. Savitz AJ, Meyer DI. Identification of a ribosome receptor in the rough endoplasmic reticulum. Nature. 1990; 346:540-544.
6. Savitz AJ, Meyer DI. 180-kD ribosome receptor is essential for both ribosome binding and protein translocation. J Cell Biol. 1993; 120:853-863.
7. Wanker EE, Sun Y, Savitz AJ, Meyer DI. Functional characterization of the 180-kD ribosome receptor *in vivo*. J Cell Biol. 1995; 130:29-39.
8. Fry CS, Kirby TJ, Kosmac K, McCarthy JJ, Peterson CA. Myogenic progenitor cells control extracellular matrix production by fibroblasts during skeletal muscle hypertrophy. Cell Stem Cell. 2017; 20:56-69.
9. Nazarian J, Bouri K, Hoffman EP, Intracellular expression profiling by laser capture microdissection: three novel components of the neuromuscular junction. Physiol Genomics. 2005; 21:70-80.

10. Chang J, Chance MR, Nicholas C, *et al.* Proteomic changes during intestinal cell maturation *in vivo*. J Proteomics. 2008; 71:530-546.
11. Tsai HY, Yang YF, Wu AT, Yang CJ, Liu YP, Jan YH, Lee CH, Hsiao YW, Yeh CT, Shen CN, Lu PJ, Huang MS, Hsiao M. Endoplasmic reticulum ribosome-binding protein 1 (RRBP1) overexpression is frequently found in lung cancer patients and alleviates intracellular stress-induced apoptosis through the enhancement of GRP78. Oncogene. 2013; 32:4921-431.
12. Fulda S, Debatin KM. Extrinsic versus intrinsic apoptosis pathways in anticancer chemotherapy. Oncogene. 2006; 25: 4798-811.
13. Gao W, Li Q, Zhu R, Jin J. La autoantigen induces ribosome binding protein 1 (RRBP1) expression through internal ribosome entry site (IRES)-mediated translation during cellular stress condition. Int J Mol Sci. 2016; 17:1174.
14. Li T, Wang Q, Hong X, Li H, Yang K, Li J, Lei B. RRBP1 is highly expressed in prostate cancer and correlates with prognosis. Cancer Manag Res. 2019; 11:3021-3027.
15. Pan Y, Cao F, Guo A, Chang W, Chen X, Ma W, Gao X, Guo S, Fu C, Zhu J. Endoplasmic reticulum ribosome-binding protein 1, RRBP1, promotes progression of colorectal cancer and predicts an unfavourable prognosis. Br J Cancer. 2015; 113:763-772.
16. Liang X, Sun S, Zhang X, Wu H, Tao W, Liu T, Wei W, Geng J, Pang D. Expression of ribosome-binding protein 1 correlates with shorter survival in Her-2 positive breast cancer. Cancer Sci. 2015; 106:740-746.
17. Wang L, Wang M, Zhang M, Li X, Zhu Z, Wang H. Expression and significance of RRBP1 in esophageal carcinoma. Cancer Manag Res. 2018; 10:1243-1249.
18. Liu S, Lin M, Ji H, Ding J, Zhu J, Ma R, Meng F. RRBP1 overexpression is associated with progression and prognosis in endometrial endometrioid adenocarcinoma. Diagn Pathol. 2019; 14:7.
19. Ma J, Ren S, Ding J, Liu S, Zhu J, Ma R, Meng F. Expression of RRBP1 in epithelial ovarian cancer and its clinical significance. Biosci Rep. 2019; 39:BSR20190656.
20. Hellen CU, Sarnow P. Internal ribosome entry sites in eukaryotic mRNA molecules. Genes Dev. 2001; 15:1593-1612.
21. Komar AA, Hatzoglou M. Exploring internal ribosome entry sites as therapeutic targets. Front Oncol. 2015; 5:233.
22. Bertolotti A, Zhang Y, Hendershot LM, Harding HP, Ron D. Dynamic interaction of BiP and ER stress transducers in the unfolded-protein response. Nat Cell Biol. 2000; 2:326-332.
23. Shen J, Chen X, Hendershot L, Prywes R. ER stress regulation of ATF6 localization by dissociation of BiP/GRP78 binding and unmasking of Golgi localization signals. Dev Cell. 2002; 3:99-111.
24. Diefenbach RJ, Diefenbach E, Douglas MW, Cunningham AL. The ribosome receptor, p180, interacts with kinesin heavy chain, KIF5B. Biochem Biophys Res Commun. 2004; 319:987-992.
25. Lee JC, Li CF, Huang HY, Zhu MJ, Marino-Enriquez A, Lee CT, Ou WB, Hornick JL, Fletcher JA. ALK oncoproteins in atypical inflammatory myofibroblastic tumours: novel RRBP1-ALK fusions in epithelioid inflammatory myofibroblastic sarcoma. J Pathol. 2017; 241:316-323.

Received May 2, 2020; Revised June 5, 2020; Accepted June 9, 2020.

[§]These authors contributed equally to this work.
**Address correspondence to:*
Rong Ma and Fanling Meng, Department of Gynecology, Harbin Medical University Cancer Hospital, Harbin, 150081, China.
E-mail: dr_marong2017@126.com (Ma R), dr_mfl1979@126.com (Meng FL)

Released online in J-STAGE as advance publication June 14, 2020.

Original Article

DOI: 10.5582/bst.2020.03086

Analysis of coagulation parameters in patients with COVID-19 in Shanghai, China

Ying Zou[1,§], Hongying Guo[1,§], Yuyi Zhang[1], Zhengguo Zhang[1], Yu Liu[1], Jiefei Wang[1], Hongzhou Lu[2,*], Zhiping Qian[1,*]

[1] Department of Severe hepatopathy, Shanghai Public Health Clinical Center, Fudan University, Shanghai, China;
[2] Department of Infectious Disease and Immunology, Shanghai Public Health Clinical Center, Fudan University, Shanghai, China.

SUMMARY To investigate the characteristic of coagulation function in 303 patients with Coronavirus disease 2019 (COVID-19), we evaluated the correlation between coagulation function and disease status. We retrospectively analyzed 303 patients diagnosed with COVID-19 and evaluated the clinical data of 240 patients who were discharged. The coagulation function of the two groups (mild and severe) was compared. Compared with the mild group, majority of patients in the severe group were male (76.9% *vs*. 49.8%) and elderly (median age 65 *vs.* 50), and the proportion with chronic underlying diseases was higher (73.1% *vs.* 36.1%). There were 209 abnormalities (69.0%) of coagulation parameters in 303 patients admitted to hospital. Comparison of various indexes of coagulation function between the two groups in admission, the proportion of abnormal coagulation indicators in the severe group was higher than that in the mild group (100% *vs.* 66.1%). The median coagulation parameters in the severe group were higher than those in the mild group: international normalized ratio (1.04 *vs.* 1.01), prothrombin time (13.8 *vs.* 13.4) seconds, activated partial thromboplastin time (43.2 *vs.* 39.2) seconds, fibrinogen (4.74 *vs.* 4.33) g/L, fibrinogen degradation products (2.61 *vs.* 0.99) μg/mL, and D-dimer (1.04 *vs.* 0.43) μg/mL, the differences were statistically significant ($p < 0.05$). Coagulation dysfunction is common in patients with COVID-19, especially fibrinogen and D-dimer elevation, and the degree of elevation is related to the severity of the disease. As the disease recovers, fibrinogen and activated partial thromboplastin time also return to normal.

Keywords COVID-19, SARS-CoV-2 , coagulation parameter, fibrinogen, D-dimer

1. Introduction

Coronavirus disease 2019 is caused by a novel beta coronavirus, on February 12, 2020, the International Committee on Taxonomy of Viruses (ICTV) named the virus SARS-CoV-2 (severe acute respiratory syndrome coronavirus 2), and on the same day, the World Health Organization (WHO) named the disease COVID-19. As of March 2, 2020, the number of confirmed cases in China had exceeded 80,000 and the number of cases outside China had exceeded 10,000, resulting in more than 3,000 deaths and a crude case fatality rate close to 3% (*1*), posing a huge threat to human life and safety. Up to date, the number of COVID-19 patients is still rapidly increasing worldwide, which is a threat to the health and lives of people all over the world. The main clinical symptoms of COVID-19 are fever, dry cough, and fatigue; while the main abnormalities in laboratory parameters are lymphopenia, elevated liver enzymes, elevated LDH, CRP, and erythrocyte sedimentation rate (*1-5*). Elevated troponin and D-dimer are observed in severe cases (*6*). In previous studies, 173 of 1,099 patients were clinically classified as severe or critically ill, with a severity rate of 15.7% (*3*). Different studies reported mortality rates varied 4.3% to 14.6%. Organ insufficiency and coagulopathy were closely associated with high mortality (*7,8*).

There have been few reports on the analysis of coagulopathy in patients with COVID-19. A previous study reported abnormalities in coagulation-related parameters in 183 patients at Wuhan Tongji Hospital at admission and during hospitalization. The study found that prothrombin time, fibrinogen, D-dimer, and fibrinogen degradation products of patients in the non-surviving group were elevated compared to those in the surviving group, suggesting that coagulopathy may be associated with prognosis, and may guide clinical treatment (*6*). To further investigate the correlation between coagulopathy and disease, we analyzed 303 patients in Shanghai diagnosed with novel coronavirus

pneumonia and followed up on the dynamic changes of coagulation function in 240 patients who achieved clinical cure and were discharged.

2. Subjects and Methods

2.1. Research subjects

Between January 20 and February 24, 2020, 324 adult patients with confirmed COVID-19 were admitted to the Shanghai Public Health Clinical Center, of which a total of 303 patients were included in the study. Among them, there was 1 mild case, 276 moderate cases, 10 severe cases, and 16 critical cases. All patients were diagnosed and classified based on the criteria in the "Diagnosis and Treatment Protocols for Novel Coronavirus Pneumonia (7th draft edition)" (*9*). As of February 24, 2020, 240 patients had been discharged, including 1 mild case, 234 moderate cases, and 5 severe cases.

2.2. Methods

Clinical data and baseline coagulation function data was collected from the 303 patients at the time of admission. Among them, the coagulation function of the 240 patients, who recovered and were discharged, were retrospectively analyzed. These cases were divided into two groups based on disease severity: mild (including mild and moderate) and severe (including severe and critical). The baseline coagulation functions of the two groups were compared to assess the correlation between coagulation function and disease severity. The coagulation function of the 240 discharged patients at admission and at discharge were compared, and the changes in coagulation function were followed up.

2.3. Statistics

Data were processed using SPSS 19.0 statistical software. Non-normally distributed measurement data were presented using the median (interquartile range), and the Mann-Whitney test was used to compare between groups (for non-normally distributed data). Qualitative data were expressed as frequencies or rates, and the chi-square test or Fisher's exact test was used for comparisons between groups. Results with $p < 0.05$ were considered statistically significant.

3. Results

3.1. Baseline characteristics of patients with COVID-19

A total of 303 patients diagnosed with COVID-19 were included in this study, consisting of 1 mild case, 276 moderate cases, 10 severe cases, and 16 critical cases. These cases were divided into two groups based on the disease severity: a mild group (including mild and moderate) and a severe group (including severe and critical); the rate of severe cases was 8.6%. There were 158 males and 145 females, the median age was 51 years (Age range: 16-88 years). The median time from the disease onset to admission was 4 days (2-8 days). Mild and severe groups showed statistically significant differences in sex ratio, age distribution, and presence of chronic underlying diseases. In the severe group, there were more males, many patients were middle-aged or elderly, and there was a higher proportion of chronic underlying diseases, including 11 cases of hypertension, 8 cases of fatty liver disease, 5 cases of coronary heart disease, 6 cases of diabetes, 3 cases of chronic bronchitis, 1 case of malignant cancer, 1 case of chronic kidney disease, 1 case of cerebral infarction, and 1 case of hypothyroidism. There were no statistically significant differences between the two groups in smoking history or time from onset to admission (Table 1).

3.2. Analysis of abnormal coagulation parameters at admission

Coagulation function examination of the 303 patients at admission revealed abnormal parameters in a total of 209 (69.0%) cases. The most common abnormal parameters were fibrinogen (FIB) (195 cases, 64.3%) followed by D-dimer (129 cases, 42.6%), prolonged prothrombin time (PT) (56 cases, 18.5%), abnormal activated partial thromboplastin time (APTT) (66 cases, 21.8%), which was increased in 57 cases (18.8%) and decreased in 9 cases (3.0%); and elevated fibrinogen degradation products (FDP) in 19 cases (6.3%). The proportion of abnormal coagulation parameters in the severe group was higher than in the mild group (100% *vs.* 66.1%), of which the proportions of abnormal fibrinogen (80.8% *vs.* 62.8%), D-dimer (80.8% *vs.* 39.0%), activated partial thromboplastin time (34.6% *vs.* 20.6%), prothrombin time (38.5% *vs.* 16.6%), and fibrinogen degradation products (19.2% *vs.* 5.1%) were higher than in the mild

Table 1. Comparison of baseline demographic characteristics of patients in the mild and severe groups

Items	Mild (n = 277)	Severe (n = 26)	Statistic	p-value
Males (patients (%))	138 (49.8%)	20 (76.9%)	$X^2 = 7.0$	0.008
Age (years)	50 (36-63)	65 (63-76)	$Z = -4.736$	< 0.001
Chronic underlying disease (patients (%))	100 (36.1%)	19 (73.1%)	$X^2 = 13.6$	< 0.001
History of smoking (patients (%))	12 (4.3%)	2 (7.7%)	/	0.607
Time from onset to admission (days)	4.0 (2.0-8.0)	5.5 (3.0-7.3)	$Z = -1.11$	0.268

group (Figure 1).

Comparison of coagulation function parameters at admission between the mild and severe groups showed that median INR, PT, APTT, FIB, FDP, and D-dimer were higher in the severe group compared to the mild group (Table 2); all differences were statistically significant (Table 3).

Further analysis of fibrinogen and D-dimer, the two most frequently abnormal coagulation function parameters, showed that about half of the patients in the mild and severe groups had a mild elevation in fibrinogen, and the proportion of patients with fibrinogen > 7.0 g/L in the severe group was significantly higher than in mild group (19.1% *vs.* 5.7%). The proportion of patients with elevated D-dimer < 2 ULN was 64.8% in the mild group but only 33.3% in the severe group. Further, in the severe group, more than 50% of patients had elevated D-dimer > 2 ULN; particularly, the proportion with D-dimer > 10 ULN was significantly higher in severe groups than in the mild group (19.0% *vs.* 3.7%) (Figure 2).

3.3. Characteristics in coagulation function at admission and at discharge

The 240 patients who were discharged included 1 mild case, 234 moderate cases, and 5 severe cases. The median time of hospital stay was 14 days (11-19 days). Comparing the coagulation function of patients at admission and at discharge showed that fibrinogen degradation products were elevated. Median INR, prothrombin time, and D-dimer at discharge were decreased compared to the values at admission, but the differences were not statistically significant. Median fibrinogen decreased and median APTT was significantly shortened (Table 4).

4. Discussion

We analyzed the baseline data of 303 patients collected at the time of admission and found a total of 26 severe and critical cases of COVID-19 diagnosed in the Shanghai area. The rate of occurrence of severe

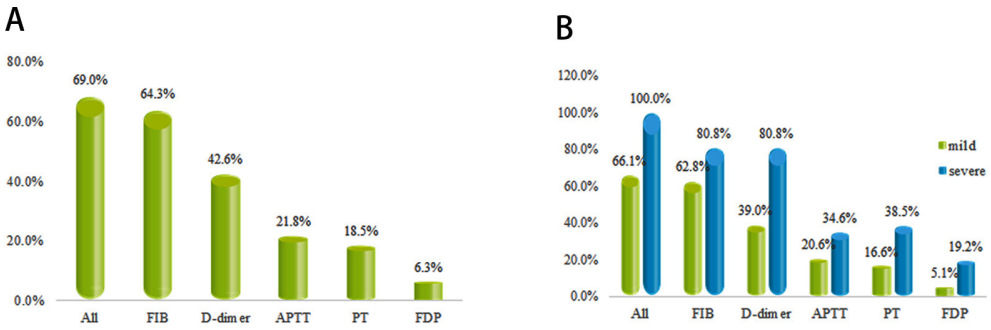

Figure 1. Proportion of abnormal coagulation function parameters at admission in the 303 patients in the mild and severe groups. A: Proportion of abnormal coagulation parameters at admission in the 303 patients. B: Proportion of abnormal coagulation parameters at admission in the mild and severe groups. Legend: green, mild; blue, severe.

Table 2. Coagulation function parameters at admission in the 303 patients

Items	Reference range	Median	Interquartile range	Maximum	Minimum
INR		1.01	0.97-1.05	2.15	0.84
PT (s)	11.0-14.0	13.4	13.0-13.8	24.4	11.6
APTT (s)	32.0-43.0	39.6	36.4-42.7	110.6	28.5
FIB (g/L)	2.0-4.0	4.4	3.65-5.41	10.5	1.34
FDP (μg/mL)	0-5.0	1.05	0.58-2.09	150	0.01
D-dimer (μg/mL)	0-0.5	0.45	0.31-0.81	20.1	0.04

The table shows the reference range, median, interquartile range, maximum, and minimum values of coagulation function parameters for the 303 admitted patients.

Table 3. Comparison of coagulation function parameters between the mild and severe groups

Items	Mild (n = 277)	Severe (n = 26)	Statistic	p-value
INR	1.01 (0.97-1.05)	1.04 (1.01-1.14)	Z = -2.965	0.003
PT (s)	13.4 (13.0-13.8)	13.8 (13.4-14.8)	Z = -2.943	0.003
APTT (s)	39.2 (36.3-42.4)	43.2 (41.0-49.7)	Z = -3.792	< 0.001
FIB (g/L)	4.33 (3.57-5.37)	4.74 (4.21-5.84)	Z = -2.080	0.038
FDP (μg/mL)	0.99 (0.52-1.98)	2.61 (1.44-4.48)	Z = -4.478	< 0.001
D-dimer (μg/mL)	0.43 (0.31-0.77)	1.04 (0.73-1.72)	Z = -5.156	< 0.001

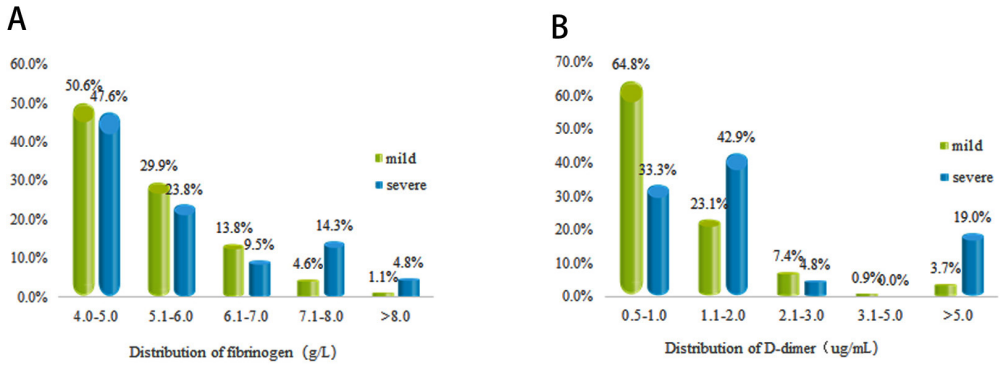

Figure 2. Distribution of fibrinogen and D-dimer values in the mild and severe groups. A: Distribution of fibrinogen (g/L), B: Distribution of D-dimer (μg/mL). Legend: green, mild; blue, severe.

Table 4. Comparison of coagulation function parameters in the 240 patients at admission and at discharge

Items	Admission	Discharge	Statistic	*p*-value
INR	1.01 (0.97-1.05)	1.00 (0.96-1.03)	Z = -1.495	0.135
PT (s)	13.4 (13.0-13.8)	13.3 (12.9-13.7)	Z = -1.477	0.140
APTT (s)	39.3 (36.4-42.2)	37.0 (34.7-39.5)	Z = -5.895	< 0.001
FIB (g/L)	4.42 (3.61-5.24)	3.82 (3.27-4.79)	Z = -4.534	< 0.001
FDP (μg/mL)	0.99 (0.52-1.93)	1.10 (0.46-1.90)	Z = -0.058	0.954
D-dimer (μg/mL)	0.44 (0.31-0.78)	0.43 (0.29-0.71)	Z = -0.717	0.473

cases was 8.6%, which was lower than previous reports (*3,7,8*). The severe cases had a relatively high proportion of males, were relatively older, and had more underlying diseases, which is consistent with previous reports (*1,3*). Analysis of coagulation function data showed that the incidence of abnormalities in conventional coagulation function parameters was higher in patients with severe cases compared to mild cases, and the magnitude of these increases was significant, suggesting that coagulopathy is more serious in severe patients, and significant coagulopathy correlates with the degree of disease severity to some extent (*6*).

The incidence of coagulopathy in all patients at the time of admission showed abnormalities of varying degrees in conventional coagulation function parameters. In particular, the incidence of abnormal fibrinogen reached 64.3% and the occurrence of abnormal D-dimer was 42.6%. These results suggest that fibrinogen and D-dimer are not only significantly increased in patients with severe cases but also increased to varying extent in a considerable proportion of patients with mild cases; however, a more significant increase was observed in patients with severe cases. This finding is consistent with previous reports (*6*). More significantly, we found that fibrinogen indicators improved significantly by the time of discharge, suggesting that fibrinogen levels normalized during recovery. This indicator may be used as a serum biomarker for predicting disease outcomes and good prognosis of COVID-19. Fibrinogen is a coagulation protein synthesized by the liver and promotes platelet aggregation, red blood cell adhesion and thrombosis, and is an important factor in coagulation and thrombosis. Based on autopsy and histopathological biopsy observations of patients with COVID-1, fibrinous exudates, intravascular hyaline thrombi, and pulmonary interstitial fibrosis were found in the alveoli, and microthrombi were found in the liver and kidney (*9*). Previous studies have reported that fibrin was abnormally elevated in the lungs of patients infected with SARS-CoV, and continuous excessive fibrin accumulation in the alveoli led to acute inflammation and chronic pulmonary fibrosis. Fibrin accumulation is a hallmark of acute respiratory distress syndrome and a reduced capacity to remove fibrin deposits results in poor clinical patient outcomes (*10*). Current research shows that SARS-CoV-2 is over 85% homologous to bat SARS-like coronavirus. So, it is speculated that a certain proportion of patients, especially critically ill patients, may have elevated fibrinogen after SARS-CoV-2 infection. Whether or not this is the underlying mechanism of the injury to the lung or other organs requires further study.

A recent retrospective analysis of 21 COVID-19-related fatalities showed that the incidence of disseminated intravascular coagulation (DIC) was 71.8% (*6*), which warns us that we must be highly vigilant about the possibility of DIC in critically ill patients. Current research suggests that cytokine release syndrome (CRS) caused by immune imbalance following SARS-CoV-2 infection may be an important cause of diffuse microvascular injury. Researchers analyzed 30 immunological parameters in the blood of 33 COVID-19 patients and speculated that the mechanism of inflammatory damage may be T cell activation following SARS-CoV-2 infection and production of a large amount of granulocyte-macrophage colony-stimulating factor

and IL-6, which induces a cascade of inflammatory factors (*11*). IL-6 can cause coagulopathies through many pathways. Cytokine storm interacts with coagulopathies to form a vicious cycle, which is directly correlated with poor prognosis (*12*). For patients with elevated IL-6, timely administration of the IL-6 inhibitor tocilizumab may improve CRS and reduce the risk of DIC (*13*). We observed a significant difference in D-dimer and FDP between the severe and mild groups. In particular, the patients in the high D-dimer interval, there was a significantly higher proportion of patients with severe cases than patients with mild cases, which may be related to the higher probability of DIC in critically ill patients. Therefore, these are important evaluation parameters for DIC. In addition to CRS caused by inflammatory factor storms in critically ill patients, septic shock occurs in a significant proportion of the population, which is also one of the common causes of DIC (*14,15*).

There are also many limitations in this study. The research data comes from a single-center clinical retrospective study. The rate of exacerbation and the incidence of coagulopathies in patients may not be representative of the entire disease population, and there was no in-depth dynamic follow-up and analysis of the relationship between coagulation function and prognosis in critically ill patients. A multi-center study with a larger sample size is needed to verify our results. Nevertheless, our study suggests that coagulopathy is common among COVID-19 patients and that DIC-related parameters are significantly elevated in patients with severe cases compared to those with mild cases. Nearly 65% of patients had elevated fibrinogen to varying degrees, and the increase was more pronounced in critically ill patients. This indicator improved correspondingly as they recovered from the disease, suggesting that fibrinogen may be associated with the disease process.

Acknowledgements

This study was supported by a hospital-level project by Shanghai Public Health Clinical Center (KY-GW-2018-18) and the National Science and Technology Major Project of China (2018ZX10302206).

References

1. Sohrabi C, Alsafi Z, O'Neill N, Khan M, Kerwan A, Al-Jabir A, Iosifidis C, Agha R. World Health Organization declares Global Emergency: a review of the 2019 Novel Coronavirus (COVID-19). Int J Surg. 2020. 2020 Apr;76:71-76.
2. Chen J, Qi T, Liu L, *et al.* Clinical progression of patients with COVID-19 in Shanghai, China. J Infect. 2020; 80:e1-e6.
3. Guan WJ, Ni ZY, Hu Y, *et al.* Clinical Characteristics of Coronavirus Disease 2019 in China. N Engl J Med. 2020; doi: 10.1056/NEJMoa2002032.
4. Yao N, Wang SN, Lian JQ, Sun YT, Zhang GF, Kang WZ, Kang W. Clinical characteristics and influencing factors of patients with novel coronavirus pneumonia combined with liver injury in Shaanxi region. Zhonghua Gan Zang Bing Za Zhi. 2020; 28:E003. (in Chinese)
5. Zhang JJ, Dong X, Cao YY, Yuan YD, Yang YB, Yan YQ, Akdis CA, Gao YD. Clinical characteristics of 140 patients infected with SARS-CoV-2 in Wuhan, China. Allergy. 2020; doi: 10.1111/all.14238.
6. Tang N, Li D, Wang X, Sun Z. Abnormal Coagulation parameters are associated with poor prognosis in patients with novel coronavirus pneumonia. J Thromb Haemost. 2020; 18:844-847.
7. Chen N, Zhou M, Dong X, Qu J, Gong F, Han Y, Qiu Y, Wang J, Liu Y, Wei Y, Xia J, Yu T, Zhang X, Zhang L. Epidemiological and clinical characteristics of 99 cases of 2019 novel coronavirus pneumonia in Wuhan, China: a descriptive study. Lancet. 2020; 395:507-513.
8. Wang D, Hu B, Hu C, Zhu F, Liu X, Zhang J, Wang B, Xiang H, Cheng Z, Xiong Y, Zhao Y, Li Y, Wang X, Peng Z. Clinical Characteristics of 138 Hospitalized Patients With 2019 Novel Coronavirus-Infected Pneumonia in Wuhan, China. JAMA. 2020; doi: 10.1001/jama.2020.1585.
9. Diagnosis and Treatment Protocol for Novel Coronavirus Pneumonia 2020; Trial Version 7, Revised. *http://www.kankyokansen.org/uploads/uploads/files/jsipc/protocol_V7.pdf* (accessed April 12, 2020).
10. Gralinski LE, Bankhead A, 3rd, Jeng S, *et al.* Mechanisms of severe acute respiratory syndrome coronavirus-induced acute lung injury. mBio. 2013 6; 4:pii: e00271-13.
11. Zhou Y, Fu B, Zheng X, Wang D, Zhao C, qi Y, Sun R, Tian Z, Xu X, Wei H. Aberrant pathogenic GM-CSF+ T cells and inflammatory CD14+CD16+ monocytes in severe pulmonary syndrome patients of a new coronavirus. bioRxiv. 2020; https://doi.org/10.1101/2020.02.12.945576.
12. Tanaka T, Narazaki M, Kishimoto T. Immunotherapeutic implications of IL-6 blockade for cytokine storm. Immunotherapy. 2016; 8:959-970.
13. Jiang H, Liu L, Guo T, Wu Y, Ai L, Deng J, Dong J, Mei H, Hu Y. Improving the safety of CAR-T cell therapy by controlling CRS-related coagulopathy. Ann Hematol. 2019; 98:1721-1732.
14. Kitchens CS. Thrombocytopenia and thrombosis in disseminated intravascular coagulation (DIC). Hematology Am Soc Hematol Educ Program. 2009; 240-246.
15. Iba T, Levi M, Levy JH. Sepsis-Induced Coagulopathy and Disseminated Intravascular Coagulation. Semin Thromb Hemost. 2020; 46:89-95.

Received April 13, 2020; Revised April 22, 2020; Accepted April 23, 2020

[§]These authors contributed equally to this work
**Address correspondence to:*
Zhiping Qian, Department of Severe hepatopathy, Shanghai Public Health Clinical Center, Fudan University. No. 2901, Caolang Road, Jinshan District, 201508, Shanghai, China.
E-mail: qianzhiping@shphc.org.cn

Hongzhou Lu, Department of Infectious Disease and Immunology, Shanghai Public Health Clinical Center, Fudan University. No. 2901, Caolang Road, Jinshan District, 201508, Shanghai, China.
E-mail: luhongzhou@fudan.edu.cn

Released online in J-STAGE as advance publication April 30, 2020.

Original Article

DOI: 10.5582/bst.2020.03197

Exploration and correlation analysis of changes in Krebs von den Lungen-6 levels in COVID-19 patients with different types in China

Mingshan Xue[1,§], Peiyan Zheng[1,§], Xiqing Bian[2,§], Zhifeng Huang[1], Huimin Huang[1], Yifeng Zeng[1], Haisheng Hu[1], Xiaoqing Liu[1], Luqian Zhou[1], Baoqing Sun[1,*], Jian-lin Wu[2,*], Nanshan Zhong[1,*]

[1] State Key Laboratory of Respiratory Disease, National Clinical Research Center for Respiratory Disease, Guangzhou Institute of Respiratory Health, First Affiliated Hospital of Guangzhou Medical University, Guangzhou, China;
[2] State Key Laboratory of Quality Research in Chinese Medicine, Macau Institute for Applied Research in Medicine and Health, Macau University of Science and Technology, Macao, China.

SUMMARY This study aimed to determine the clinical significance of Krebs von den Lungen-6 (KL-6) in patients with COVID-19, so as to find a marker with high sensitivity, specificity and easy detection to evaluate the lung injury and inflammation of COVID-19. Sixty-three COVID-19 patients and 43 non-COVID-19 patients with similar clinical phenotypes and/or imaging findings were enrolled to test the levels of KL-6 using chemiluminescent immunoassay. In addition, the blood gas, imaging and lymphocyte factors tests were collected from all participants. The data was finally analyzed using multivariate statistical analysis. The results showed KL-6 levels in COVID-19 patients were higher than those in non-COVID-19 patients ($P < 0.001$). Moreover, the KL-6 levels in severe and critically severe patients were significantly upregulated compared with patients with mild and common type ($P < 0.05$). Meanwhile, the imaging evaluation showed a significant correlation between KL-6 and pulmonary lesion area ($P < 0.05$). KL-6 was also found to be significantly correlated with oxygenation index and oxygen partial pressure difference of alveolar artery ($PA\text{-}aDO_2$) (Both $P < 0.01$). In conclusion, KL-6 could be an indicator to evaluate the progression of COVID-19, which is parallel to the level of lung injury and inflammation in patients. Moreover, it can also reflect the pulmonary ventilation function.

Keywords COVID-19, lung, Krebs von den Lungen-6 (KL-6)

1. Introduction

The 2019 novel coronavirus pneumonia (COVID-19) was initially identified in Wuhan, China in December 2019, and emerged as a global pandemic, which affected greater than 3,500,000 people globally, including more than 110,000 deaths by May, 2020, and rising. Based on its partial homology with SARS-CoV-2 virus, the novel coronavirus of this pandemic was named COVID-19 by the World Health Organization (WHO) (*1*) and confirmed to be the seventh member of the coronavirus family of *beta-coronavirus* (*2*). COVID-19 can cause symptoms of acute nonspecific respiratory infection, such as fever, dry cough, shortness of breath, as well as many pulmonary manifestations, such as diarrhea and muscle soreness; in addition, many patients present no clinical symptoms, which will cause the virus to spread widely (*2-4*). Many severe patients can develop septic shock, acute respiratory distress syndrome, disseminated intravascular coagulation (DIC), and multiple organ failure during progressive progression (*5*). Severe COVID-19 cases might lead to death when they suffer from cardiovascular disease, diabetes, liver failure, and heart failure (*6,7*). Therefore, it is urgent to find an easily, simple and effective diagnosis approach for COVID-19 to reduce mortality.

Current diagnostic approaches for COVID-19 include nucleic acid detection, chest CT, epidemiological history and clinical manifestations (*8-10*). However, nucleic acid detection is time consuming and an incorrect sample collection may lead to false-positive results. Additionally, the specificity of CT is low and the cost is high. Moreover, in clinical practice, the detection standard varied partly with rapidly growing awareness

of COVID-19 (*7,8*). Hence, timely and accurate diagnosis of COVID-19 is still important for detection and therapy of patients.

Krebs von den Lungen-6 (KL-6), a high molecular weight mucinous glycoprotein, is more highly expressed in injured or regenerating epithelial cells than in normal epithelial cells (*11,12*). KL-6 plays an important role in pulmonary inflammatory damage, mainly due to its ability to specifically identify the function of type 1 alveolar epithelial cells, thus as a biomarker to predict risk of illness or death of pneumonia patients (*13*). Angiotensin-converting enzyme 2 (ACE2) mainly exists in type 1 alveolar epithelium (*14*). Receptor binding domain (RBD) glycoprotein, the functional receptor of COVID-19, could closely bind to ACE2, thus resulting in significant reduction of the number of viruses for infecting cells (*15*). Hence, the pathogenesis of COVID-19 might be related to KL-6. In the present study, we explored the changes of KL-6 levels in COVID-19 and non-COVID-19 patients, aiming to investigate the pathogenesis and auxiliary diagnostic markers of COVID-19, as well as further analyze its transmission characteristics. The flow chart of the experiment is shown in Figure 1.

2. Materials and Methods

2.1. Study design and patients

A total of 63 COVID-19 cases were involved, which were collected and collated by the First Affiliated Hospital of Guangzhou Medical University between February 1, 2020 and March 15, 2020. According to the standard of COVID-19 medical protocol issued by national health commission, the patients were divided into two groups: a mild and common type group (N = 30), as well as a severe and critically severe type group (N = 33), by evaluation of results of clinical symptoms, imaging and blood gas (standard atmospheric pressure). However, due to lack of follow-up data in part of the COVID-19 patients, some patients were excluded in the process of collating information. Finally, 6 patients with mild or normal type and 15 patients with severe or critical type were included in the longitudinal follow-up analysis. In addition, 43 gender and age-matched confirmed non-COVID-19 patients with similar clinical phenotypes and/or imaging findings were enrolled. The clinical parameters of all participants were collected and summarized in Table 1. This study was Approved by the ethics committee of First Affiliated Hospital of Guangzhou Medical University (Ethics number 2020-77).

2.2. Diagnosis

The patients were recruited according to guidelines of diagnosis and treatment of COVID-19 including clinical characteristics and typical epidemiological history. Inclusion criteria were as follows: *i*) COVID-19 was positive after PCR detection of nucleic acid in respiratory or blood samples; *ii*) The sequence of virus genes in respiratory or blood samples showed a high homology to COVID-19. Meanwhile, we also referred to the diagnostic and grading criteria of Daniel *et al.* 2020 (*16*), Jin *et al.* 2020 (*17*) and Corman *et al.* 2020 (*1*). Briefly, the clinical manifestations were consistent with fever and/or respiratory symptoms, imaging features of COVID-19 infection, normal or decreased white blood cells, and normal or decreased lymphocyte count.

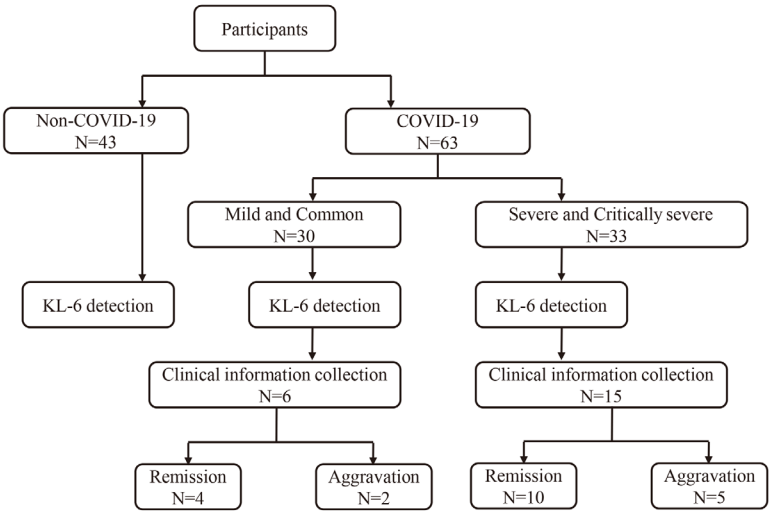

Figure 1. The flow chart of the experiment.

Table 1. The clinicopathologic characteristics of participants

Variables	Non-COVID-19	Non-COVID-19		*P* value
		Mild and Common	Severe and Critically Severe	
N	43	6	15	
Age, years	51.70 ± 3.27	55.00 ± 18.84	57.20 ± 14.25	0.015
Gender, male/female	30/13	2/4	12/3	0.098
KL-6, U/mL	173.9 ± 63.40	241.2 ± 207.90	676.6 ± 506.70	0.001
CRP, mg/L	-	4.77 ± 3.59	8.38 ± 6.77	0.027
LDH, U/L	-	411.00 ± 359.40	492.30 ± 718.40	0.151
Blood creatinine, umol/L	-	79.77 ± 22.93	90.32 ± 44.48	0.159
ALT, U/L	-	41.35 ± 45.43	55.06 ± 50.20	0.121
AST, U/L	-	42.07 ± 26.28	171.10 ± 856.40	0.014
Oxygenation index	-	3.99 ± 1.60	2.21 ± 2.11	0.001
PA-aO_2	-	145.30 ± 69.50	219.40 ± 125.10	0.003
Venous blood cell analysis				
White blood cell, 10^9/L	-	5.16 ± 1.68	9.29 ± 3.88	0.001
Neutrophil count, 10^9/L	-	3.48 ± 1.57	7.40 ± 3.72	0.001
Lymphocyte count, 10^9/L	-	1.07 ± 0.34	0.97 ± 0.61	0.001
Eosinophil count, 10^9/L	-	0.11 ± 0.06	0.22 ± 0.28	0.037
Red blood cell, 10^{12}/L	-	3.66 ± 0.55	2.97 ± 0.62	0.001
Platelet count, 10^9/L	-	273.5 ± 104.0	178.40 ± 80.30	0.001
Electrolyte				
K, mmol/L	-	3.86 ± 0.31	4.40 ± 5.88	0.001
Na, mmol/L	-	138.40 ± 1.78	141.10 ± 6.29	0.001
CI, mmol/L	-	104.4 ± 2.77	106.4 ± 8.04	0.030
Ca, mmol/L	-	2.23 ± 0.10	2.25 ± 0.18	0.432

ALT, Alanine transaminase; AST, Glutamic oxalacetic transaminase; CRP, C-reactive protein; KL-6, Krebs von den Lungen-6; LDH, Lactate dehydrogenase; PA-aO_2, Partial pressure difference of oxygen in alveolar air artery.

2.3. Sample collection and preservation

5 mL venous blood samples were collected, divided into individual tubes and stored at 0-4°C for inspection, and the other blood was centrifuged at 3,000 rpm for 30 min at room temperature to obtain serum. Urine samples were collected, stored at 0-4°C and measured within 24 hours. Feces samples (5 g) were collected and stored at room temperature until analysis.

2.4. KL-6 detection

The levels of KL-6 in serum were measured using chemiluminescence immunity (KAESER 1000) according to the manufacturers' protocol.

2.5. Imaging evaluation

Due to the condition limitation of severe patients and for the purpose of dynamic observation of the lesion change level, we also included the results of DR results. The appearance, size, and location of pulmonary infection lesions in DR and CT reports were both evaluated. Coronal plane was used for evaluation of DR and CT. CT was also assessed from four planes: subclavicular, aortic arch, hilum, and superior diaphragm. According to the grading standards reported by Chung *et al.* (*18*) and Lei *et al.* (*19*), > 50% intrapulmonary lesion progression from 24 to 48 hours was classified as the severe classification.

2.6. Statistical analysis

R software (Bell Laboratories Version 4.0.0), SPSS 22.0 software (SPSS Inc., Chicago, IL, USA) and GraphPad Prism 5.0 (G San Diego, CA, US) were used for statistical analysis. Comparisons in three groups or between two groups were made by ANOVA or Student's *t*-test. P value < 0.05 was considered to be statistically significant.

3. Results

3.1. Participants characteristics

As shown in Table 1, the levels of KL-6 in patients with COVID-19 were significantly higher than those in non-COVID-19 type ($P < 0.001$). Moreover, the levels of AST in patients with severe and critically severe were upregulated in comparison with those in patients with mild and common type, and the difference of AST levels between the two groups was significant ($P < 0.05$). Additionally, no electrolyte disturbance was observed in COVID-19 patients.

3.2. Changes of KL-6 level in COVID-19 patients with different types

To detect the potential roles of KL-6 in progression of COVID-19 disease, we assessed the change of KL-6 levels in COVID-19 patients with different types. As

illustrated in Figure 2A, the KL-6 level of COVID-19 patients was significantly higher than that of non-COVID-19 controls, and the overall levels of KL-6 in severe and critically severe patients were significantly higher than that in mild and common patients (both $P < 0.01$). The overall levels of KL-6 in patients with COVID-19 after remission showed a decreasing trend. During hospitalization, the levels of KL-6 rose briefly due to changes in the condition, but gradually decreased with the overall improvement of the condition in the later period; moreover, the length of hospitalization for mild and common type of patients was relatively short (Figure 2B). However, not all COVID-19 patients improved during hospitalization. For example, in this study, a total of 5 critically severe patients have aggravated conditions during hospitalization. According to Figure 2C, KL-6 levels in 2 of them showed a significant upward trend in the first 16 days. Taken together, the KL-6 level of the patients with aggravation of the disease was stable and increased; however, the change trend of KL-6 in patients with mild and common type was basically stable due to their mild condition. In this study, 2 cases of mild and common type were aggravated, among which 1 case showed a significant upward trend of KL-6 level.

3.3. Imaging analysis of pulmonary lobe involvement

To further clarify the clinical significance of KL-6 in COVID-19 patients, the phenotypic data in imaging reports of COVID-19 patients were investigated. There was no significant change of lesion size in mild and common group, however, we observed a significant reduction in lesions of severe and critically severe stages of remission. Additionally, There was a significant correlation between KL-6 and pulmonary lesion area. ($r = -0.14$, $P < 0.05$; Table 2).

3.4. Inflammatory index analysis

Inflammatory index analysis showed that lymphocytes of severe and critically severe patients have a temporary

Table 2. Imaging findings of the COVID-19 patient's lungs

Variables	Mild and Common, *N*	Severe and Critically Severe, *N*
Lung involvement area		
0%	0	0
1-25%	6	0
26-50%	0	1
51-75%	0	11
76-100%	0	3
Morphologic		
Patchy shadows	6 (100.0)	15 (100.0)
Consolidations	4 (66.7)	9 (60.0)
Pleural thickening	0	3 (20.0)
Bronchiolectasis	1 (16.7)	4 (26.7)
Atelectasis	0	1 (6.7)
Tuberosis	1 (16.7)	4 (26.7)
Hydrothorax	0	7 (46.7)
Mediastinal lymphadenectasis	0	4 (26.7)
Emphysema	0	6 (40.0)
Pulmonary fibrosis	0	1 (6.7)

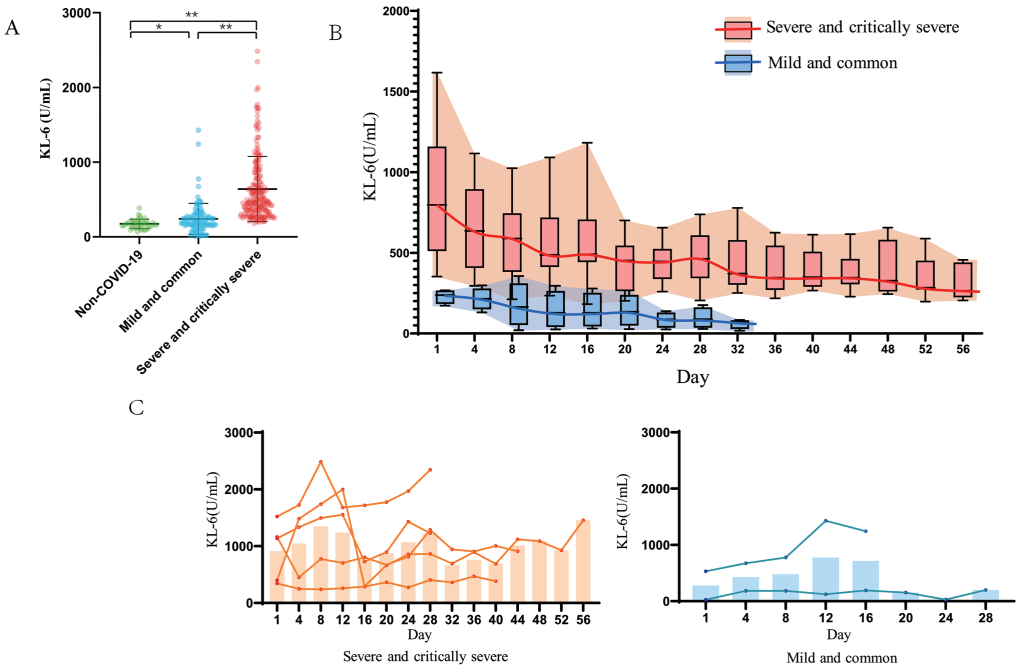

Figure 2. KL-6 level in COVID-19 patients with different types. (A) The differences in non- COVID-19 controls group, mild and common patients group and severe and critically severe patients group. (B) Changes in KL-6 levels in remission patients with COVID-19; **(C)** Changes in KL-6 level in patients with aggravating COVID-19. KL-6, Krebs von den Lungen-6.

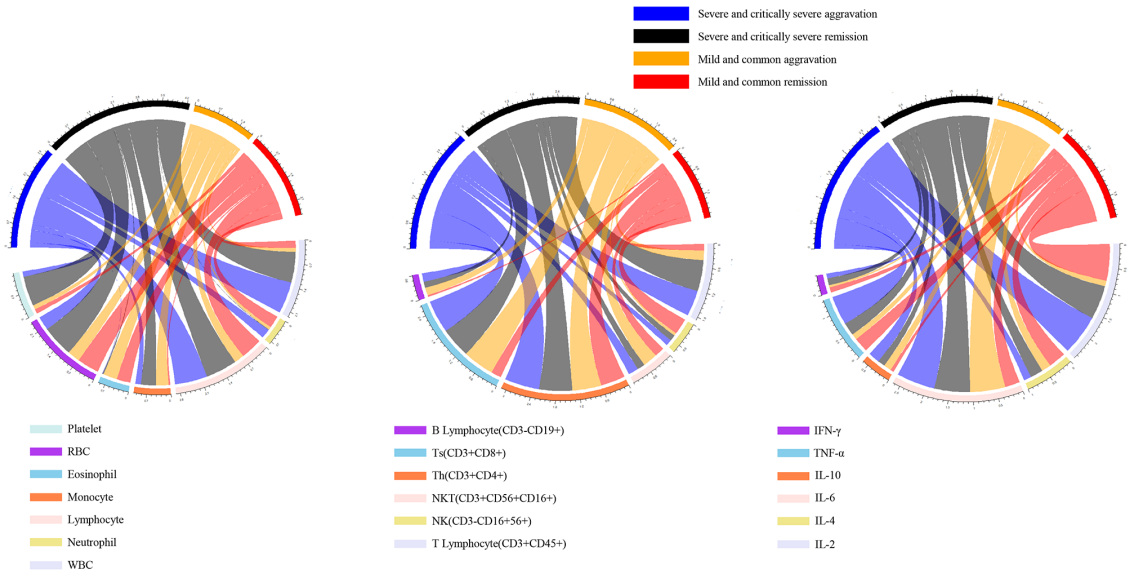

Figure 3. Correlation analysis of KL-6 level with leukocyte, lymphocyte subsets and inflammatory factors in COVID-19 patients. IFN, Interferon; IL, Interleukin; NK, Natural killer; NKT, Natural killer T lymphocyte; Th, Helper T lymphocyte; TNF, Tumor necrosis factor; Ts, Suppressor T lymphocyte.

decline at the time of admission, and then increase to normal with remission of the disease. The levels of T lymphocytes (CD3+), helper T lymphocytes (CD3+CD4+) and inhibitory T lymphocytes (CD3+CD8+) increased gradually with progression of the COVID-19 patients, while there was no significant changes in B lymphocytes (CD3-CD19+) and NK cells (CD3-CD16+56+). Next, the correlation analysis of leukocyte, lymphocyte subsets and inflammatory cytokines with KL-6 levels was conducted. The results revealed that there was a significant correlation between the levels of KL-6 and T lymphocyte(CD3+CD45+) in severe and critically severe patients (r = -0.24, P < 0.05; Figure 3). Moreover, the Ts (CD3+CD8+) and Th (CD3+CD4+) lymphocyte subsets were both closely related to KL-6 levels in all COVID-19 patients (r = -0.19 and -0.25, both P < 0.05). Additionally, IL-6 and IL-10 were significantly correlated with KL-6 levels, respectively (r = 0.38 and 0.19, both P < 0.05).

3.5. Correlation analysis of blood gas and KL-6 in patients

According to Figure 4, 81.5% of severe and critically severe patients had an oxygenation index (PaO_2/FiO_2) of less than 3.00 within 5 days of admission. In general, KL-6 was significantly correlated with CO_2 partial pressure, arterial alveolar blood oxygen partial pressure difference and oxygenation index (PaO_2/FiO_2) under normal atmospheric pressure in COVID-19 patients (r = 0.19, 0.48 and -0.45, all P < 0.01).

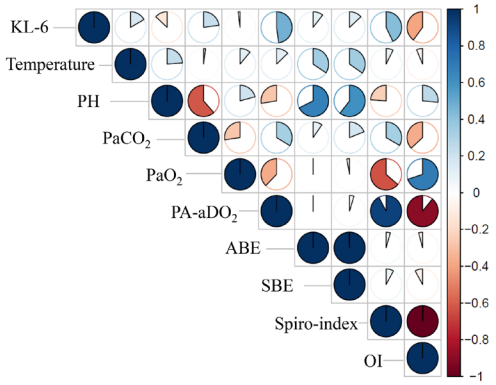

Figure 4. Correlation analysis of blood gas and KL-6 in patients. $PA\text{-}aDO_2$: Alveolar-arterial oxygen differential; ABE: Actual alkali excess; SBE: Standard alkali excess; Spiro-index: Respiratory Index; OI: Oxygenation index.

4. Discussion

According to the follow-up investigation of in-patient conditions, the levels of KL-6 were different with change of COVID-19 patients' condition. Moreover, the expression level of KL-6 was significantly correlated with oxygenation index and arterial alveolar oxygen partial pressure difference. At the same time, it was also consistent with the change of the pulmonary lesion area. In particular, in patients with COVID-19, no obvious electrolyte abnormality was observed.

In this study, the levels of KL-6 in COVID-19 patients was found to be higher than in non-COVID-19 patients with similar symptoms. During the course

of the disease, the levels of KL-6 were parallel to the changes of the disease, especially in severe and critical severe patients. Actually, with aggravation of the disease, a large amount of viral replication infiltration could destroy the alveolar epithelium, cause damage to the basement membrane, increase pulmonary vascular permeability, and result in localized pulmonary edema (*13*). At the same time, a clear membrane is formed, which leads to symptoms of chest tightness and shortness of breath (*20*). In our study, the levels of KL-6 were consistent with the severity of the disease and the progressive changes in the course of the disease. Therefore, we speculated that it could reflect the damage of alveolar epithelium in patients with COVID-19.

Besides, the lymphocyte count of some patients with severe and critically severe COVID-19 was lower than normal, and gradually increased to normal with the recovery of immune function, which was consistent with the characteristics of other viral infections. Through the detection of lymphocyte subsets, we found that the total number of CD3+ T lymphocytes increased with the progress of the disease, and at the same time, auxiliary T lymphocytes (Th CD3+CD4+) and inhibitory T lymphocytes (Ts CD3+CD8+) also increased to regulate the immune function of the body. No significant changes were observed in CD3-CD19+ B lymphocytes and CD3-CD16+56+ of NK cells. It was found that KL-6 was significantly correlated with changes of cytokine IL-6 in the whole course of disease. IL-6 was one of the cytokines which could lead to fever and increase of alveolar epithelial exudation (*21*). Early rapid replication of the virus may lead to a large amount of airway and alveolar epithelial and endothelial cell apoptosis, and induce release of a large amount of pro-inflammatory cytokines and chemokines (*20*). We speculated that the level of KL-6 was correlated with some T lymphocytes and inflammatory factors and could reflect the level of lung inflammation. Oxygenation index (PaO_2/FiO_2) in 81.5 % of patients with severe and critical type was less than 3.00 on day 5 and rose to normal with remission. COVID-19 can cause lung interstitial injury. In addition, the partial pressure difference of the alveolar artery is also related to the severity and improvement of the disease. KL-6 is significantly correlated with the above two indicators. Under the action of infection and inflammation, interstitial edema and destruction of pulmonary vascular endothelium will occur in the lungs, and the respiratory membrane ventilation efficiency will be significantly reduced. In our study about imaging report, the pulmonary interstitial fibrosis induced by severe viral pneumonia was also found to have an influence on lung ventilation function and abnormal blood gas indicators. KL-6 is one of the indicators for assessing the degree of pulmonary interstitial fibrosis and is related to the prognosis of the disease. In addition, KL-6 was related to the oxygenation index and the differential pressure of alveolar arterial oxygen and could reflect the pulmonary ventilation function in our study. Therefore, KL-6 could be used as a key indicator to evaluate the degree of damage of alveolar epithelial cells.

The study showed that lung lobe involvement was higher in severe and critically severe patients than in mild and common patients. Moreover, in the aggravation stage, the progress of lung lesion area in COVID-19 patients was significantly correlated with the level of KL-6. Hydrothorax, pleural thickening, and Mediastinal lymphadenectasis due to heavy infection are also more common in severe and critically severe patients. From the perspective of vision, patients with severe and critically severe COVID-19 had a wider lung involvement area, which was consistent with the degree of lung damage.

Compared to detecting biomarkers in COVID-19 by nucleic acid detection and chest CT, measurement of the levels of KL-6 were rapid, sensitive, and inexpensive. Several studies suggest that KL-6 is associated with lung cancer (*22,23*). However, no articles have been reported about the relationship of KL-6 with COVID-19. Therefore, KL-6 could be regarded as a novel biomarker for COVID-19. In our study, the levels of KL-6 were closely related to IL-6, IL-10, $PaCO_2$, PaO_2/FiO_2 and pulmonary lesion area. These results suggested that KL-6 is a useful prognostic indicator for COVID-19.

Although promising results were obtained, this study also has some limitations. For example, the number of patients was not sufficient to perform a valid statistical analysis. To investigate the significance of KL-6 expression, a larger number of patients with COVID-19 is required for a prospective study.

5. Conclusion

In summary, KL-6 can be used as an auxiliary evaluation index of lung injury due to COVID-19, and can reflect lung ventilation function and oxygen intake level of patients. In addition, KL-6 could be used as a new biomarker in the future for screening and evaluating COVID-19 by virtue of its high sensitivity, specificity and easy detection.

Funding: This study was supported by Zhejiang University special scientific research fund for COVID-19 prevention and control (2020XGZX040).

Conflict of Interest: The authors declare that they have no competing interests.

References

1. Corman VM, Landt O, Kaiser M. *et al.* Detection of 2019 novel coronavirus (2019-nCoV) by real-time RT-PCR. Euro Surveill. 2020; 25:2000045.
2. Zhu Y, Li C, Chen L. *et al.* A novel human coronavirus

OC43 genotype detected in mainland China. Emerg Microbes Infect. 2018; 7:173.
3. Yang XL, Hu B, Wang B, Wang MN, Zhang Q, Zhang W, Wu LJ, Ge XY, Zhang YZ, Daszak P, Wang LF, Shi ZL. Isolation and Characterization of a Novel Bat Coronavirus Closely Related to the Direct Progenitor of Severe Acute Respiratory Syndrome Coronavirus. J Virol. 2015; 90:3253-3256.
4. Wang C, Horby PW, Hayden FG, Gao GF. A novel coronavirus outbreak of global health concern. Lancet. 2020; 395:470-473.
5. Hui DS, E IA, Madani TA, Ntoumi F, Kock R, Dar O, Ippolito G, McHugh TD, Memish ZA, Drosten C, Zumla A, Petersen E. The continuing 2019-nCoV epidemic threat of novel coronaviruses to global health - The latest 2019 novel coronavirus outbreak in Wuhan, China. Int J Infect Dis. 2020; 91:264-266.
6. Malik YS, Sircar S, Bhat S, Sharun K, Dhama K, Dadar M, Tiwari R, Chaicumpa W. Emerging novel coronavirus (2019-nCoV)-current scenario, evolutionary perspective based on genome analysis and recent developments. Vet Q. 2020; 40:68-76.
7. Wu Z, McGoogan JM. Characteristics of and Important Lessons From the Coronavirus Disease 2019 (COVID-19) Outbreak in China: Summary of a Report of 72314 Cases From the Chinese Center for Disease Control and Prevention. JAMA. 2020; doi: 10.1001/jama.2020.2648.
8. To KK, Tsang OT, Chik-Yan Yip C. *et al.* Consistent detection of 2019 novel coronavirus in saliva. Clin Infect Dis. 2020; ciaa149. doi: 10.1093/cid/ciaa149.
9. Zu ZY, Jiang MD, Xu PP, Chen W, Ni QQ, Lu GM, Zhang LJ. Coronavirus Disease 2019 (COVID-19): A Perspective from China. Radiology. 2020; 200490. doi: 10.1148/radiol.2020200490.
10. Sharfstein JM, Becker SJ, Mello MM. Diagnostic Testing for the Novel Coronavirus. JAMA. 2020; doi: 10.1001/jama.2020.3864.
11. Kohno N, Awaya Y, Oyama T, Yamakido M, Akiyama M, Inoue Y, Yokoyama A, Hamada H, Fujioka S, Hiwada K. KL-6, a Mucin-like Glycoprotein, in Bronchoalveolar Lavage Fluid from Patients with Interstitial Lung Disease. Am Rev Respir Dis. 1993; 148:637-642.
12. Ishizaka A, Matsuda T, Albertine KH, Koh H, Tasaka S, Hasegawa N, Kohno N, Kotani T, Morisaki H, Takeda J, Nakamura M, Fang X, Martin TR, Matthay MA, Hashimoto S. Elevation of KL-6, a lung epithelial cell marker, in plasma and epithelial lining fluid in acute respiratory distress syndrome. Am J Physiol Lung Cell Mol Physiol. 2004; 286:L1088-1094.
13. Hu C, Wu C, Yang E, Huang H, Xu D, Hou Y, Zhao J, Li M, Xu Z, Zeng X, Wang Q. Serum KL-6 is associated with the severity of interstitial lung disease in Chinese patients with polymyositis and dermatomyositis. Clin Rheumatol. 2019; 38:2181-2187.
14. Chen Y, Guo Y, Pan Y, Zhao ZJ. Structure analysis of the receptor binding of 2019-nCoV. Biochem Biophys Res Commun. 2020; 525:135-140.
15. Hamming I, Timens W, Bulthuis ML, Lely AT, Navis G, van Goor H. Tissue distribution of ACE2 protein, the functional receptor for SARS coronavirus. A first step in understanding SARS pathogenesis. J Pathol. 2004; 203:631-637.
16. Chu DKW, Pan Y, Cheng SMS, Hui KPY, Krishnan P, Liu Y, Ng DYM, Wan CKC, Yang P, Wang Q, Peiris M, Poon LLM. Molecular Diagnosis of a Novel Coronavirus (2019-nCoV) Causing an Outbreak of Pneumonia. Clin Chem. 2020; 66:549-555.
17. Jin YH, Cai L, Cheng ZS. *et al.* A rapid advice guideline for the diagnosis and treatment of 2019 novel coronavirus (2019-nCoV) infected pneumonia (standard version). Mil Med Res. 2020; 7:4.
18. Chung M, Bernheim A, Mei X, Zhang N, Huang M, Zeng X, Cui J, Xu W, Yang Y, Fayad ZA, Jacobi A, Li K, Li S, Shan H. CT Imaging Features of 2019 Novel Coronavirus (2019-nCoV). Radiology. 2020; 295:202-207.
19. Lei J, Li J, Li X, Qi X. CT Imaging of the 2019 Novel Coronavirus (2019-nCoV) Pneumonia. Radiology. 2020; 295:18.
20. Fu Y, Cheng Y, Wu Y. Understanding SARS-CoV-2-Mediated Inflammatory Responses: From Mechanisms to Potential Therapeutic Tools. Virol Sin. 2020; 1-6.
21. Tanaka T, Narazaki M, Kishimoto T. Interleukin (IL-6) Immunotherapy. Cold Spring Harb Perspect Biol. 2018; 10:a028456.
22. Tanaka S, Hattori N, Ishikawa N, Shoda H, Takano A, Nishino R, Okada M, Arihiro K, Inai K, Hamada HJIjoc. Krebs von den Lungen-6 (KL-6) is a prognostic biomarker in patients with surgically resected nonsmall cell lung cancer. Int J Cancer. 2012; 130:377-387.
23. Takanashi S, Nishina N, Nakazawa M, Kaneko Y, Takeuchi TJR. Usefulness of serum Krebs von den Lungen-6 for the management of myositis-associated interstitial lung disease. Rheumatology (Oxford). 2019; 58:1034-1039.

Received May 29, 2020; Revised June 8, 2020; Accepted June 11, 2020.

[§]These authors contributed equally to this work.

**Address correspondence to:*
Baoqing Sun and Nanshan Zhong, State Key Laboratory of Respiratory Disease, National Clinical Research Center for Respiratory Disease, Guangzhou Institute of Respiratory Health, First Affiliated Hospital of Guangzhou Medical University, Guangzhou 510120, China.
E-mail: sunbaoqing@vip.163.com (Sun BQ); nanshan@vip.163.com (Zhong NS)

Jian-lin Wu, State Key Laboratory of Quality Research in Chinese Medicine, Macau Institute for Applied Research in Medicine and Health, Macau University of Science and Technology, Macao, China.
E-mail: jlwu@must.edu.mo

Released online in J-STAGE as advance publication June 21, 2020.

Original Article

DOI: 10.5582/bst.2020.03180

Are inflammation-based markers useful in patients with hepatocellular carcinoma and clinically significant portal hypertension after liver resection?

Li Qin[1], Chuan Li[1,*], Fei Xie[2], Zhenxia Wang[3], Tianfu Wen[1]

[1] Department of Liver Surgery, West China Hospital of Sichuan University, Chengdu, Sichuan, China;
[2] Department of Hepato-pancreato-biliary Surgery, First People's Hospital of Neijiang, Neijiang, China;
[3] Department of Hepato-pancreato-biliary Surgery, Chengdu Second People's Hospital, Chengdu, Sichuan, China.

SUMMARY Inflammation-based markers are considered prognostic indicators for patients with hepatocellular carcinoma (HCC) after liver resection. However, there is little information concerning whether they are useful for HCC patients with clinically significant portal hypertension (CSPH). In this study, 1452 patients were enrolled. Independent risk factors for recurrence-free survival (RFS) and overall survival (OS) were analyzed for patients with and without CSPH. For HCC patients without CSPH, multivariate analysis suggested that microvascular invasion (MVI), neutrophil-to-lymphocyte ratio (NLR) ≥ 3, platelet-to-lymphocyte ratio (PLR) ≥ 150, tumor size > 5 cm, and the presence of a satellite lesion were independently associated with RFS. MVI, NLR ≥ 3, PLR ≥ 150, and advanced Barcelona clinical liver cancer (BCLC) stage contributed to mortality. However, neither NLR nor PLR showed any prognostic power in HCC patients with CSPH. For HCC patients with CSPH, tumor size > 5 cm, MVI, satellite lesion, and albumin-bilirubin (ALBI) grade were independent risk factors for RFS, whereas tumor size > 5 cm, MVI, multiple tumors, ALBI grade and advanced BCLC stage showed prognostic power for OS. Our study confirmed CSPH influences the predictive ability of inflammation-based markers. This result reminds us to pay more attention to the influence of CSPH when we apply inflammation-based markers in patients with HCC after liver resection.

Keywords hepatocellular carcinoma, neutrophil-to-lymphocyte ratio, platelet-to-lymphocyte ratio, clinically significant portal hypertension

1. Introduction

Hepatocellular carcinoma (HCC) often arises from the cirrhotic liver, which may coexist with portal hypertension and hypersplenism manifested as thrombocytopenia and/or leukocytopenia. Liver resection is widely perceived as a curative treatment for patients with HCC, but some investigators have suggested that clinically significant portal hypertension (CSPH) is a contraindication for liver resection (*1*). On the other hand, some researchers have also argued that liver resection can be safely performed in HCC patients with CSPH (*2,3*).

Many risk factors for postoperative recurrence and mortality for HCC patients have been proposed by previously published investigations. Recently, some studies confirmed that the presence of a systemic inflammatory response, which was assessed by neutrophil-to-lymphocyte ratio (NLR), platelet-to-lymphocyte ratio (PLR), and other measurements, contributed to tumor growth, metastasis and poor therapeutic outcomes in patients with HCC (*4-6*). Both NLR and PLR can be easily calculated using laboratory tests. However, serum platelet counts and lymphocyte and neutrophil counts will be impacted by portal hypertension. Accordingly, whether NLR and PLR are suitable for HCC patients with portal hypertension is unknown. Unfortunately, few published investigations have noted the adverse impact of CSPH on inflammation-based markers. In the present study, we aimed to clarify this issue.

2. Materials and Methods

Patients with HCC who underwent liver resection between 2013 and 2019 at West China Hospital of Sichuan University were retrospectively reviewed. Patients who underwent re-resection, had ruptured HCC, received preoperative antitumor treatment, had a positive surgical margin, or had other types of

tumors were excluded. All HCCs were confirmed by postoperative pathology. The ethics committee of West China Hospital approved this study (No. 170062).

2.1. Follow-up

All laboratory tests were performed one week before the operation. After liver resection, patients were regularly followed up every 3 months during the first two postoperative years and then very 6 months after 2 years. Antiviral drugs (entecavir, lamivudine or tenofovir) were conventionally administered to patients with positive hepatitis B virus (HBV)-DNA load before and after resection. The routine follow-up included blood cell tests, liver function tests, serum alpha-fetoprotein (AFP) measurement, HBV-DNA tests, visceral ultrasonography, computed tomography or magnetic resonance imaging and chest radiography. Bone scintigraphy was performed whenever HCC recurrence was suspected. Postoperative recurrence was defined as positive imaging findings compared with the preoperative examination values or as confirmed by biopsy or resection.(*7*)

2.2. Definitions

High AFP was defined as > 400 ng/mL (*7*). Preoperative HBV DNA load > 10^4 copies/mL was considered to be a high preoperative HBV DNA load (*8*). Clinically significant portal hypertension (CSPH) was defined by the presence of esophagogastric varices and/or a platelet count < 100 × 10^9/L in association with splenomegaly (*9*). The definitions of neutrophil-to-lymphocyte ratio (NLR), platelet-to-lymphocyte ratio (PLR), prognostic nutrition index (PNI), systemic immune-inflammation index (SII), aspartate aminotransferase-to-platelet count ratio index (APRI) and albumin-bilirubin (ALBI) grade are listed in Table 1(*10-15*). NLR ≥ 3 was defined as being high (*10*). PLR ≥ 150 was considered high (*10*). The cut-off value of PNI was 45, as reported in the literature (*11*). SII ≥ 330 was considered high (*12*). PRI ≥ 0.5 was considered high (*13,14*). ALBI values were divided into 3 grades: grade 1 (less than -2.60), grade 2 (between -2.60 and -1.39) and grade 3 (above -1.39) (*15*).

2.3. Statistical analysis

All statistical analyses were performed in SPSS 26.0 (SPSS Company, Chicago, IL) for Windows. All continuous variables were analyzed using one-way analysis of variance. Binary variables were compared by using the χ^2 test or Fisher's exact test. The Kaplan-Meier method was applied to determine the recurrence-free survival (RFS) and overall survival, and the log-rank test was performed to test the survival differences. Multivariable analysis was carried out using Cox regression analysis to identify independent risk factors for OS and RFS. All variables with a P value < 0.1 in the univariate analysis were taken into the multivariate analysis. A P value of < 0.05 was considered statistically significant.

3. Results

A total of 1,452 patients were included in this study. The clinical and demographic data of this study are shown in Table 2. Patients were followed up regularly until death or the termination of this study (April 2020). The minimum follow-up period of this study was 3 months. During a mean of 33.7 ± 18.5 months of follow-up, 1,027 patients suffered from recurrence, and 810 patients died.

3.1. Independent prognostic factors for RFS and OS in patients without CSPH

In patients without CSPH, multivariate analysis revealed that the presence of microvascular invasion (MVI) (HR = 1.681, 95% CI = 1.372-2.060, P < 0.001), NLR ≥ 3 (HR = 1.222, 95% CI = 1.015-1.472, P = 0.035), PLR ≥ 150 (HR = 1.272, 95% CI = 1.058-1.529, P = 0.011), tumor size larger than 5 cm (HR = 1.693, 95% CI = 1.306-2.195, P < 0.001) and the presence of a satellite lesion (HR1.263, 95% CI = 1.026-1.554, P = 0.028) were independently associated with postoperative recurrence (Table 3). As shown in Table 4, presence of MVI (HR = 1.756, 95% CI = 1.335-2.309, P < 0.001), NLR ≥ 3 (HR = 1.274, 95% CI = 1.032-1.571, P = 0.024), PLR ≥ 150 (HR = 1.428, 95% CI = 1.161-1.756, P = 0.001), and Barcelona Clinic Liver Cancer (BCLC) stage (HR = 2.100, 95% CI = 1.614-2.732, P < 0.001) were independent risk factors for OS.

The 1-, 3-, and 5-year RFS were 74.4%, 41.2 and 32.9% respectively for patients with low NLR, and 64.0%, 26.2% and 14.6% respectively for patients

Table 1. Definitions of inflammation-based markers in this study

Variables	Definitions
Neutrophil-to-lymphocyte ratio	Absolute neutrophil count divided by the lymphocyte count
Platelet-to-lymphocyte ratio	Platelet count divided by lymphocyte count
Prognostic nutrition index	Serum albumin (g/L) + 5 × lymphocyte count (10^9/L).
Systemic immune-inflammation index	Platelet counts × neutrophil counts/lymphocyte counts
Aspartate aminotransferase-to-platelet count ratio index	[(Aspartate aminotransferase/upper limit of normal)/platelet count (10^9/L)] × 100
Albumin-bilirubin grade	($\log_{10}$ bilirubin (μmol/L) × 0.66) + (albumin (g/L) × -0.085)

Table 2. Clinical and demographic data of current study

Variables	N/mean ± SD
Male/female	1229/223
Age (years)	51.1 ± 12.0
Tumor size (cm)	7.1 ± 3.7
Multiple tumors	351
Presence of MVI	836
The number of patients with high AFP	609 (ranged from 401 to 256360 ng/mL)
The number of patients with high HBV-DNA	648 (ranged from 1.01×10^4 copies/mL to 7.65×10^7 copies/mL)
The number of patients with high NLR	387 (ranged from 3.0 to 14.2)
The number of patients with high PLR	260 (ranged from 150 to 903)
The number of patients with high SII	577 (ranged from 330 to 5501)
The number of patients with low PNI	326 (ranged from 32.95 to 44.98)
ALBI grade 1/2/3	981/471/0
BCLC stage 0 and A/B/C	672/162/618
Presence of CSPH	527

Abbreviations: ALBI, albumin-bilirubin; AFP, alpha-fetoprotein; APRI, Aspartate aminotransferase-to-platelet count ratio index; BCLC stage, Barcelona Clinic Liver Cancer stage; CSPH, clinically significant portal hypertension; HBV, hepatitis B virus; MVI, microvascular invasion; NLR, neutrophil to lymphocyte ratio; PLR, platelet to lymphocyte ratio, PNI, Prognostic nutrition index; SD, standard deviation; SII, Systemic immune-inflammation index.

Table 3. Univariate and multivariate analyses of predictors for postoperative recurrence in patients without clinically significant portal hypertension

Variable	Univariate analysis	Multivariate analysis		
	P	HR	95% CI	*P*
Age > 60 years	0.868			
Male	0.729			
Tumor size > 5 cm	< 0.001	1.693	1.306-2.195	< 0.001
Multiple tumors	0.018			0.982
Poor tumor differentiation	0.002			0.529
AFP > 400 ng/mL	< 0.001			0.112
High HBV-DNA load	0.886			
Presence of MVI	< 0.001	1.681	1.372-2.060	< 0.001
Satellite lesion	0.001	1.263	1.026-1.554	0.028
NLR ≥ 3	< 0.001	1.222	1.015-1.472	0.035
PNI < 45	0.001			0.322
PLR ≥ 150	< 0.001	1.272	1.058-1.529	0.011
SII ≥ 330	0.002			0.439
APRI ≥ 0.5	0.039			0.785
ALBI grade	0.001			0.073
BCLC stage	< 0.001			0.586

Abbreviations: ALBI, albumin-bilirubin; AFP, alpha-fetoprotein; APRI, Aspartate aminotransferase-to-platelet count ratio index; BCLC stage, Barcelona Clinic Liver Cancer stage; CI, confidence interval; HBV, hepatitis B virus; HR, hazard ratio; MVI, microvascular invasion; NLR, neutrophil to lymphocyte ratio; PLR, platelet to lymphocyte ratio, PNI, Prognostic nutrition index; SII, Systemic immune-inflammation index.

Table 4. Univariate and multivariate analyses of predictors for postoperative mortality in patients without clinically significant portal hypertension

Variable	Univariate analysis	Multivariate analysis		
	P	HR	95% CI	*P*
Age > 60 years	0.983			
Male	0.657			
Tumor size > 5 cm	< 0.001			0.242
Multiple tumors	0.008			0.271
Poor tumor differentiation	< 0.001			0.999
AFP > 400 ng/mL	< 0.001			0.101
High HBV-DNA load	0.426			
Presence of MVI	< 0.001	1.756	1.335-2.309	< 0.001
Satellite lesion	0.032			0.624
NLR ≥ 3	< 0.001	1.274	1.032-1.571	0.024
PNI < 45	0.003			0.785
PLR ≥ 150	< 0.001	1.428	1.161-1.756	0.001
SII ≥ 330	0.001			0.593
APRI ≥ 0.5	0.021			0.394
ALBI grade	0.002			0.239
BCLC stage	< 0.001	2.100	1.614-2.732	< 0.001

Abbreviations: ALBI, albumin-bilirubin; AFP, alpha-fetoprotein; APRI, Aspartate aminotransferase-to-platelet count ratio index; BCLC stage, Barcelona Clinic Liver Cancer stage; CI, confidence interval; HBV, hepatitis B virus; HR, hazard ratio; MVI, microvascular invasion; NLR, neutrophil to lymphocyte ratio; PLR, platelet to lymphocyte ratio, PNI, Prognostic nutrition index; SII, Systemic immune-inflammation index.

with high NLR ($P < 0.001$, Figure 1A). The 1-, 3-, and 5-year OS were 91.5%, 61.2 and 39.6% respectively for patients with low NLR, and 88.5%, 43.7% and 26.3% respectively for patients with high NLR ($P < 0.001$, Figure 1B). The 1-, 3-, and 5-year RFS of patients with low and high PLR were 75.4%, 41.9%, 32.5% and 62.8%, 25.0%, 15.5% respectively. A significant difference was observed ($P < 0.001$, Figure 1C). The 1-, 3-, and 5-year OS of patients with low PLR were 92.6%, 62.7%, and 40.9% respectively, which were significantly better than those with low PLR (85.8%, 40.5%, 23.2% respectively, $P < 0.001$, Figure 1D)

3.2. Independent prognostic factors for RFS and OS in patients with CSPH

Among patients with CSPH, as presented in Table 5, the multivariate analysis confirmed that tumor size

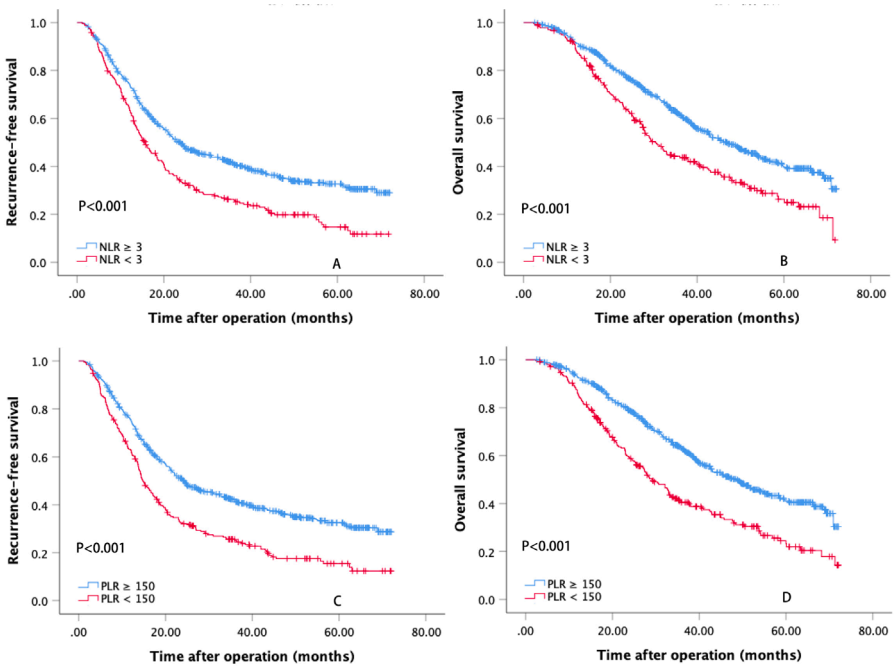

Figure 1. The recurrence-free (A) and overall (B) survival curves of patients with high and low neutrophil to lymphocyte ratios. The recurrence-free (C) and overall (D) survival curves of patients with high and low platelet to lymphocyte ratios.

Table 5. Univariate and multivariate analyses of predictors for postoperative recurrence in patients with clinically significant portal hypertension

Variable	Univariate analysis	Multivariate analysis		
	P	HR	95% CI	*P*
Age > 60 years	0.529			
Male	0.432			
Tumor size > 5 cm	< 0.001	1.485	1.173-1.879	0.001
Multiple tumors	0.007			0.743
Poor tumor differentiation	0.011			0.998
AFP ≥ 400 ng/mL	0.188			
High HBV-DNA load	0.824			
Presence of MVI	< 0.001	1.875	1.495-2.351	< 0.001
Satellite lesion	< 0.001	1.532	1.187-1.976	0.001
NLR ≥ 3	0.078			0.294
PNI < 45	0.179			
PLR ≥ 150	0.836			
SII ≥ 330	0.263			
APRI ≥ 0.5	0.166			
ALBI grade	0.006	1.333	1.098-1.619	0.004
BCLC stage	< 0.001			0.140

Abbreviations: ALBI, albumin-bilirubin; AFP, alpha-fetoprotein; APRI, Aspartate aminotransferase-to-platelet count ratio index; BCLC stage, Barcelona Clinic Liver Cancer stage; CI, confidence interval; HBV, hepatitis B virus; HR, hazard ratio; MVI, microvascular invasion; NLR, neutrophil to lymphocyte ratio; PLR, platelet to lymphocyte ratio, PNI, Prognostic nutrition index; SII, Systemic immune-inflammation index.

Table 6. Univariate and multivariate analyses of predictors for postoperative mortality in patients with clinically significant portal hypertension

Variable	Univariate analysis	Multivariate analysis		
	P	HR	95% CI	*P*
Age > 60 years	0.785			
Male	0.721			
Tumor size > 5 cm	< 0.001	1.398	1.003-1.948	0.048
Multiple tumors	0.063	0.656	0.489-0.882	0.005
Poor tumor differentiation	0.005			0.214
AFP > 400 ng/mL	0.142			
High HBV-DNA load	0.367			
Presence of MVI	< 0.001	1.598	1.188-2.150	0.002
Satellite lesion	0.007			0.051
NLR ≥ 3	0.097			0.572
PNI < 45	0.012			0.287
PLR ≥ 150	0.543			
SII ≥ 330	0.052			0.466
APRI ≥ 0.5	0.320			
ALBI grade	0.002	1.389	1.117-1.726	0.003
BCLC stage	< 0.001	2.209	1.490-3.276	< 0.001

Abbreviations: ALBI, albumin-bilirubin; AFP, alpha-fetoprotein; APRI, Aspartate aminotransferase-to-platelet count ratio index; BCLC stage, Barcelona Clinic Liver Cancer stage; CI, confidence interval; HBV, hepatitis B virus; HR, hazard ratio; MVI, microvascular invasion; NLR, neutrophil to lymphocyte ratio; PLR, platelet to lymphocyte ratio, PNI, Prognostic nutrition index; SII, Systemic immune-inflammation index.

greater than 5 cm (HR = 1.484, 95% CI = 1.173-1.879, $P = 0.001$), MVI (HR = 1.875, 95% CI = 1.495-2.351, $P < 0.001$), satellite lesion (HR = 1.532, 95% CI = 1.187-1.976, $P = 0.001$) and ALBI grade (HR = 1.333, 95% CI = 1.098-1.619, $P = 0.004$) independently predicted postoperative recurrence.

As shown in Table 6, tumor size greater than 5 cm (HR = 1.398, 95% CI = 1.003-1.948, $P = 0.048$), multiple tumors (HR = 0.656, 95% CI = 0.489-0.882, $P = 0.005$), MVI (HR = 1.598, 95% CI = 1.188-2.150,

Table 7. Comparison of clinicopathological characteristics of patients with or without clinically significant portal hypertension

Variable	Patients without CSPH	Patients with CSPH	*P* values
Age	50.5 ± 12.2	52.2 ± 11.6	< 0.001
Female/male	150/775	73/454	0.230
Tumor size (cm)	7.7 ± 3.9	6.0 ± 3.1	< 0.001
MVI (yes/no)	564/361	272/255	0.001
Multiple tumors (yes/no)	217/708	134/393	0.400
Poor tumor differentiation	195/730	71/456	< 0.001
AFP > 400 ng/mL	408/516	200/327	0.020
High HBV-DNA load	397/528	251/276	0.083
Satellite lesion	149/776	80/447	0.641
NLR	2.6 ± 2.2	2.7 ± 1.7	0.519
PLR	130.9 ± 87.8	64.9 ± 30.2	< 0.001
PNI	49.5 ± 5.6	47.6 ± 5.2	< 0.001
SII	489.1 ± 591.4	198.5 ± 126.9	< 0.001
APRI	0.82 ± 0.72	1.09 ± 1.83	< 0.001
Neutrophil	3.6 ± 1.6	3.1 ± 1.5	< 0.001
Lymphocyte	1.6 ± 0.6	1.3 ± 0.5	< 0.001
Albumin	41.4 ± 4.4	40.9 ± 4.3	0.059
AST	47.5 ± 31.3	49.2 ± 36.3	0.350
ALBI grade (grade 1/2)	663/262	318/209	< 0.001
BCLC stage (0/A *vs.* B/C)	393/532	279/248	< 0.001

Abbreviations: ALBI, albumin-bilirubin; AFP, alpha-fetoprotein; APRI, Aspartate aminotransferase-to-platelet count ratio index; BCLC stage, Barcelona Clinic Liver Cancer stage; CSPH, clinically significant portal hypertension; HBV, hepatitis B virus; MVI, microvascular invasion; NLR, neutrophil to lymphocyte ratio; PLR, platelet to lymphocyte ratio, PNI, Prognostic nutrition index; SII, Systemic immune-inflammation index.

P = 0.002), ALBI grade (HR = 1.389, 95% CI = 1.117-1.726, *P* = 0.003) and BCLC stage (HR = 2.209, 95% CI = 1.490-3.276, *P* < 0.001) were independent risk factors in the multivariate analysis (Table 6).

3.3. Comparison of clinicopathological characteristics of patients with versus without CSPH

As listed in Table 7, large tumors, MVI, poor tumor differentiation, high preoperative AFP, high PLR, high SII, low APRI and advanced tumors were more often observed in patients without CSPH, whereas older patients, lower PNI, low preoperative lymphocyte count, low preoperative neutrophil count and ALBI grade 2 were more often found in those with CSPH.

4. Discussion

In this study, we confirmed that NLR and PLR may be prognostic predictors for HCC patients without CSPH, but not for those with CSPH. Moreover, ALBI grade may be a surrogate predictive marker for those with CSPH.

In this study, both NLR and PLR predicted the outcomes of HCC patients without CSPH, but not in those with CSPH. Many studies have suggested that both NLR and PLR could predict the postoperative prognosis of patients with HCC after liver resection (*6,10*). There are some potential mechanisms by which high NLR and PLR could contribute to poor prognosis. First, both neutrophils and platelets could secrete some factors that could promote angiogenesis, tumor progression and metastasis (*16,17*). Second, lymphocytes are very important anticancer cells (*18,19*). However, many previous investigations ignored the adverse influence of CSPH on neutrophils, platelets and lymphocytes. CSPH results in low platelet counts and even low white blood cell counts. As shown in Table 7, high PLR was rare in those with CSPH due to a low preoperative platelet count. Moreover, both neutrophils and lymphocytes were reduced in patients with CSPH, though it seems that lymphocytes decreased slightly more than neutrophils. The discrepancy in the magnitudes of the lymphocyte and neutrophil declines may explain why the NLR was not a prognostic predictor for patients with CSPH. However, few previous studies ignored the impact of CSPH on markers of the systemic inflammatory response. Our results could also explain why the predictive ability of NLR and PLR was controversial among previous investigators. In this study, larger tumor size, more MVI and higher AFP level were observed in HCC patients without CSPH. The tolerance for surgical procedures of patients with CSPH may be worse than those without CSPH due to thrombocytopenia. Accordingly, some HCC patients with CSPH cannot tolerate liver resection, such as those with very large tumors or advanced BCLC stage. Because, in this situation, we need to remove a lot of liver parenchyma, and the surgical procedure is more complicated.

It was interesting that SII was not a prognostic predictor, even in patients without CSPH, although this marker was calculated using neutrophils, lymphocytes and platelets. Hu *et al.* (*12*) reported that circulating tumor cell levels were significantly higher and the prognosis was poorer in HCC patients with a high SII. They divided HCC patients into high- and low-SII groups by using a cut-off of 330, which was also used in the current study (*12*). However, some investigations confirmed that SII is a good predictor for patients with HCC, but they proposed other optimal cut-off values (*20,21*). For example, Wang *et al.* (*21*) used 305 as the best cut-off value of SII, whereas Fu *et al.* (*20*) used 226 as the optimal cut-off value of SII. Further study is needed to determine the best cut-off level of SII from the view of predicting the outcome of patients who underwent liver resection for HCC.

There are some limitations in this study. This is a retrospective study and lacks validation. Moreover, there are many biomarkers of the systemic inflammatory response, only some of which we measured. Different from previous studies, we assessed the influence of inflammation-based markers on prognosis of HCC patients with or without CSPH respectively. Our study

confirmed that these biomarkers can be impacted by CSPH, especially those calculated from platelets, neutrophils, lymphocytes and albumin.

In conclusion, CSPH could influence the predictive capacity of biomarkers of the systemic inflammatory response. NLR and PLR only showed prognostic power in HCC patients without CSPH, whereas poor liver function assessed by ALBI grade contributed to a poor prognosis for HCC patients with CSPH following liver resection. In clinical practice, we should not ignore the adverse influence of CSPH on inflammation-based biomarkers in predicting the outcomes of patients with HCC after liver resection.

Acknowledgements

This study was supported by grants from the State Key Scientific and Technological Research Programs (2017ZX10203207-003-0020), the National Natural Science Foundation of China (81900576), and the Science and Technological Supports Project of Sichuan Province (2019YJ0149).

References

1. Bruix J, Sherman M, Llovet JM, Beaugrand M, Lencioni R, Burroughs AK, Christensen E, Pagliaro L, Colombo M, Rodes J, HCC EPoEo. Clinical management of hepatocellular carcinoma. Conclusions of the Barcelona-2000 EASL conference. European Association for the Study of the Liver. J Hepatol. 2001; 35:421-430.
2. Giannini EG, Savarino V, Farinati F, Ciccarese F, Rapaccini G, Marco MD, Benvegnu L, Zoli M, Borzio F, Caturelli E, Chiaramonte M, Trevisani F, Italian Liver Cancer g. Influence of clinically significant portal hypertension on survival after hepatic resection for hepatocellular carcinoma in cirrhotic patients. Liver Int. 2013; 33:1594-1600.
3. Jang CW, Kwon HJ, Kong H, Ha H, Han YS, Chun JM, Kim SG, Hwang YJ. Impact of clinically significant portal hypertension on surgical outcomes for hepatocellular carcinoma in patients with compensated liver cirrhosis: a propensity score matching analysis. Ann Hepatobiliary Pancreat Surg. 2016; 20:159-166.
4. Sanghera C, Teh JJ, Pinato DJ. The systemic inflammatory response as a source of biomarkers and therapeutic targets in hepatocellular carcinoma. Liver Int. 2019; 39:2008-2023.
5. Zheng J, Seier K, Gonen M, Balachandran VP, Kingham TP, D'Angelica MI, Allen PJ, Jarnagin WR, DeMatteo RP. Utility of Serum Inflammatory Markers for Predicting Microvascular Invasion and Survival for Patients with Hepatocellular Carcinoma. Ann Surg Oncol. 2017; 24:3706-3714.
6. Goh BK, Kam JH, Lee SY, Chan CY, Allen JC, Jeyaraj P, Cheow PC, Chow PK, Ooi LL, Chung AY. Significance of neutrophil-to-lymphocyte ratio, platelet-to-lymphocyte ratio and prognostic nutrition index as preoperative predictors of early mortality after liver resection for huge (>/=10 cm) hepatocellular carcinoma. J Surg Oncol. 2016; 113:621-627.
7. Li C, Shen JY, Zhang XY, Peng W, Wen TF, Yang JY, Yan LN. Predictors of Futile Liver Resection for Patients with Barcelona Clinic Liver Cancer Stage B/C Hepatocellular Carcinoma. J Gastrointest Surg. 2018; 22:496-502.
8. Huang G, Li PP, Lau WY, Pan ZY, Zhao LH, Wang ZG, Wang MC, Zhou WP. Antiviral Therapy Reduces Hepatocellular Carcinoma Recurrence in Patients With Low HBV-DNA Levels: A Randomized Controlled Trial. Ann Surg. 2018; 268:943-954.
9. Takemura N, Aoki T, Hasegawa K, Kaneko J, Arita J, Akamatsu N, Makuuchi M, Kokudo N. Hepatectomy for hepatocellular carcinoma after perioperative management of portal hypertension. Br J Surg. 2019; 106:1066-1074.
10. Yamamura K, Sugimoto H, Kanda M, Yamada S, Nomoto S, Nakayama G, Fujii T, Koike M, Fujiwara M, Kodera Y. Comparison of inflammation-based prognostic scores as predictors of tumor recurrence in patients with hepatocellular carcinoma after curative resection. J Hepatobiliary Pancreat Sci. 2014; 21:682-688.
11. Chan AW, Chan SL, Wong GL, Wong VW, Chong CC, Lai PB, Chan HL, To KF. Prognostic Nutritional Index (PNI) Predicts Tumor Recurrence of Very Early/Early Stage Hepatocellular Carcinoma After Surgical Resection. Ann Surg Oncol. 2015; 22:4138-4148.
12. Hu B, Yang XR, Xu Y, Sun YF, Sun C, Guo W, Zhang X, Wang WM, Qiu SJ, Zhou J, Fan J. Systemic immune-inflammation index predicts prognosis of patients after curative resection for hepatocellular carcinoma. Clin Cancer Res. 2014; 20:6212-6222.
13. Wang H, Xue L, Yan R, Zhou Y, Wang MS, Cheng MJ, Huang HJ. Comparison of FIB-4 and APRI in Chinese HBV-infected patients with persistently normal ALT and mildly elevated ALT. J Viral Hepat. 2013; 20:e3-10.
14. Luo H, Li C, Chen L. Preoperative albumin-bilirubin grade combined with aspartate aminotransferase-to-platelet count ratio index predict outcomes of patients with hepatocellular carcinoma within Milan criteria after liver resection. Biosci Trends. 2019; 13:176-181.
15. Johnson PJ, Berhane S, Kagebayashi C, *et al.* Assessment of liver function in patients with hepatocellular carcinoma: a new evidence-based approach-the ALBI grade. J Clin Oncol. 2015; 33:550-558.
16. Kuang DM, Zhao Q, Wu Y, Peng C, Wang J, Xu Z, Yin XY, Zheng L. Peritumoral neutrophils link inflammatory response to disease progression by fostering angiogenesis in hepatocellular carcinoma. J Hepatol. 2011; 54:948-955.
17. Palumbo JS, Talmage KE, Massari JV, La Jeunesse CM, Flick MJ, Kombrinck KW, Jirouskova M, Degen JL. Platelets and fibrin(ogen) increase metastatic potential by impeding natural killer cell-mediated elimination of tumor cells. Blood. 2005; 105:178-185.
18. Wang M, Li C, Wen TF, Peng W, Chen LP. Postoperative Low Absolute Lymphocyte Counts may Predict Poor Outcomes of Hepatocellular Carcinoma After Liver Resection. Chin Med J (Engl). 2016; 129:536-541.
19. Li C, Wen TF, Yan LN, Li B, Wang WT, Yang JY, Xu MQ. Postoperative neutrophil-to-lymphocyte ratio plus platelet-to-lymphocyte ratio predicts the outcomes of hepatocellular carcinoma. J Surg Res. 2015; 198:73-79.

20. Fu H, Zheng J, Cai J, Zeng K, Yao J, Chen L, Li H, Zhang J, Zhang Y, Zhao H, Yang Y. Systemic Immune-Inflammation Index (SII) is Useful to Predict Survival Outcomes in Patients After Liver Transplantation for Hepatocellular Carcinoma within Hangzhou Criteria. Cell Physiol Biochem. 2018; 47:293-301.
21. Wang C, He W, Yuan Y, Zhang Y, Li K, Zou R, Liao Y, Liu W, Yang Z, Zuo D, Qiu J, Zheng Y, Li B, Yuan Y. Comparison of the prognostic value of inflammation-based scores in early recurrent hepatocellular carcinoma after hepatectomy. Liver Int. 2020; 40:229-239.

Received May 25, 2020; Revised June 26, 2020; Accepted July 5, 2020.

*Address correspondence to:
Chuan Li, Department of Liver Surgery, West China Hospital of Sichuan University, Chengdu 610041, Sichuan Province, China.
E-mail: lichuan@scu.edu.cn

Released online in J-STAGE as advance publication July 8, 2020.

Original Article

DOI: 10.5582/bst.2020.03167

High C-reactive protein/albumin ratio associated with reduced survival due to advanced stage of intrahepatic cholangiocarcinoma

Hisao Kano[1], Yutaka Midorikawa[1,*], Peipei Song[2], Hisashi Nakayama[1], Masamichi Moriguchi[1], Tokio Higaki[1], Shingo Tsuji[3], Tadatoshi Takayama[1]

[1] Department of Digestive Surgery, Nihon University School of Medicine, Tokyo, Japan;
[2] National Center for Global Health and Medicine, Tokyo, Japan;
[3] Genome Science Division, Research Center for Advanced Science and Technology, The University of Tokyo, Tokyo, Japan.

SUMMARY C-reactive protein (CRP)- and albumin (Alb)-based scoring systems are available for predicting the prognosis of patients with diverse forms of gastrointestinal cancer, but their utility for patients with intrahepatic cholangiocarcinoma (ICC) is still unclear. This study aimed to elucidate whether a high CRP/Alb ratio is associated with the surgical outcome of ICC patients. Patients who underwent initial and curative resection for ICC were included in this study, and were divided into the High and Low CRP/Alb groups based on their preoperative CRP and Alb values. The surgical outcomes were compared between the two groups. The median CRP/Alb ratio amongst 88 patients was 0.033 (range, 0.019-3.636); 44 patients with CRP/Alb > 0.033 were allocated to the High CRP/Alb group and 44 patients were allocated to the Low CRP/Alb group. The operative data did not differ between the two groups, while the tumor status was more advanced in the High CRP/Alb group. The median overall survival was 2.4 years (95% CI, 1.4-3.3) and 8.9 years (3.8-NA) in the High and Low CRP/Alb groups, respectively ($P < 0.001$), and recurrence-free survival was 0.5 years (95% CI, 0.3-0.7) and 7.7 years (1.3-NA), respectively ($P < 0.001$). In a multivariate analysis, the independent factors for overall survival were High CRP/Alb ($P = 0.017$) and multiple nodules ($P = 0.008$). Taken together, the survival of ICC patients in the High CRP/Alb group was reduced compared to that of patients in the Low CRP/Alb group due to the advanced stage of the tumor as well as malnutrition.

Keywords intrahepatic cholangiocarcinoma, C-reactive protein/albumin ratio, prognostic marker

1. Introduction

Both inflammation and nutrition-based prognostic systems such as the Glasgow prognostic score (GPS) and C-reactive protein/Albumin (CRP/Alb) ratio are brief and useful markers for surgical outcomes in patients with diverse forms of gastroenterological cancer, such as esophageal (*1*), gastric (*2*), colorectal (*3,4*), and pancreatic cancer (*5,6*). In primary liver cancer, high scores of GPS and CRP/Alb ratio have also been associated with reduced survival after operation in patients with hepatocellular carcinoma (*7-9*), although it is still unclear whether CRP/Alb ratio can predict survival in patients with intrahepatic cholangiocarcinoma (ICC) (*10,11*).

ICC makes up approximately 5% of all primary liver cancer cases, and prognosis is very poor because of the possibility of relapse both outside and inside the liver, even when a patient undergoes liver resection at an early stage (*12,13*). Therefore, stratification of ICC patients based on the risk of recurrence would be helpful for identifying candidates for postoperative adjuvant therapy (*14,15*). In addition to clinicopathological findings (*16,17*) and surgical procedures (*18,19*), various types of predictive marker, such as aspartate aminotransferase/neutrophil ratio (*20*), platelet/lymphocyte ratio (*21*), albumin/gGTP ratio (*22*), and neutrophil/lymphocyte ratio (*23*), have been reported as being negatively associated with patient survival after resection of ICC.

In this study, we classified patients who underwent curative resection for ICC according to the prognostic system, CRP/Alb ratio, and compared their surgical outcomes. Then, we elucidated whether a high CRP/Alb ratio was associated with the survival of patients with ICC.

2. Materials and Methods

2.1. Patients

Patients undergoing curative liver resection for ICC from 2000 to 2018 at Nihon University Itabashi Hospital were included in this study; each participant provided written informed consent, and the institutional review board of Nihon University approved this study. All the patients were closely observed during each of their outpatient office visits. All clinical investigations were conducted according to the principles of the Declaration of Helsinki.

2.2. Classification

Patients with ICC, which was diagnosed by two pathologists with more than 5 years' experience in the field of liver pathology, were divided into the two classes based on the preoperative CRP/Alb ratio. The cut-off value was determined as the median, and those patients with a CRP/Alb ratio higher than the cut-off value were allocated to the High CRP/Alb group, and the other patients to the Low CRP/Alb group.

2.3. Surgical procedures

Liver resection was performed for all patients based on the criteria regarding the number of tumors and liver function (*24*). Transection of the liver was performed under ultrasonographic guidance using the clamp-crushing method and the inflow blood occlusion technique (*25*). Systemic lymph nodes dissection was not routinely performed; only those that were diagnosed as metastatic before or during operation were removed. Anatomic resection was defined as any type of systematic resection of the portal regions based on Couinaud's classification. Major liver resection was defined as resection of three or more segments. Curative resection was defined as the complete removal of recognizable viable ICC diagnosed preoperatively or intraoperatively with macroscopically tumor-free surgical margins.

2.4. Follow-up after operation

All patients were followed for postoperative recurrence as described previously (*26*). Briefly, tumor marker levels, including those of carcinoembryonic antigen and carbohydrate antigen 19-9 (CA19-9), were measured, and imaging studies, including computed tomography and ultrasonography, were performed every three months in all patients. Recurrence was diagnosed by dynamic computed tomography and/or by gadolinium-ethoxybenzyl-diethylenetriamine pentaacetic acid-enhanced magnetic resonance imaging, and 18F-fluorodeoxyglucose-positron emission tomography. The date of recurrence was defined as the date of examination when the recurrent ICC was noted.

2.5. Statistical analysis

Data collected from each group were statistically analyzed using Fisher's exact test and the Wilcoxon rank-sum test. Survival curves were generated using the Kaplan–Meier method and compared using the Wilcoxon test. Prognostic factors for survival were identified using the Cox proportional hazards regression model. A P value of less than 0.10 was set as the cut-off value for elimination. The following 11 variables, considered potential confounders, were examined: age (≥ 70 versus < 70 years), sex, positive for hepatitis B or C virus, indocyanine green clearance rate at 15 minutes (ICGR15) (≥ 15 versus < 15%), frequency of esophageal varices, tumor size (≥ 5.0 versus < 5.0 cm), tumor number (single versus multiple), tumor thrombus, serum carcinoembryonic antigen level (≥ 5.0 versus < 5.0 ng/mL), CA19-9 level (≥ 37 versus < 37 ng/mL), and CRP/Alb ratio. In all analyses, a P value < 0.05 was considered to be statistically significant.

3. Results

3.1. Patients

The median CRP/Alb ratio amongst 88 patients who underwent initial and curative resection for ICC was 0.033 (range, 0.019-3.636), from whom 44 patients with a CRP/Alb ratio > 0.033 were allocated to the High CRP/Alb group (median, 0.139; range, 0.034-3.636), and 44 patients with a CRP/Alb ratio < 0.033 were allocated to the Low CRP/Alb group (median, 0.023; range, 0.019-0.032) (Figure 1).

Patient background did not differ between the two groups, except for CA 19-9, which was significantly higher in the High CRP/Alb group (P = 0.005) (Table 1).

3.2. Operative data

Operation data and postoperative complication rates did not differ between the two groups (Table 2). Two patients (for bile leakage and an intra-abdominal abscess) and one patient (for wound infection) underwent re-operation in the High and Low CRP/Alb groups, respectively, but

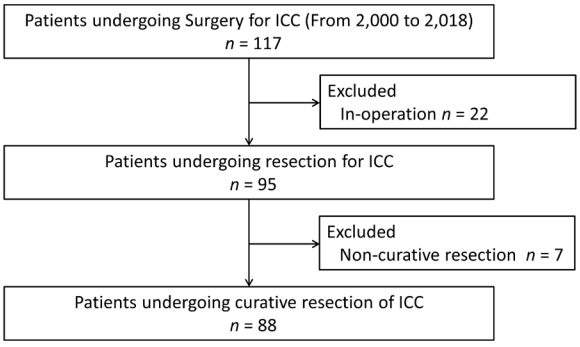

Figure 1. Flow diagram illustrating the recruitment of patients with ICC. ICC, intrahepatic cholangiocarcinoma.

Table 1. Patient background

Variables	High CRP/Alb (n = 44)	Low CRP/Alb (n = 44)	P value
Age, years	68 (23-84)	69 (41-84)	0.622
Sex, male (%)	28 (63.6)	33 (75.0)	0.355
Alcoholic, n (%)	8 (18.1)	9 (20.4)	1
Diabetes mellitus, n (%)	9 (20.4)	9 (20.4)	1
HBV, n (%)	1 (2.2)	7 (15.9)	0.057
HCV, n (%)	5 (11.3)	6 (13.6)	1
Varices, n (%)	2 (4.5)	1 (2.2)	1
Child-Pugh, A (%)	42 (95.4)	44 (100)	0.494
ICGR15, %	8.8 (1.9-26.8)	9.4 (2.0-33.4)	0.667
CEA, ng/mL	3.3 (0.2-175.1)	2.8 (0.4-71.5)	0.362
CA19-9, U/mL	82.8 (0.5-117800)	22.5 (0.1-39950)	0.005

Data are presented as median with range, if not specified. HBV, hepatitis B virus; HCV, hepatitis C virus; ICGR15, indocyanine green clearance rate at 15 minutes; CEA, carcinoembryonic antigen; CA19-9, carbohydrate antigen 19-9.

Table 2. Operative data

Variables	High CRP/Alb (n = 44)	Low CRP/Alb (n = 44)	P value
Operation data			
Operation time, min	392 (168-869)	381 (170-795)	0.229
Bleeding, mL	326 (20-1,752)	352 (29-11,002)	0.442
Transfusion, n (%)	2 (4.5)	4 (9.0)	0.116
Major resection, n (%)	21 (47.7)	22 (50.0)	1
Anatomic resection, n (%)	35 (79.5)	29 (65.9)	0.231
Complications			
Overall, n (%)	19 (43.1)	11(25.0)	0.114
Morbidity, n (%)	10 (22.7)	8 (18.1)	0.792
Re-operation, n (%)	2 (4.5)	1 (2.2)	1
Mortality, n (%)	0	0	1
Pathology			
Multiple, n (%)	15 (34.0)	5 (11.3)	0.020
Size, cm (range)	5.2 (1.8-12.3)	3.4 (1.0-10.5)	0.001
Differentiation grade, mod, (%)	39 (88.6)	41 (93.1)	0.713
Vascular invasion, n (%)	32 (72.7)	20 (47.7)	0.026
Tumor exposure, n (%)	11 (25.0)	5 (11.3)	0.165
Cirrhosis	2 (4.5)	3 (6.8)	1

Data are presented as median, if not specified.

there was no in-hospital death in this series. Histological findings for the resected specimens showed that tumor status was more advanced in the High CRP/Alb group; multiple nodules (P = 0.020) and vascular invasion (P = 0.026) were more frequent, and tumor size was larger (P = 0.001), in the High CRP/Alb group.

3.3. Survival

After a median follow-up of 1.4 years (range, 0.3 to 10.3 years), a total of 48 patients (54.5%) experienced recurrence; 28 patients (58.3%) in the remnant liver, 11 patients (12.5%) in distant sites, and nine patients with both intra- and extra-hepatic recurrences (Table 3). Extrahepatic recurrence was more frequent in the Low CRP/Alb group (30.3% vs 66.6%, P = 0.027). Treatment for recurrent ICC did not differ between the two groups.

Median overall survival was 2.4 years (95% confidence interval [CI], 1.4-3.3) and 8.9 years (3.0-NA; P < 0.001) in the High CRP/Alb and the Low CRP/Alb groups, respectively (Figure 2A), and recurrence-free survival was 0.5 years (95% CI, 0.3-0.7) and 7.7 years (1.3-NA; P < 0.001), respectively (Figure 2B). The 5-year rate of overall survival was 19.1% and 65.0%, and that of recurrence-free survival was 14.4% and 55.9% in the two groups, respectively.

Table 3. Treatment for recurrence

Variables	High CRP/Alb (n = 33)	Low CRP/Alb (n = 15)	P value
Recurrent sites			0.004
Intrahepatic	23 (69.6)	5 (33.3)	
Distant sites	3 (9.0)	8 (53.3)	
Both	7 (21.2)	2 (13.3)	
Treatments			0.410
Second resection	5 (15.1)	2 (13.3)	
TACE/TAI	9 (27.2)	1 (6.6)	
Chemotherapy	12 (36.3)	8 (24.2)	
Radiation therapy	4 (12.1)	1 (6.6)	
None	3 (9.0)	3 (20.0)	

Data are presented as median with range, if not specified. TACE, transcatheter arterial chemoembolization; TAI, transcatheter arterial infusion.

In a multivariate analysis, the independent factors

affecting overall survival were High CRP/Alb (hazard ratio [HR], 2.82, 95% CI, 1.20-7.17; $P = 0.017$) and the presence of multiple nodules (HR, 3.98, 95% CI, 1.42-11.09; $P = 0.008$) (Table 4). The independent factors affecting recurrence were High CRP/Alb ratio (HR, 3.28, 95% CI, 1.64-6.80; $P < 0.001$) and the presence of multiple nodules (HR, 7.67, 95% CI, 3.57-16.50; $P < 0.001$) (Table 5).

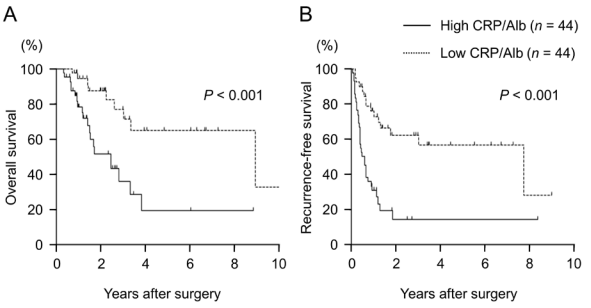

Figure 2. Surgical outcomes of patients undergoing resection for ICC. (A) Overall survival of patients in the High CRP/Alb group is significantly less than that of patients in the Low CRP/Alb group ($P = 0.001$). **(B)** Recurrence-free survival of patients in the High CRP/Alb group is significantly less than that of patients in the Low CRP/Alb group ($P < 0.001$). CRP, C-reactive protein; Alb, albumin; ICC, intrahepatic cholangiocarcinoma.

4. Discussion

We demonstrate that a high preoperative CRP/Alb ratio is related to advanced tumor stage and reduced survival in patients with ICC. This is the first report showing the utility of a scoring system based on inflammation and nutritional status (CRP/Alb ratio) for stratifying patients after resection of ICC.

GPS was originally proposed as a prognostic marker for patients with non-small lung cell cancer, which was superior to clinical stage or performance status (*27*). It was later shown that GPS reflected malnutrition status based on the systemic inflammation response, "cancer cachexia" (*28*). Given that many ICC patients experience early recurrence even after curative resection, it is possible that patient survival is longer in our Low CRP/Alb group, and in the GPS-Low group in the Pan *et al.* (*11*) study, due to the possible continuation of cancer treatments for recurrent tumors, including chemotherapy, radiation therapy, transcatheter arterial chemoembolization, and infusion.

Table 4. Prognostic factors for survival

Variables	Univariate		Multivariate	
	Hazard ratio	*P* value	Hazard ratio	*P* value
Age	1.02 (0.47-2.17)	0.958		
Sex	1.19 (0.53-2.52)	0.657		
Viral hepatitis	0.79 (0.26-1.93)	0.635		
ICGR15	1.08 (0.46-2.94)	0.864		
Varices	0.92 (0.33-2.15)	0.864		
Size	2.59 (1.23-5.47)	0.012	1.37 (0.56-3.24)	0.477
Multiple	6.45 (2.56-15.73)	< 0.001	3.98 (1.42-11.09)	0.008
Tumor Thrombus	1.87 (0.87-4.24)	0.106		
CEA	0.74 (0.27-1.72)	0.511		
CA19-9	0.98 (0.45-2.08)	0.965		
CRP/Alb ratio	3.76 (1.70-9.16)	< 0.001	2.82 (1.20-7.17)	0.017

ICGR15, indocyanine green clearance rate at 15 minutes; CEA, carcinoembryonic antigen; CA19-9, carbohydrate antigen 19-9.

Table 5. Prognostic factors for recurrence

Variables	Univariate		Multivariate	
	Hazard ratio	*P* value	Hazard ratio	*P* value
Age	0.73 (0.40-1.30)	0.293		
Sex	1.14 (0.62-2.22)	0.666		
Viral hepatitis	0.56 (0.24-1.15)	0.123		
ICGR15	0.68 (0.29-1.39)	0.310		
Varices	1.59 (0.25-5.18)	0.548		
Size	2.09 (1.17-3.70)	0.012	1.12 (0.57-2.14)	0.727
Multiple	8.40 (4.25-16.36)	< 0.001	7.67 (3.57-16.50)	< 0.001
Tumor Thrombus	1.85 (1.03-3.43)	0.038	1.19 (0.61-2.38)	0.603
CEA	1.08 (0.55-1.98)	0.809		
CA19-9	1.49 (0.83-2.68)	0.174		
CRP/Alb ratio	3.81 (2.07-7.35)	< 0.001	3.28 (1.64-6.80)	< 0.001

ICGR15, indocyanine green clearance rate at 15 minutes; CEA, carcinoembryonic antigen; CA19-9, carbohydrate antigen 19-9.

It has been reported that GPS and CRP/Alb ratio are positively associated with primary liver cancer progression; tumor stage is more advanced in patients with a higher GPS (*7,11*) and CRP/Alb ratio (*8,9*). Consequently, both overall and recurrence-free survival of patients in these studies were without exception significantly reduced in the high GPS and CRP/Alb ratio groups. Consistent with this, tumor status was more advanced in the High CRP/Alb group in our study; multiple tumors and vascular invasion were more frequent, tumors were larger, and serum CA19-9 levels were higher. Given that liver function, indicated by variables such as frequency of varices, Child-Pugh classification, and ICGR15, did not differ between the two groups, we attributed reduced survival in patients from the High/CRP group to the advanced stage of the tumor and the poor nutritional status of patients with a cancer burden.

In the studies reported above, cut-off values for the CRP/Alb ratio were determined using area under the curve of receiver operating characteristic curves (*9*) or X-tile plots (*8*), or were defined as the median value (*10*), and its range was from 0.024 to 0.033. Given that cut-off values for CRP/Alb ratio were from 0.018 to 0.10 for the other types of gastroenterological cancer (*1-3,5,6*), the value of 0.033 used in this study was appropriate.

There are several limitations of this study. First, tumor status was more advanced in the High CRP/Alb group, as in previous reports. Consequently, progressive cancer greatly influenced surgical outcomes and it is not yet clear whether nutritional status can contribute to the improvement of post-operational patient survival. In order to elucidate the relationship between nutritional status and survival, surgical outcomes should be compared after matching patient background and tumor stage between the two groups, using a much larger cohort. Second, the presence of any causal relationship between high CRP/Alb ratio and tumor progression remains unknown. Given that tumor status is more advanced in high GPS and high CRP/Alb ratio groups in previous primary liver cancer studies (*7-9,11*), we speculate that the deviation of tumor progression in the High CRP/Alb group in this study is not accidental, which needs to be clarified in the future.

In conclusion, survival of ICC patients in the High CRP/Alb group was significantly less than that of patients in the Low/CRP group. This is partly because the nutritional status of high CRP/Alb ratio patients negatively affected survival, but mainly because CRP/Alb ratio is associated with tumor progression, which dictated surgical outcome in patients with ICC.

Acknowledgements

This work was supported by the Japan Agency for Medical Research and Development (AMED) under Grant Number JP18hk0102049 and a grants-in-aid of The 106th Annual Congress of JSS Memorial Surgical Research Fund, Tokyo, Japan.

References

1. Tamagawa H, Aoyama T, Tamagawa A, Komori K, Maezawa Y, Kano K, Murakawa M, Atsumi Y, Hara K, Kazama K, Numata M, Oshima T, Yukawa N, Masuda M, Rino Y. Influence of the Preoperative C-Reactive Protein-to-Albumin Ratio on Survival and Recurrence in Patients With Esophageal Cancer. Anticancer Res. 2020; 40:2365-2371.
2. Kudou K, Saeki H, Nakashima Y, *et al.* C-reactive protein/albumin ratio is a poor prognostic factor of esophagogastric junction and upper gastric cancer. J Gastroenterol Hepatol. 2019; 34:355-363.
3. Shibutani M, Maeda K, Nagahara H, Iseki Y, Ikeya T, Hirakawa K. Prognostic Significance of the Preoperative Ratio of C-Reactive Protein to Albumin in Patients with Colorectal Cancer. Anticancer Res. 2016; 36:995-1001.
4. Ishizuka M, Nagata H, Takagi K, Horie T, Kubota K. Inflammation-based prognostic score is a novel predictor of postoperative outcome in patients with colorectal cancer. Ann Surg. 2007; 246:1047-1051.
5. Murakawa M, Yamamoto N, Kamioka Y, Kamiya M, Kobayashi S, Ueno M, Morimoto M, Atsumi Y, Aoyama T, Tamagawa H, Yukawa N, Rino Y, Masuda M, Morinaga S. Clinical Implication of Pre-operative C-reactive Protein-Albumin Ratio as a Prognostic Factor of Patients With Pancreatic Ductal Adenocarcinoma: A Single-institutional Retrospective Study. In Vivo. 2020; 34:347-353.
6. Liu Z, Jin K, Guo M, Long J, Liu L, Liu C, Xu J, Ni Q, Luo G, Yu X. Prognostic Value of the CRP/Alb Ratio, a Novel Inflammation-Based Score in Pancreatic Cancer. Ann Surg Oncol. 2017; 24:561-568.
7. Ishizuka M, Kubota K, Kita J, Shimoda M, Kato M, Sawada T. Impact of an inflammation-based prognostic system on patients undergoing surgery for hepatocellular carcinoma: a retrospective study of 398 Japanese patients. Am J Surg. 2012; 203:101-106.
8. Wu MT, He SY, Chen SL, Li LF, He ZQ, Zhu YY, He X, Chen H. Clinical and prognostic implications of pretreatment albumin to C-reactive protein ratio in patients with hepatocellular carcinoma. BMC Cancer. 2019; 19:538.
9. Shimizu T, Ishizuka M, Suzuki T, Tanaka G, Shiraki T, Sakuraoka Y, Matsumoto T, Kato M, Aoki T, Kubota K. The Value of the C-Reactive Protein-to-Albumin Ratio is Useful for Predicting Survival of Patients with Child-Pugh Class A Undergoing Liver Resection for Hepatocellular Carcinoma. World J Surg. 2018; 42:2218-2226.
10. Nakao Y, Yamashita YI, Arima K, Miyata T, Itoyama R, Yusa T, Umezaki N, Yamao T, Nakagawa S, Okabe H, Imai K, Chikamoto A, Baba H. Clinical Usefulness of Perioperative C-reactive Protein/Albumin Ratio in Patients With Intrahepatic Cholangiocarcinoma: A Retrospective Single Institutional Study. Anticancer Res. 2019; 39:2641-2646.
11. Pan QX, Su ZJ, Zhang JH, Wang CR, Ke SY. Glasgow Prognostic Score predicts prognosis of intrahepatic cholangiocarcinoma. Mol Clin Oncol. 2017; 6:566-574.
12. Cai Y, Cheng N, Ye H, Li F, Song P, Tang W. The current management of cholangiocarcinoma: A comparison of current guidelines. Biosci Trends. 2016; 10:92-102.

13. Chan KM, Tsai CY, Yeh CN, Yeh TS, Lee WC, Jan YY, Chen MF. Characterization of intrahepatic cholangiocarcinoma after curative resection: outcome, prognostic factor, and recurrence. BMC Gastroenterol. 2018; 18:180.
14. Ke Q, Lin N, Deng M, Wang L, Zeng Y, Liu J. The effect of adjuvant therapy for patients with intrahepatic cholangiocarcinoma after surgical resection: A systematic review and meta-analysis. PloS One. 2020; 15:e0229292.
15. Wang L, Deng M, Ke Q, Lou J, Zheng S, Bi X, Wang J, Guo W, Li F, Wang J, Zheng Y, Li J, Cheng S, Zhou W, Zeng Y. Postoperative adjuvant therapy following radical resection for intrahepatic cholangiocarcinoma: A multicenter retrospective study. Cancer Med. 2020; 9:2674-2685.
16. Sakamoto Y, Kokudo N, Matsuyama Y, Sakamoto M, Izumi N, Kadoya M, Kaneko S, Ku Y, Kudo M, Takayama T, Nakashima O; Liver Cancer Study Group of Japan. Proposal of a new staging system for intrahepatic cholangiocarcinoma: Analysis of surgical patients from a nationwide survey of the Liver Cancer Study Group of Japan. Cancer. 2016; 122:61-70.
17. Nathan H, Aloia TA, Vauthey JN, Abdalla EK, Zhu AX, Schulick RD, Choti MA, Pawlik TM. A proposed staging system for intrahepatic cholangiocarcinoma. Ann Surg Oncol. 2009; 16:14-22.
18. Wu ZF, Wu XY, Zhu N, Xu Z, Li WS, Zhang HB, Yang N, Yao XQ, Liu FK, Yang GS. Prognosis after resection for hepatitis B virus-associated intrahepatic cholangiocarcinoma. World J Gastroenterol. 2015; 21:935-943.
19. Zhou R, Lu D, Li W, *et al.* Is lymph node dissection necessary for resectable intrahepatic cholangiocarcinoma? A systematic review and meta-analysis. HPB 2019; 21:784-92.
20. Liu L, Wang W, Zhang Y, Tan W, Zhu S, Chen X, Min J, Shang C, Chen Y. Declined Preoperative Aspartate Aminotransferase to Neutrophil Ratio Index Predicts Poor Prognosis in Patients with Intrahepatic Cholangiocarcinoma after Hepatectomy. Cancer Res Treat. 2018; 50:538-550.
21. Chen Q, Dai Z, Yin D, Yang LX, Wang Z, Xiao YS, Fan J, Zhou J. Negative impact of preoperative platelet-lymphocyte ratio on outcome after hepatic resection for intrahepatic cholangiocarcinoma. Medicine. 2015; 94:e574.
22. Jing CY, Fu YP, Shen HJ, Zheng SS, Lin JJ, Yi Y, Huang JL, Xu X, Zhang J, Zhou J, Fan J, Ren ZG, Qiu SJ, Zhang BH. Albumin to gamma-glutamyltransferase ratio as a prognostic indicator in intrahepatic cholangiocarcinoma after curative resection. Oncotarget. 2017; 8:13293-13303.
23. Chen Q, Yang LX, Li XD, Yin D, Shi SM, Chen EB, Yu L, Zhou ZJ, Zhou SL, Shi YH, Fan J, Zhou J, Dai Z. The elevated preoperative neutrophil-to-lymphocyte ratio predicts poor prognosis in intrahepatic cholangiocarcinoma patients undergoing hepatectomy. Tumour Biol. 2015; 36:5283-5289.
24. Kokudo N, Hasegawa K, Akahane M, *et al.* Evidence-based Clinical Practice Guidelines for Hepatocellular Carcinoma: The Japan Society of Hepatology 2013 update (3rd JSH-HCC Guidelines). Hepatol Res. 2015; 45:123-127.
25. Takayama T, Makuuchi M, Kubota K, Harihara Y, Hui AM, Sano K, Ijichi M, Hasegawa K. Randomized comparison of ultrasonic vs clamp transection of the liver. Arch Surg. 2001; 136:922-928.
26. Song P, Midorikawa Y, Nakayama H, Higaki T, Moriguchi M, Aramaki O, Yamazaki S, Aoki M, Teramoto K, Takayama T. Patients' prognosis of intrahepatic cholangiocarcinoma and combined hepatocellular-cholangiocarcinoma after resection. Cancer Med. 2019; 8:5862-5871.
27. Forrest LM, McMillan DC, McArdle CS, Angerson WJ, Dunlop DJ. Evaluation of cumulative prognostic scores based on the systemic inflammatory response in patients with inoperable non-small-cell lung cancer. Br J Cancer. 2003; 89:1028-1030.
28. McMillan DC. Systemic inflammation, nutritional status and survival in patients with cancer. Curr Opin Clin Nutr Metab Care. 2009; 12:223-226.

Received May 20, 2020; Revised June 1, 2020; Accepted June 3, 2020.

**Address correspondence to:*
Yutaka Midorikawa, Department of Digestive Surgery, Nihon University School of Medicine. 30-1, Oyaguchikami-machi, Itabashi-ku, Tokyo 173-8610, Japan.
E-mail: mido-tky@umin.ac.jp

Released online in J-STAGE as advance publication June 5, 2020.

Letter

DOI: 10.5582/bst.2020.03305

Promoting social engagement of the elderly to cope with aging of the Chinese population

Yi Wang[1], Chengchao Zhou[1,2,*]

[1] Centre for Health Management and Policy, School of Public Health, Cheeloo College of Medicine, Shandong University, Ji'nan, Shandong, China;
[2] NHC Key Lab of Health Economics and Policy Research (Shandong University), Ji'nan, Shandong, China.

SUMMARY China is in a stage of rapid aging of its population, and its old-age dependency ratio has been increasing for decades. The acceleration of aging of the population and the increasing old-age dependency ratio will significantly increase the pressure on social security and public services, highlight the need for the effective supply of labor, and weaken the demographic dividend, which will continue to affect social vitality, the power to innovate, and potential economic growth rates. Promoting social engagement has been widely recognized as an effective strategy to address these challenges. Such an approach not only promotes the development of social productivity, but it also alleviates the social burden. Actively promoting the social engagement of the elderly is an important task in gerontology in China. Although the development of social engagement of the elderly is on the rise, the infrastructure and institutions to provide social engagement need to be enhanced. Improving social engagement in China is not just the responsibility of older adults themselves but also of the country and society as a whole. In the future, the entire society will fully understand the special role of older adults and increase their value through social engagement to achieve active and healthy aging in China.

Keywords social engagement, aging of the population, old-age dependency ratio, China

1. Introduction

Aging of the population is a worldwide problem. How do policy-makers help people remain independent and active as they age? How can the quality of life among older people be improved as people are living longer? These questions are even more difficult and challenging for China, which is the world's most populous country with the largest aging population (*1*). China is in a stage of rapid aging of the population. The number of people aged 65 and older in China was 176 million in 2019 (*2*), accounting for 12.6% of the total population. According to data from the World Bank (*3*), the older population is estimated to reach 240 million in 2030, accounting for 16.9% of the total population, and 354 million in 2050, accounting for 26.1%. Although aging symbolizes the great success of development, it is also one of China's biggest challenges. The acceleration of aging of the population will significantly increase the pressure on social security and public services, highlight the need for the effective supply of labor, and weaken the demographic dividend, which will continue to affect social vitality, the power to innovate, and potential economic growth rates (*4*). At present, China faces the problem of an increasing number of older people as well as a reduction in the labor force and an increase in the dependency ratio. Reaching its "Lewis turning point" (*5*), China's working-age population is decreasing and its elderly population is increasing, causing the old-age dependency ratio to increase from 11.9% in 2010 to 17.8% in 2019. This exceeds the average ratio worldwide, and the gap is widening (Figure 1). The old-age dependency ratio refers to the proportion of older dependents (people older than 64) to the working-age population (those ages 15-64), reflecting the burden of old-age dependency on society (*6*). Traditional thinking often regards the older population as a "burden" and views aging as a "problem," thus obscuring the potential of older people. The concept of *Active Aging* was devised to solve the challenges of aging and explore the potential of older people.

2. Active Aging and social engagement

In 1996, the World Health Organization (WHO) first proposed the concept of *Active Aging*. Social engagement is the core and essence of the concept of *Active Aging*, highlighting the fact that the elderly have an equal right

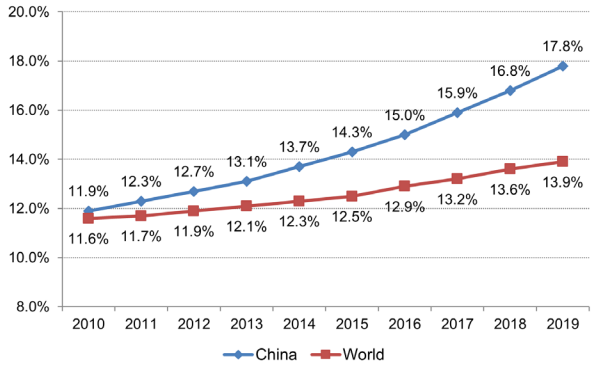

Figure 1. Trends of the old-age dependency ratio in China and the world from 2010 to 2019. Data source: The World Bank, *https://data.worldbank.org.cn/indicator/SP.POP.DPND.OL?end=2019&name_desc=true&start=2010&view=chart*

to engage in a social life, which is defined as "the process of optimizing opportunities for health, engagement, and security in order to enhance quality of life as people age" (*7*). *Active Aging* recognizes that older people have a right to social engagement and that such a right should be restored if lost. Accordingly, older people will cease to be the source of social problems and instead become the solution to those problems, changing from a consumer of social wealth to a creator of wealth, changing from a drag on social development to a promoter of development, and fundamentally defining an identity like the young and middle-aged. The WHO believes that if governments implement *Active Aging* policies and programs to enhance the health, engagement, and safety of older people, then those countries will be able to deal with aging.

3. The role of social engagement in coping with aging in Chinese population

Promoting social engagement has been widely recognized as an effective strategy to cope with aging of the population, and especially in China today. First, reemployment of the older population can promote the development of social productivity to a certain extent. Nowadays in China, one couple needs to take care of two children and four elderly parents in a typical family (*8*). In order to curb the continuing increase in the old-age dependency ratio, China implemented the two-child policy in 2016 to increase the expected labor force (*9*). However, the two-child policy only addresses the "denominator." Encouraging the social engagement of the elderly can fundamentally solve the problem of the increasing dependency ratio in terms of the "numerator." According to data from the China Association of Senior Scientists and Technologists, the number of older scientific and technological workers has reached more than 6 million, accounting for 15% of the total number of scientific and technological personnel in China (*10*). Older scientific and technological workers with senior professional titles account for a large proportion of the country's senior technical personnel. Older scientific and technological workers have worked hard in various fields such as education, scientific research, culture, health, and industrial and agricultural production for a long time. They have accumulated rich practical experience and made major contributions to the country's scientific and technological progress and economic and social development. If retired senior professionals continue to devote themselves to economic and cultural development, this will further spur the momentum for sustainable economic and social development. Older people in general also have a wealth of political experience, extensive knowledge and experience, technical proficiency, and usually have a strong desire to participate in society. In addition, most of the elderly are in good mental and physical condition and have the ability to engage in production, labor, social management, scientific research, creation of art, helping and teaching the next generation, and other social affairs. Second, social engagement can also alleviate the social burden caused by aging. After retirement, the main arenas for older people are the family and society, and the proportion of elderly people living alone or living separately from their adult children continues to increase as families in China shrink. Most of the elderly want to be independent and may not want to live with their children (*11*). However, older people can enrich their own lives in their later years and improve their own quality of life through hobby circles and educational groups. Older people in local hobby circles can promote traditional Chinese culture, such as Beijing opera and Yangko dances. More importantly, the elderly will no longer feel lonely in their later years. A growing number of studies have indicated the important role of social engagement in promoting health and reducing the burden of caregiving among older adults (*12,13*). A study has also suggested that older people who engage in group activities have lower medical costs (*14*).

4. Policy background and the way of social engagement in China

Actively promoting the social engagement of the elderly is an important task in gerontology in China. As early as 1996, Article 4 of the "Law of the People's Republic of China on the Protection of the Rights and Interests of the Elderly" specifically stipulates that the state and society will improve conditions for the elderly "to participate in social development," thus establishing social engagement as a basic right of the elderly (*15*). The National Population Development Plan (2016-2030) issued by the State Council in 2016 proposed encouraging the elderly to actively engage in family development, mutual assistance for the aged, community governance, and social welfare activities (*16*). In 2017, the "Thirteenth Five-Year Plan for Healthy Aging"

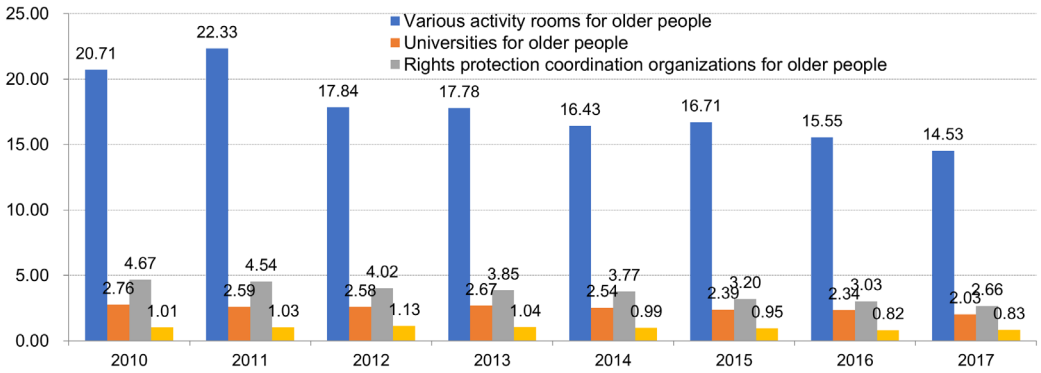

Figure 2. Number of institutions providing social engagement services to older adults in China from 2010 to 2017 (per 10,000 older individuals). Data source: Ministry of Civil Affairs, People's Republic of China, *http://www.mca.gov.cn/article/sj/tjgb/* (*Note*: The latest national data prior to 2017 are available).

issued by the National Health Commission clearly stated the need to provide daily care and support for the elderly living separately from their children, to encourage them to actively participate in society, and to promote the health of the elderly (*17*).

At present, the best form of social engagement among older people is mainly through various social organizations (*18*). Social organizations of older people are large organizations involved in self-education, self-management, self-service, community-building, and social development. Social organizations for older people play an increasingly important role as the population rapidly ages. Although social engagement among older people is increasing, it is still relatively limited in China at present. The number of institutions and organizations providing social engagement services to older adults in China tended to decline from 2010 to 2017 (Figure 2). This indicates that the rate at which the elderly are engaging socially lags behind the growth rate of the older population within the content of rapid aging in China.

5. Policy recommendations

There are some suggestions and pathways to improve the level of social engagement. First, the reemployment of older adults needs to increase. Human resources or departments to promote employment of the elderly need to create a database to collect information on relevant resources and to establish a forum where the elderly can regularly interact and receive information about employment opportunities. Suitable platforms should be created to capitalize on the advantages of older adults so that older adults and children, adolescents, young people, and even the middle-aged can help each other. The government should further construct public facilities for older people. Many recreational, developmental, and modern activities require corresponding venues or settings, such as places to play chess or cards, venues for community organizations, etc. Last but not least, an awareness of the importance of social engagement should be cultivated among older adults by expanding informational campaigns and active advocacy so that they actively participate in and integrate into social life. Overall, improving social engagement in China is not just the responsibility of older adults themselves but also of the country and society as a whole. In the future, the entire society will fully understand the special role of older adults and increase their value through social engagement to achieve active and healthy aging in China.

References

1. Hsu M, Liao PJ, Zhao M. Demographic change and long-term growth in China: Past developments and the future challenge of aging. Rev Dev Econ..2018; 22:928-952.
2. National Bureau of Statistics. National data. 2020. *http://data.stats.gov.cn/easyquery.htm?cn=C01* (accessed August 15, 2020)
3. World Bank. Population estimates and projections. 2020. *https://databank.worldbank.org/source/population-estimates-and-projections* (accessed August 15, 2020)
4. Fu T. Population Aging and pension pressure in China. Modern Economic Information. 2010;162+164. (in Chinese)
5. Wei Z, Kwan F. Revisit China's lewis turning point: An analysis from a regional perspective. Asian Econ J. 2018; 32:333-357.
6. Aisa R, Pueyo F. Population aging, health care, and growth: A comment on the effects of capital accumulation. J Popul Econ. 2013; 26:1285-1301.
7. World Health Organization. Active Ageing: A Policy Framework. 2002.
8. Li G, Li Z, Lv X. The ageing population, dependency burdens and household commercial insurance purchase: Evidence from China. Applied Economics Letters. 2020.
9. Wang W. Population aging, family planning policy adjustment and China economic growth. China Economic Quarterly. 2016; 16:67-96. (in Chinese)
10. China Association of Senior Scientists and Technologists. Historical developments. 2017. *http://www.casst.org.cn/cms/contentmanager.do?method=view&pageid=view&id=cms0fc8e35e0865f* (accessed August 15, 2020)

11. Li Y, Lu J. Social engagement of the elderly in China: Implications, the status quo, and challenges. Population and Family Planning. 2018; 255:14-17. (in Chinese)
12. Walker E, Ploubidis G, Fancourt D. Social engagement and loneliness are differentially associated with neuro-immune markers in older age: Time-varying associations from the English Longitudinal Study of Ageing. Brain Behav Immun. 2019; 82:224-229.
13. Liu J, Rozelle S, Xu Q, Yu N, Zhou T. Social engagement and elderly health in China: Evidence from the China Health and Retirement Longitudinal Survey (CHARLS). Int J Environ Res Public Health. 2019; 16:278.
14. Otsuki T. Older community residents who participate in group activities have higher daily physical activity levels and lower medical costs. Asia-Pac J Public He. 2018; 30:629-634.
15. Ministry of Civil Affairs, People's Republic of China. Law of the People's Republic of China on the Protection of the Rights and Interests of the Elderly. 1996. *http://www.mca.gov.cn/article/gk/fg/ylfw/202002/20200200024078.shtml* (accessed August 15, 2020)
16. State Council, People's Republic of China. The National Population Development Plan (2016-2030) 2016. *http://www.gov.cn/zhengce/content/2017-01/25/content_5163309.htm* (accessed August 15, 2020)
17. National Health Commission, People's Republic of China. Thirteenth Five Year Plan for Healthy Aging. 2017. *http://www.nhc.gov.cn/lljks/zcwj2/201703/86fd489301c64c46865bd98c29e217f2.shtml* (accessed August 15, 2020)
18. Yan X. In this new situation, we should actively respond to the problem of the advent of an aging population. Social Science Forum. 2019. (in Chinese)

Received July 22, 2020; Revised August 18, 2020; Accepted August 23, 2020.

**Address correspondence to:*
Chengchao Zhou, Centre for Health Management and Policy, School of Public Health, Cheeloo College of Medicine, Shandong University; NHC Key Lab of Health Economics and Policy Research (Shandong University), Ji'nan, 250012, Shandong, China .
E-mail: zhouchengchao@sdu.edu.cn

Released online in J-STAGE as advance publication August 26, 2020.

BST
BioScience Trends

Guide for Authors

1. Scope of Articles

BioScience Trends (Print ISSN 1881-7815, Online ISSN 1881-7823) is an international peer-reviewed journal. *BioScience Trends* devotes to publishing the latest and most exciting advances in scientific research. Articles cover fields of life science such as biochemistry, molecular biology, clinical research, public health, medical care system, and social science in order to encourage cooperation and exchange among scientists and clinical researchers.

2. Submission Types

Original Articles should be well-documented, novel, and significant to the field as a whole. An Original Article should be arranged into the following sections: Title page, Abstract, Introduction, Materials and Methods, Results, Discussion, Acknowledgments, and References. Original articles should not exceed 5,000 words in length (excluding references) and should be limited to a maximum of 50 references. Articles may contain a maximum of 10 figures and/or tables. Supplementary Data are permitted but should be limited to information that is not essential to the general understanding of the research presented in the main text, such as unaltered blots and source data as well as other file types.

Brief Reports definitively documenting either experimental results or informative clinical observations will be considered for publication in this category. Brief Reports are not intended for publication of incomplete or preliminary findings. Brief Reports should not exceed 3,000 words in length (excluding references) and should be limited to a maximum of 4 figures and/or tables and 30 references. A Brief Report contains the same sections as an Original Article, but the Results and Discussion sections should be combined.

Reviews should present a full and up-to-date account of recent developments within an area of research. Normally, reviews should not exceed 8,000 words in length (excluding references) and should be limited to a maximum of 10 figures and/or tables and 100 references. Mini reviews are also accepted, which should not exceed 4,000 words in length (excluding references) and should be limited to a maximum of 5 figures and/or tables and 50 references.

Policy Forum articles discuss research and policy issues in areas related to life science such as public health, the medical care system, and social science and may address governmental issues at district, national, and international levels of discourse. Policy Forum articles should not exceed 3,000 words in length (excluding references) and should be limited to a maximum of 5 figures and/or tables and 30 references.

Communications are short, timely pieces that spotlight new research findings or policy issues of interest to the field of global health and medical practice that are of immediate importance. Depending on their content, Communications will be published as "Comments" or "Correspondence". Communications should not exceed 1,500 words in length (excluding references) and should be limited to a maximum of 2 figures and/or tables and 20 references.

Editorials are short, invited opinion pieces that discuss an issue of immediate importance to the fields of global health, medical practice, and basic science oriented for clinical application. Editorials should not exceed 1,000 words in length (excluding references) and should be limited to a maximum of 10 references. Editorials may contain one figure or table.

News articles should report the latest events in health sciences and medical research from around the world. News should not exceed 500 words in length.

Letters should present considered opinions in response to articles published in *BioScience Trends* in the last 6 months or issues of general interest. Letters should not exceed 800 words in length and may contain a maximum of 10 references. Letters may contain one figure or table.

3. Editorial Policies

For publishing and ethical standards, BioScience Trends follows the Recommendations for the Conduct, Reporting, Editing, and Publication of Scholarly Work in Medical Journals (*http://www.icmje.org/recommendations*) issued by the International Committee of Medical Journal Editors (ICMJE), and the Principles of Transparency and Best Practice in Scholarly Publishing (*https://doaj.org/bestpractice*) jointly issued by the Committee on Publication Ethics (COPE), the Directory of Open Access Journals (DOAJ), the Open Access Scholarly Publishers Association (OASPA), and the World Association of Medical Editors (WAME).

BioScience Trends will perform an especially prompt review to encourage innovative work. All original research will be subjected to a rigorous standard of peer review and will be edited by experienced copy editors to the highest standards.

Ethics: *BioScience Trends* requires that authors of reports of investigations in humans or animals indicate that those studies were formally approved by a relevant ethics committee or review board. For research involving human experiments, a statement that the participants gave informed consent before taking part (or a statement that it was not required and why) should be indicated. Authors should also state that the study conformed to the provisions of the Declaration of Helsinki (as revised in 2013). When reporting experiments on animals, authors should indicate whether the institutional and national guide for the care and use of laboratory animals was followed.

Conflict of Interest: All authors are required to disclose any actual or potential conflict of interest including financial interests or relationships with other people or organizations that might raise questions of bias in the work reported. If no conflict of interest exists for each author, please state "There is no conflict of interest to disclose".

Submission Declaration: When a manuscript is considered for submission to *BioScience Trends*, the authors should confirm that 1) no part of this manuscript is currently under consideration for publication elsewhere; 2) this manuscript does not contain the same information in whole or in part as manuscripts that have been published, accepted, or are under review elsewhere, except in the form of an abstract, a letter to

the editor, or part of a published lecture or academic thesis; 3) authorization for publication has been obtained from the authors' employer or institution; and 4) all contributing authors have agreed to submit this manuscript.

Cover Letter: The manuscript must be accompanied by a cover letter prepared by the corresponding author on behalf of all authors. The letter should indicate the basic findings of the work and their significance. The letter should also include a statement affirming that all authors concur with the submission and that the material submitted for publication has not been published previously or is not under consideration for publication elsewhere. The cover letter should be submitted in PDF format. For example of Cover Letter, please visit: Download Centre (*https://ircabssagroup.com/downcentre*).

Copyright: When a manuscript is accepted for publication in *BioScience Trends*, the transfer of copyright is necessary. A JOURNAL PUBLISHING AGREEMENT (JPA) form will be e-mailed to the authors by the Editorial Office and must be returned by the authors as a scan. Only forms with a hand-written signature are accepted. This copyright will ensure the widest possible dissemination of information. Please note that your manuscript will not proceed to the next step in publication until the JPA Form is received. In addition, if excerpts from other copyrighted works are included, the author(s) must obtain written permission from the copyright owners and credit the source(s) in the article.

Peer Review: *BioScience Trends* uses single-blind peer review, which means that reviewers know the names of the authors, but the authors do not know who reviewed their manuscript. The external peer review is performed for research articles by at least two reviewers, and sometimes the opinions of more reviewers are sought. Peer reviewers are selected based on their expertise and ability to provide high quality, constructive, and fair reviews. For research manuscripts, the editors may, in addition, seek the opinion of a statistical reviewer. Consideration for publication is based on the article's originality, novelty, and scientific soundness, and the appropriateness of its analysis.

Suggested Reviewers: A list of up to 3 reviewers who are qualified to assess the scientific merit of the study is welcomed. Reviewer information including names, affiliations, addresses, and e-mail should be provided at the same time the manuscript is submitted online. Please do not suggest reviewers with known conflicts of interest, including participants or anyone with a stake in the proposed research; anyone from the same institution; former students, advisors, or research collaborators (within the last three years); or close personal contacts. Please note that the Editor-in-Chief may accept one or more of the proposed reviewers or may request a review by other qualified persons.

Language Editing: Manuscripts prepared by authors whose native language is not English should have their work proofread by a native English speaker before submission. If not, this might delay the publication of your manuscript in *BioScience Trends*.

The Editing Support Organization can provide English proofreading, Japanese-English translation, and Chinese-English translation services to authors who want to publish in *BioScience Trends* and need assistance before submitting a manuscript. Authors can visit this organization directly at *http://www.iacmhr.com/iac-eso/support.php?lang=en*. IAC-ESO was established to facilitate manuscript preparation by researchers whose native language is not English and to help edit works intended for international academic journals.

4. Manuscript Preparation

Manuscripts are suggested to be prepared in accordance with the "Recommendations for the Conduct, Reporting, Editing, and Publication of Scholarly Work in Medical Journals", as presented at *http://www.ICMJE.org*.

Manuscripts should be written in clear, grammatically correct English and submitted as a Microsoft Word file in a single-column format. Manuscripts must be paginated and typed in 12-point Times New Roman font with 24-point line spacing. Please do not embed figures in the text. Abbreviations should be used as little as possible and should be explained at first mention unless the term is a well-known abbreviation (*e.g.* DNA). Single words should not be abbreviated.

Title page: The title page must include 1) the title of the paper (Please note the title should be short, informative, and contain the major key words); 2) full name(s) and affiliation(s) of the author(s), 3) abbreviated names of the author(s), 4) full name, mailing address, telephone/fax numbers, and e-mail address of the corresponding author; and 5) conflicts of interest (if you have an actual or potential conflict of interest to disclose, it must be included as a footnote on the title page of the manuscript; if no conflict of interest exists for each author, please state "There is no conflict of interest to disclose"). Please visit Download Centre and refer to the title page of the manuscript sample.

Abstract: The abstract should briefly state the purpose of the study, methods, main findings, and conclusions. For articles that are Original Articles, Brief Reports, Reviews, or Policy Forum articles, a one-paragraph abstract consisting of no more than 250 words must be included in the manuscript. For Communications, Editorials, News, or Letters, a brief summary of main content in 150 words or fewer should be included in the manuscript. Abbreviations must be kept to a minimum and non-standard abbreviations explained in brackets at first mention. References should be avoided in the abstract. Three to six key words or phrases that do not occur in the title should be included in the Abstract page.

Introduction: The introduction should be a concise statement of the basis for the study and its scientific context.

Materials and Methods: The description should be brief but with sufficient detail to enable others to reproduce the experiments. Procedures that have been published previously should not be described in detail but appropriate references should simply be cited. Only new and significant modifications of previously published procedures require complete description. Names of products and manufacturers with their locations (city and state/country) should be given and sources of animals and cell lines should always be indicated. All clinical investigations must have been conducted in accordance with Declaration of Helsinki principles. All human and animal studies must have been approved by the appropriate institutional review board(s) and a specific declaration of approval must be made within this section.

Results: The description of the experimental results should be succinct but in sufficient detail to allow the experiments to be analyzed and interpreted by an independent reader. If necessary, subheadings may be used for an orderly presentation. All figures and tables must be referred to in the text.

Discussion: The data should be interpreted concisely without repeating material already presented in the Results section. Speculation is permissible, but it must be well-founded, and discussion of the wider implications of the findings is encouraged. Conclusions derived from the study should be included in this section.

Acknowledgments: All funding sources should be credited in the Acknowledgments section. In addition, people who contributed to the work but who do not meet the criteria for authors should be listed along with their contributions.

References: References should be numbered in the order in which they appear in the text. Citing of unpublished results, personal communications, conference abstracts, and theses in the reference list is not recommended but these sources may be mentioned in the text. In the reference list, cite the names of all authors when there are fifteen or fewer authors; if there are sixteen or more authors, list the first three followed by *et al*. Names of journals should be abbreviated in the style used in PubMed. Authors are responsible for the accuracy of the references. The EndNote Style of *BioScience Trends* could be downloaded at **EndNote** (*https://ircabssagroup.com/examples/BioScience_Trends.ens*).

Examples are given below:

Example 1 (Sample journal reference):

Inagaki Y, Tang W, Zhang L, Du GH, Xu WF, Kokudo N. Novel aminopeptidase N (APN/CD13) inhibitor 24F can suppress invasion of hepatocellular carcinoma cells as well as angiogenesis. Biosci Trends. 2010; 4:56-60.

Example 2 (Sample journal reference with more than 15 authors):

Darby S, Hill D, Auvinen A, *et al*. Radon in homes and risk of lung cancer: Collaborative analysis of individual data from 13 European case-control studies. BMJ. 2005; 330:223.

Example 3 (Sample book reference):

Shalev AY. Post-traumatic stress disorder: Diagnosis, history and life course. In: Post-traumatic Stress Disorder, Diagnosis, Management and Treatment (Nutt DJ, Davidson JR, Zohar J, eds.). Martin Dunitz, London, UK, 2000; pp. 1-15.

Example 4 (Sample web page reference):

World Health Organization. The World Health Report 2008 – primary health care: Now more than ever. *http://www.who.int/whr/2008/whr08_en.pdf* (accessed September 23, 2010).

Tables: All tables should be prepared in Microsoft Word or Excel and should be arranged at the end of the manuscript after the References section. Please note that tables should not in image format. All tables should have a concise title and should be numbered consecutively with Arabic numerals. If necessary, additional information should be given below the table.

Figure Legend: The figure legend should be typed on a separate page of the main manuscript and should include a short title and explanation. The legend should be concise but comprehensive and should be understood without referring to the text. Symbols used in figures must be explained. Any individually labeled figure parts or panels (A, B, *etc*.) should be specifically described by part name within the legend.

Figure Preparation: All figures should be clear and cited in numerical order in the text. Figures must fit a one- or two-column format on the journal page: 8.3 cm (3.3 in.) wide for a single column, 17.3 cm (6.8 in.) wide for a double column; maximum height: 24.0 cm (9.5 in.). Please make sure that the symbols and numbers appeared in the figures should be clear. Please make sure that artwork files are in an acceptable format (TIFF or JPEG) at minimum resolution (600 dpi for illustrations, graphs, and annotated artwork, and 300 dpi for micrographs and photographs). Please provide all figures as separate files. Please note that low-resolution images are one of the leading causes of article resubmission and schedule delays.

Units and Symbols: Units and symbols conforming to the International System of Units (SI) should be used for physicochemical quantities. Solidus notation (*e.g*. mg/kg, mg/mL, mol/mm^2/min) should be used. Please refer to the SI Guide *www.bipm.org/en/si/* for standard units.

Supplemental data: Supplemental data might be useful for supporting and enhancing your scientific research and *BioScience Trends* accepts the submission of these materials which will be only published online alongside the electronic version of your article. Supplemental files (figures, tables, and other text materials) should be prepared according to the above guidelines, numbered in Arabic numerals (*e.g.*, Figure S1, Figure S2, and Table S1, Table S2) and referred to in the text. All figures and tables should have titles and legends. All figure legends, tables and supplemental text materials should be placed at the end of the paper. Please note all of these supplemental data should be provided at the time of initial submission and note that the editors reserve the right to limit the size and length of Supplemental Data.

5. Submission Checklist

The Submission Checklist will be useful during the final checking of a manuscript prior to sending it to *BioScience Trends* for review. Please visit Download Centre and download the Submission Checklist file.

6. Online Submission

Manuscripts should be submitted to *BioScience Trends* online at *http://www.biosciencetrends.com*. The manuscript file should be smaller than 5 MB in size. If for any reason you are unable to submit a file online, please contact the Editorial Office by e-mail at *office@biosciencetrends.com*

7. Accepted Manuscripts

Proofs: Galley proofs in PDF format will be sent to the corresponding author *via* e-mail. Corrections must be returned

to the editor (*proof-editing@biosciencetrends.com*) within 3 working days.

Offprints: Authors will be provided with electronic offprints of their article. Paper offprints can be ordered at prices quoted on the order form that accompanies the proofs.

Page Charge: Page charges will be levied on all manuscripts accepted for publication in *BioScience Trends* ($140 per page for black white pages; $340 per page for color pages). Under exceptional circumstances, the author(s) may apply to the editorial office for a waiver of the publication charges at the time of submission.

Misconduct: *BioScience Trends* takes seriously all allegations of potential misconduct and adhere to the ICMJE Guideline (*http://www.icmje.org/recommendations*) and COPE Guideline (*http://publicationethics.org/files/Code_of_conduct_for_journal_editors.pdf*). In cases of suspected research or publication misconduct, it may be necessary for the Editor or Publisher to contact and share submission details with third parties including authors' institutions and ethics committees. The corrections, retractions, or editorial expressions of concern will be performed in line with above guidelines.

(As of June 2020)

BioScience Trends
Editorial and Head Office
Pearl City Koishikawa 603,
2-4-5 Kasuga, Bunkyo-ku,
Tokyo 112-0003, Japan.
E-mail: office@biosciencetrends.com